VÂNIA DINORA PEREIRA FRAGUITO CORREIA

JURASSIC DINOFLAGELLATE CYST BIOSTRATIGRAPHY OF THE LUSITANIAN BASIN, WEST-CENTRAL PORTUGAL, AND ITS RELEVANCE TO THE OPENING OF THE NORTH ATLANTIC AND PETROLEUM GEOLOGY

Doutoramento em Ciências do Mar, da Terra e do Ambiente, ramo Geociências
Especialidade em Geologia

Trabalho efetuado sob a orientação de:

Professor Doutor Paulo Fernandes
(UAlg – Universidade do Algarve)

Doutora Zélia Pereira
(LNEG – Laboratório Nacional de Energia e Geologia)

Doutor James Brian Riding
(BGS – British Geological Survey)

UNIVERSIDADE DO ALGARVE

Faculdade de Ciências e Tecnologia

2018

Caption of the photomicrograph in the cover:

Luehndea spinosa Morgenroth 1970. Vale das Fontes section, lower Toarcian (*Dactylioceras polymorphum* AB), sample PVF8.

Jurassic dinoflagellate cyst biostratigraphy of the Lusitanian Basin, west-central Portugal, and its relevance to the opening of the North Atlantic and petroleum geology

Declaração de autoria de trabalho

Declaro ser a autora deste trabalho, que é original e inédito. Autores e trabalhos consultados estão devidamente citados no texto e constam da listagem de referências incluída.

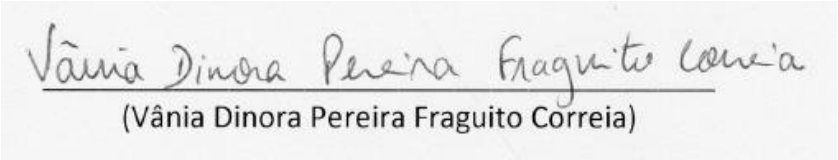

To my mother

"There is grandeur in this view of life, with its several powers
having been originally breathed into a few forms or into one;
and from so simple a beginning endless forms
most beautiful and most wonderful have been, and are being evolved."
Charles Darwin

Agradecimentos/Acknowledgements

E porque juntos vamos mais longe, agora no culminar da realização de um propóstito académico e pessoal há muito ansiado, gostaria de expressar os meus sinceros agradecimentos a todos aqueles que enriqueceram esta caminhada de quatro anos:

Em primeiro lugar, aos meus orientadores, Zélia Pereira, Paulo Fernandes e James Brian Riding, por todos os (valiosos!) ensinamentos, disponibilidade, motivação constante e, acima de tudo, acreditarem que eu era capaz. Sem vós, este trabalho de Doutoramento, simplesmente, não teria acontecido! E porque, para mim, são muito mais que orientadores, estou-vos muito agradecida pela amizade e carinho com que sempre me trataram.

Jim, I'm deeply grateful for your commitment with this project and for spending so much of your precious time in this work. Thank you for having me trained with so much effort and patience, and for all your positive energy and friendship!

Em segundo lugar, à Fundação para a Ciência e Tecnologia por me ter concedido uma bolsa de Doutoramento (SFRH/BD/93950/2013), imprescindível para a realização deste projecto de investigação.

Ao Luís Vitor Duarte, pelo incentivo à reflexão e exigência, por toda a dedicação e energia transmitida ao longo das várias fases deste percurso e por acreditar sempre no sucesso deste projecto.

À Maria Helena Henriques, pela força e entusiasmo expressados desde o início, total empenho e rigor durante esta colaboração, bem como o estímulo à minha autonomia e confiança no trabalho realizado.

Ao Professor Artur Sá pela confiança depositada em mim e por me ter aberto as portas deste fantástico mundo da (micro)Paleontologia!

À Marisa Borges e Gilda Lopes por toda a coragem transmitida, partilha de conhecimentos e vivências e, em especial, por serem uma inspiração para mim nesta aventura pela Palinologia!

Ao Bruno Rodrigues por todas as dicas "burocráticas" iniciais e à Francesca Galasso pelo apoio no trabalho de microscopia de fluorescência.

Ao Sr Fernando Oliveira e D. Irene Sousa pela dedicação e rapidez na preparação laboratorial das amostras.

À Márcia e Margarida por todo o companheirismo e boa disposição; ao Filipe Barreira por toda a colaboração no grafismo e sugestões essenciais na elaboração deste trabalho; à Vera Figueiredo pela ajuda nos mapas, *posters* e pelo interesse em ouvir "o ponto de situação" do meu trabalho, mesmo durante a hora de almoço! A toda a maravilhosa equipa de Geologia do LNEG em S. Mamede de Infesta por me terem acolhido tão carinhosamente na vossa "casa" e pelo suporte prestado ao longo destes quatro anos.

À Patrícia Rita e ao Bruno Rodrigues Teixeira pelo incentivo à proactividade e crítica científica e, em particular, pelo apoio e excelente companhia durante a viagem e estadia em Jaén! Também ao Jorge de Carvalho pela ajuda na amostragem e partilha das belas paisagens do Cabo Mondego.

À Mariana Fernandes, Lisete Fernandes e Pedro Tavares pelas sugestões, tempo e "espaço" dispendidos!

Às minhas sempre amigas Catarina, Lisete, Lisa, Marisa e Rita por todo o apoio e interesse e pelos bons momentos de descontração, essenciais para "desligar" das preocupações do trabalho, mesmo que às vezes nem se tenham apercebido disso… À Sónia Xavier, pelas preciosas sugestões de técnicas de concentração e relaxamento.

A toda a minha família pelo incentivo em ir mais além e serem as raízes da minha determinação em atingir esta meta que, ao início, parecia inalcansável... Sem vós, mãe, pai, irmã, primos, padrinhos, tios e avós, a concretização deste sonho não teria sido possível.

Ao Carlos, por me fazer acreditar e ter dado a coragem necessária para embarcar nesta viagem. Pelo amor, companheirismo, compreensão e ser a luz em todos os momentos de dúvida…Mais que tudo, por me ter ajudado a crescer, tornado-me uma pessoa mais segura, serena e feliz.

E à Bia, Amy e Yma por não permitirem que os meus dias em casa fossem monótonos, por trazerem o conforto, alegria e energia à minha vida, essenciais para relativizar todas as dificuldades ao longo deste percurso.

Estou profundamente grata a todos vós!

Abstract

The biostratigraphy of the Lusitanian Basin is based mainly on macrofossils and microfossils (foraminifera, nannofossils and ostracods). Compared to these works, palynological studies are scarce in the Lusitanian Basin. Dinoflagellate cysts are a powerful biostratigraphical and paleoenvironmental tool and, their study may be a major contribution for the Lusitanian Basin background. In this project, the Lower and Middle Jurassic of the Lusitanian Basin was investigated for palynological and palaeoenvironmental analyses. Eight sections were sampled: São Pedro de Moel, Brenha, Peniche, Fonte Coberta, Maria Pares, Vale das Fontes, São Gião e Cabo Mondego; 358 samples of marls and marly limestones were studied in detail.

The palynological response to the Toarcian Oceanic Anoxic Event (T-OAE) was examined in the Lower Jurassic sections of Maria Pares, Vale das Fontes and Peniche. A low diversity dinoflagellate cyst flora, typical of the Sub-Boreal Realm, was recovered from the *Emaciaticeras emaciatum* and *Dactylioceras polymorphum* ammonite biozones (ABs). Prior to the T-OAE, dinoflagellates thrived in the Lusitanian Basin. The *Hildaites levisoni* AB represents the T-OAE and the overlying strata, and is characterised by a profound reduction in dinoflagellate cyst relative abundances, causing the extinction of *Luehndea spinosa* and disappearance of *Nannoceratopsis* spp. This dinoflagellate cyst "blackout" reflects significant environmental stress, such as marine anoxia, elevated temperatures and reduced salinity, with the former two probably being most important.

A comprehensive investigation of the Early and Middle Jurassic stratigraphical palynology of the Lusitanian Basin was undertaken and a palynostratigraphical chart is proposed based, especially, in dinoflagellate cysts. The Sinemurian material examined in São Pedro de Moel was barren of dinoflagellate cysts, however the Pliensbachian and Toarcian successions are characterised by relatively low diversities, but biostratigraphically significant. *Luehndea spinosa* dominates the uppermost Pliensbachian–lowermost Toarcian, and is an index species. The *Luehndea spinosa* and *Mendicodinium microscabratum* dinoflagellate cyst biozones were defined, both of which are subdivided into two dinoflagellate cyst subbiozones. The Middle Jurassic samples of São Gião and Cabo Mondego successions are correlated to ammonite biozones spanning *Pleydellia aalensis* to *Zigzagiceras zigzag*. The Cabo Mondego section largely yielded relatively abundant palynomorph associations. By contrast, the

São Gião outcrop, which only includes the Toarcian–Aalenian transition, produced sparse assemblages. The uppermost Toarcian to lowermost Bajocian is characterised by a low diversity dinoflagellate cyst association. Above this (*Witchellia laeviuscula* AB) is a markedly more diverse assemblage. The trend of increasing dinoflagellate cyst diversity continued at the Bajocian–Bathonian transition. The acritarchs, prasinophytes, pollen and spores observed in this study are typical of Jurassic assemblages worldwide.

The palynostratigraphical scheme proposed in this project may be used in future hydrocarbon investigation of the Lusitanian Basin. The fluorescence colour of palynomorphs and spore-pollen colours (TAI) analyses, suggest that most of the Lower and Middle Jurassic sediments of the Lusitanian Basin are between the immature and mature phases for oil generation. This work is presented as a significant contribution to the Lusitanian Basin background, especially for biostratigraphy.

Keywords

Biostratigraphy; Dinoflagellate cysts; Lusitanian Basin; Jurassic; Palynology; Toarcian Oceanic Anoxic Event;

Resumo

A Bacia Lusitânica é uma bacia sedimentar Mesozoica, que se desenvolveu na Margem Oeste da Península Ibérica. A sua origem e evolução está relacionada com sucessivas fases de rifting do continente Pangea que conduziram à abertura do Oceano Atlântico Norte durante o Triássico ?Médio–Superior e o Cretácico Inferior. A bioestratigrafia da Bacia Lusitânica assenta, maioritariamente, na informação de macrofósseis (amonites, braquiópodes e corais) e microfósseis (foraminíferos, nanofósseis e ostracodos). Comparado com estes trabalhos, as investigações palinológicas na Bacia Lusitânica são escassas, em particular, o estudo dos quistos de dinoflagelados.

Os principais objectivos deste estudo de investigação são: i) estabelecer a palinoestratigrafia do Jurássico da Bacia Lusitânica e propor um esquema biozonal com base nos quistos de dinoflagelados ii) investigar as semelhanças e diferenças das associações de dinoflagelados entre a Bacia Lusitânica e outras bacias em Portugal (e.g. Bacia Algarvia), Europa, Austrália ou América; iii) realizar correlações biozonais entre os quistos de dinoflagelados e outros grupos fósseis (e.g. amonites, foraminíferos, nanofósseis); iv) estudar a paleoecologia/paleobiologia e realizar palinoestratigrafia de alta resolução com base nos quistos de dinoflagelados em afloramentos da Bacia Lusitânica que conservam eventos importantes do Jurássico, como por exemplo, o Evento Anóxico Oceânico do Toarciano (*T-OAE – Toarcian Oceanic Anoxic Event*), os Estratotipos Global de Limite (*GSSP - Global Boundary Stratotype Section and Point*) da base dos andares do Toarciano em Peniche e Bajociano na praia da Murtinheira, Cabo Mondego, e Estratotipo Auxiliar (*ASSP - Auxiliary Stratotype Section and Point*) do andar Batoniano no Cabo Mondego; v) perceber em que medida este depocentro atuou como "ponte" de ligação entre as províncias Boreal, do Norte da Europa, e Tetsiana, do Sul da Europa; vi) contribuir para os conhecimentos da paleoceanografia e paleogeografia da Bacia Lusitânica no Jurássico, durante as primeiras fases de abertura do Oceano Atlântico Norte, com base na distribuição dos quistos de dinoflagelados.

Os dinoflagelados são seres unicelulares que, na sua fase móvel, possuem dois flagelos, um transversal, e outro longitudinal. A maioria das espécies modernas são marinhas e parte constituinte do fitoplâncton. Cerca de 50% das espécies são autotróficas e, portanto, importantes produtores primários, que terão surgido no Triássico Médio. Estes seres, na forma de quistos de dinoflagelados, deixaram um

importante registo fóssil nas rochas marinhas, nomeadamente no Jurássico, e são, assim, importantes marcadores bioestratigráficos e paleoambientais.

Neste trabalho foram amostradas e investigadas 358 amostras de rochas sedimentares (margas e calcários margosos) do Jurássico Inferior e Médio da Bacia Lusitânica. Análises palinológicas detalhadas foram realizadas na sucessão entre o Sinemuriano superior e Batoniano inferior, que compreendeu o estudo de oito afloramentos da Bacia Lusitânica: São Pedro de Moel, Brenha, Peniche, Fonte Coberta, Maria Pares, Vale das Fontes, São Gião e Cabo Mondego.

Foi investigada a resposta dos palinomorfos às alterações paleoambientais ocorridas durante o T-OAE, com base no estudo de três importantes cortes do Jurássico Inferior, Maria Pares, Vale das Fontes e Peniche, onde está registado este evento. Nas amostras estudadas foram reconhecidas as biozonas de amonite *Emaciaticeras emaciatum* (Pliensbaquiano superior), *Dactylioceras polymorphum*, *Hildaites levisoni* e *Hildoceras bifrons* (Toarciano). Foi registada uma baixa diversidade de quistos de dinoflagelados, típica da província Sub-Boreal, uma área de transição entre as províncias Boreal e Tetsiana, comprovando que a Bacia Lusitânica terá sido uma área de ligação entre as duas províncias. A espécie dominante é a *Luehndea spinosa*, característica de águas frias da província Boreal. Antes do registo do T-OAE (base da biozona de amonite *Hildaites levisoni*), a população de dinoflagelados era, em geral, abundante, mas no início deste evento observou-se uma redução acentuada da abundância e diversidade dos quistos de dinoflagelados, mas também um aumento de prasinofitas. Este estudo evidenciou que as alterações paleoambientais relacionadas com o T-OAE causaram a extinção da *Luehndea spinosa* e o desaparecimento de outras espécies de quistos de dinoflagelados, nomeadamente formas de *Nannoceratopsis* spp. Comparando e integrando estes resultados palinológicos com o registo de outros grupos fósseis, em particular do nanoplâncton, percebe-se que estes bioeventos foram causados não só pela anóxia, mas também pelo aumento abrupto da temperatura e redução da salinidade das águas oceânicas. Este cenário, que na generalidade é similar aos de outras bacias Europeias, indica que a anóxia terá ocorrido não só no fundo marinho mas também ao longo da coluna de água. A localização relativamente confinada da Bacia Lusitânica, no enquadramento paleogeofráfico do Toarciano, pode ser um dos fcatores para explicar o longo período de recuperação da população de dinoflagelados observado nesta bacia. Esta parte do trabalho relaciona-se com os objectivos propostos de ii) a vi), referentes ao Jurássico Inferior.

O estudo dos cortes de S. Pedro de Moel, Brenha, Peniche, Fonte Coberta, Maria Pares e Vale das Fontes, que constituem a sucessão entre o Sinemuriano superior e o Toarciano superior, permitiu estabelecer um quadro palinoestratigráfico do Jurássico Inferior da Bacia Lusitânica. Não foram encontrados taxa de quistos de dinoflagelados no Sinemuriano superior de S. Pedro de Moel. No entanto, a associação de quistos de dinoflagelados identificados nas amostras do Pliensbaquiano e Toarciano, composta por *Luehndea spinosa*, *Mancodinium semitabulatum*, *Mendicodinium microscabratum*, *Nannoceratopsis gracilis*, *Nannoceratopsis senex* e *Scriniocassis priscus*, revela-se bioestratigraficamente importante. Destaca-se a *Luehndea spinosa*, espécie marcadora do intervalo entre o Pliensbaquiano superior e Toarciano inferior. Foram definidas as biozonas de quistos de dinoflagelados *Luehndea spinosa* e *Mendicodinium microscabratum*, ambas sendo compostas por duas sub-biozonas. Assim, atingem-se os pontos descritos de i) a iii) para o Jurássico Inferior.

A palinoestratigrafia do Jurássico Médio (Aaleniano–Batoniano inferior) foi estudada nos cortes de S. Gião e Cabo Mondego e foi reconhecido o intervalo entre as biozonas de amonites *Pleydellia aalensis* a *Zigzagiceras zigzag*. A sucessão do Toarciano superior–Aaleniano inferior em S. Gião revelou-se palinologicamente pouco produtiva. Contudo, nas amostras do afloramento do Cabo Mondego foram observados taxa de quistos de dinoflagelados característicos do Jurássico Médio, em especial a partir do Bajociano inferior (biozona de amonite *Witchellia laeviuscula*), em que ocorre um aumento da abundância e diversidade deste grupo. Ainda assim, a associação identificada neste estudo da Bacia Lusitânica possui pouca riqueza, quando comparada com outras no norte e este da Europa e Ártico. Este facto pode estar relacionado com a posição paleogeografica isolada da Bacia Lusitânica durante o Jurássico Médio. Os restantes taxa identificados neste estudo, em especial do grupo dos esporos e pólens, estão de acordo com as associações definidas noutras bacias do Jurássico. Em geral, os palinomorfos continentais possuem intervalos mais longos quando comparados com os quistos de dinoflagelados e, por isso, menos úteis do ponto de vista bioestratigráfico. No entanto, destaca-se o registo do esporo *Kraeuselisporites reissingeri* e dos pólens *Araucariacites australis*, *Classopollis* spp. e *Callialasporites* spp. Desta forma cumprem-se os propósitos acima enunciados de i) a vi) para o Jurássico Médio (Aaleniano–Batoniano inferior).

O Jurássico Inferior e Médio da Bacia Lusitânica foi também investigado, de forma genérica, sobre os níveis de maturação orgânica. Para este efeito foram analisadas

39 amostras, compreendidas entre o Sinemuriano superior e o Caloviano superior, em microscopia de fluorescência ultra-violeta e determinação da cor dos esporos e pólens (TAI - Thermal Alteration Index). Os resultados sugerem que a maioria das amostras enquadra-se na fase de produção de petróleo líquido enquanto que, o intervalo compreendido entre o Pliensbaquiano superior e Toarciano inferior encontra-se na fase imatura. Por estas técnicas serem muito subjetivas, para um estudo mais aprofundado é necessário complementar este trabalho com outras metodologias mais precisas, como por exemplo o poder reflector da vitrinite.

Em conclusão, neste trabalho está descrito e discutido em detalhe o estudo palinológico do Jurássico Inferior e Médio da Bacia Lusitânica, onde estão também estabelecidas análises bioestratigráficas e paleoambientais com base, maioritariamente, no registo dos quistos de dinoflagelados. Foram estabelecidas correlações com outros grupos grupos fósseis e bacias da mesma idade e, assim, com este estudo acrescentam-se informações na investigação da paleoceanografia e paleogeografia do Jurássico. Os objetivos inicialmente propostos foram atingidos na totalidade, embora se ressalve a impossibilidade do estudo palinoestratigráfico detalhado do Batoniano médio e superior e do Caloviano, por falta de controlo bioestratigráfico. Espera-se que este projeto seja um contributo significativo para o conhecimento da Bacia Lusitânica, em particular para a estratigrafia, e que os resultados aqui obtidos sejam uma ferramenta útil em futuras estratégias relacionadas com atividadades geológicas de importância no desenvolvimento económico do país, nomeadamente na prospecção de hidrocarbonetos.

Palavras-chave

Bacia Lusitânica; Bioestratigrafia; Evento Anóxico Oceânico do Toarciano; Jurássico; Palinologia; Quistos de dinoflagelados.

Contents

List of Figures

List of Plates

List of Tables

Supplement B - Digital Supplementary Data

Table S6. The palynomorph assemblages from the upper Pliensbachian succession of the Fonte Coberta section (five samples, numbered FC1 to FC5), subdivided into six groups. The numbers in the cells represent percentages of the specified taxon within the overall palynoflora; blank spaces indicate the absence of the respective form.

Table S7. The palynomorph assemblages from the Cabo Mondego section subdivided into six groups. The numbers in the cells represent percentages of the specified taxon within the overall palynoflora; blank spaces indicate the absence of the respective form and the asterisked numbers correspond to barren samples.

Table S8. The palynomorph assemblages from the São Gião succession subdivided into six groups. The numbers in the cells represent percentages of the specified taxon within the overall palynoflora; blank spaces indicate the absence of the respective form and the asterisked numbers correspond to barren samples.

Table S9. List of the 15 extra samples from the middle Jurassic (?middle Bathonian–upper Callovian) of Cabo Mondego studied for microscopy and TAI (Chapter V).

List of acronyms and abbreviations

AB: Ammonite Biozone
AOM: Amorphous Organic Matter
ASSP: Auxiliary Stratotype Section and Point
CIA: Colour Image Analyses
GSSP: Global boundary Stratotype Section and Point
HEC: Hydroxyethylcellulose
member LML: Lumpy Marls and Limestones
member MLLF: Marly Limestones with *Leptaena* Facies
member MLOF: Marly Limestones with Organic Facies
member MLUP: Marls and Limestones with *Uptonia* and *Pentacrinus*
member MMLHH: Marls and Marly Limestones with *Hildaites* and *Hildoceras*
member MMLSB: Marls and Marly Limestones with Sponge Bioconstructions
member PPL: Praia Pedra Lisa
member TNL: Thin Nodular Limestones
members CC1–CC5: Cabo Carvoeiro 1–5
RGB: Red Green Blue
SCI: Spore Colour Index
SCI: Spore Colour Index
Section Br: Brenha
Section CM: Cabo Mondego
Section FC: Fonte Coberta
Section MP: Maria Pares
Section P: Peniche
Section PM: S. Pedro de Moel
Section SG: São Gião
Section VF: Vale das Fontes
TAI: Thermal Alteration Index
T-OAE: Toarcian Oceanic Anoxic Event
UV: Ultraviolet rays
D.p.: Dactylioceras polymorphum
E.e.: Emaciaticeras emaciatum
H.l.: *Hildaites levisoni*

CHAPTER I

General introduction

Chapter I cover:

Peniche section, Lower Jurassic

Chapter I. General introduction

1. Structure of the thesis

The present PhD thesis is based on four papers in indexed journals. Three papers are published and available online and the other is submitted. Additionally, a fifth paper is in preparation. Those papers are listed and numbered as below:

Paper 1

Correia, V.F., Riding, J.B., Fernandes, P., Duarte, L.V., Pereira, Z. 2017a. The palynology of the lower and middle Toarcian (Lower Jurassic) in the northern Lusitanian Basin, western Portugal. *Review of Palaeobotany and Palynology* 237, 75–95. http://dx.doi.org/10.1016/j.revpalbo.2016.11.008

Paper 2

Correia, V.F., Riding, J.B., Duarte, L.V., Fernandes, P., Pereira, Z. 2017b. The palynological response to the Toarcian Oceanic Anoxic Event (Early Jurassic) at Peniche, Lusitanian Basin, western Portugal. *Marine Micropaleontology* 137, 46-63. http://dx.doi.org/10.1016/j.marmicro.2017.10.004

Paper 3

Correia, V.F., Riding, J.B., Duarte, L.V., Fernandes, P., Pereira, Z. 2018. The Early Jurassic palynostratigraphy of the Lusitanian Basin, western Portugal. *Geobios*, in press. https://doi.org/10.1016/j.geobios.2018.03.001

Paper 4

Correia, V.F., Riding, J.B., Henriques, M.H., Fernandes, P., Pereira, Z. Wiggan, N. J. The Middle Jurassic palynostratigraphy of the northern Lusitanian Basin, Portugal**.** *Newsletters on Stratigraphy*, submitted.

Paper 5

Correia, V.F., Fernandes, P., Riding, J.B., Pereira, Z. The value of fluorescence microscopy in routine source-rock analysis: Lower-Middle Jurassic successions from the Lusitanian Basin, Portugal (in preparation).

In Chapter I, in addition to the presentation of the thesis structure, several important subjects which give better comprehension of the theme studied and discussed in this PhD work are also briefly introduced, such as the motivation that led us to initiate this project, as well the main objectives. A general introduction to the basic dinoflagellate aspects, sampling field trips and laboratory and office methodologies are also described in this chapter.

Chapter II is especially dedicated to the palaeoecological effects of the Toarcian Oceanic Anoxic Event (T-OAE) on marine palynomorphs in Lusitanian Basin, focusing the dinoflagellate response, as a major component of microplankton. These local data are compared with coeval Toarcian basins and palaeobiological interpretations are discussed in the European context. The Lower Jurassic dinoflagellate cyst provincialism of the northern hemisphere is also analysed. For simplify the presentation of this study and to avoid repeated ideas, this chapter is a composite work from papers 1 and 2. In paper 1 the palynological records from Maria Pares and Vale das Fontes sections (northern Lusitanian Basin) are presented, and the Peniche results are described and discussed in paper 2. These papers 1 and 2 are are available on Supplement A, of the Digital Supplementary Data.

The Lower Jurassic palynostratigraphy, mainly based on dinoflagellate cysts bioevents, is presented and associated to coeval European basins in Chapter III. This chapter is adapted from paper 3. The biostratigraphical information of Chapter II are also integrated here (but not pictured) and quoted as “Correia et al. (2017a,b), corresponding to papers 1 and 2, respectively. Chapter IV reports the Aalenian to lower Bathonian (Middle Jurassic) palynological data, in a biostratigraphical perspective. This chapter is based on paper 4 (submitted).

In Chapter V the qualitative fluorescence results, complemented with spores and pollen colour analyses - Thermal Alteration Index (TAI) are illustrated, from the palynomorphs of the Lusitanian Basin, comprising the entire Lower and Middle Jurassic succession, allowing vertical and lateral comparisons. Are discussed, several methodological aspects of this tool in source-rocks analyses, as well its advantages and limitations. A fifth manuscript (paper 5) is being prepared with the information outlined in this chapter.

The overall and most significant conclusions of this PhD study are summarised in Chapter VI. Here is also evaluated the contribution of this work to scientific background and geological applications in Lusitanian Basin. In this chapter, some ideas

are advanced for future palynological studies to be developed in the Lusitanian Basin and in other Basins. In digital format, Supplements A–C within the folder Digital Supplementary Data are provided. Supplement A contains copies of the published papers 1, 2 and 3. In Supplement B are the Excel files with Tables S1–9 corresponding to the overall palynological data (in percentages) of the eight sections studied in detail (qualitative and semi-quantitative). In Table S9 are listed 15 extra samples from ?middle Bathonian and Callovian, that were collected for the fluorescence microscopical analyses (Chapter V). Preliminary qualitative results from these samples were presented as a poster in the 50th Annual Meeting of the AASP – The Palynological Society, at Nottingham (Keyworth, British Geological Survey), 3–7 of September 2017, and the pdf with this contribution, out of this PhD project, is within the Supplement C.

2. State of the art and scientific problem

The Lusitanian Basin is a Mesozoic sedimentary basin that developed in the western Iberian Margin. Its origin and evolution are related to the successive rifting phases of Pangaea that led to the opening of the North Atlantic Ocean during the Middle?–Upper Triassic to uppermost part of Lower Cretaceous interval. Changes in sedimentary facies and the thicknesses of the Mesozoic have allowed the division of the Lusitanian Basin into three different sub-basins separated by major regional faults (Fig. 1.1; Kullberg et al., 2013). The first of these is the Septentrional sector which is bounded to the south by the Nazaré Fault. The Central sector is bounded by the Nazaré Fault to the north and the Arrife Baixo–Vale Inferior Tejo fault system to the south. Finally the Meridional sector is developed to south through the Torres Vedras-Montejunto fault. The Lusitanian Basin successions also extend offshore where they are recognised in seismic surveys and in numerous exploration wells. Four successive rifting phases occurred before the formation of the first oceanic crust in the Aptian. The stratigraphy of the Lusitanian Basin reflects these four rifting phases, forming four main sedimentary cycles of Triassic-Sinemurian, Pliensbachian-Oxfordian, Kimmeridgian-early Berriasian and late Berriasian-late Aptian age. The first cycle records the evolution from alluvial environments to lacustrine (evaporites) and shallow marine carbonate environments. The second cycle consists entirely of marine carbonates. The third records the evolution from marine carbonates to deltaic and alluvial environments, and the fourth cycle records a mix of shallow marine carbonates and clastic littoral-lacustrine environments. These sedimentary cycles are bounded by disconformities or

angular unconformities that are related to tectonics and/or sea level changes (Kullberg et al., 2013).

The previous extensive research on the stratigraphy and biostratigraphy of the Lusitanian Basin are summarized in Azerêdo et al. (2003), Rey et al. (2006), Reis et al. (2010) and Kullberg et al. (2013). The biostratigraphy of the Lusitanian Basin is based mainly on macrofossils (ammonites, brachiopods and corals) and microfossils (foraminifera, nannofossils and ostracods). Compared to these works, palynological studies are scarce in the Lusitanian Basin. Cretaceous palynomorphs have received more attention (Trincão 1990, Heimhofer et al. 2007, 2012, Mendes et al. 2011), due mainly to the first appearance of angiosperm pollen. Previous studies on the Jurassic palynology of the Lusitanian Basin are those by Davies (1985), Mohr and Schmidt (1988), van Erve and Mohr (1988), Smelror et al. (1991), Bucefalo Palliani and Riding (1999a; 2003), Barrón and Azerêdo (2003), Oliveira et al. (2007a) and Barrón et al. (2013). Only Davies (1985) and Bucefalo Palliani and Riding (1999a; 2003) discusses dinoflagellate cysts, but not in detail; the others describe spores, pollen and acritarchs.

Therefore, there is no detailed work on the Jurassic dinoflagellate cysts of the Lusitanian Basin. Dinoflagellate cysts are a powerful biostratigraphical and paleoenvironmental tool (e.g. Riding et al., 1999; 2013; Castro, 2006; Borges et al., 2011; 2012; Hssaida et al., 2014; Wiggan et al., 2017) and their study is presented as major contribution for the Lusitanian Basin background. Consequently, this PhD project was motivated with the goal to establish the research of the palynological assemblages, especially centred on dinoflagellate cysts, from the Jurassic (principally Lower and Middle) of the Lusitanian Basin. The base of this work will also contribute for the improvement of paleoenvironmental knowledge of the Jurassic period, particularly in the Lusitanian Basin, and to present a biostratigraphical framework based on dinoflagellate cysts for the most important geological units of the Lusitanian Basin. The use of this fossil group to determine the rock age is very important for hydrocarbon exploration, where the determination of subsurface geology is made by using boreholes.

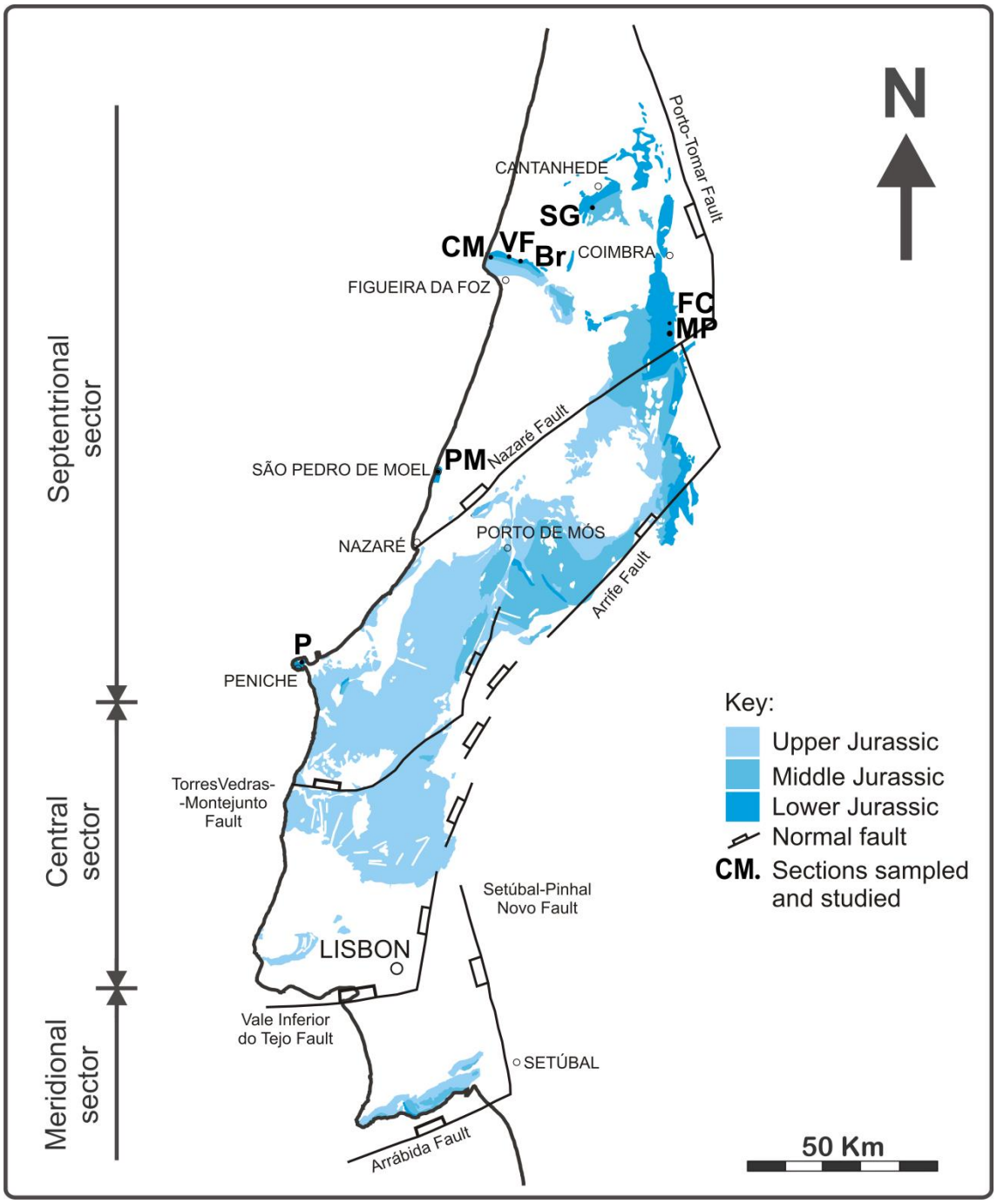

Figure 1.1. The geographic and geological setting of the Lusitanian Basin of western-central Portugal (adapted from Figueiredo, 2009 and Kullberg et al., 2013). The eight sections sampled and studied in this PhD project are indicated by the abreviations: **MP** = Maria Pares (40° 3' 10"N; 8° 27' 25"W); **FC** = Fonte Coberta (40° 3' 44"N; 8° 27' 31"W); **Br** = Brenha (40° 11' 49"N; 8° 49' 55"W); **VF** = Vale das Fontes (40° 12' 10"N; 8° 51' 31"W); **SG** = São Gião (40°18' 12.63" N; 8°37'17.58"W); **CB** = Cabo Mondego (40°12'1.26" N; 8°54'10.4"W); **PM** = São Pedro de Moel (39° 43' 18"N; 9° 02' 56"W); **P** = Peniche (39° 22' 15"N; 9° 23' 07"W).

3. Objectives

The objectives of this research project were to:

i. Establish the Jurassic dinoflagellate cyst palynostratigraphy of the Lusitanian Basin and propose a biozonal scheme based on dinoflagellate cysts. This may help in future conventional and non-conventional hydrocarbon exploration or exploitation of the onshore and offshore Lusitanian Basin.
ii. Investigate the similarities and differences in the dinoflagellate cyst assemblages between the Lusitanian Basin and the associations described elsewhere in Portugal (i.e. the Algarve Basin), Europe, Australia or America and formulate explanations for any differences that were observed;
iii. Establish biozonal correlations between the dinoflagellate cyst biostratigraphy and the biostratigraphy based on other fossil groups (e.g. ammonites, foraminifera, nannofossils);
iv. Study the palaeobiology/palaeoecology and high resolution palynostratigraphy based on dinoflagellate cysts of important stratigraphical sections that record Jurassic key events. These are the Toarcian Oceanic Anoxic Event (T-OAE), the Global boundary Stratotype Section and Points (GSSPs) for the Toarcian Stage at Peniche and the Bajocian Stage at Murtinheira, Cabo Mondego and the Auxiliary Stratotype Section and Point (ASSP) for the Bathonian stage at Cabo Mondego. The dinoflagellate cyst associations of these important sections will help in the establishment of characteristic assemblages or biozones indicative of these stages and contribute for the palaeoenvironmental characterization of the Lusitanian Basin during these Jurassic events.
v. Investigate to what extent the Lusitanian Basin acted as a 'bridge' between the North European Boreal and the South European Tethyan realms, based on the distribution of dinoflagellate cyst taxa;
vi. Improve the Jurassic palaeoceanography and palaeogeography of the Lusitanian Basin in relation to the initial phases of the opening of the North Atlantic Ocean;

4. Sampling field trips

To achieve the goals of this project, four sampling campaigns were outlined. Eight outcrops were selected to be sampled (Fig. 1.1) considering the following aspects: the most representative lithostratigraphical Jurassic sections of the Lusitanian Basin and

their national and international scientific relevance (e.g. the GSSPs); the lithological type of each section, as the more suitable lithologies for palynological studies include mudrocks, especially marls and marly limestones; previous biostratigraphical studies of each section, i.e., to achieve an accurate and useful palynostratigraphical scheme, was took in account the boundaries between the biozones defined by other fossil groups, particularly ammonites, but also foraminifera and nannofossils. In most of the sampled outcrops, the stratigraphical positions of the samples were delineated on the lithological logs of that sections studied earlier by others. These four sampling field trips took place in the Lusitanian Basin during the first three years (2014–2016) of this PhD project, in which two were dedicated to Lower Jurassic, and the other two to Middle Jurassic. The Table 1.1 referes all the sampled successions, their chronology and lithostratigraphy, as well the number of samples collected per section. An overview of the sampled lithostratigraphical units of the Lusitanian Basin is pictured in Fig. 1.2. Nevertheless, the lithology, cronostratigraphy and lithostratigraphic units of all studied sections are described in detail in the following Chapters II, III and IV.

In the first campaign the Lower Jurassic of the northern Lusitanian Basin was visited and the Maria Pares (Fig. 1.3), Vale das Fontes (Fig. 1.4) and Brenha (Fig. 1.5) sections were sampled. The samples from S. Pedro de Moel and Fonte Coberta sections (Fig. 1.1) were collected at the rock repository of Coimbra University. In the second field trip we sampled the Peniche section at Ponta do Trovão (Fig. 1.6). The Middle Jurassic (lower Aalenian– lower Bajocian) was sampled at the outcrops of São Gião (Fig. 1.7) and Cabo Mondego, at Murtinheira beach (includes the Bajocian GSSP) (Fig. 1.8) during the third campaign. The Bathonian ASSP succession at Cabo Mondego (Fig. 1.9) was visited during the fourth sampling campaign. There are no comprehensive biostratigraphical studies on the remaining Bathonian and Callovian of the Cabo Mondego succession. For that reason, this part of the outcrop was not sampled in detail. However, 15 extra samples (Table S9) were collected from the ?middle Bathonian to upper Callovian strata for the work on the palynomorphs fluorescence (Chapter V), in order to have data encompassing the entire Lower and Middle Jurassic stratigraphical column. In total, 358 samples were collected (Table 1.1).

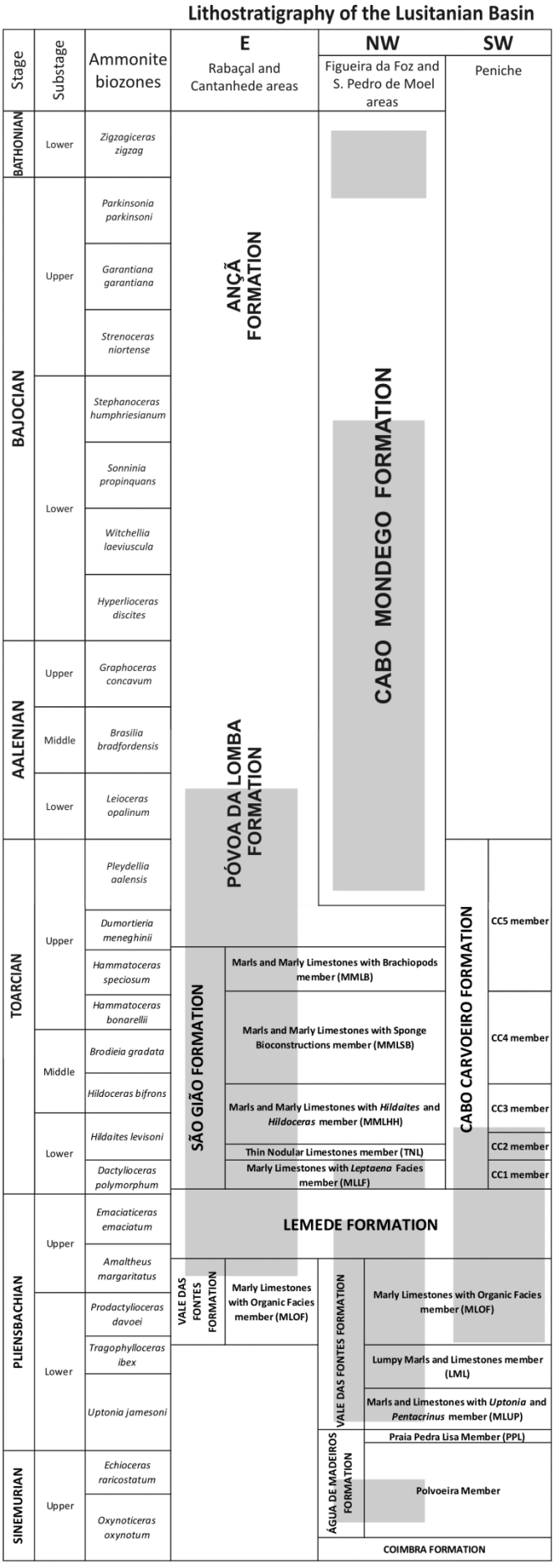

Figure 1.2. Summary of the ammonite biostratigraphy and lithostratigraphy of the Lower and Middle Jurassic (upper Sinemurian to lower Bathonian) of the eastern and western sectors of the Lusitanian Basin, central-western Portugal, based on Duarte and Soares (2002), Azerêdo et al. (2003), Duarte (2007) and Duarte et al. (2014a,b). The grey shading indicates the lithostratigraphical units sampled and studied in detail in the present PhD project.

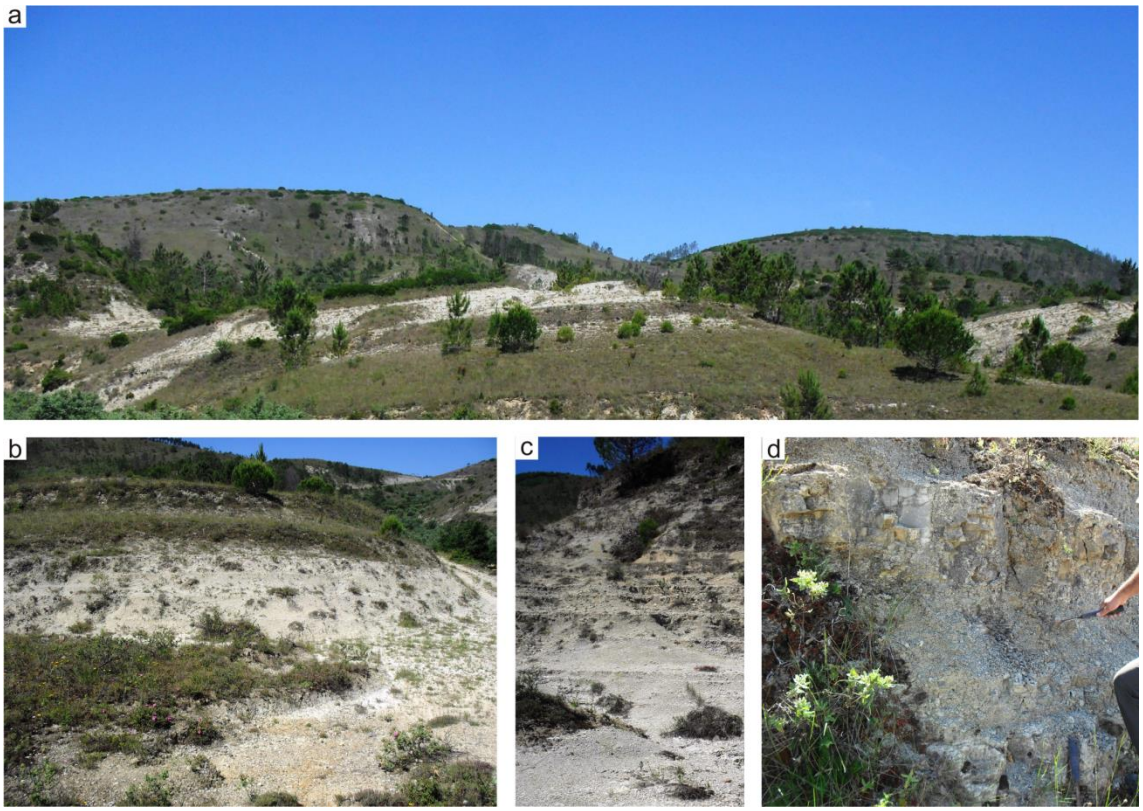

Figure 1.3. Maria Pares section: panoramic view of the outcrop (a); general aspect of the sampled area, corresponding to the MLLF, TNL (b) and MMLHH members (c); detail of limestones– marls alternation at the MMLSB member in which the sample PZ56 was collected (d).

Figure 1.4. Vale das Fontes section: general view of the sampled outcrop (a); note the greyish colour of the marls within the MLLF member (b, c), compared with the brownish aspect of the TNL member (d), properly called Chocolate Marls (corresponding to the sample PVF14).

Figure 1.5. Brenha section: general view of the sampled outcrop corresponding to the Vale das Fontes Formation(a); aspect of the LML member (b) and detail of a dark marl (corresponding to the sample Br19) collected within the MLOF member (c); general view of the Lemede Formation at Brenha.

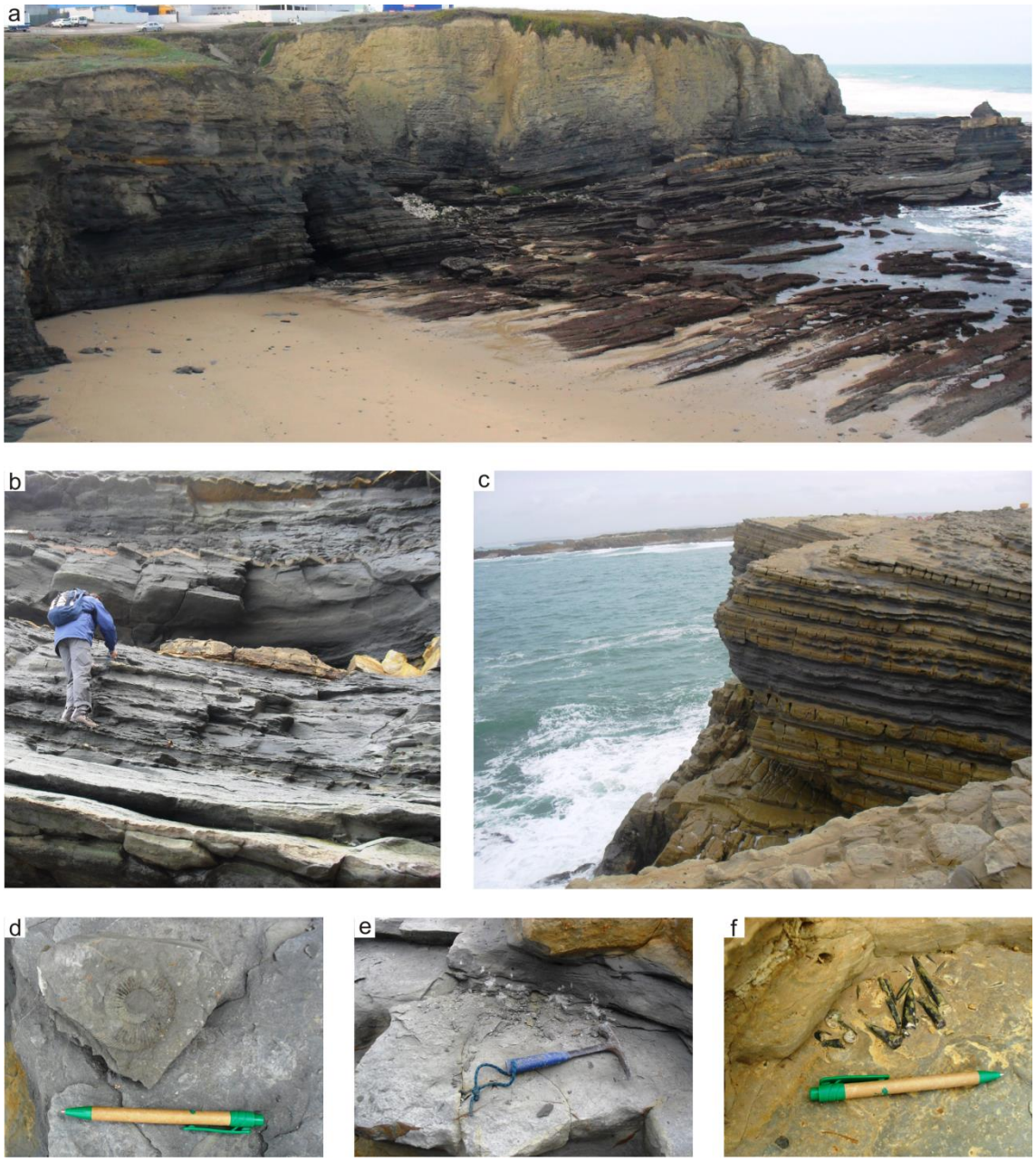

Figure 1.6. Peniche section: panoramic view of the Toarcian part/Cabo Carvoeiro Formation (a); aspect during the sampling of the CC2 member (b); view of part of the Pliensbachian strata (c); ammonoide within the CC1 member/*Dactylioceras polymorphum* AB (d); sampling of the Pliensbachian–Toarcian transition (e); belemnite agglomerate in the Lemede Formation (Pliensbachian) strata (f).

Figure 1.7. São Gião section, corresponding to Póvoa da Lomba Formation: general view of the Aalenian part of the outcrop (a); view of the Toarcian–Aalenian transition, in which the pine (near the bag) marks the boundary (b); detail of the collected marl of bed 26 (sample SG26) from the Aalenian (c).

Figure 1.8. Cabo Mondego section, corresponding to the Cabo Mondego Formation: general view of the Bajocian GSSP outcrop at the Murtinheira beach (a); detail of the Aalenian–Bajocian transition (b), in which the red circle corresponds to the Aalenian/Bajocian boundary, i.e., the Bajocian GSSP (b); detail of the Toarcian–Alenian transition sampling (c), in which the limestone bed with the number 31 (in green) is the first layer of Aalenian and was sampled the marl above 32 (sample M32); transversal view of an ammonite *Brasilia gigantea* (d). Credits of photo (a): Maria Helena Henriques.

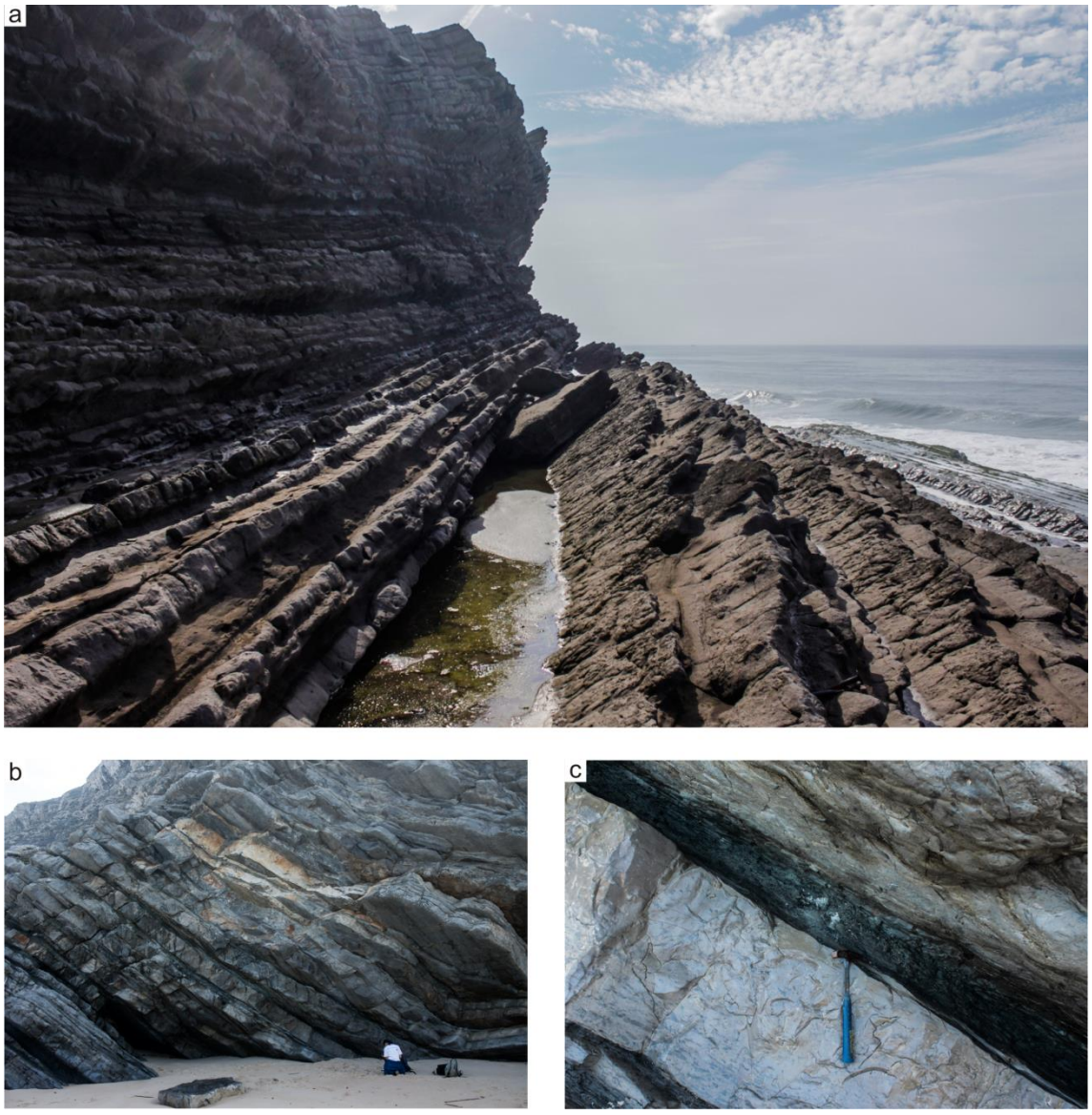

Figure 1.9. Cabo Mondego section/ Cabo Mondego Formation: general view of the Bathonian ASSP outcrop (a), in which the bed below the water, in first view, marks the base of the Bathonian; general aspects (b) and detail (c) of the lower Bajocian sampling, within the *Stephanoceras humphriesianum* AB. Credits of photos: Jorge de Carvalho.

5. Laboratory and office work

Standard palynological preparation techniques were used in order to extract the organic residues (Wood et al., 1996; Traverse, 2007; Riding and Warny 2008; see also, Castro 2006, chapter 5 and Borges 2012, chapter 3):

i. The first stage consisted in cleaning and disaggreagation of the rocks;
ii. The second task, and the most important, is the demineralization, which was the use of hydrochloric acid (HCl 33%) for removal of the carbonates, and hydrofluoric acid (HF 48%) for removal of the silicates. Heavy liquids ($ZnCl_2$ and $ZnBr_2$) to concentrate the organic particles were not used, instead we applied the "swirling" technique; the residues were not oxidised as well;
iii. The third stage was screening the residues using a 15 µm mesh sieve;
iv. The final palynomorph concentrates were stained with Safranin O. Neverthless, at least one slide of each sample was not stained, for control and for the study described in Chapter V;
v. Finally, at this stage the organic residues were ready for microscope slide preparation, and we used and the dispersant agent Hydroxyethylcellulose (HEC) and Entellan® as mounting medium. Were mounted a minimum of three slides per sample: one unstained and two stained.

This procedure was done in the palynology laboratories of CIMA, University of the Algarve, and LNEG (Portuguese Geological Survey), São Mamede Infesta-Porto, Portugal. The unused sample material, aqueous residues, microscope slides and figured specimens are curated in the collections of LNEG, São Mamede de Infesta.

In the qualitative and semi-quantitative palynological analyses was used a Bresser® microscope incorporated with a digital microcamera 5 MP. As much as possible, depending of the palynomorph preservation, all palynomorph specimens were identified at the species or genus level and separated by six groups: dinoflagellate cysts, acritarchs, prasinophytes, foraminiferal test linings, spores and pollen. In the majority of the samples, were counted at least 300 palynomorphs. However, if the material was sparse, were counted as many specimens as possible from two microscope slides. The qualitative palynomorphs fluorescence study (Chapter V) was undertaken in the University of the Algarve using an Olympus BX 51 microscope equipped with a metal halide lamp fluorescence unit XCite Series 120Q and with a violet and Blue 12 filter

block that yields awavelength band of 390 and 490 nm. In this project, in total were studied 358 samples from the Lower and Middle Jurassic of the Lusitanian Basin (Table 1.1).

Table 1.1. Overview of the chronological and lithostratigraphical units of each sampled section. It is also presented the number of collected samples per section and totals.

EPOCH	Stage	Formations	Sections	Nº collected samples
LOWER JURASSIC	Sinemurian	Água de Madeiros	S. Pedro de Moel	12
	Pliensbachian	Vale das Fontes, Lemede	Brenha	22
	Pliens.-Toarcian	Vale das Fontes, Lemede, Cabo Carvoeiro	Peniche (Toarcian GSSP)	72
	Toarcian	São Gião	Vale das Fontes	14
	Pliens.-Toarcian	Cale das Fontes, Lemede, São Gião	Rabaçal area: Maria Pares and Fonte Coberta	94
			Sub-total	214
MIDDLE JURASSIC	Aalenian	Póvoa da Lomba	São Gião	47
	Aalenian-Bajocian	Cabo Mondego	Cabo Mondego (Murtinheira, Bajocian GSSP)	68
	Bajocian-Bathonian	Cabo Mondego	Cabo Mondego (Bathonian ASSP)	14
	Bathonian, Callovian	Cabo Mondego	Cabo Mondego (extra samples)	15
			Sub-total	144
			TOTAL	**358**

6. Dinoflagellates: general aspects

Dinoflagellates are single-celled organisms that occur usually as motile cells with two flagella: the tranverse flagellum is ribbon-like with multiple waves, which encircles the cell within a transverse furrow called the cingulum; the longitudinal flagellum, is whip-like, only with one or few waves which beats posteriorly, and proximally is within a longitudinal furrow termed the sulcus (Fig. 1.10). The etymology of "Dinoflagellata" was inspired from the Greek word *dinos*, meaning "whirling rotation", and from the Latin word *flagellum*, that means "small whip" (Fensome et al., 1996).

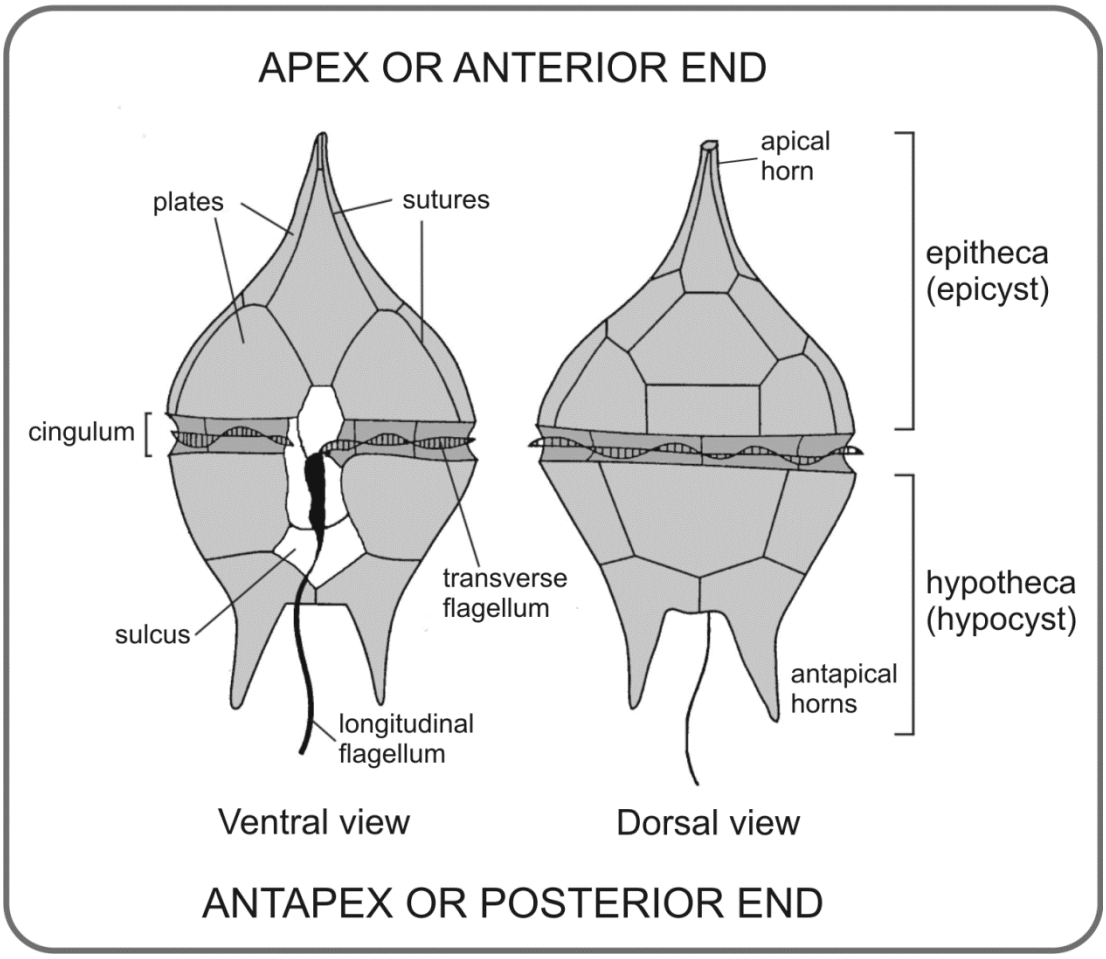

Figure 1.10. General morphology and principal terminology of a thecate motile dinoflagellate. Note that the terms "epitheca" and "hypotheca" of the living cell, are equivalent of "epicyst" and "hypocyst" of the fossil dinoflagellate, respectivally (adapted from Evitt, 1985 and Borges, 2012).

The evolutionary position of dinoflagellates was a subject of an intense discussion, considered algae or protists, but nowadays preferably called as alveolates. In terms of taxonomy, in the present time dinoflagellates are treated under the botanical nomenclature, International Code of Nomenclature for algae, fungi and plants (ICN), and this group forms the Division Dinoflagellata. The updated taxonomical table is available at the Dinoflaj2 site (http://dinoflaj.smu.ca/wiki/Master_Table). Therefore, the organisms of this division are characterized by having, at least in some stage of their life cycle, a motile stage with two dissimilar flagella and/or a special kind of nucleus, called dinokaryon, with the chromossomes constantly condensed during the mitotic cycle and with no histones.

Around 50% of living dinoflagellates are autotrophic and the others are heterotrophic or mixotrophic. Some can also be parasitic or autotrophic symbionts. Most of the living species are marine (~ 1600) but others can inhabit in freshwater environments. Dinoflagellates, together with diatoms and coccolithophores, form a major element of the marine eukaryotic phytoplankton and are significant primary produceres. The growth and distribution of dinoflagellates is influenced by several ecological factors, such as light, nutrients, salinity, ocean currents, water depth and temperature (Fensome et al., 1996).

The live cycle of dinoflagellates can involve asexual and sexual reproduction phases and is schematic summarized in Fig. 1.11: (a) during favorable environmental conditions, dinoflagellate populations can expand by binary fission, yielding successive motile and haploid schizonts generations; (b) other times the haploid cells can function as gametes and fuse to form a zygote; (c) this diploid zygote can constructs a new theca forming a motile zygote (planozygote); (d) some species, under unfavorable conditions, can form a thicker and resistant wall underneath the theca and, among other cellular changes, loose the flagella; (e) the cell becomes non-motile (hypnozygote), the theca wall (with cellulose) is destroyed by bacteria and the organic resistant cyst wall (with dinosporin) is exposed; (f) this resting cyst behaves as a sedimentary particle and following an obligatory dormancy period, when the biotic conditions are again favorable, (g) the protoplast excysts and the cycle closes with meiotic divisions, producing new haploid cells; (h) the remaning resting cysts can be geologically preserved and seems to be the origin of most fossil dinoflagellate cysts (Evitt, 1985).

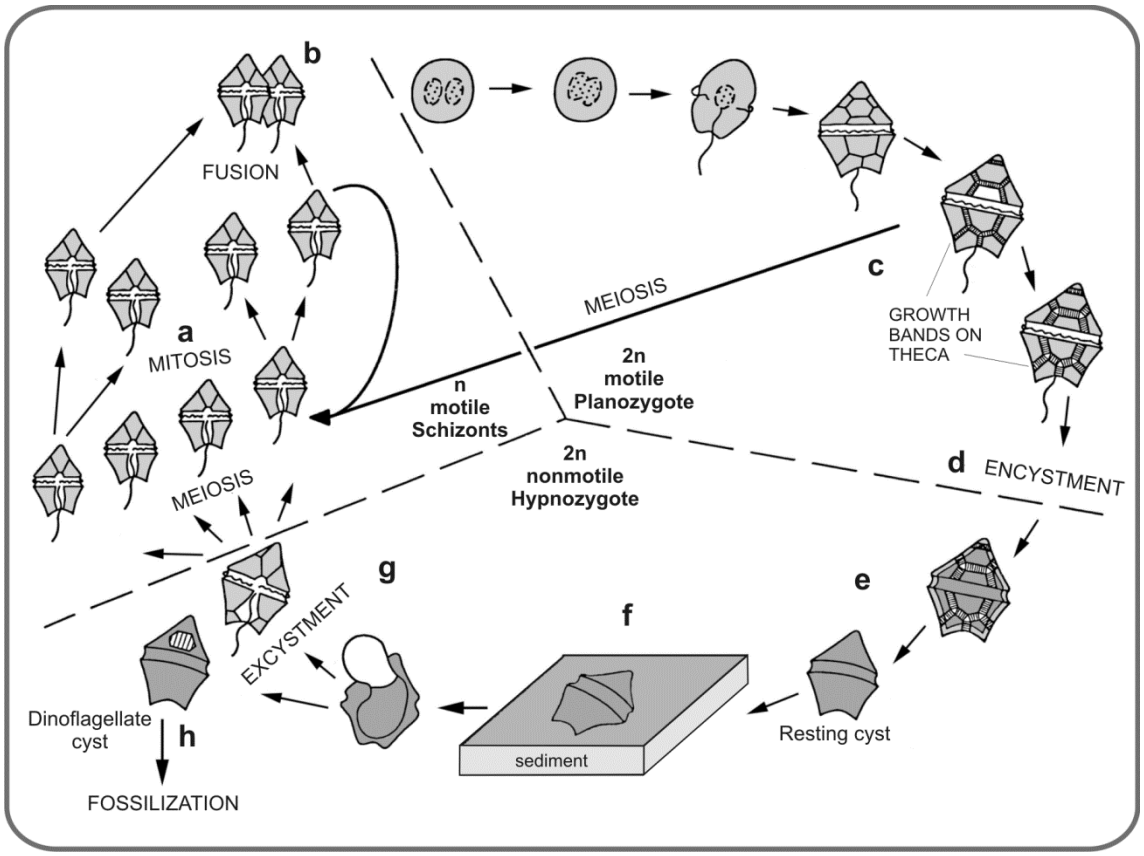

Figure 1.11. Schematic life cycle of a resting cyst–producing dinoflagellate, involving vegetative and sexual reproduction; n = haploid; 2n = diploid (adapted from Evitt, 1985 and Borges, 2012).

The resting cysts of dinoflagellates represent a rich and diverse fossil record from the Middle Triassic to the present. Although Sarjeant (1978) recognised the specimen of *Arpylorus antiquus* from Silurian of northern Africa as the oldest occurrence of a dinoflagellate cyst, this hypothesis was not accepted by the scientific community. Most dinoflagellate cysts became preserved in the fossil record because one or more layers are formed with dinosporin, a very resistant organic substance, similar to sporopollenin. For this reason, the study of dinoflagellate cysts are included in Paleopalynology, which is, according with Traverse (2007), "the study of the organic microfossils that are found in maceration preparations of sedimentary rocks." Cysts are produced inside the dinoflagellate theca. Only around 15% of the living dinoflagellate species, mostly marine, produce fossilizable cysts (Head, 1996) and it is assumed that the same percentage formed resistant organic-walled cysts in the past. These, and more aspects related with fossil dinoflagellates, are discussed in detail in Evitt (1985), Fensome et al. (1996), Castro (2006, chapter 4) and Borges (2012, Vol. II).

CHAPTER II

The palynological response to the
Toarcian Oceanic Anoxic Event

Chapter II cover:

Luehndea spinosa Morgenroth 1970. Vale das Fontes section, lower Toarcian (*Dactylioceras polymorphum* AB), sample PVF8.

Chapter II. The palynological response to the Toarcian Oceanic Anoxic Event

Adapted from the papers 1 and 2:

Correia, V.F., Riding, J.B., Fernandes, P., Duarte, L.V., Pereira, Z. 2017a. The palynology of the lower and middle Toarcian (Lower Jurassic) in the northern Lusitanian Basin, western Portugal. *Review of Palaeobotany and Palynology* 237, 75–95. http://dx.doi.org/10.1016/j.revpalbo.2016.11.008

Correia, V.F., Riding, J.B., Duarte, L.V., Fernandes, P., Pereira, Z. 2017b. The palynological response to the Toarcian Oceanic Anoxic Event (Early Jurassic) at Peniche, Lusitanian Basin, western Portugal. *Marine Micropaleontology* 137, 46-63. http://dx.doi.org/10.1016/j.marmicro.2017.10.004

Abstract

The uppermost Pliensbachian and lower Toarcian (Early Jurassic) in the Lusitanian Basin was examined for palynomorphs. Three successions were sampled for this purpose: Maria Pares, Vale das Fontes and Peniche, the Toarcian Global boundary Stratotype Section and Point (GSSP). In total, 103 samples were studied. The material spans the *Emaciaticeras emaciatum* (uppermost Pliensbachian), *Dactylioceras polymorphum*, *Hildaites levisoni* and *Hildoceras bifrons* ammonite biozones (ABs). Dinoflagellate cysts, acritarchs, prasinophytes, foraminiferal test linings and terrestrial palynomorphs were documented. A low diversity dinoflagellate cyst flora, typical of the Sub-Boreal Realm, was recovered from the *Emaciaticeras emaciatum* and *Dactylioceras polymorphum* ABs. The dominant element is the cold water species *Luehndea spinosa*, which is an index for the Pliensbachian to earliest Toarcian, and is thought to have migrated from the more northerly Boreal Realm. Prior to the Toarcian Oceanic Anoxic Event (T-OAE), dinoflagellates thrived in the Lusitanian Basin, except during a brief warm period in the earliest Toarcian. Despite the latter, the recovery from this event was relatively rapid and was characterised by a return to relatively cool temperatures. The *Hildaites levisoni* AB represents the T-OAE and the overlying strata, and is characterised by a profound reduction in dinoflagellate cyst relative abundances.

This dinoflagellate cyst 'blackout', and the associated rise of prasinophytes, reflects significant environmental stress, such as marine anoxia, elevated temperatures and reduced salinity, with the former two probably being most important. The low proportions of dinoflagellate cysts following the T-OAE indicates a protracted recovery phase from the bottom and water column anoxia developed throughout the Lusitanian Basin.

Keywords

Dinoflagellate cysts; Palaeobiology; Palynomorphs; Toarcian Oceanic Anoxic Event (T-OAE); Lusitanian Basin, Portugal.

1. Introduction

This study is a documentation of the palynology of the uppermost Pliensbachian and lower Toarcian (Lower Jurassic) strata at Maria Pares, Vale das Fontes and Peniche sections in the Lusitanian Basin, western Portugal. The principal aim was to investigate the response of marine microplankton to the Toarcian Oceanic Anoxic Event (T-OAE).

The Vale das Fontes and Maria Pares sections are located between Figueira da Foz and Rabaçal in the northern Lusitanian Basin (Fig. 2.1). The Peniche section is located at Ponta do Trovão, on a peninsula close to Peniche city (Fig. 2.1). An exceptionally expanded, well exposed and well preserved Pliensbachian-Toarcian transition is part of this coastal succession, which was chosen as the Global boundary Stratotype Section and Point (GSSP) for the Toarcian Stage (Elmi, 2006; Rocha et al., 2016). The Pliensbachian-Toarcian boundary is primarily based on a relative abundance of the ammonite *Dactylioceras* and secondarily on the inceptions of several calcareous nannofossils. These bioevents define the base of Toarcian Stage at the base of Bed 15e (Rocha et al., 2016).

Previous studies on the Jurassic palynology of the Lusitanian Basin are those by Davies (1985), Mohr and Schmidt (1988), van Erve and Mohr (1988), Smelror et al. (1991), Bucefalo Palliani and Riding (1999a; 2003), Barrón and Azerêdo (2003), Oliveira et al. (2007a) and Barrón et al. (2013). Only three of these publications included material from the Toarcian (Davies, 1985; Oliveira et al., 2007a; Barrón et al. 2013), and even in these dinoflagellate cysts were not discussed in detail. Davies (1985) is a purely biostratigraphical study, and Oliveira et al. (2007a) and Barrón et al. (2013)

mainly discussed pollen and spores. Pliensbachian and Toarcian calcareous nannofossils of the Peniche section were studied by Perilli & Duarte (2006), Oliveira et al. (2007a), Mattiolli et al. (2008, 2013) and Reggiani et al. (2010).

These three sections include one of the major Phanerozoic environmental perturbations, the T-OAE. This was the earliest of the major Mesozoic-Cenozoic oceanic anoxic events (Jenkyns, 2010). The T-OAE is global and caused marine extinction and stratification, anoxia, and a rapid increase in seawater temperatures at ~182 Ma (e.g. Harries and Little, 1999; Cohen et al., 2007; Suan et al., 2008a, b; 2010; 2011; Al-Suwaidi et al., 2010; 2016; Gómez and Arias, 2010; Izumi et al., 2012; Danise et al., 2013; Xu et al, 2017). This event is characterised by a negative carbon isotope excursion ($\delta^{13}C$), recorded in marine carbonates and sedimentary organic matter. This characteristic geochemical signal has been confidently recognised in the Lusitanian Basin (Duarte et al., 2004, 2007; Hesselbo et al., 2007; Suan et al., 2008a; Pittet et al., 2014). The T-OAE may have been caused by a massive carbon injection into the atmosphere from oceanic gas hydrates, and/or methane release from sedimentary rocks due to intrusive volcanism (Hesselbo et al., 2000; Kemp et al., 2005; McElwain et al., 2005; Svensen et al., 2007; Hesselbo and Pieńkowski, 2011; van de Schootbrugge et al., 2013). It may have been terminated by fire-feedbacks to atmospheric oxygen concentrations (Baker et al., 2017). The more recent Paleocene-Eocene Thermal Maximum (PETM, ~56 Ma) was also a short-lived interval of elevated temperatures caused by an injection of greenhouse gases into the atmosphere. However, the PETM only caused relatively minor and localised marine anoxia in comparison to the T-OAE (Cohen et al., 2007; Kender et al., 2012).

The distribution and growth of dinoflagellates, which are planktonic organisms, are influenced by factors such as light, nutrients, ocean currents, oxygen levels, salinity, temperature and water depth (Taylor and Pollingher, 1987; Dale, 1996). Toarcian marine plankton populations would therefore have been significantly affected by the T-OAE. Hence, research on Toarcian dinoflagellate cysts and other marine microplankton will help the understanding of this major environmental perturbation (e.g. Prauss, 1996; Prauss et al., 1991; Bucefalo Palliani et al., 2002).

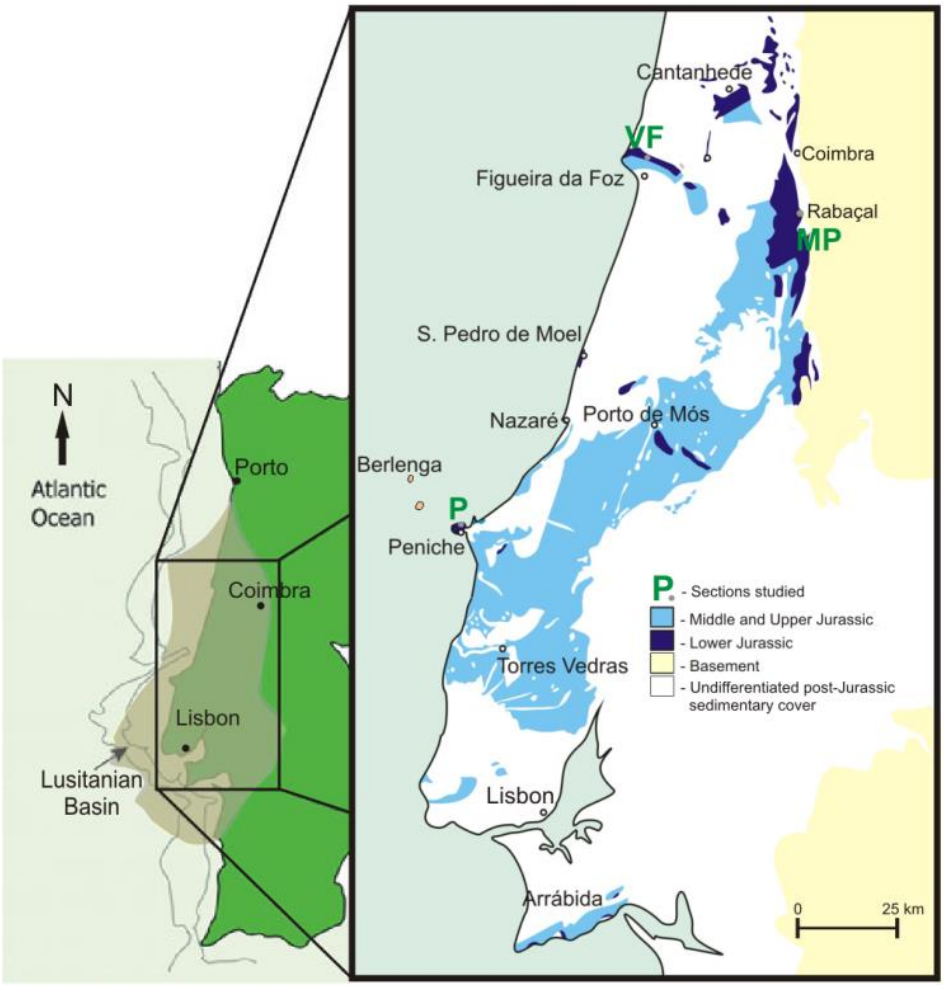

Figure 2.1. The location and geological setting of the Lusitanian Basin of western Portugal (adapted from Duarte et al., 2010). The coordinates of the Maria Pares section(MP), close to Zambujal village in the Rabaçal area are 40°3'10''N, 8°27'25''W; the Vale das Fontes section (VF) in the Figueira da Foz area are 40°12'10''N, 8°51'31''W; and the Peniche section (P), which is the Toarcian GSSP near to Peniche city, are 39°22'15''N, 9°23'07''W.

2. Geological background

The Lusitanian Basin is a major marine depocentre on the Atlantic coastal margin in western central Portugal (Fig. 2.1). This basin is oriented NE-SW, and is 300 km in length and 150 km wide. The depocentre is filled by a maximum thickness of 5 km of Mesozoic (Middle?–Upper Triassic to uppermost part of Lower Cretaceous) strata, but most of the succession is Jurassic (Rasmussen et al., 1998; Kullberg et al., 2013). Its initiation and evolution were associated with the fragmentation of Pangaea during the opening of the North Atlantic.

The Lower and Middle Jurassic ammonite faunas of the Lusitanian Basin are indicative of a Sub-Boreal (Atlantic) affinity (Mouterde et al., 1979). However,

occasional diverse and mixed ammonite associations are suggestive of sporadic communication between the Boreal and Tethyan Realms (Terrinha et al., 2002). The earliest Toarcian *Dactylioceras polymorphum* AB of the Tethyan region is broadly coeval with the *Dactylioceras tenuicostatum* AB in the Sub-Boreal and Sub-Mediterranean provinces. Succeeding the Tethyan *Dactylioceras polymorphum* AB, the *Hildaites levisoni* AB is equivalent to the *Harpoceras serpentinum* AB of the Sub-Mediterranean and Sub-Boreal provinces (Fig. 2.2; Elmi et al., 1989; Page, 2003; Simms et al., 2004).

Substage	Ammonite Provinces		
	Tethyan	**Sub-Mediterranean**	**Sub-Boreal**
Middle Toarcian	*Hildoceras bifrons*	*Hildoceras bifrons*	*Hildoceras bifrons*
Lower Toarcian	*Hildaites levisoni*	*Harpoceras serpentinum*	*Harpoceras falciferum*
	Dactylioceras polymorphum	*Dactylioceras tenuicostatum*	*Dactylioceras tenuicostatum*

Figure 2.2. Correlation of the lower Toarcian ABs in the Tethyan, Sub-Mediterranean and Sub-Boreal provinces, adapted from Page (2003).

Most of the Toarcian of the northern and central Lusitanian Basin comprises the São Gião Formation, which is included in the oldest first order sedimentary cycle (Soares et al., 1993; Azerêdo et al., 2003, 2014), mainly composed of fossiliferous marl-limestone alternations (Duarte, 1997, 2007; Duarte et al., 2001; Comas-Rengifo et al., 2013; Reolid and Duarte, 2014). This unit is subdivided into five members and spans the *Dactylioceras polymorphum* to the lowermost *Dumortieria meneghinni* ABs (Fig. 2.3; Duarte and Soares, 2002; Duarte, 2007). The type section of the São Gião Formation is within the Maria Pares succession in the Coimbra-Rabaçal region, located in the northern part of the Lusitanian Basin (Fig. 2.1). This section exposes a continuous upper Plienbachian–Aalenian succession with ammonite faunas throughout (Mouterde et al., 1964-65; Henriques, 1992; 1995). Although the Pliensbachian to Toarcian sections of the Lusitanian Basin are dominated by hemipelagic deposits (e.g. Duarte et al., 2001, 2010; Duarte, 2007), the lower Toarcian succession exhibits a broader range of facies (Duarte, 1997; Duarte and Soares, 2002; Duarte et al., 2004; Pittet et al., 2014). The lowermost beds consist of fossiliferous grey marl and limestone couplets

belonging to the *Dactylioceras polymorphum* AB. The lowermost *Hildaites levisoni* AB is represented by sparsely fossiliferous, thin, nodular limestones, that locally include a basal unit termed the Chocolate Marls (see Duarte, 1997; Pittet et al., 2014); this marly facies is absent in the Maria Pares section. The middle *Hildaites levisoni* AB normally comprises limestones often rich in brachiopods. Marl-limestone alternations, similar to those in the lowermost Toarcian, constitute the upper part of the *Hildaites levisoni* and the *Hildoceras bifrons* ABs.

Lower Jurassic strata are especially well developed in the Peniche area (Duarte et al., 2017). Here, the upper Pliensbachian and lower Toarcian are represented by an expanded succession of interbedded fossiliferous limestones, marls and calcarenites (Wright and Wilson, 1984; Duarte, 1997, 2007; Duarte and Soares, 2002). The upper Pliensbachian comprises the uppermost part of the Vale das Fontes Formation and the majority of the Lemede Formation. The Vale das Fontes and Lemede formations represent the *Amaltheus margaritatus*, *Emaciaticeras emaciatum* and lowermost *Dactylioceras polymorphum* ABs (Fig. 2.3). The Vale das Fontes Formation is composed of interbedded relatively thick (ca. 10 cm–1 m) marls and thinner (<10 cm) limestones, both of which are abundantly fossiliferous (Duarte et al., 2010; Silva et al., 2011, 2015). The overlying Lemede Formation is heavily bioturbated and also cyclic; it comprises interbedded relatively thick (~10 cm–40 cm) limestones and thinner (<10 cm) marl interbeds. Both lithotypes are richly fossiliferous (Duarte and Soares, 2002; Comas-Rengifo et al., 2016). In this study, only the uppermost Lemede Formation was studied (Figs. 2.3).

The Toarcian of the Peniche region is represented by the Cabo Carvoeiro Formation, which is subdivided into five members (Duarte and Soares, 2002). These are numbered and prefixed with Cabo Carvoeiro, but are frequently abbreviated (i.e. CC1–CC5; Fig. 2.3). In this study only the CC1, CC2 and lowermost CC3 members were analysed, and this succession is correlated to the *Dactylioceras polymorphum* and *Hildaites levisoni* ABs (Figs. 2.3). The CC1 member is a succession of fossiliferous greyish marls and marly limestones. By contrast, the CC2 member comprises interbedded relatively fine-grained conglomerates and sandy limestones/marls, and is sparsely fossiliferous. The CC3 member is dominated by marly limestone and greyish marls with rare brachiopods (Duarte and Soares, 2002).

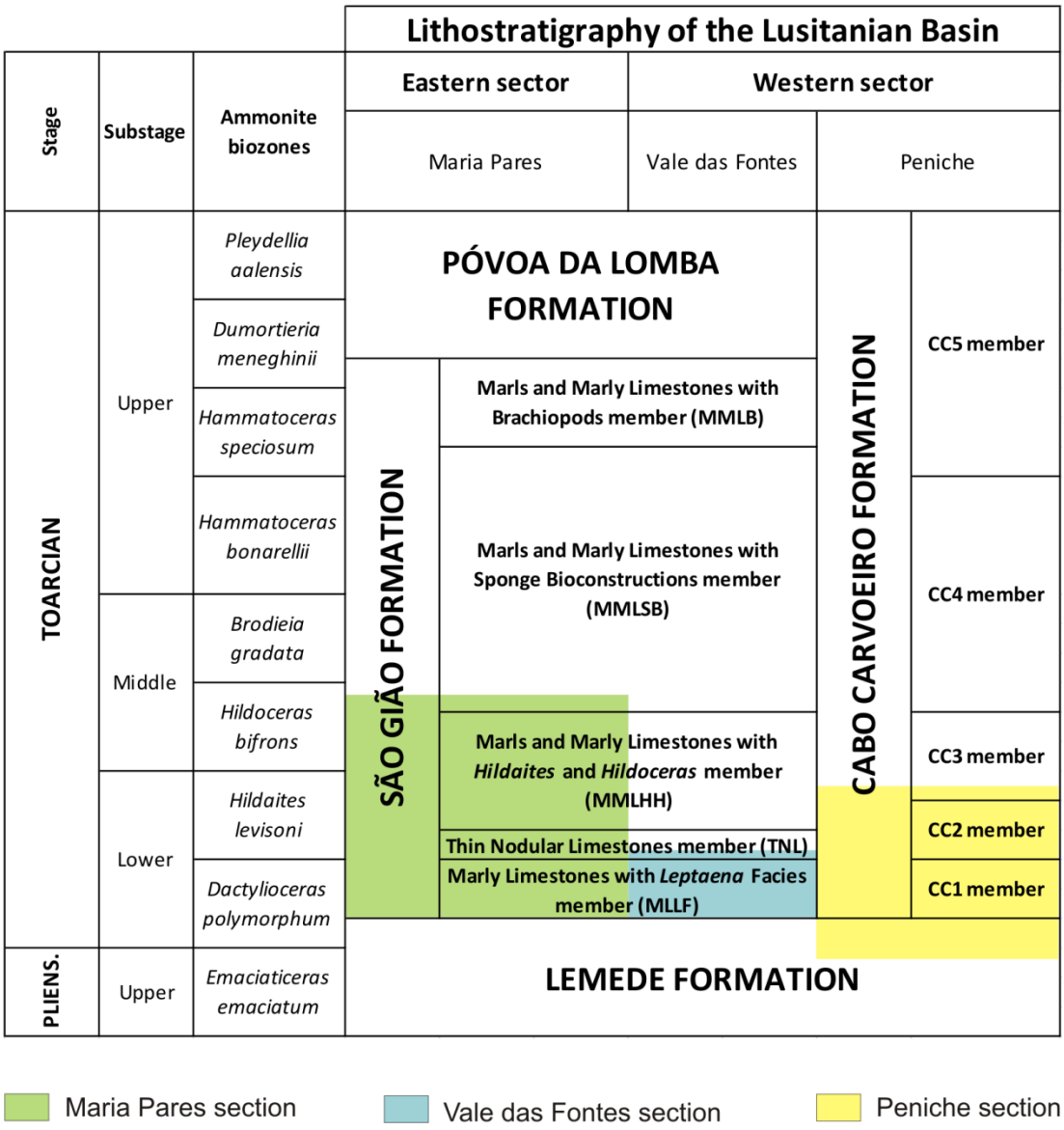

Figure 2.3. The ammonite biostratigraphy and lithostratigraphy of the Toarcian of the eastern and western sectors of the Lusitanian Basin. The color shading indicates the lithostratigraphical units studied in the present work.The ammonite biostratigraphy and lithostratigraphy of the upper Pliensbachian and Toarcian successions of the Lusitanian Basin are based on Duarte and Soares (2002) and Duarte (2007) and with the biostratigraphical data of Silva et al. (2011) and Comas-Rengifo et al. (2016).

3. Material and methods

In this study three sections were sampled: two Toarcian outcrops from the northern part of the Lusitanian Basin and one succession from the southern Lusitanian Basin at Peniche (Fig. 2.1), comprising the upper Pliensbachian to middle Toarcian, in a total of 103 samples.

In the Maria Pares section, in the Rabaçal area, 54 samples (prefixed PZ) were collected (Figs. 2.1, 2.4). This is the type section of the São Gião Formation (Duarte, 1995, 1997, 2007; Duarte and Soares, 2002), and four members were sampled. These are the Marly Limestones with *Leptaena* Facies (MLLF), the Thin Nodular Limestones (TNL), the Marls and Marly Limestones with *Hildaites* and *Hildoceras* (MMLHH), and the Marls and Marly Limestones with Sponge Bioconstructions (MMLSB) members.

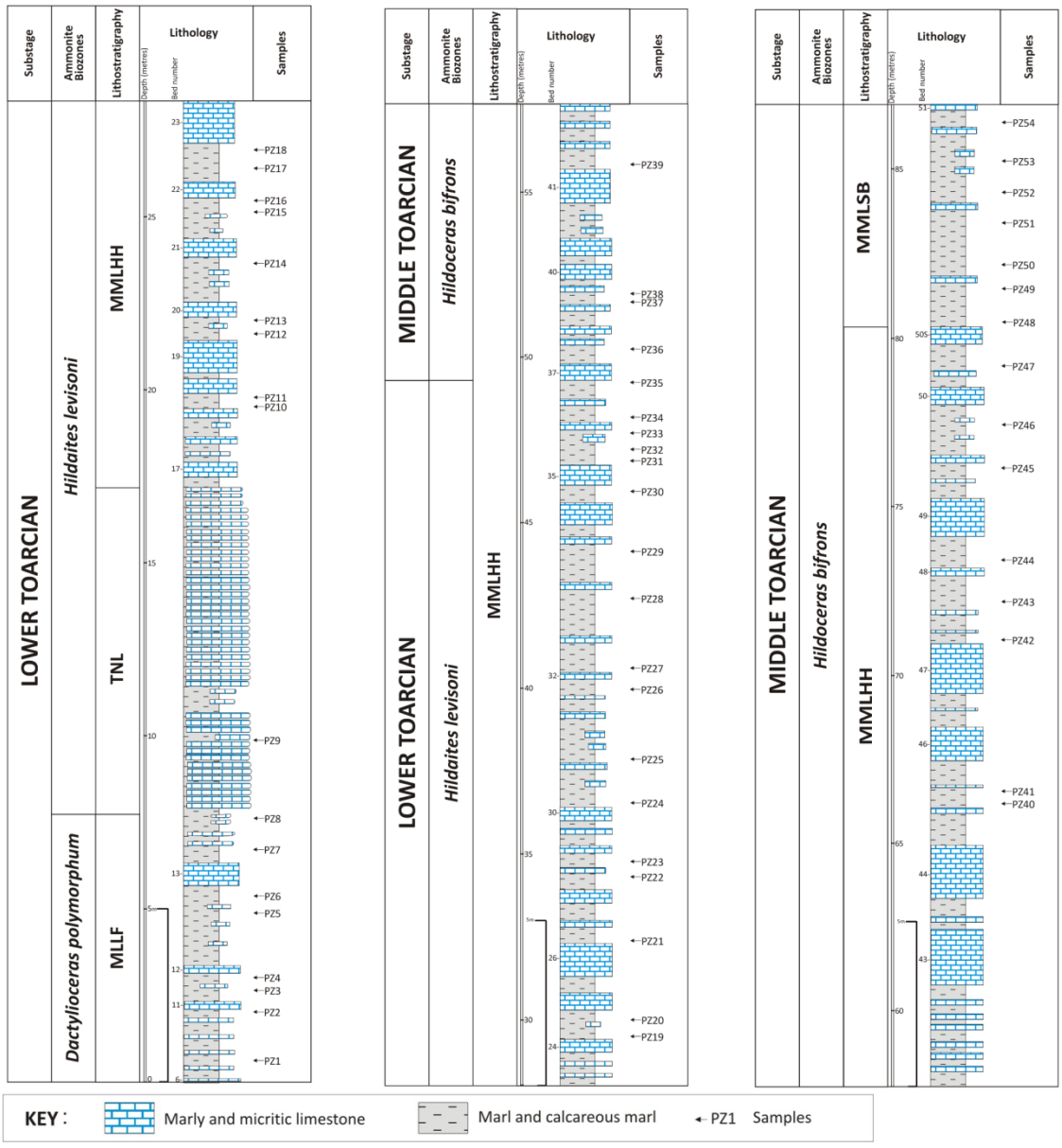

Figure 2.4. The lithological log of the lower and middle Toarcian succession in the Maria Pares section (modified from Duarte, 1995), with the positions of the palynomorph samples PZ1–PZ54 indicated. The ammonite biozones are based on, and modified from, Mouterde et al. (1964-1965) and Elmi et al. (1989). MLLF = Marly Limestones with *Leptaena* Facies member; TNL = Thin Nodular Limestones member; MMLHH = Marls and Marly Limestones with *Hildaites* and *Hildoceras* member; MMLSB = Marls and Marly Limestones with Sponge Bioconstructions member.

Other section examined was at Vale das Fontes, near the coast at Boa Viagem Mountain in the Cape Mondego region (see Duarte, 1995, 1997). Here, 14 samples (prefixed PVF) were taken from the base of the São Gião Formation (Figs. 2.1, 2.5). They are all from the MLLF and the lowermost TNL members.

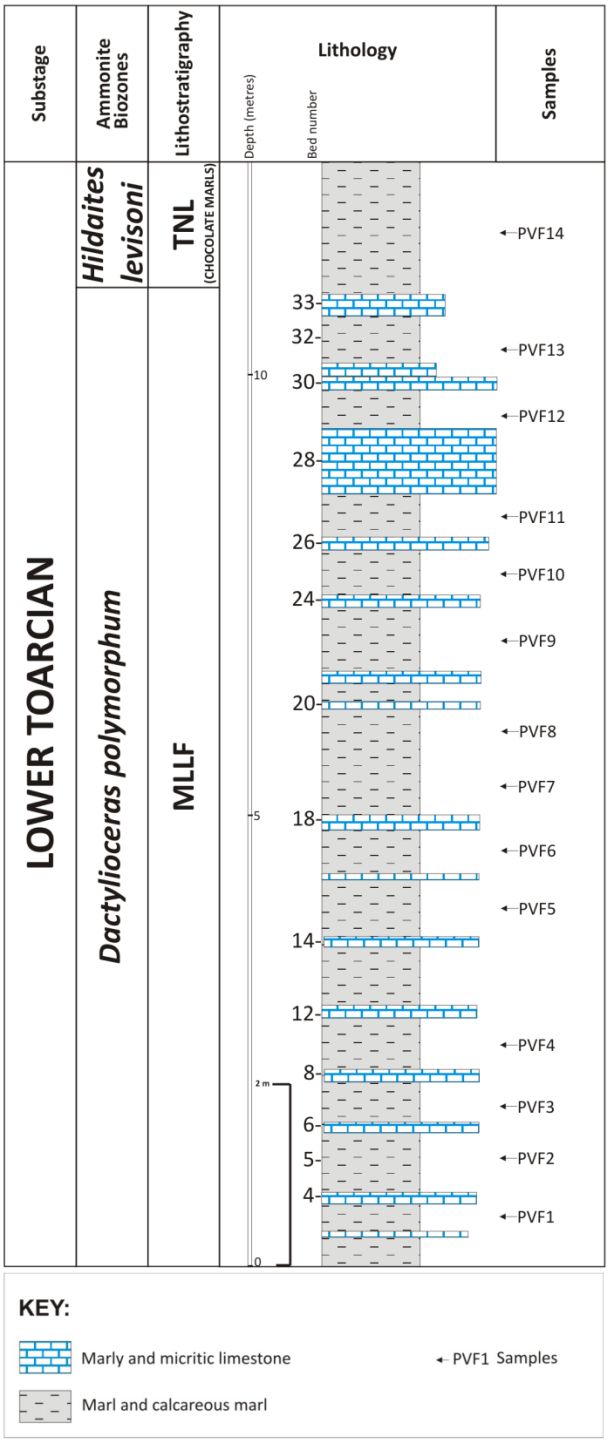

Figure 2.5. The lithological log of the lower Toarcian succession in the Vale das Fontes section (modified from Duarte, 1995), with the positions of the palynomorph samples PVF1–PVF14 indicated. The ammonite biozones are based on, and modified from, Mouterde et al., 1978 and Elmi et al. (1989). MLLF = Marly Limestones with *Leptaena* Facies member; TNL = Thin Nodular Limestones member.

In the Peniche section, at Ponta do Trovão, 45 samples were collected (prefixed P). The reference datum used in the Peniche log (0 m) was the boundary between the Lemede and Cabo Carvoeiro formations (Fig. 2.6). The seven samples below the datum boundary include a minus sign (e.g. P-7) and the sample numbers above this horizon only comprise the number (e.g. P34). Here, the upper part of Lemede Formation and the lowest three members of Cabo Carvoeiro Formation (CC1, CC2 and the lowest part of CC3 members) were sampled (Fig. 2.3). Therefore, the studied samples span the *Emaciaticeras emaciatum*, *Dactylioceras polymorphum*, *Hildaites levisoni* and *Hildoceras bifrons* ABs. Pittet et al. (2014) located the T-OAE in the equivalent of sample PZ9 in the Maria Pares section and sample PVF14 in the Vale das Fontes section. The T-OAE interval in the Peniche section is between samples P15 and P24, according with Hesselbo et al. (2007).

The samples were prepared using standard palynological techniques (Wood et al., 1996; Riding and Warny 2008), however the organic residues were not oxidised. The post-mineral acid residues were sieved through a 15 µm mesh sieve. All the final palynomorph concentrates were stained with Safranin to increase body colour. If possible, at least 300 palynomorphs were counted for each sample; if not, the maximum number of specimens from two microscope slides were used. All the remaining raw sample material, aqueous residues, microscope slides and figured specimens are curated in the collections of LNEG (Portuguese Geological Survey), São Mamede de Infesta, Portugal.

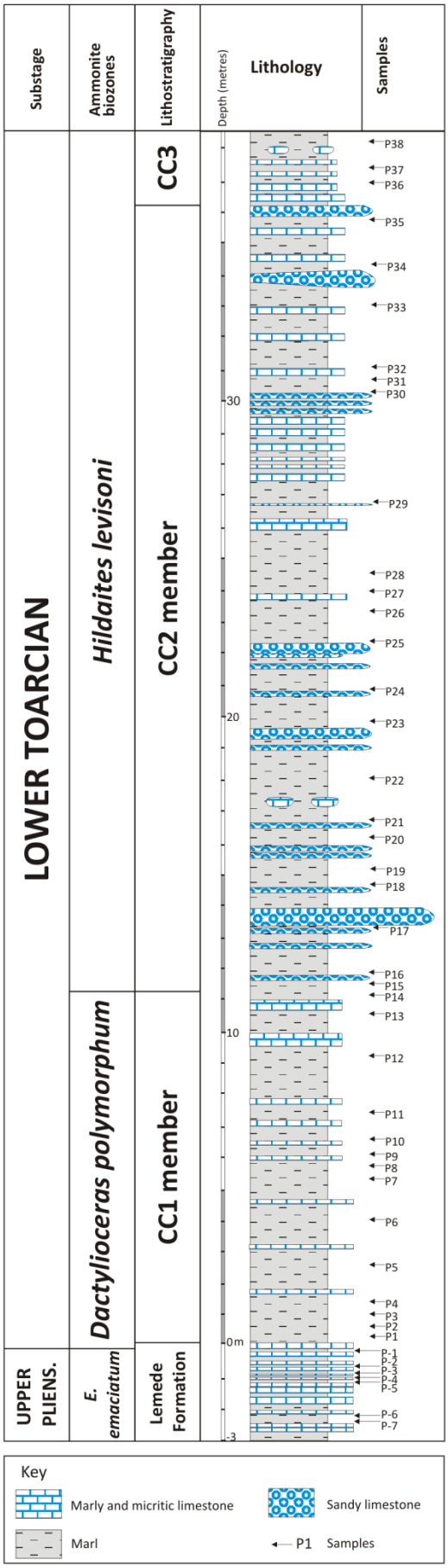

Figure 2.6. The lithological log of the uppermost Pliensbachian and lower Toarcian succession in the Peniche section The log is modified from Hesselbo et al. (2007) and Barrón et al. (2013), and indicates the positions of the palynomorph samples P-7 to P38. The ammonite biozones are based on, and modified from, Mouterde (1955), Elmi et al. (1989) and Comas-Rengifo et al. (2016).
CC1–3 = Cabo Carvoeiro Formation members 1–3. Toarcian GSSP = Toarcian Global boundary Stratotype Section and Point, immediately above sample P-1. T-OAE = Toarcian Oceanic Anoxic Event, between samples P15 and P24.

4. Palynology and biostratigraphy

In this section, the uppermost Pliensbachian–middle Toarcian palynofloras from the Maria Pares, Vale das Fontes and Peniche successions are described and interpreted, based largely on dinoflagellate cysts biostratigraphy. The percentages of the principal dinoflagellate cyst taxa, the aggregate percentages of the marine palynomorphs and the relative abundances of the six major palynomorph groups (i.e., dinoflagellate cysts, acritarchs, prasinophytes, foraminiferal test linings, spores and pollen) are illustrated in Figs. 2.7–2.14. Selected palynomorphs are pictured in Plates 2.1–2.4 and the digital supplementary Tables S1–S3.1 give comprehensive palynomorph datasets for each of the two sections. All identified palynomorphs are documented and the data presented as percentages of the overall palynofloras. These supplementary tables are available as Excel format in Supplement B of the Digital Supplementary Data. The palynomorph taxa at and below species level that were recorded herein, or were mentioned in the text, are listed in Appendix 1 with their respective author citations. Appendix 2 documents our concepts of *Nannoceratopsis gracilis* and *N. senex*.

4.1. The Maria Pares section

The samples in this section are assigned to the lower and middle Toarcian *Dactylioceras polymorphum*, *Hildaites levisoni* and *Hildoceras bifrons* ABs of the Tethyan scheme (Figs. 2.3, 2.4; Mouterde et al., 1964-1965; Elmi et al., 1989). Two samples, PZ14 and PZ37, proved entirely barren of palynomorphs (Table S1). However, eight dinoflagellate cyst taxa were encountered throughout this section: *Luehndea spinosa*, *Mancodinium semitabulatum*, *Mendicodinium microscabratum*, *M. spinosum* subsp. *spinosum*, *Mendicodinium* sp., *Nannoceratopsis ambonis*, *N. gracilis* and *N. senex* (Figs. 2.7; Plate 2.1; Table S1).

Luehndea spinosa was recorded from samples PZ1 to PZ8 (Table S1). All these occurrences are in the MLLF member within the *Dactylioceras polymorphum* AB. Based on the known range of *Luehndea spinosa* elsewhere in Europe, the Maria Pares succession is no older than late Pliensbachian (*Amaltheus margaritatus* AB), and no younger than earliest Toarcian (*Dactylioceras polymorphum* AB) (Morgenroth, 1970; Riding, 1987; Bucefalo Palliani and Riding, 1997a,b; 2000; 2003; Bucefalo Palliani et al., 1997a). The presence of *Luehndea spinosa* in the Maria Pares section is consistent with the findings of Davies (1985), who recorded this species, as *Luehndea* sp. A, at Brenha, Peniche and Maria Pares (Zambujal) in the Lusitanian Basin between the late

Pliensbachian (*Emaciaticeras emaciatum* AB) and the early Toarcian (*Dactylioceras polymorphum* AB).

In the Maria Pares section, the lowest occurrences of *Mancodinium semitabulatum, Nannoceratopsis gracilis* and *Nannoceratopsis senex* are all in sample PZ1. *Mancodinium semitabulatum* ranges throughout the entire succession, but *Nannoceratopsis ambonis, N. gracilis* and *N. senex* are confined to the MLLF, TNL and the lowermost MMLHH members (*Dactylioceras polymorphum* and *Hildaites levisoni* ABs) (Table S1). In Europe, the consistent range bases of *Mancodinium semitabulatum, Nannoceratopsis ambonis, N. gracilis* and *N. senex* are all late Pliensbachian (Morgenroth, 1970; Woollam and Riding, 1983; Bucefalo Palliani and Riding, 2003; Poulsen and Riding, 2003). *Mancodinium semitabulatum* ranges from the Pliensbachian to the early Bajocian (Riding, 1984a; Feist Burkhardt and Wille 1992; Riding and Thomas 1992), and *Nannoceratopsis ambonis* extends from the late Pliensbachian to the late Bajocian (Riding, 1984b). The overall ranges of *Nannoceratopsis gracilis* and *N. senex* are late Pliensbachian to early Bajocian (Feist Burkhardt and Monteil, 1997; Poulsen and Riding, 2003). The presence of these four species is hence entirely consistent with an early Toarcian age for the succession.

Mendicodinium spp. was recorded sporadically, and in low abundances, between samples PZ16 and PZ54 at Maria Pares (Table S1). This interval spans the *Hildaites levisoni* and *Hildoceras bifrons* ABs. Three taxa were recognised: *Mendicodinium microscabratum*; *M. spinosum* subsp. *spinosum* and *Mendicodinium* sp. Representatives of the typically, but not exclusively, southern European genus *Mendicodinium* are not present in the *Dactylioceras polymorphum* AB herein (Table S1). This is in contrast to the records from the lowermost Toarcian *Dactylioceras tenuicostatum* AB reported by Bucefalo Palliani et al. (1997b) from central Italy, and those from the earliest Pliensbachian to the middle Toarcian (*Hildoceras bifrons* AB) of the Lusitanian Basin documented by Davies (1985) and Bucefalo Palliani and Riding (2003).

In the Maria Pares section, the relative abundance of dinoflagellate cysts decreased markedly at the T-OAE in the lower part of the *Hildaites levisoni* AB (sample PZ9). Above that level, the occurrences of dinoflagellate cysts remained low throughout the remainder of the *Hildaites levisoni* AB and in the *Hildoceras bifrons* AB (Figs. 2.7, 2.8, Table S1). With the transition for the *Hildaites levisoni* AB occur a shift in the local sedimentation, becoming more carbonated and siliciclastic (Duarte, 1997; Duarte et al., 2004; Duarte et al., 2007) with a higher continental influence (Rodrigues et al., 2016).

This fact may also explain the low abundances of dinoflagellate cysts during the *Hildaites levisoni* AB in this section (Fig. 2.7).

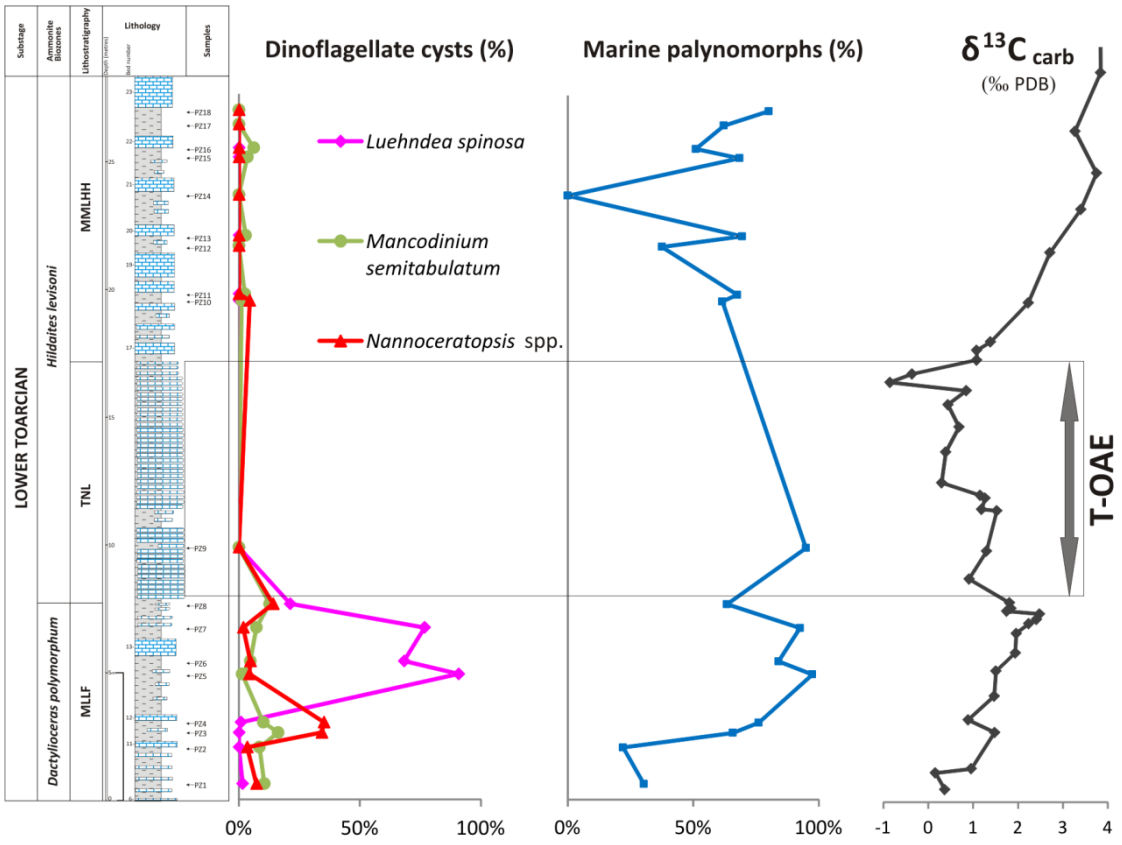

Figure 2.7. The relative proportions of the dinoflagellate cysts *Luehndea spinosa*, *Mancodinium semitabulatum* and *Nannoceratopsis* spp., expressed as a percentage of the overall palynoflora, from the lower Toarcian (*Dactylioceras polymorphum* and *Hildaites levisoni* ABs) in the Maria Pares section. *Mendicodinium* spp. are not included. The plot with the percentages of all marine palynomorphs (i.e. acritarchs, dinoflagellate cysts, foraminiferal test linings and prasinophytes) includes *Mendicodinium* spp. The right hand column illustrates the carbon isotope records of Pittet et al. (2014) for the Maria Pares section. T-OAE = Toarcian Oceanic Anoxic Event.

In the *Dactylioceras polymorphum* AB, *Luehndea spinosa* dominates the dinoflagellate cyst assemblages. In samples PZ5, PZ6 and PZ7, this species represents 90.8%, 68.2% and 76.7% of the palynoflora respectively (Fig. 2.7, Table S1). It is possible that this abundance peak represents a transgressive event, such as interpreted by Duarte et al. (2004) and Duarte (2007) for the whole lower Toarcian succession (see also Pittet et al., 2014). *Nannoceratopsis gracilis* and *N. senex* are also relatively common in the *Dactylioceras polymorphum* AB, but they never exceed 20% of the

overall palynoflora (Fig. 2.7). *Nannoceratopsis ambonis* is rare, and is only present in sample PZ8 (Table S1). *Mancodinium semitabulatum* is present throughout the *Dactylioceras polymorphum, Hildaites levisoni* and *Hildoceras bifrons* ABs, and is the only species present in all three of these biozones. The range top of consistent *Nannoceratopsis* is in sample PZ8, in the *Dactylioceras polymorphum* AB. In the majority of the *Hildaites levisoni* AB, and throughout the *Hildoceras bifrons* AB, *Mancodinium semitabulatum* is present persistently in low numbers, occasionally co-occurring with sparse representatives of *Mendicodinium* spp. (Table S1).

Marine palynomorphs exhibit significant change throughout the Maria Pares section. Dinoflagellate cysts dominate the palynomorph assemblages in the middle and upper part of the *Dactylioceras polymorphum* AB (Fig. 2.7). In contrast, prasinophytes dominate throughout the *Hildaites levisoni* and *Hildoceras bifrons* ABs (Figure 2.8, Table S1). Most of the prasinophytes are either large, dispersed specimens of *Tasmanites*, or clumps of small (c. 20 µm diameter) bodies which are referable to *Halosphaeropsis liassica* (Plate 2.2(12); see Mädler 1968; Bucefalo Palliani and Riding, 2000, fig. 7I). Acritarchs, largely *Micrhystridium* spp., and foraminiferal test linings are also frequently present throughout this succession.

Pteridophyte spores such as *Cyathidites* spp., *Ischyosporites variegatus* and *Leptolepidites* spp., and the gymnosperm pollen grains *Alisporites* spp. and *Classopollis classoides* (Figs. 2.8; Plate 2.2), dominate some samples. However, these terrestrially derived palynomorphs do not exhibit any coherent or specific trends. The two lowermost samples from the *Dactylioceras polymorphum* AB (PZ1 and PZ2) are especially rich in spores and pollen, notably *Alisporites* spp. and *Classopollis classoides* (Table S1). In contrast, between samples PZ3 and PZ9, marine palynomorphs consistently dominate. Although marine palynomorphs dominate most samples, some of those stratigraphically above PZ9 exhibit a relatively high terrestrial influence (Figs. 2.7, 2.8, Table S1).

During the T-OAE (sample PZ9), acritarchs, dinoflagellate cysts and foraminiferal test linings are entirely absent. The only marine palynomorphs present are prasinophytes, small clumps of these fossils dominate the assemblage. Including dispersed specimens of *Tasmanites* spp., prasinophytes comprise 94.9% of the overall palynoflora in sample PZ9. This dominance of prasinophytes, largely in the absence of dinoflagellate cysts, is typical of the T-OAE throughout Europe (Wille, 1982a,b; Loh et al., 1986; Prauss; 1989; 1996; Prauss and Riegel 1989; Prauss et al., 1991; Bucefalo

Palliani and Riding, 1999b; 2000; Bucefalo Palliani et al., 2002). Pteridophyte spores, including *Cyathidites* spp. and *Leptolepidites* spp., are present in low proportions in sample PZ9 (5.1%), but no pollen grains were encountered (Table S1).

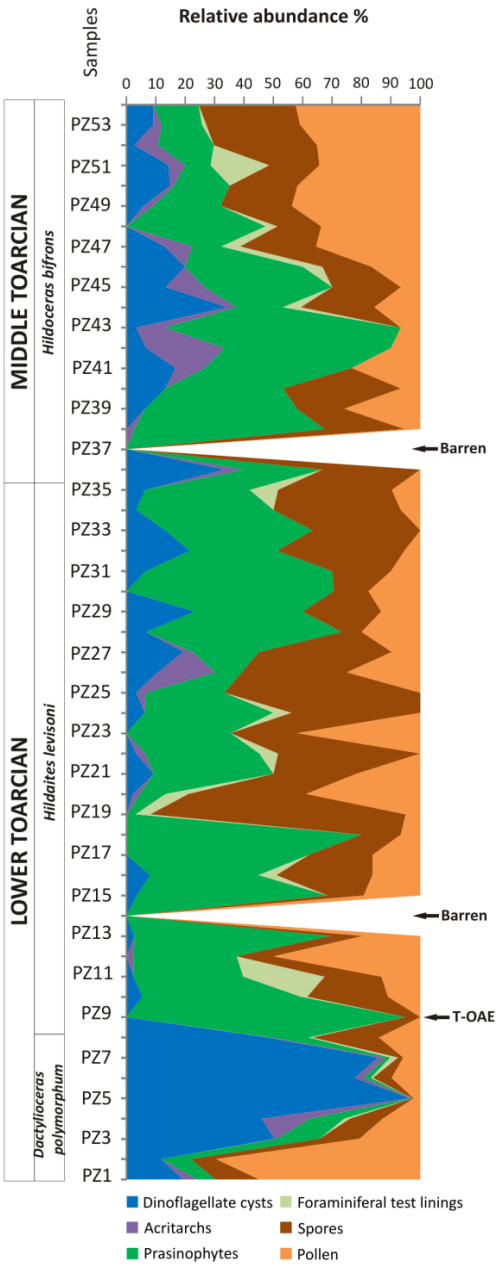

Figure 2.8. The relative abundances, expressed as percentages, of the six main palynomorph groups recorded from the lower and middle Toarcian (*Dactylioceras polymorphum*, *Hildaites levisoni* and *Hildoceras bifrons* ABs) of the Maria Pares section (samples PZ1–PZ54). Samples PZ14 and PZ37 are entirely devoid of palynomorphs. Note the dominance of prasinophytes in the T-OAE (sample PZ9). T-OAE = Toarcian Oceanic Anoxic Event.

4.2. The Vale das Fontes section

We examined fourteen samples from the lower Toarcian MLLF and TNL members of the São Gião Formation succession at Vale das Fontes, Boa Viagem Mountain (Figs. 2.1, 2.5). All proved palynologically productive and correlate with the *Dactylioceras polymorphum* and *Hildaites levisoni* AB of the Tethyan scheme (Figs.

2.2, 2.5; Table S2; Mouterde et al., 1980; Elmi et al., 1989). Only one sample (PVF14) is assigned to the *Hildaites levisoni* AB. It was not possible to collect more samples from this AB because this section does not expose strata above this level. In this area (Figueira da Foz) the Toarcian outcrops are very difficult to observe and this section is the best one for palynological studies, due the higher strata of marls. Five dinoflagellate cyst species were recorded: *Luehndea spinosa*, *Mancodinium semitabulatum*, *Nannoceratopsis ambonis*, *N. gracilis* and *N. senex* (Figs. 2.9; Plate 2.1; Table S2). This dinoflagellate cyst association is substantially similar to those from the coeval part of the Maria Pares section, but represenatatives of *Mendicodinium* were not found at Vale das Fontes. Dinoflagellate cysts are relatively common in the middle and upper part of the MLLF member (*Dactylioceras polymorphum* AB, samples PVF1-PVF13), but are absent in the TNL member (*Hildaites levisoni* AB, sample PVF14) (Figs. 2.9, 2.10; Table S2).

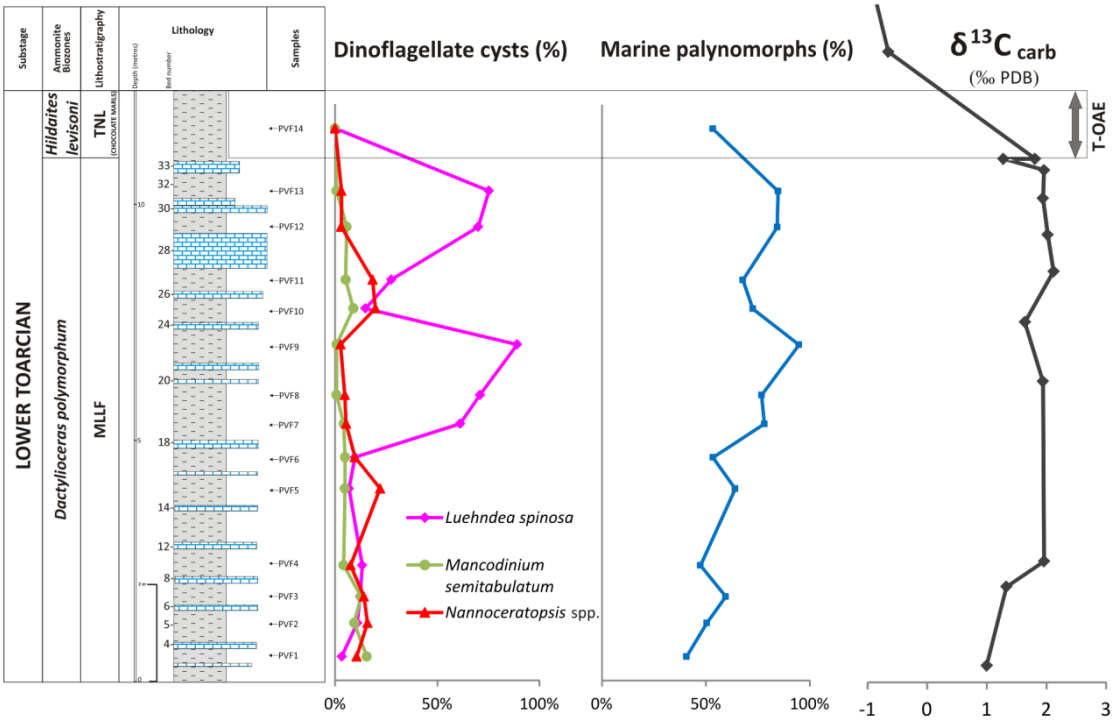

Figure 2.9. The relative proportions of the dinoflagellate cysts *Luehndea spinosa*, *Mancodinium semitabulatum* and *Nannoceratopsis* spp., expressed as a percentage of the overall palynoflora, from the lower Toarcian (*Dactylioceras polymorphum* and *Hildaites levisoni* ABs) in the Vale das Fontes section. *Mendicodinium* spp. are not included. The plot with the percentages of all marine palynomorphs (i.e. acritarchs, dinoflagellate cysts, foraminiferal test linings and prasinophytes) include *Mendicodinium* spp. The right hand column illustrates the carbon isotope records of Duarte et al. (2007) and Pittet et al. (2014) for the Vale das Fontes section. T-OAE = Toarcian Oceanic Anoxic Event.

As in the Maria Pares section, *Luehndea spinosa* was found throughout the MLLF member/*Dactylioceras polymorphum* AB at Vale das Fontes. It is the most abundant dinoflagellate cyst in most of the samples (PVF4, PVF6–PVF9, PVF11–PVF13). In the middle and upper part of this unit/biozone, in samples PVF8, PVF9, PVF12 and PVF13, *Luehndea spinosa* attains 70.9%, 89.1%, 70.0% and 75.3% of the overall palynoflora respectively (Fig. 2.9; Table S2). As at Maria Pares, this major acme may represent the general transgressive event that occurred during the early Toarcian (Duarte et al., 2004; Duarte, 2007; Pittet et al., 2014). The acme and the pattern of occurrences of this species at Vale das Fontes is unsurprisingly virtually identical to that at Maria Pares. The main acme of *Luehndea spinosa* occurs stratigraphically below the T-OAE, and has two distinctive peaks with an intervening low level, giving a distinctive 'swallow tail' pattern (Figs. 2.7, 2.9). The presence of this species confirms that the MLLF member is no younger than earliest Toarcian (subsection 4.1).

Mancodinium semitabulatum, Nannoceratopsis gracilis and *N. senex* are also consistently present throughout the MLLF member at Vale das Fontes. These species are persistent and relatively common, but they never exceed 16% (Table S2). As with *Luehndea spinosa*, the distribution of *Mancodinium semitabulatum* and *Nannoceratopsis* spp. appears to be similar to those at Maria Pares. There are minor acmes of *Mancodinium semitabulatum* and *Nannoceratopsis* spp. stratigraphically below the abundance peak of *Luehndea spinosa* (Figs. 2.7, 2.9; Table S2). *Nannoceratopsis ambonis* is rare, as in the Maria Pares section. This species is sparsely present only in samples PVF2 and PVF5 in the lower part of the *Dactylioceras polymorphum* AB (Table S2). The occurrence of *Mancodinium semitabulatum* and *Nannoceratopsis* spp. is compatible with an early Toarcian age for this succession (subsection 4.1).

Only samples PVF1 and PVF4 in the lower part of the *Dactylioceras polymorphum* AB at Vale das Fontes exhibit more terrestrial than marine influence, due mainly to the abundance of *Classopollis classoides* (Table S2). However, in the middle and upper *Dactylioceras polymorphum* AB (samples PVF7–PVF13), marine elements dominate, reaching a maximum of 94.7% of all palynomorphs in sample PVF9, largely due the abundance of *Luehndea spinosa* (Fig. 2.9; Table S2). As in the Maria Pares section, this marine acme reflects the dominance of dinoflagellate cysts stratigraphically below the

T-OAE. There are five dinoflagellate cyst abundance peaks in samples PVF7, PVF8, PVF9, PVF12 and PVF13, (Fig. 2.9; Table S2).

Acritarchs (*Micrhystridium* spp.), foraminiferal test linings and prasinophytes are present in all the samples. Spores, such as *Cyathidites* spp. and *Kraeuselisporites reissingeri*, are also consistently present, generally in low percentages. Gymnospermous pollen, largely *Classopollis classoides* and *Alisporites* spp., are relatively common throughout (Table S2). There is a general decrease in the relative abundance of pollen up-section, but no other obvious coherent trends in the non-dinoflagellate cyst palynomorphs (Fig. 2.10). During the T-OAE (sample PVF14), no acritarchs or dinoflagellate cysts were recorded. This relatively sparse assemblage is dominated by indeterminate spores; foraminiferal test linings, pollen and prasinophytes are also present (Table S2).

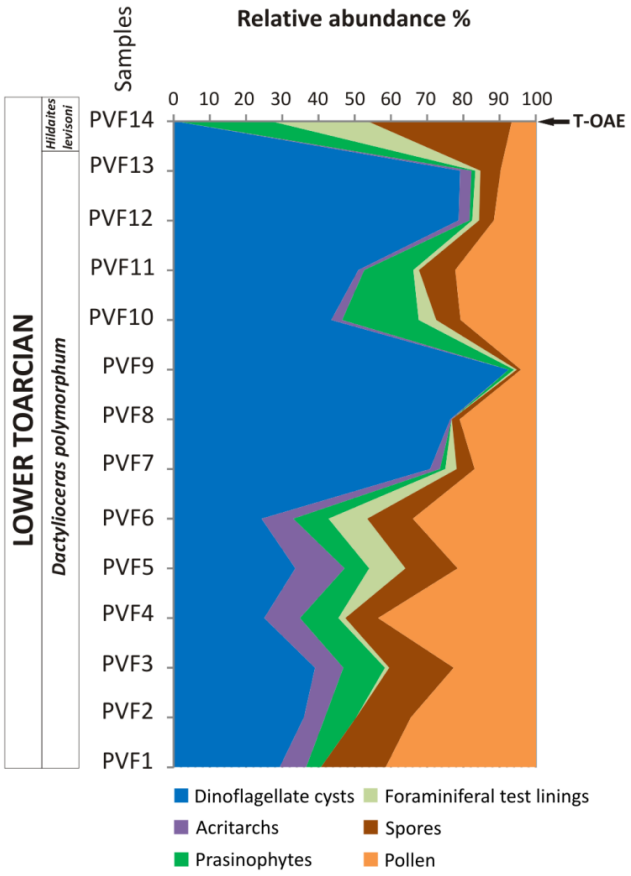

Figure 2.10. The relative abundances, expressed as percentages, of the six main palynomorph groups recorded from the lower Toarcian (*Dactylioceras polymorphum* and *Hildaites levisoni* ABs) of the Vale das Fontes section (samples PVF1–PVF14).
T-OAE = Toarcian Oceanic Anoxic Event.

Plate 2.1. Selected dinoflagellate cysts from Toarcian of the Maria Pares and Vale das Fontes sections of the Lusitanian Basin, west-central Portugal. All specimens are housed in the collections of the LNEG (Portuguese Geological Survey), S. Mamede de Infesta, Portugal. The sample number, slide number and England Finder coordinates are provided. All the scale bars represent 20 μm.

1. *Nannoceratopsis gracilis* Alberti 1961 emend. Evitt 1962. Vale das Fontes section, lower Toarcian (*Dactylioceras polymorphum* AB), sample PVF10, slide 1, R47/1. Right lateral view. Note the dorsal antapical horn and the microreticulate autophragm.
2. *Nannoceratopsis senex* van Helden 1977. Vale das Fontes section, lower Toarcian (*Dactylioceras polymorphum* AB), sample PVF2, slide 1, Q57. Right lateral view. Note the single antapical horn and the microreticulate autophragm.
3. *Nannoceratopsis ambonis* Drugg 1978 emend. Riding 1984. Vale das Fontes section, lower Toarcian (*Dactylioceras polymorphum* AB), sample PVF2, slide 1, Y36/1. Left lateral view. Note the prominent dark sagittal rim and the microreticulate autophragm.
4. *Mendicodinium spinosum* Bucefalo Palliani et al. 1997 subsp. *spinosum* (autonym). Maria Pares section, lower Toarcian (*Hildaites levisoni* AB), sample PZ26, slide 1, F49/1. Oblique dorsal view. Note the spines and the smooth autophragm.
5. *Mendicodinium microscabratum* Bucefalo Palliani et al. 1997. Maria Pares section, lower Toarcian (*Hildaites levisoni* AB), sample PZ16, slide 1, T36/1. Right lateral view. Note the microscabrate autophragm.
6. *Mendicodinium* sp. Maria Pares section, lower Toarcian (*Hildaites levisoni* AB), sample PZ29, slide 1, M33/3. Oblique left lateral view. Note that this form is larger than most Toarcian specimens of *Mendicodinium*; the width is 40 μm.
7. *Luehndea spinosa* Morgenroth 1970. Vale das Fontes section, lower Toarcian (*Dactylioceras polymorphum* AB), sample PVF8, slide 1, O24. Mid-ventral view, high focus. Note the prominent cingulum, interrupted by the sulcus.
8. *Luehndea spinosa* Morgenroth 1970. Vale das Fontes section, lower Toarcian (*Dactylioceras polymorphum* AB), sample PVF10, slide 1, Y27/3. Dorsal view, high focus. Note the uninterrupted cingulum.
9. *Luehndea spinosa* Morgenroth 1970. Maria Pares section, lower Toarcian (*Dactylioceras polymorphum* AB), sample PZ5, slide 1, O22/2. Oblique dorsal view. Note the antapical (1"") plate.
10. *Mancodinium semitabulatum* Morgenroth 1970. Maria Pares section, lower Toarcian (*Hildaites levisoni* AB), sample PZ32, slide 1, D42. Oblique ventral-left lateral view. Note the well-preserved precingular plates which are involved in the formation of the 'disintegration' archaeopyle, in which all the epicystal plates are lost, apparently one-by-one. The anterior sulcal plate (the sulcal tongue) is visible; this is clearly not involved in archaeopyle formation.
11. *Mancodinium semitabulatum* Morgenroth 1970. Vale das Fontes section, lower Toarcian (*Dactylioceras polymorphum* AB), sample PVF1, slide 1, H56/2. Oblique right lateral-ventral view. Note the clearly detached 7" plate, which is immediately adjacent to the much narrower anterior sulcal plate (sulcal tongue).
12. *Mancodinium semitabulatum* Morgenroth 1970. Maria Pares section, lower Toarcian (*Hildaites levisoni* AB), sample PZ32, slide 1, K39. Slightly oblique dorsal view. Note the anterior sulcal plate (sulcal tongue) and the release of all the epicystal plates during archaeopyle formation.

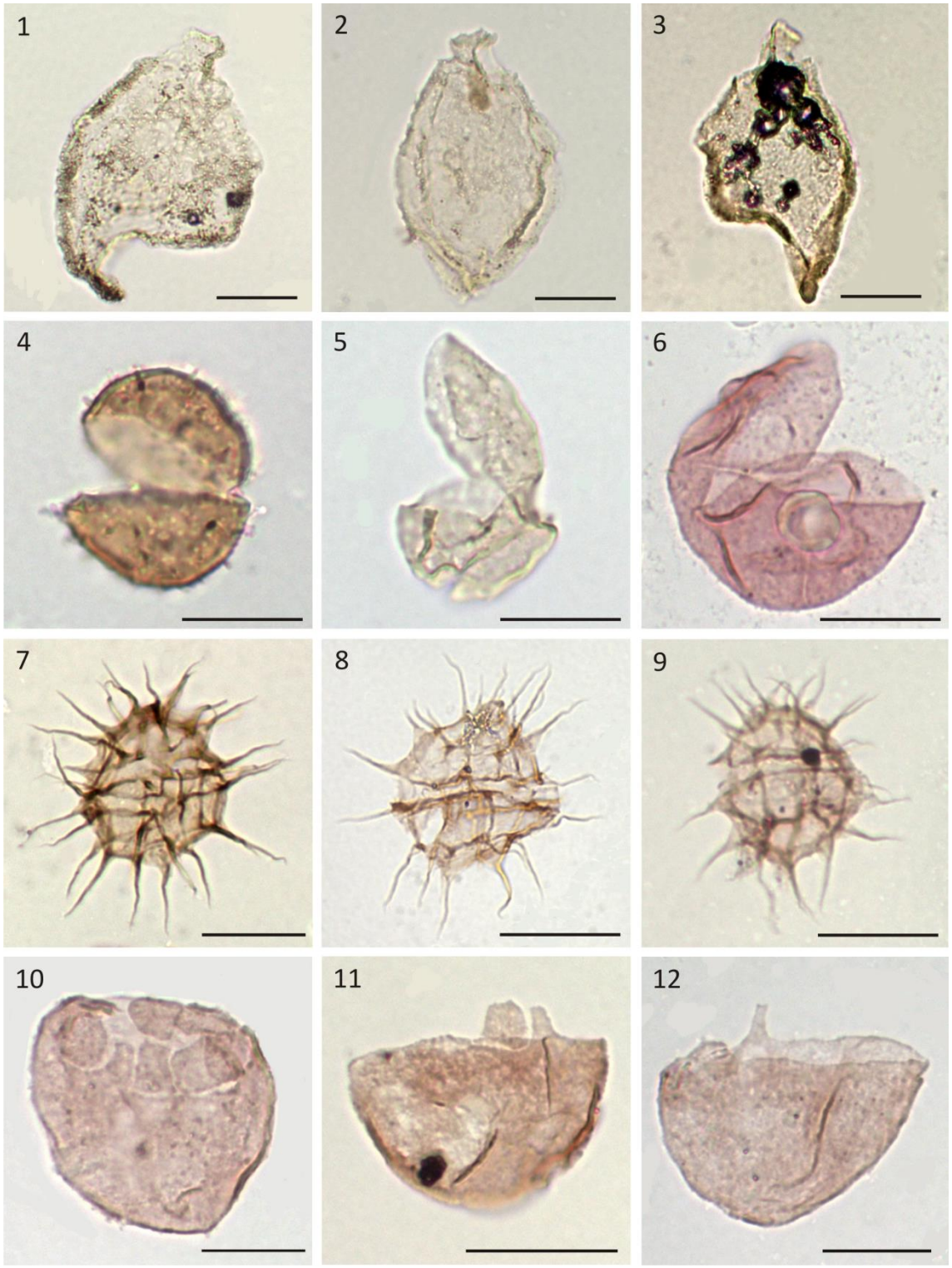

Plate 2.1 (caption on previous page)

Plate 2.2. Selected miscellaneous microplankton, pollen and spores from the Toarcian of the Maria Pares and Vale das Fontes sections of the Lusitanian Basin, west-central Portugal. All specimens are housed in the collections of the LNEG (Portuguese Geological Survey), S. Mamede de Infesta, Portugal. The sample number, slide number and England Finder coordinates are provided. All the scale bars represent 20 μm.

1. *Cyathidites* sp. Maria Pares section, lower Toarcian (*Hildaites levisoni* AB), sample PZ20, slide 1, F50.
2. *Ischyosporites variegatus* (Couper 1958) Schulz 1967. Maria Pares section, lower Toarcian (*Hildaites levisoni* AB), sample PZ19, slide 1, J51.
3. Tetrad of *Kraeuselisporites reissingeri* (Harris 1957) Morbey 1975. Vale das Fontes section, lower Toarcian (*Dactylioceras polymorphum* AB), sample PVF5, slide 1, E34/3.
4. Tetrad of *Leptolepidites* sp. Vale das Fontes section, lower Toarcian (*Dactylioceras polymorphum* AB), sample PVF13, slide 1, H28.
5. *Lycopodiacidites rugulatus* (Couper 1958) Schulz 1967. Maria Pares section, lower Toarcian (*Hildaites levisoni* AB), sample PZ19, slide 1, J37/2.
6. *Alisporites* sp. *sensu lato.* Maria Pares section, lower Toarcian (*Hildaites levisoni* AB), sample PZ15, slide 1, S70/4.
7. *Araucariacites australis* Cookson 1947 ex Couper 1958. Vale das Fontes section, lower Toarcian (*Dactylioceras polymorphum* AB), sample PVF5, slide 1, O40.
8. *Cerebropollenites macroverrucosus* (Thiergart 1949) Schulz 1967. Vale das Fontes section, lower Toarcian (*Dactylioceras polymorphum* AB), sample PVF1, slide 1, P41.
9. Tetrad of *Classopollis classoides* (Pflug 1953) Pocock & Jansonius 1961. Vale das Fontes section, lower Toarcian (*Dactylioceras polymorphum* AB), sample PVF2, slide 1, K39/3.
10. *Micrhystridium* sp. Vale das Fontes section, lower Toarcian (*Dactylioceras polymorphum* AB), sample PVF2, slide 1, E54/3.
11. *Tasmanites* sp. Vale das Fontes section, lower Toarcian (*Dactylioceras polymorphum* AB), sample PVF10, slide 1, J49/3.
12. Clump of *Halosphaeropsis liassica* Mädler 1968. Vale das Fontes section, lower Toarcian (*Dactylioceras polymorphum* AB), sample PVF2, slide 1, R58/2.

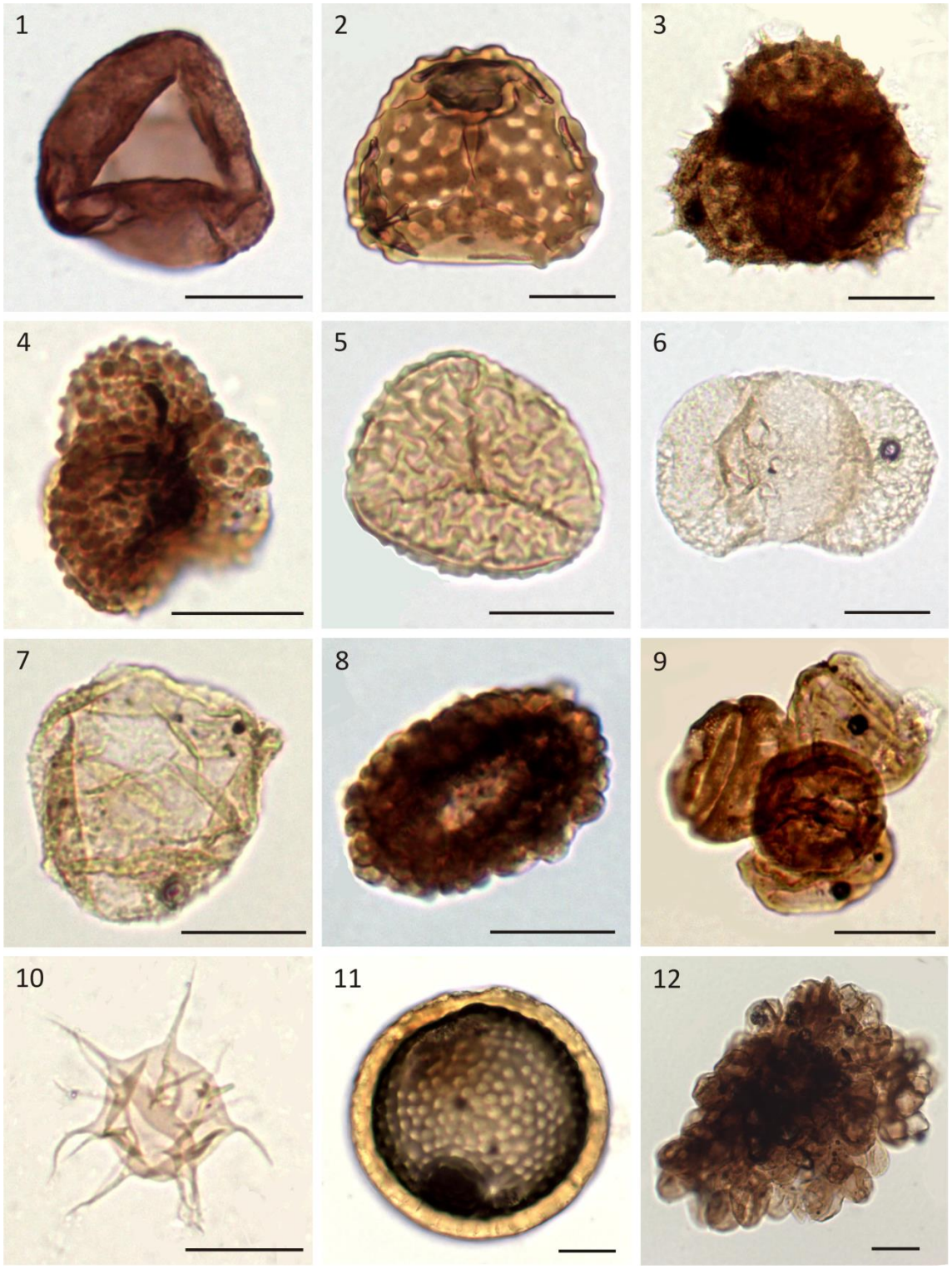

Plate 2.2 (caption on previous page)

4.3. Peniche section

4.3.1. The Emaciaticeras emaciatum *AB (samples P-7 to P-1)*

Seven samples were analysed from the uppermost part of the Lemede Formation of latest Pliensbachian age, and are referable to the uppermost *Emaciaticeras emaciatum* AB (Figs. 2.3, 2.6). All proved palynologically productive. The dinoflagellate cyst species *Luehndea spinosa*, *Mancodinium semitabulatum*, *Nannoceratopsis gracilis* and *Nannoceratopsis senex* were recorded. *Luehndea spinosa*, where present, was the most abundant species; it attained 92% of the overall palynobiota in sample P-6, where it was the only dinoflagellate cyst recorded. It comprised 86.3% and 73.3% in samples P-7 and P-1 respectively, and was the most common dinoflagellate cyst in sample P-2 (13.0%). However, this distinctive taxon was absent in samples P-5 to P-3 (Fig. 2.11; Table S3.1).

Mancodinium semitabulatum, Nannoceratopsis gracilis and *Nannoceratopsis senex* were also recorded in all the horizons except P-6. These species were present in relatively low percentages. *Mancodinium semitabulatum* was most prominent, attaining 17.1% of the overall assemblage in sample P-3. By contrast, *Nannoceratopsis* spp. proved relatively sparse, representing 0.3% to 2.4% in all the samples except P-6 and P-3 (Table S3.1). Other marine palynomorphs encountered were acritarchs, mainly *Micrhystridium* spp. and *Polygonium jurassicum*, foraminiferal test linings and prasinophytes. These groups were present in relatively low proportions, but foraminiferal test linings represented a high relative abundance in sample P-4 (Fig. 2.12). The records of the distinctive acritarch *Polygonium jurassicum* (Plate 2.4(1–3)) in the *Emaciaticeras emaciatum* to lower *Hildaites levisoni* ABs (Table S3.1) extend the known range of this species. It was previously known from the earliest Toarcian of southern Europe (Bucefalo Palliani et al., 1996; Bucefalo Palliani and Mattioli, 1998).

The pteridophyte spores *Cyathidites* spp., *Ischyosporites variegatus*, *Kraeuselisporites reissingeri* and *Leptolepidites* spp. were recorded throughout in minor proportions (0.3% to 3.5%), except in sample P-6. *Kraeuselisporites reissingeri* was consistently present throughout the *Emaciaticeras emaciatum* and *Dactylioceras polymorphum* ABs, with occasional occurrences in the *Hildaites levisoni* AB (samples P16 and P33; Table S3.1). This distribution is similar to that in the northern Lusitanian Basin, where it is confined to the *Dactylioceras polymorphum* AB. Gymnosperm pollen were present in higher proportions than trilete spores. The most common form was

Classopollis classoides which represented 85.0% of the association in sample P-5. *Alisporites* spp., *Araucariacites australis* and *Cerebropollenites macroverrucosus* were also identified; these forms comprised between 0.3% in P-6 and 6.0% in P-4 (Table S3.1). The middle part of the uppermost *Emaciaticeras emaciatum* AB (samples P-5 to P-2) was dominated by gymnospermous pollen. This is largely due the high relative abundances of *Classopollis classoides* in this interval. *Classopollis classoides* was the most abundant continental palynomorph throughout. By contrast, samples P-7, P-6 and P-1 exhibited high levels of marine influence (Fig. 2.13), largely due the dominance of *Luehndea spinosa* (Figs. 2.11; Table S3.1).

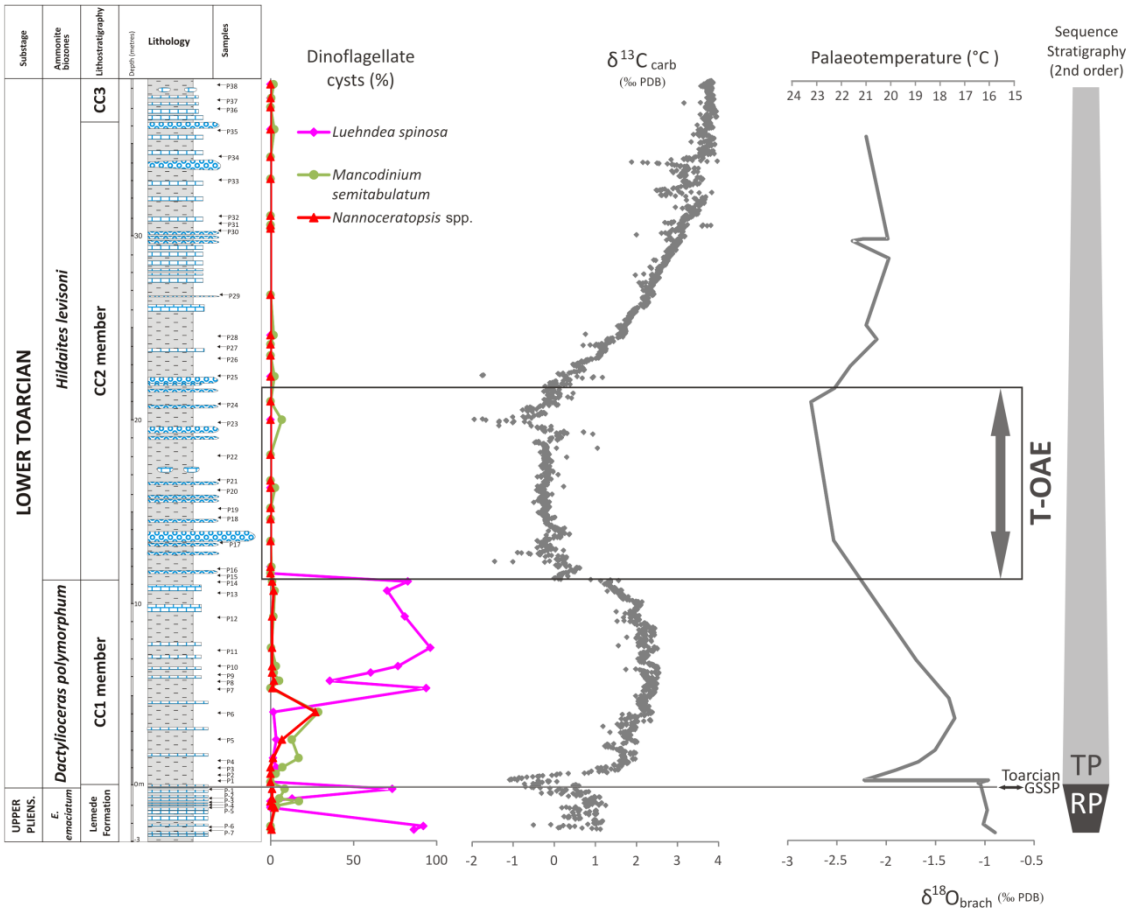

Figure 2.11. Dinoflagellate cyst relative abundances, the $\delta^{13}C_{carb}$ record, the temperature profile based on $\delta^{18}O$ and the sequence stratigraphy of the uppermost Pliensbachian (*Emaciaticeras emaciatum* AB) and lower Toarcian (*Dactylioceras polymorphum* and *Hildaites levisoni* ABs) in the Peniche section, western Portugal. The first (left hand) column depicts the relative proportions of the dinoflagellate cysts *Luehndea spinosa*, *Mancodinium semitabulatum* and *Nannoceratopsis* spp. expressed as a percentage of the overall marine palynofloras. The second column depicts the carbon isotope ($\delta^{13}C_{carb}$) record of Hesselbo et al. (2007). The third column represents temperature profile inferred from the $\delta^{18}O$ record of Suan et al. (2008a). The fourth (right hand) column illustrates the sequence stratigraphy of Duarte (2007); two second order cycles are illustrated. TP = transgressive phase; RP = regressive phase.

4.3.2. The Dactylioceras polymorphum *AB (samples P1 to P14)*

Fourteen horizons (P1–14) were sampled from the earliest Toarcian *Dactylioceras polymorphum* AB, representing the CC1 member of the Cabo Carvoeiro Formation (Fig. 2.11). The lowermost sample (P1) proved devoid of palynomorphs. By contrast, the overlying 13 samples all yielded relatively abundant palynomorph associations (Table S3.1). The dinoflagellate cyst floras proved similar to those from the underlying *Emaciaticeras emaciatum* AB. However, the high relative abundances (73.3%) of *Luehndea spinosa* observed in the uppermost Lemede Formation (subsection 4.3.1) abruptly decreased to between 1.5% and 3.4% in the lowermost Toarcian (samples P2 to P6; Table S3.1). This phenomenon was termed the Pliensbachian-Toarcian boundary event (Littler et al., 2010; Korte et al., 2015). Here, the most abundant dinoflagellate cyst was *Mancodinium semitabulatum*, which attained 28.7% in sample P6. *Nannoceratopsis* spp. also increased in relative abundance in samples P4 to P6; in the latter horizon this genus represented 27%. In sample P7, *Luehndea spinosa* massively increased to 93.8% and this dominance continued to the top of the *Dactylioceras polymorphum* AB (82.7% in sample P14). The latter occurrence represented the range top of this species. The maximum value was 96.2% in sample P11 (Table S3.1). The signature of the latter peak occurrence, together with 82.7% in sample P14, is virtually identical to that observed in the northern Lusitanian Basin at Maria Pares and Vale das Fontes (Fig. 2.14). Between samples P7 and P14, where *Luehndea spinosa* was dominant, *Mancodinium semitabulatum*, *Nannoceratopsis gracilis* and *Nannoceratopsis senex* were present in low proportions. *Nannoceratopsis gracilis* exhibited significant intraspecific variability (Plate 2.3 (4–7)), and *Nannoceratopsis ambonis* and *Scriniocassis weberi* were recorded in extremely low numbers in samples P9 and P10 (Table S3.1). The latter is a gonyaulacacean species and a marker for the late Pliensbachian to Aalenian (Woollam and Riding, 1983; Davies, 1985; Feist-Burkhardt and Wille, 1992; Poulsen and Riding, 2003).

Miscellaneous marine palynomorphs (i.e. acritarchs, foraminiferal test linings and prasinophytes) in the *Dactylioceras polymorphum* AB were similar to those from the underlying *Emaciaticeras emaciatum* AB. The acritarchs included *Micrhystridium* spp. and *Polygonium jurassicum*, and were sporadically common. Prasinophytes were intermittent and sparse, but slightly more diverse than in the underlying samples, with

Cymatiosphaera sp. cf. *C. pachytheca*, clumps of *Halosphaeropsis liassica* and *Tasmanites* spp. present. *Halosphaeropsis liassica* is characteristic of the early Toarcian (Mädler, 1968; Bucefalo Palliani and Riding, 2000). Foraminiferal test linings occurred throughout in significant proportions in samples P8 and P9 (Fig. 2.12, Table S3.1).

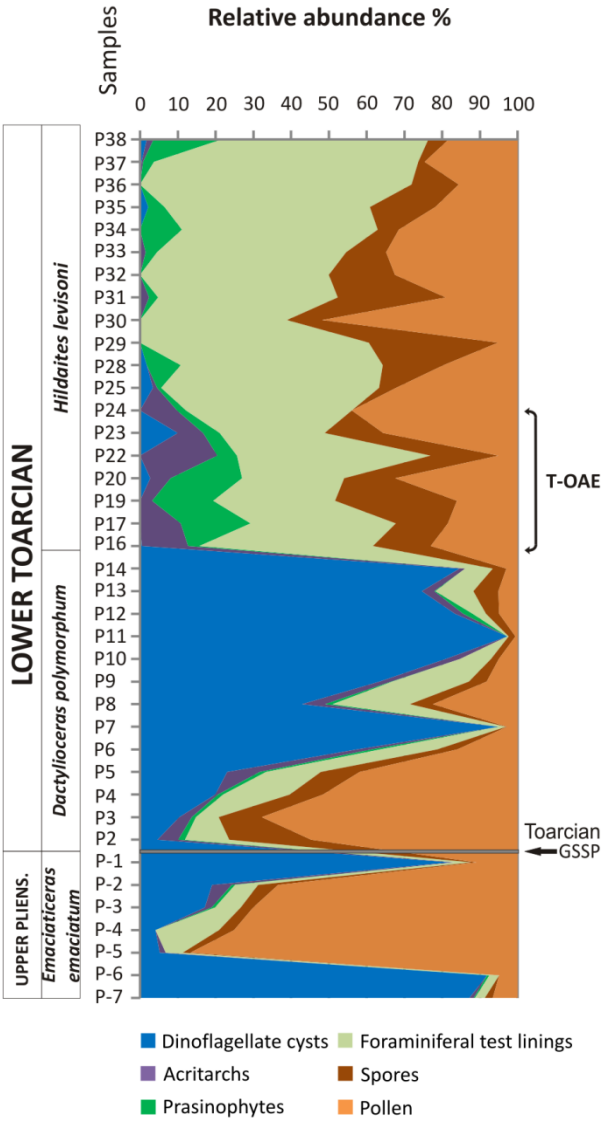

Figure 2.12. The relative abundances of the six palynomorph groups, expressed as percentages of the overall palynoflora, from the uppermost Pliensbachian (*Emaciaticeras emaciatum* AB) and the lower Toarcian (*Dactylioceras polymorphum* and *Hildaites levisoni* ABs) of the Peniche section, western Portugal. Note that the samples P1, P15, P18, P21, P26 and P27 are entirely devoid of palynomorphs, and were not illustrated here in order to achieve better visualisation of the marine palynobiotas. Toarcian GSSP = Toarcian Global boundary Stratotype Section and Point.

Pteridophyte spores proved moderately diverse with *Calamospora tener*, *Concavisporites granulosus*, *Cyathidites* spp., *Kraeuselisporites reissingeri*, *Leptolepidites* spp. and *Osmundacidites wellmanii* present. These normally occurred in low numbers, but *Kraeuselisporites reissingeri* attained 9.5% in sample P2. The gymnosperm pollen comprised *Alisporites* spp., *Araucariacites australis*, *Cerebropollenites macroverrucosus*, *Classopollis classoides*, *Exesipollenites* spp. and *Spheripollenites* spp. The latter was present throughout the lower Toarcian. As in the

underlying AB, *Classopollis classoides* remained the most abundant terrestrial palynomorph in the lower part of this interval (samples P2 to P6 and P8). Its relative abundance decreased in the upper part of the *Dactylioceras polymorphum* AB. Therefore, terrestrial palynomorphs rapidly diminished upsection, due to the decrease in *Classopollis classoides* and the increase of *Luehndea spinosa*, leading to a strong marine influence in this part of the section (Figs. 2.12, 2.13; Table S3.1).

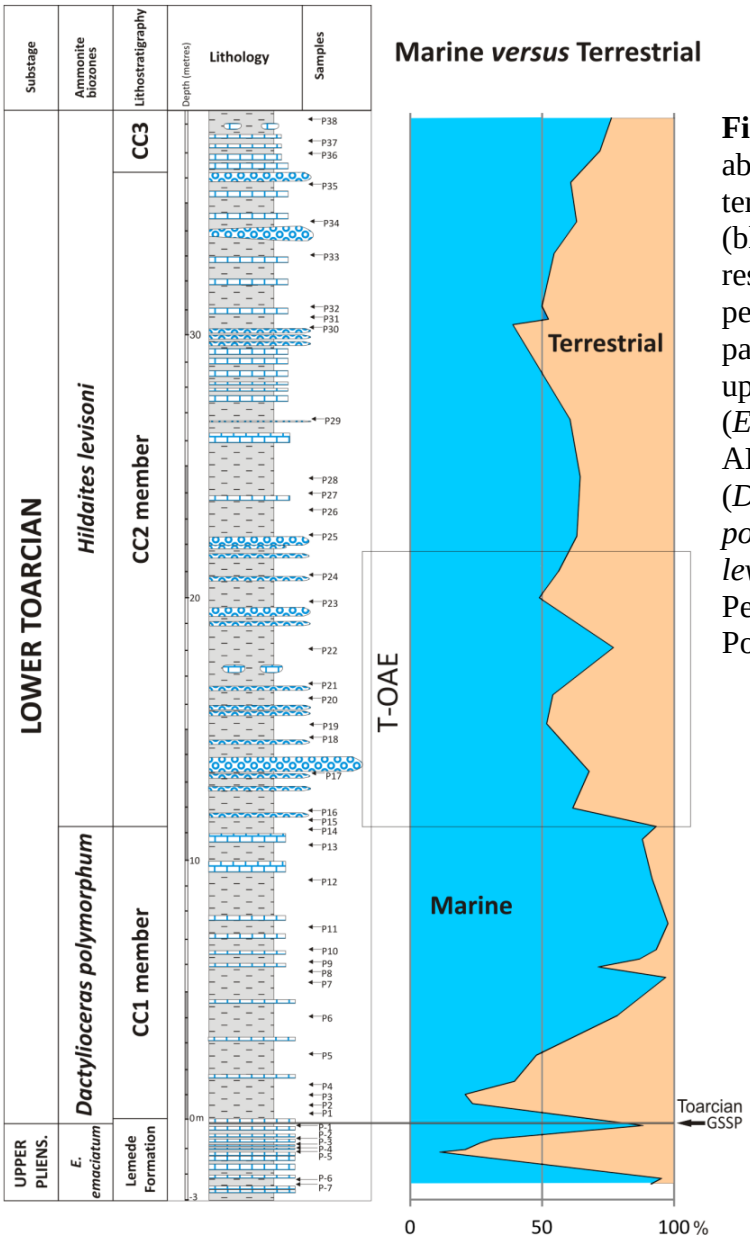

Figure 2.13. The relative abundance of marine and terrestrial palynomorphs (blue and brown shading respectively), expressed as percentages of the overall palynoflora from the uppermost Pliensbachian (*Emaciaticeras emaciatum* AB) and lower Toarcian (*Dactylioceras polymorphum* and *Hildaites levisoni* ABs) of the Peniche section, western Portugal.

4.3.3. The Hildaites levisoni *AB (samples P15 to P38)*

The *Hildaites levisoni* AB was most intensively sampled in this study, with 24 horizons collected from the CC2 and base of CC3 members of the Cabo Carvoeiro Formation (Fig. 2.11). All of these proved sparse, except P15, P18, P21, P26 and P27 which were barren (Table S3.1). The T-OAE is present in this succession, and is represented by samples P15 to P24 (Figs. 2.11–2.14). The dinoflagellate cyst associations were extremely low in diversity and relative proportions throughout the *Hildaites levisoni* AB. Only *Mancodinium semitabulatum* (samples P16–P38) and *Mendicodinium microscabratum* (samples P23 and P25) were recorded. *Mancodinium semitabulatum* attained 6.7% of the palynobiota in sample P23 in the CC2 member, and was the only dinoflagellate cyst species present in the CC3 member. *Mendicodinium microscabratum* was encountered in low proportions from the middle of the *Hildaites levisoni* AB (Table S3.1). *Mendicodinium microscabratum* was recorded from the *Hildaites levisoni* and *Hildoceras bifrons* ABs of the northern Lusitanian Basin. *Mendicodinium microscabratum* was documented in the earliest Toarcian of central Italy by Bucefalo Palliani et al. (1997b) and in the early Toarcian of Peniche by Davies (1985) as *Mendicodinium* sp. A. *Luehndea spinosa*, *Nannoceratopsis* spp. and *Scriniocassis weberi* were absent throughout the *Hildaites levisoni* AB. This scenario is entirely consistent with coeval successions in the northern Lusitanian Basin.

The miscellaneous microplankton taxa throughout this succession are rather conservative. The acritarch associations were similar to those in the two underlying ABs. *Micrhystridium* sp. and *Polygonium jurassicum* were present sparsely in the *Hildaites levisoni* AB. However, acritarchs were significantly more frequent in the lowermost T-OAE than in the overlying recovery succession (Fig. 2.12). In particular, they represented 20.5% of the palynobiota in sample P22 (Table S3.1). The prasinophyte associations of the *Hildaites levisoni* AB were similar in taxonomic composition to those in the underlying *Dactylioceras polymorphum* AB, except that *Cymatiosphaera* sp. cf. *C. pachytheca* was absent. However, prasinophytes were substantially more prevalent than in either of the two underlying ABs. Within the *Hildaites levisoni* AB these distinctive palynomorphs, which largely comprised *Halosphaeropsis liassica* and *Tasmanites* spp., were markedly more common in the T-OAE interval than in the overlying succession (Fig. 2.12). They were most common in P17 (18.5%), P19 (16.2%) and P20 (18.9%) (Table S3.1).

Plate 2.3. Selected dinoflagellate cysts from the uppermost Pliensbachian and lower Toarcian of the Peniche section of the Lusitanian Basin, western Portugal. All specimens are housed in the collections of the LNEG (Portuguese Geological Survey), S. Mamede de Infesta, Portugal. The sample number, slide number and England Finder coordinates are provided. All the scale bars represent 20 μm.

1. *Luehndea spinosa* Morgenroth 1970. Lower Toarcian (*Dactylioceras polymorphum* AB), sample P9, slide 1, X37. Oblique lateral view, high focus. Note the cingulum and the antapical (1"") plate.
2. *Luehndea spinosa* Morgenroth 1970. Lower Toarcian (*Dactylioceras polymorphum* AB), sample P12, slide 1, N27/4. Dorsal view, high focus. Note the uninterrupted cingulum.
3. *Luehndea spinosa* Morgenroth 1970. Upper Pliensbachian (*Emaciaticeras emaciatum* AB), sample P-6, slide 1, H28/2. Oblique dorsal view, high focus. Note the uninterrupted cingulum and the antapical (1"") plate.
4. *Nannoceratopsis gracilis* Alberti 1961. Lower Toarcian (*Dactylioceras polymorphum* AB), sample P6, slide 1, D45/4. Left lateral view. Note the rounded ventral antapical horn.
5. *Nannoceratopsis gracilis* Alberti 1961. Lower Toarcian (*Dactylioceras polymorphum* AB), sample P6, slide 1, G28/3. Right lateral view. Note the short dorsal antapical horn and the less pronounced ventral antapical horn.
6. *Nannoceratopsis gracilis* Alberti 1961. Lower Toarcian (*Dactylioceras polymorphum* AB), sample P6, slide 1, G20/4. Right lateral view. Note the long dorsal antapical horn.
7. *Nannoceratopsis gracilis* Alberti 1961. Lower Toarcian (*Dactylioceras polymorphum* AB), sample P10, slide 1, Q20/4. Right lateral view. Note the moderate width, comparing with the specimens in 4, 5 and 6.
8. *Nannoceratopsis ambonis* Drugg 1978. Lower Toarcian (*Dactylioceras polymorphum* AB), sample P10, slide 1, T25/3. Left lateral view. Note the prominent, thick sagittal rim.
9. *Nannoceratopsis senex* van Helden 1977. Upper Pliensbachian (*Emaciaticeras emaciatum* AB), sample P-4, slide 1, M50/3. Left lateral view. Note the single antapical horn.
10. *Mancodinium semitabulatum* Morgenroth 1970. Lower Toarcian (*Dactylioceras polymorphum* AB), sample P6, slide 1, O27/4. Dorsal view, high focus. Note the anterior sulcal plate (the sulcal tongue) and the well-preserved precingular plates (the 1" and 7") which are involved in the formation of the 'disintegration' style archaeopyle.
11. *Scriniocassis weberi* Gocht 1964. Lower Toarcian (*Dactylioceras polymorphum* AB), sample P9, slide 1, R36/1. Dorsal view, high focus. Note the coarse reticulum and the 2P archaeopyle.
12. *Mendicodinium microscabratum* Bucefalo Palliani et al. 1997. Lower Toarcian (*Hildaites levisoni* AB), sample P23, slide 1, L24/4. Dorsal view. Note the microscabrate autophragm and the epicystal archaeopyle.

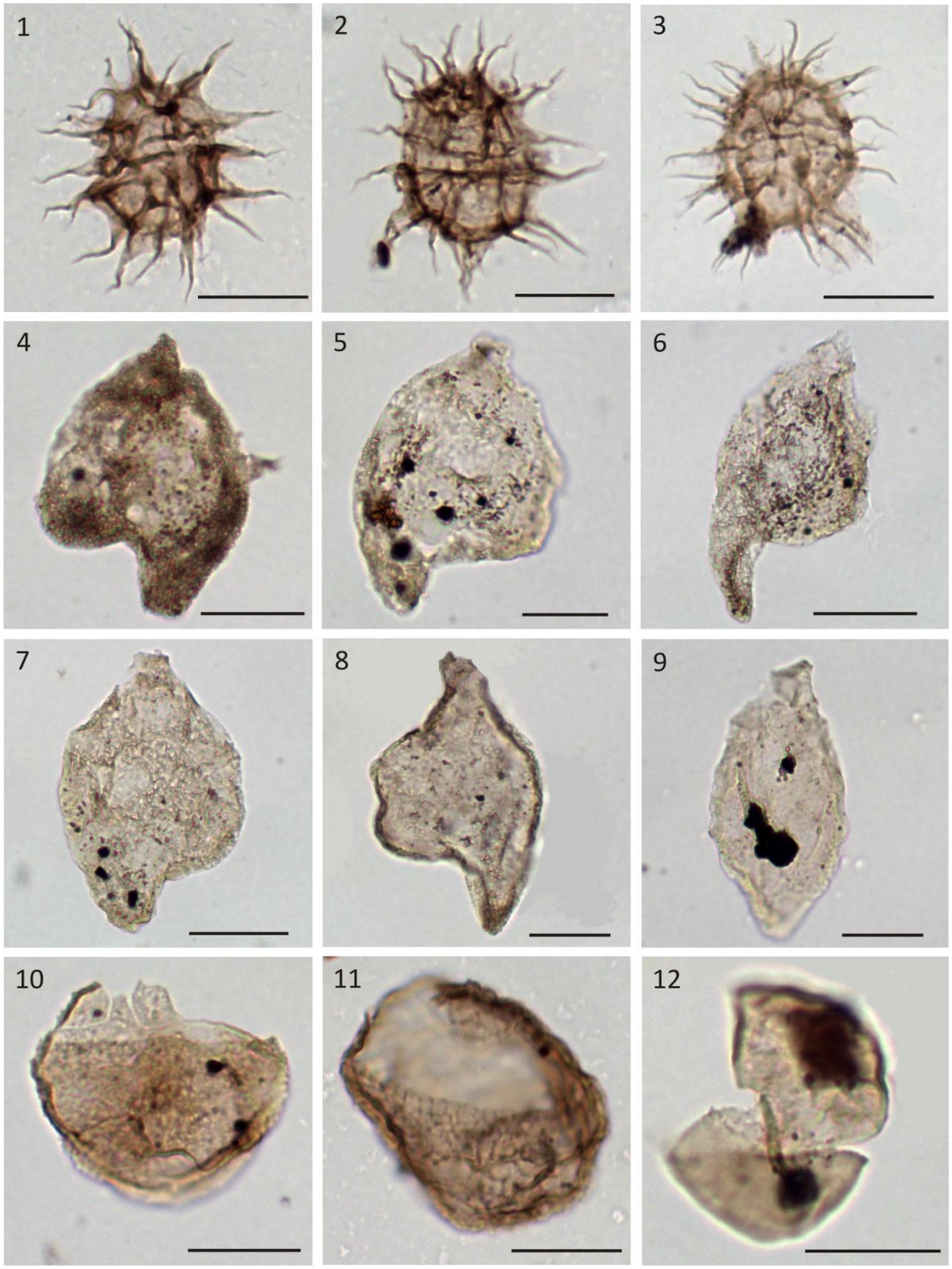

Plate 2.3 (caption on previous page)

Plate 2.4. Selected palynomorphs from the uppermost Pliensbachian and lower Toarcian of the Peniche section of the Lusitanian Basin, western Portugal. All specimens are housed in the collections of the LNEG (Portuguese Geological Survey), S. Mamede de Infesta, Portugal. The sample number, slide number and England Finder coordinates are provided. All the scale bars represent 20 μm.

1. *Polygonium jurassicum* Bucefalo Palliani et al. 1996. Lower Toarcian (*Dactylioceras polymorphum* AB), sample P5, slide 1, J25/3.
2. *Polygonium jurassicum* Bucefalo Palliani et al. 1996. Lower Toarcian (*Dactylioceras polymorphum* AB), sample P6, slide 1, T38.
3. *Polygonium jurassicum* Bucefalo Palliani et al. 1996. Lower Toarcian (*Hildaites levisoni* AB), sample P16, slide 1, G43/2.
4. *Micrhystridium* sp. Lower Toarcian (*Hildaites levisoni* AB), sample P38, slide 1, T46.
5. Indeterminate acritarch. Lower Toarcian (*Hildaites levisoni* AB), sample P17, slide 1, V48.
6. *Cymatiosphaera* sp. cf. *C. pachytheca* Eisenack 1957. Lower Toarcian (*Dactylioceras polymorphum* AB), sample P13, slide 1, F34/3.
7. *Osmundacidites wellmanii* Couper 1953. Lower Toarcian (*Dactylioceras polymorphum* AB), sample P3, slide 1, O64.
8. *Striatella* sp. Lower Toarcian (*Hildaites levisoni* AB), sample P25, slide 1, B33.
9. *Concavisporites granulosus* Tralau 1968. Lower Toarcian (*Hildaites levisoni* AB), sample P16, slide 1, T46/4.
10. *Cerebropollenites macroverrucosus* (Thiergart 1949) Schulz 1967. Upper Pliensbachian (*Emaciaticeras emaciatum* AB), sample P-4, slide 1, T35/3.
11. Foraminiferal test lining. Lower Toarcian (*Hildaites levisoni* AB), sample P23, slide 1, N47/4.
12. Foraminiferal test lining. Lower Toarcian (*Hildaites levisoni* AB), sample P23, slide 1, X23/4.

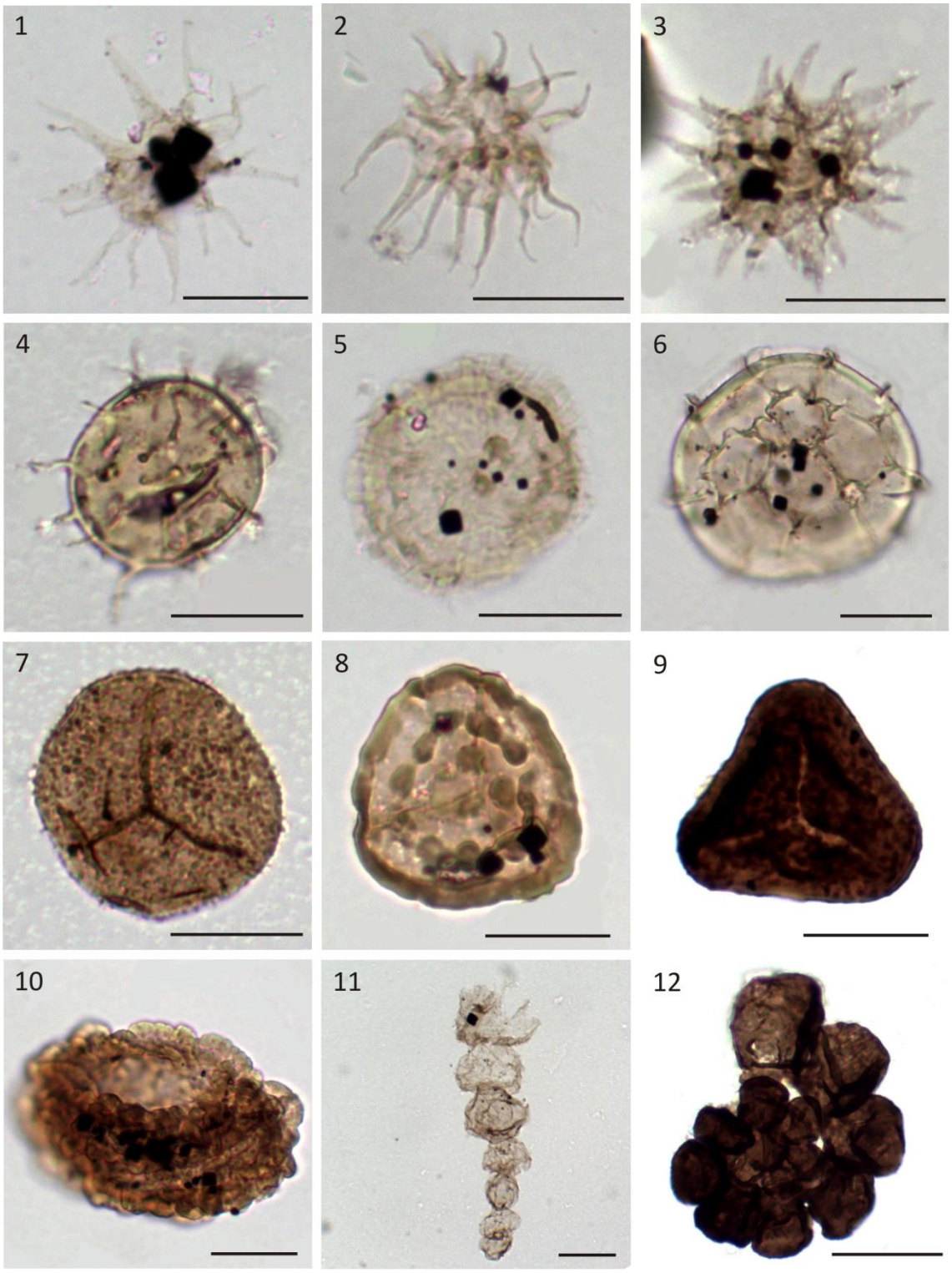

Plate 2.4 (caption on previous page)

These relative proportions never attained the very high relative abundances of prasinophytes observed in coeval strata at the Maria Pares section in the northern Lusitanian Basin. Foraminiferal test linings were present in high relative abundances throughout. The relative proportions were generally higher in the samples above the T-OAE (Fig. 2.12); the maximum was 71.9% in P36 (Table S3.1).

The pteridophyte spores from the *Hildaites levisoni* AB included *Concavisporites granulosus*, *Cyathidites* spp., *Ischyosporites variegatus*, *Kraeuselisporites reissingeri*, *Leptolepidites* spp. and *Todisporites granulatus*. Generally, spores were slightly more common in this AB, for example 34.2% in sample P29 and 28.6% in P31. The gymnosperm pollen comprised the same six taxa recorded in the underlying *Dactylioceras polymorphum* AB. However, *Alisporites* spp., *Araucariacites australis* and *Cerebropollenites macroverrucosus* proved extremely sporadic. By contrast, *Classopollis classoides*, *Exesipollenites* spp. and *Spheripollenites* spp. were much more consistent (Table S3).

In summary, in the *Hildaites levisoni* AB, dinoflagellate cysts were relatively sparse. However, the relative abundance of foraminiferal test linings and prasinophytes considerably increased; prasinophytes were especially prominent in the T-OAE interval. But overall, the marine influence was diminished in comparison with the underlying *Dactylioceras polymorphum* and *Emaciaticeras emaciatum* ABs (Fig. 2.13). The percentages of spores and pollen in the *Hildaites levisoni* AB were markedly higher than in the middle and upper parts of the underlying *Dactylioceras polymorphum* AB, but were lower than in the lowermost part of the overall succession studied (Figs. 2.12, 2.13; Table S3).

4.4. Overview of the uppermost Pliensbachian to middle Toarcian palynostratigraphy of the Lusitanian Basin

This relatively low diversity dinoflagellate cyst assemblage at Maria Pares, Vale das Fontes and Peniche sections is entirely consistent with a late Pliensbachian to early Toarcian age (Woollam and Riding, 1983; Feist-Burkhardt and Wille, 1992; Riding and Thomas, 1992; Bucefalo Palliani and Riding 2003; Poulsen and Riding 2003). The taxa encountered were *Luehndea spinosa*, *Mancodinium semitabulatum*, *Mendicodinium microscabratum*, *Mendicodinium spinosum* subsp. *spinosum*, *Mendicodinium* sp., *Nannoceratopsis ambonis*, *Nannoceratopsis gracilis*, *Nannoceratopsis senex* and *Sriniocassis weberi*. The most abundant, and stratigraphically diagnostic, species was

Luehndea spinosa which occurs throughout the *Emaciaticeras emaciatum* and *Dactylioceras polymorphum* ABs. Its range is late Pliensbachian to earliest Toarcian (e.g. Poulsen and Riding, 2003, fig. 3). This occurrence confirms the age of the MLLF member and the uppermost Lemede Formation and the CC1 member. *Nannoceratopsis* spp. were also confined to the *Emaciaticeras emaciatum* and *Dactylioceras polymorphum* ABs. The three species recorded here range from the Pliensbachian to Bajocian (e.g. Morgenroth, 1970; Wiggan et al., 2017). By contrast, *Mancodinium semitabulatum* was present throughout the entire successions studied. This species has a Pliensbachian to Bajocian range in Europe (Woollam and Riding, 1983; Feist-Burkhardt and Götz, 2016; Wiggan et al., 2017).

The consistent presence of significant levels of terrestrial palynomorphs indicates a marine depositional setting relatively close to continental sources. The most abundant continental palynomorph recorded throughout the three sections was *Classopollis classoides* (Tables S1, S2, S3.1). *Classopollis* is a gymnosperm pollen genus produced by plants belonging to the extinct Mesozoic conifer family Cheirolepidiaceae (Francis, 1983). These were thermophilic and xerophytic conifers that tolerated semiarid conditions, and lived in both coastal and upland environments (Pocock and Jansonius, 1961; Batten, 1975; Filatoff, 1975; Srivastava, 1976). These plants covered large areas, but their abundance declined sharply with increasing palaeolatitude (Vakhrameev, 1981; Riding et al. 2013). *Classopollis* have previously been reported from the Lower Jurassic of the Lusitanian Basin by Davies (1985), Oliveira et al. (2007a) and Barrón et al. (2013). The presence of *Classopollis classoides*, and the absence of *Callialasporites*, is a characteristic of the late Sinemurian to early Toarcian interval (Helby et al. 1987; Quattrocchio et al., 2011). *Spheripollenites* spp. was present throughout the Toarcian and this long-ranging pollen genus was also recorded from the Pliensbachian to Aalenian of the Lusitanian Basin by Davies (1985). The bryophyte spore *Kraeuselisporites reissingeri* is also present in the three successions studied here, between *Emaciaticeras emaciatum* to *Hildaites levisoni* the ABs (Tables S1, S2, S3.1). The range of this species is Late Triassic to Early Jurassic (Rhaetian–early Sinemurian) of northwest Europe according to Morbey (1978) and Morbey and Dunay (1978). However, Barrón et al. (2010) reported *Kraeuselisporites reissingeri* from the Toarcian–Aalenian succession (the Aalenian GSSP) at Fuentelsaz, Spain. The non-dinoflagellate cyst palynomorphs are entirely consistent with an Early Jurassic age (e.g. Srivastava, 1987; 2011; Weiss, 1989; Ziaja, 2006).

5. The effects of the Toarcian Oceanic Anoxic Event (T-OAE)

In this section the palaeoecological and palaeobiological effects caused by the T-OAE on the palynofloras, especially on dinoflagellate cysts, are discussed. Firstly and in particular in the Peniche section (Fig. 2.15), and secondly in the Lusitanian Basin in general, comparing these data with coeval European basins (Figs 2.16, 2.17).

5.1. Peniche section, as an extensive studied section

The dinoflagellate cyst record at Peniche section is analysed, and interpreted in conjunction with previous studies on Early Jurassic calcareous nannofossils (Fig. 2.15). The previous extensive and detailed studies in this succession, integrated with the present work, allow us to recognised four planktonic phases (Fig. 2.15; Table 2.1). The digital supplementary Table S3.2 give the marine taxa percentages of the overall marine palynobiota. These percentages of the overall marine grains were used in Fig. 2.15, in order to compare the dinoflagellate cysts with nannofossils abundance variations, excluding the terrestrial input.

Table 2.1. A concise summary of the four plankton phases recognised herein, which are described in detail in section 5. The *Emaciaticeras emaciatum*, *Dactylioceras polymorphum* and *Hildaites levisoni* ABs are abbreviated to *E.e.*, *D.p.* and *H.l.* respectively in column 2. The temperatures are taken from Suan et al. (2008a). The grey shading represents a brief warm period in the earliest Toarcian.

Phase	Palaeoecological plankton response	Age (and biozone)	Samples	Palaeotemperature	Notes
4	Plankton crisis	Early Toarcian (*H.l.*)	P15 to P38	warm/hot (ca. 20-24°C)	Plankton 'blackout' (during and after T-OAE)
3	Earliest Toarcian plankton abundance	Early Toarcian (*D.p.*)	P6 to P14	cool (ca. 17-19°C)	Abundant *Luehndea spinosa*
2	Recovery of dinoflagellates from the earliest Toarcian warming	Early Toarcian (*D.p.*)	P2 to P5	cooling (ca. 20-17°C)	Recovery of dinoflagellate populations
Event	Earliest Toarcian warming	Earliest Toarcian	P1	warming (ca. 16-21°C)	No palynomorphs
1	Latest Pliensbachian plankton abundance	Latest Pliensbachian (*E.e.*)	P-7 to P-1	cool (ca. 16°C)	Abundant *Luehndea spinosa*

5.1.1. Plankton phase 1 (samples P-7 to P-1)

In this interval, the most prominent dinoflagellate cyst in the uppermost Pliensbachian was *Luehndea spinosa*. Two relative abundance peaks were present, which are indicative of maximum marine influence (Figs. 2.13, 2.15). Mattioli et al. (2008) studied coeval calcareous nannofossils from the section, and found that the upper

Emaciaticeras emaciatum AB is characterised by abundant biota. These include prominent *Schizosphaerella*, a probably calcareous dinoflagellate cyst genus (Bown, 1987), which exhibited three relative abundance peaks (Fig. 2.15). Therefore, plankton phase 1 is termed the 'latest Pliensbachian plankton abundance' (Fig. 2.15; Table 2.1).

The late Pliensbachian was a relatively cool interval, with temperatures between 10 and 20 °C throughout the Laurasian Seaway in western Europe (Korte and Hesselbo, 2011; Korte et al., 2015, fig. 2). Specifically, in the *Emaciaticeras emaciatum* AB of the Lusitanian Basin, $\delta^{18}O_{brachiopod}$ values from diagenetically resistant material indicate temperatures of ~16 °C (Fig. 2.11; Table 2.1; Suan et al., 2008a). Moreover, $\delta^{18}O_{belemnite}$ and Mg/Ca data from northern Spain indicate that late Pliensbachian water masses cooled and became significantly more saline (van de Schootbrugge et al., 2005). It therefore appears that *Luehndea spinosa*, the other dinoflagellate cysts and the probably calcareous dinoflagellate cyst *Schizosphaerella* thrived in the relatively cool, saline waters of the Iberian Peninsula at this time. Relatively diverse dinoflagellate cyst assemblages in the Mesozoic and Cenozoic frequently appear to have preferred relatively cool waters (e.g. Head et al., 2001; Bowman et al., 2013; Hennissen et al., 2017). Furthermore, significant migrations towards the equator from high latitudes are known to have occurred during cold intervals (e.g. Sluijs et al., 2005; Prauss, 2006; Riding and Michoux, 2013).

5.1.2. Plankton phase 2 (samples P2 to P5)

The uppermost sample (P-1) from the 'latest Pliensbachian plankton abundance phase', was dominated by the dinoflagellate cysts *Luehndea spinosa* and *Mancodinium semitabulatum*. By contrast, the overlying sample (P1), proved barren. At this horizon, negative $\delta^{13}C$ and $\delta^{18}O$ excursions occur (Fig. 2.11; Hesselbo et al., 2007; Suan et al., 2008a; Korte et al., 2015). These indicate an abrupt environmental change, including a rise in temperature, which appear to have adversely affected the dinoflagellates. The calcareous nannofossils were similarly affected (Fig. 2.15; Mattioli et al., 2008). However, *Luehndea spinosa*, *Mancodinium semitabulatum* and *Nannoceratopsis* spp., reappeared in low relative abundances in the immediately overlying strata in the *Dactylioceras polymorphum* AB (samples P2–P5). This recovery from the brief earliest Toarcian warming in sample P1 was gradual and sustained during the lower part of the *Dactylioceras polymorphum* AB (Figs. 2.11, 2.15). The recovery of calcareous

nannofossils was more rapid, with a significant relative abundance peak in the lower *Dactylioceras polymorphum* AB (Fig. 2.15). These increases in plankton appear to have been driven by cooling temperatures (Korte et al., 2015, fig. 2). The abrupt and brief warming immediately above the Pliensbachian-Toarcian boundary apparently triggered a sharp decrease in phytoplankton, but did not cause a general biotal crisis. In the benthic fossil record in the Lusitanian Basin, the Pliensbachian-Toarcian transition is characterised by an increase in the relative abundances of foraminifera and ostracods (Pinto, 2008; Rita et al., 2016, figs. 6, 8). This phase is therefore referred to as the 'recovery of dinoflagellates from the earliest Toarcian warming' event (Fig. 2.15; Table 1).

5.1.3. Plankton phase 3 (samples P6 to P14)

In this phase, between sample P6 to the uppermost *Dactylioceras polymorphum* AB (sample P14), there was a pronounced increase in dinoflagellate cyst relative abundances. This was caused by an increase in *Luehndea spinosa* (Fig. 2.11; Table S3.2). This trend is consistent with the northern Lusitanian Basin where the relative abundance of *Luehndea spinosa* in the middle and upper *Dactylioceras polymorphum* AB appears to have correlative significance (Fig. 2.14). This increase is apparently due to the continuing decrease in temperatures during the earliest Toarcian (Korte et al., 2015, fig. 2). As in the *Emaciaticeras emaciatum* AB, the relatively cool conditions favoured *Luehndea spinosa*, which was a typical northern Europe, cool-adapted, form (Riding, 1987; Riding and Hubbard, 1999; Riding et al., 1999; Bucefalo Palliani and Riding, 2000). The $\delta^{18}O_{brachiopod}$ of the *Dactylioceras polymorphum* AB at Peniche indicates water temperatures between 16 and 20°C (Fig. 2.11; Table 2.1; Suan et al., 2008a). The high relative abundances of *Luehndea spinosa* in the *Emaciaticeras emaciatum* and *Dactylioceras polymorphum* ABs of the Lusitanian Basin can be explained by favourable ecological conditions for this species in this region, principally cool seawater. However, salinity fluctuations and the early Toarcian transgressive event may also have been influential. Duarte et al. (2004, 2007), Duarte (2007) and Pittet et al. (2014) identified an early Toarcian transgressive event in the Lusitanian Basin that may have enhanced the dominance of dinoflagellate cysts during the middle and upper parts of *Dactylioceras polymorphum* AB (Figs 2.7, 2.9, 2.11, 2.14) Mattioli et al. (2008) interpreted the calcareous nannofossils from this interval as cool-adapted.

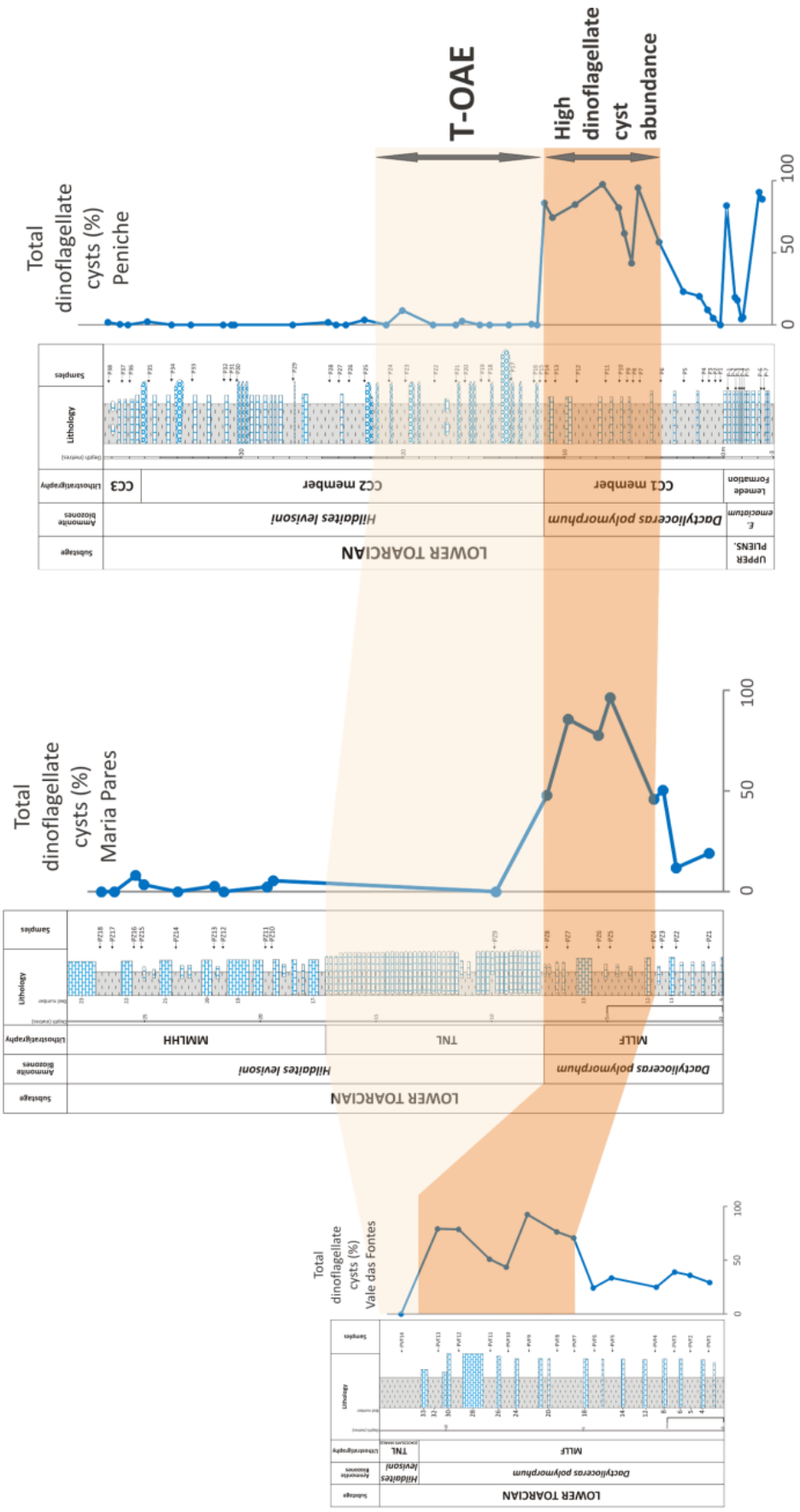

Figure 2.14. The uppermost Pliensbachian to lower Toarcian dinoflagellate cyst relative abundances, expressed as percentages of the overall palynoflora, observed at Peniche, (right hand column), Maria Pares (central column) and Vale das Fontes (left hand column) in Lusitanian Basin, western Portugal. The dark shaded interval denotes the correlation of the maximum relative abundance of dinoflagellate cysts in the upper part of the *Dactylioceras polymorphum* AB, immediately below the T-OAE in the Lusitanian Basin.

The Toarcian species of *Nannoceratopsis* were also typically cold water forms (Riding and Hubbard, 1999; Riding et al., 1999). However, in the Lusitanian Basin, *Nannoceratopsis gracilis* and *N. senex* were present in both the *Emaciaticeras emaciatum* and *Dactylioceras polymorphum* ABs in low relative abundances, compared to *Luehndea spinosa* (Fig. 2.11; Table S2). It is possible that the nutrient and salinity levels were not optimal for *Nannoceratopsis* spp., but were favourable for *Luehndea spinosa*. *Mancodinium semitabulatum* was a more cosmopolitan species (Bucefalo Palliani and Riding, 2003; Mantle and Riding, 2012), and hence was apparently not influenced by low temperatures and rising sea levels as the other dinoflagellate cyst taxa were.

The calcareous nannofossil and dinoflagellate cyst records during this interval in the Lusitanian Basin are strikingly similar (Fig. 2.15; Mattioli et al., 2008). Both were abundant during the middle part of *Dactylioceras polymorphum* AB, before decreasing in the upper part. However, the dinoflagellate cysts did not decline as fast as the calcareous nannofossils in the upper *Dactylioceras polymorphum* AB. Hence, we hypothesise that a rise in sea level, with a consequent increase in the area of continental shelf, and relatively low seawater temperatures led to the high bioproductivity of phytoplankton in the Lusitanian Basin at this time. Plankton phase 3 is therefore termed the 'earliest Toarcian plankton abundance' (Fig. 2.15; Table 1).

5.1.4. Plankton phase 4 (samples P15 to P38)

The lowermost sample from this phase, P15 (*Hildaites levisoni* AB), entirely lacked palynomorphs (Table S3.1). This horizon is coincident with the inception of the T-OAE in the Lusitanian Basin (Hesselbo et al., 2007; Suan et al., 2008b; 2010). This major environmental perturbation lies between samples P15 and P24, as indicated by $\delta^{13}C$ data (Fig. 2.11; Hesselbo et al., 2007; Suan et al., 2008a). From this point, the relative abundance of dinoflagellate cysts sharply decreased as compared to the progressive increase in the underlying *Dactylioceras polymorphum* AB (Figs. 2.11, 2.12, 2.14, 2.15). This dinoflagellate cyst 'blackout' appears to be related to the significant environmental changes associated with the T-OAE. The oxygen reduction close to the sediment-water interface occasionally reached the photic zone (Mattioli et al., 2008), and hence would have profoundly affected plankton productivity. Cyst-

forming dinoflagellates are affected by bottom water anoxia, which completely inhibits excystment in the benthic zone. Moreover, hypoxia reduces the rate of germination in modern dinoflagellates (Anderson et al. 1987; Kremp and Anderson 2000). The dinoflagellate cyst 'blackout' during the T-OAE has also been discussed by Loh et al. (1986), Prauss (1989), Prauss et al. (1991), Bucefalo Palliani and Riding (1999b) and Bucefalo Palliani et al. (2002).

Mattioli et al. (2008, 2013) reported that when $\delta^{13}C$ values began to decrease in the T-OAE, the densities of calcareous nannofossils drastically declined, and they remained low during the entire T-OAE interval and above it. Furthermore, Fraguas et al. (2012) described a significant calcareous nannofossil extinction event associated with the temperature increase at the *Dactylioceras tenuicostatum–Harpoceras serpentinum* AB boundary. Hence, the calcareous nannofossil record is analogous and coeval with the response of dinoflagellate cysts to the T-OAE, and these floras are similar to those from the northern Lusitanian Basin (Fig. 2.14). The calcareous nannofossil abundance decrease during the T-OAE has also been recorded in France, Germany, central Italy and northern Spain (Bucefalo Palliani and Mattioli, 1998; Mattioli et al., 2008; Fraguas et al., 2012). However, in these areas, the abundance of calcareous nannofossils increased after the T-OAE. Throughout Europe, except western Portugal, the recolonisation of calcareous nannofossils after this environmental perturbation coincides with dinoflagellate cyst floras, for which the record became re-established in the *Hildoceras bifrons* AB (Bucefalo Palliani et al., 2002). Calcareous nannoplankton is meroplanktonic, and thus is heavily dependent on conditions in the water column. Thecate (motile) dinoflagellates are largely confined to the photic zone, but their resting cysts are benthic and non-motile (Dale, 1983). This means that cyst-producing dinoflagellates are also highly sensitive to the ecology of the benthic zone. It is remarkable that, despite their different life cycles, the 'phytoplankton blackout' is recorded by both these planktonic groups, indicating that the profoundly stressed conditions associated with the T-OAE affected both the water column and the sea bed (Bucefalo Palliani et al., 2002). For this reason, plankton phase 4 is named the 'plankton crisis' (Fig. 2.15; Table 1).

The seawater temperatures in the Lusitanian Basin during the *Hildaites levisoni* AB were generally higher (20–24°C) than in the *Dactylioceras polymorphum* AB (16–21°C) (Table 1; Suan et al., 2008a). The abrupt low levels of dinoflagellate cysts at the base of the *Hildaites levisoni* AB coincided with a rise in temperature (Fig. 2.11). After

the T-OAE, temperatures diminished slightly, but the relative abundances of dinoflagellate cysts remained very low. Van de Schootbrugge et al. (2005) also demonstrated the relationship between dinoflagellate cyst relative abundances with temperature and salinity, using belemnite Mg/Ca and $\delta^{18}O$ from material from northern Spain. Their data demonstrate high dinoflagellate cyst relative abundances before the T-OAE in cool and high salinity marine settings. During the T-OAE seawater temperatures rapidly rose, and the salinity and dinoflagellate cyst relative abundances decreased, as in the Lusitanian Basin. In addition to the anoxia and the rise in temperatures, low salinity may be another abiotic factor that helps to explain the dinoflagellate cyst 'blackout'. Mattioli et al. (2008) suggested that the high levels of the calcareous nannofossil genus *Calyculus* during the T-OAE, together with low relative abundances of calcareous nannofossils, are due to a decrease in salinity. *Calyculus* is an atypical genus because it is characteristic of stressed environments. The relatively low salinities may be due a southward current of low density water from the Arctic into the Tethys (Bjerrum et al., 2001) or increased continental runoff (Röhl et al., 2001).

Either or both these factors would have enhanced stratification and, consequently, anoxia. The replacement of calcareous nannofossils and dinoflagellates, which were both abundant in the *Dactylioceras polymorphum* AB, for prasinophytes (Bucefalo Palliani et al., 2002; Mattioli and Pittet, 2004; van de Schootbrugge et al., 2005) also indicates low salinity surface waters. Prasinophytes are an opportunistic group of green algae, which do not necessarily require a sustained benthic phase in their life cycle (Tappan, 1980). The non-motile stage of their life cycle, the phycomata, is typically relatively short (Tappan 1980, p. 809). This gives them a significant competitive advantage (through rapid to exponential reproduction rates) if the benthos is compromised by anoxia, and nutrients are sporadically supplied to the surface waters from deeper levels in the water column. Prasinophytes have been referred to as 'disaster taxa' and first evolved in the less well oxygenated Proterozoic and Palaeozoic ocean surfaces (Falkowski et al., 2004; van de Schootbrugge et al., 2013).

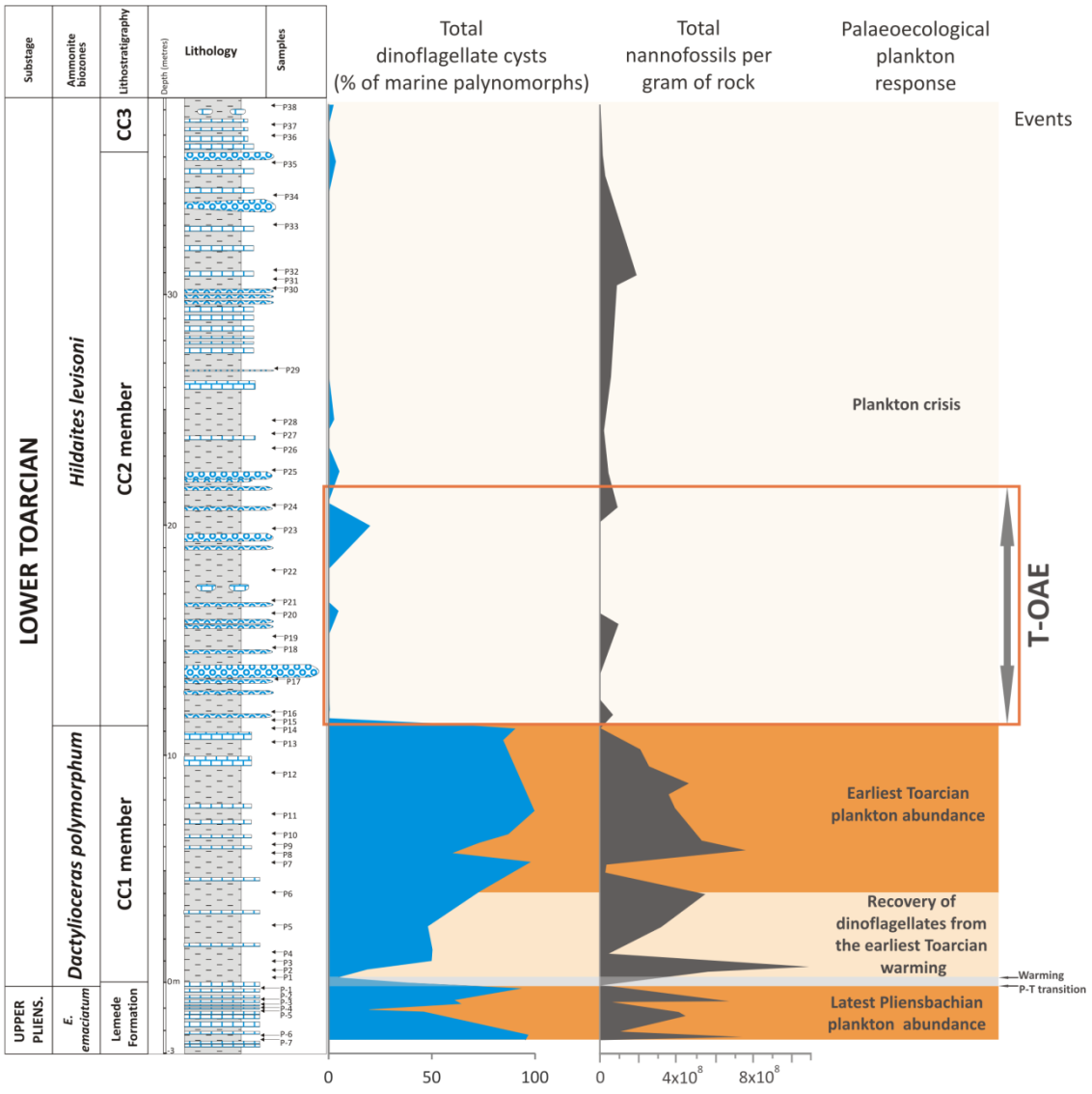

Figure 2.15. The total dinoflagellate cysts expressed as a percentage of the overall marine palynobiota plotted against the total calcareous nannofossils per gram of rock (taken from Mattioli et al., 2008) in the uppermost Pliensbachian (*Emaciaticeras emaciatum* AB) to the lower Toarcian (*Hildaites levisoni* AB) at Peniche, western Portugal. The four plankton phases described in section 5 are also plotted against the two microfossil records.

The apparent extinction of the dinoflagellate cyst *Luehndea spinosa* appears to be directly related to the stressed environmental conditions associated with the T-OAE. The higher relative abundances of this species in the latest Pliensbachian and earliest Toarcian are related to relatively low seawater temperatures (Fig. 2.11; Table 1). As a typical north European species, *Luehndea spinosa* preferred relatively low temperatures and was apparently stressed to extinction by the sudden temperature rise in the *Hildaites levisoni* AB. As for *Luehndea spinosa*, changes in seawater temperature appeared to have caused important alterations in other planktonic groups. For example, Peti and Thibault (2017) documented small average sizes of *Schizosphaerella* during the T-OAE interval in the Paris Basin. These data suggest that the *Schizosphaerella* size fluctuations are correlated with climatic change, with the smaller average size being a response to the warmer conditions.

Nannoceratopsis was also absent in the *Hildaites levisoni* AB; this is consistent with the northern Lusitanian Basin (Figs. 2.7, 2.9). Thus, *Nannoceratopsis* did not recolonise the Lusitanian Basin following the T-OAE in the *Hildaites levisoni* and the *Hildoceras bifrons* ABs. By contrast, Bucefalo Palliani and Riding (2003, fig. 3) documented *Nannoceratopsis gracilis* and *N. senex* in the *Harpoceras serpentinum* AB, following the T-OAE. This disappearance of *Luehndea spinosa* and *Nannoceratopsis* spp. during this event in the Lusitanian Basin indicates differences between the T-OAE in western Portugal compared to elsewhere in Europe, where the dinoflagellate cyst populations recovered relatively rapidly. The recovery elsewhere was due to the floras recolonising shelfal areas from shallow water intertidal/littoral refugia where tidal action prevented the development of anoxia. It appears that, in the Lusitanian Basin, which was in a relatively enclosed position (Fig. 2.16), environmental conditions were especially stressful during the T-OAE. Therefore, the vertical extent of anoxia may have been more extensive, probably attaining the photic zone. On the other hand, it seems likely that seawater temperatures were very high and/or salinity was lowered more than elsewhere in Europe. Only the cosmopolitan dinoflagellate cyst *Mancodinium semitabulatum* and *Mendicodinium microscabratum*, which had an isolated and sparse occurrence, survived during the T-OAE at Peniche. *Mancodinium semitabulatum* was present, albeit sporadically and in low numbers, throughout the entire succession in the three ABs studied herein and hence appears to be a highly resilient species (Figs. 2.7, 2.9, 2.11).

In the Lusitanian Basin, other fossil groups became extinct. These include brachiopods (Comas-Rengifo et al., 2013; 2015), some species of calcareous nannofossils (Perilli and Duarte, 2006) and the metacopinid ostracods (Cabral et al., 2011; 2013). Alternatively, others, such as the calcareous nannofossil *Discorhabdus ignotus* (see Mattioli et al., 2013), were temporarily restricted to refugia, due to the hostile environmental conditions associated with the T-OAE. At Peniche, Rita et al. (2016, fig. 9) reported an interval devoid of benthic foraminifera only at the middle *Hildaites levisoni* AB, coincident with the end of the $\delta^{13}C$ negative excursion. In the upper part of the *Hidaites levisoni* AB, after the reestablishment of favourable oxygenated marine environments, the apparent decrease of seawater temperatures, and normal levels of nutrients and salinity, these groups recovered (Pinto, 2008; Comas-Rengifo et al., 2013, 2015; Rita et al., 2016). In this study, the barren interval for foraminifera of Rita et al. (2016) coincides with samples P23 and P24. Both these samples yielded foraminiferal test linings (Table S3.1). The reason for this apparent disparity is not obvious. It is possible that the foraminifera here did not attain maturity; foraminiferal test linings only represent small morphotypes which cannot presently be linked to their agglutinated and/or calcareous counterparts (Stancliffe 1996).

Foraminiferal test linings were relatively abundant throughout the *Hildaites levisoni* AB (Fig. 2.12; Table S3.1). This is not deemed to be the result of preservation bias mitigating against the presence of dinoflagellate cysts under anoxic conditions. The reason why foraminiferal test linings are common in this interval may be due to a combination of their adaptability and relative mobility, coupled with the concomitant reduction in dinoflagellate cysts. These remains of benthic foraminifera could have survived the effects of bottom water anoxia by rapid adaptation (Hart et al. 2003; Reolid et al. 2014).

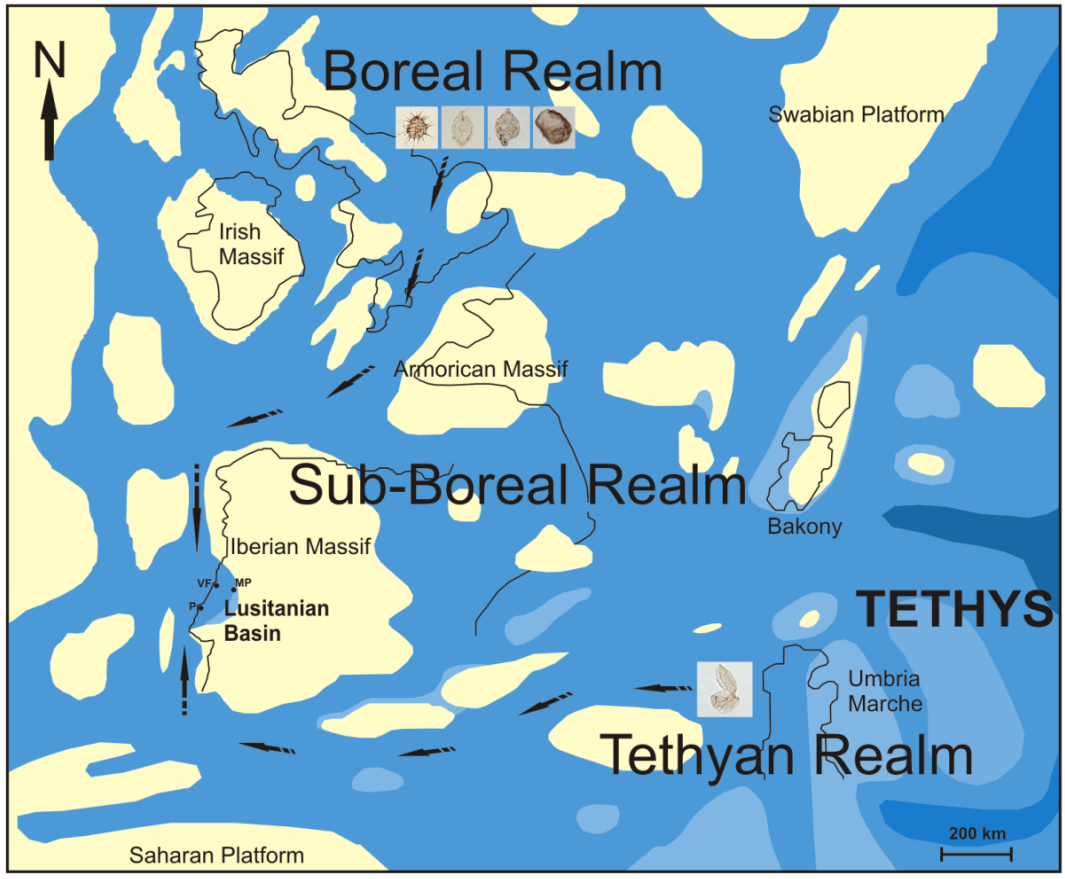

Key:

- Emergent areas (in the Jurassic)
- Deep marine waters
- Shallow marine waters
- Open ocean
- Dinoflagellate migrations
- Present day emergent areas
- *Luehndea spinosa*
- *Nannoceratopsis senex*
- *Nannoceratopsis gracilis*
- *Scriniocassis weberi*
- *Mendicodinium* spp.
- Location of the sections studied:
  MP: Maria Pares
  VF: Vale das Fontes
  P: Peniche

Figure 2.16. The Toarcian palaeogeography of the western Tethys region, modified from Thierry and Barrier (2000), with the interpreted dinoflagellate migrations between the Boreal and Tethyan Realms depicted; these are explained in subsection 6.3.

5.2.Lusitanian Basin: comparison with coeval European basins

The T-OAE significantly suppressed all biotas, especially benthic ones, due to intense bottom water anoxia. This event directly caused some extinctions (Harries and Little, 1999; Bucefalo Palliani et al., 2002; Caswell et al., 2009; Caswell and Coe, 2012; 2013). In the Lusitanian Basin, the T-OAE caused the virtual disappearance of all dinoflagellate cyst taxa, including the extinction of *Luehndea spinosa*, within the lowermost part of the *Hildaites levisoni* AB. This disappearance event and the extinction of *Luehndea spinosa* are consistent with other northern Europe and mediterranean basins (Figs. 2.7, 2.9, 2.11, 2.17). Clearly the dinoflagellate assemblage was responding to a major palaeoenvironmental change.

In north of Europe (Boreal Realm), the dinoflagellate cyst record became re-established in the *Hildoceras bifrons* AB by floras returning from refugia in the littoral zone when marine environments became re-oxygenated (Fig. 2.17; Bucefalo Palliani et al., 2002). Furthermore, there was significant speciation in north of Europe and surrounding regions at this time (Riding, 1984c; Riding et al., 1991; 1999). This renewal and diversification did not occur in the Lusitanian Basin and throughout the southern Europe (Tethyan Realm) basins (Fig. 2.17; Bucefalo Palliani and Riding, 2003). An example of this is that *Nannoceratopsis gracilis* and *N. senex* are absent immediately above the T-OAE in the Lusitanian Basin (Figs. 2.7, 2.9, 2.11, 2.17). Farther north, these species quickly became re-established in the *Harpoceras falciferum* AB (Fig. 2.17; Riding, 1987, fig. 3; Bucefalo Palliani and Riding, 2000, fig. 3).

The range top of *Luehndea spinosa* throughout Europe is within the *Dactylioceras polymorphum* AB or equivalent (Figs. 2.2, 2.17). This bioevent was observed slightly stratigraphically higher, in the uppermost part of the *Dactylioceras polymorphum* AB, in the Lusitanian Basin (Figs. 2.7, 2.9, 2.11, 2.17). The dinoflagellate cyst disappearance event or 'blackout' appears to occur slightly earlier in the southern Europe when calibrated to the early Toarcian ammonite biostratigraphy (Figs. 2.2, 2.17). This may be indicative of preservational artefacts and/or there may be some minor diachroneity between the ammonite zones of the southern province and further north. Apparently only *Mancodinium semitabulatum* recolonised the Lusitanian Basin in the *Hildaites levisoni* and *Hildoceras bifrons* ABs (Figs. 2.7, 2.9, 2.11, 2.17). Bucefalo Palliani and Riding (2003, fig. A3.4) documented the occurrence of *Nannoceratopsis gracilis* and *N. senex* in the *Harpoceras falciferum* AB, following the T-OAE throughout Europe. However, although it was a cosmopolitan genus,

Nannoceratopsis did not recolonise the Lusitanian Basin during the lower–middle Toarcian (Fig. 2.17).

In summary, phytoplankton, i.e. calcareous nannofossils and dinoflagellates, was dramatically adversely affected by anoxia and increased temperatures during the T-OAE in the Lusitanian Basin. Both groups declined abruptly in the lowermost part of the *Hildaites levisoni* AB (Figs. 2.11, 2.12, 2.14, 2.15; Mattioli et al., 2008). However, unlike the benthic groups, and calcareous nannofossils and dinoflagellates elsewhere in Europe (Fig. 2.17), the phytoplankton apparently did not recover after the T-OAE during the upper part of the *Hidaites levisoni* AB. This marked disparity is highly intriguing; plankton groups are generally one of the pioneers in recolonisation following ecological crises (e.g. Eshet et al., 1995). This scenario is somewhat counterintuitive as consumers and predators in the trophic structure require primary producers (i.e. phytoplankton). Nevertheless, it appears that microplankton were more severely affected by the anoxia, and changes in temperature and salinity, than at least some of the higher trophic levels in the Lusitanian Basin. Of these abiotic factors, in the case of dinoflagellate populations, anoxia is deemed to have been most influential as this entirely inhibits excystment (Anderson et al. 1987; Martindale and Aberhan 2017). Temperature may also have been a highly influential factor, and probably was the major cause of the demise of *Luehndea spinosa*. Dinoflagellates have specific temperature windows where excystment is possible (Kremp and Anderson 2000, fig. 5). Many dinoflagellates may have (or have had) light and salinity preferences, but these factors largely tend only to reduce germination rates (Anderson et al. 1987). The relatively enclosed position of the Lusitanian Basin during the Toarcian, preventing the reestablishment of marine circulation patterns at this time (Fig. 2.16), could also contributed to this long recovery phase of the plankton from the effects of the T-OAE in this area (Fig. 2.17).

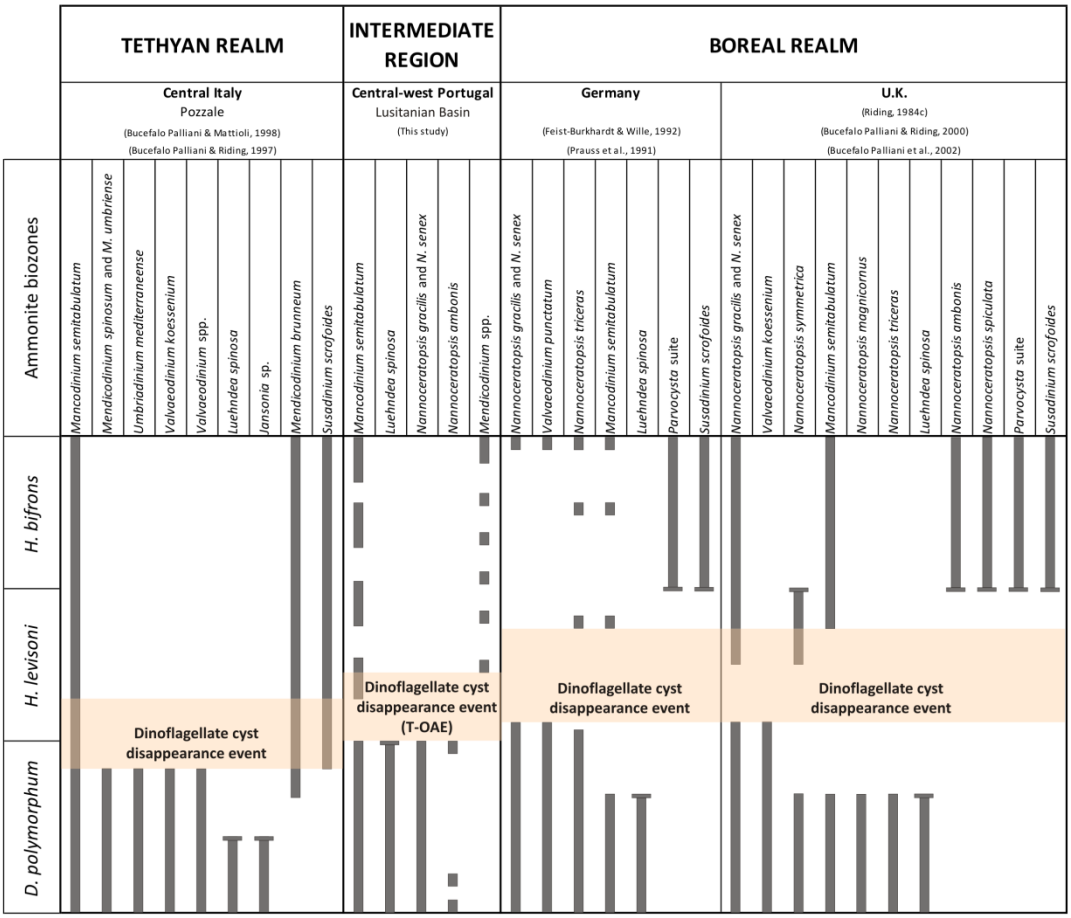

Figure 2.17. A comparison of the stratigraphical ranges of selected dinoflagellate cysts from the lower and middle Toarcian (*Dactylioceras polymorphum* to *Hildoceras bifrons* ABs or their equivalents) of the major European basins. In the Tethyan Realm (southern Europe), the ranges are based on data from central Italy. Data from Germany and U.K. are depicted for the Boreal Realm (northern Europe). The dinoflagellate floras recorded in the present study from the northern Lusitanian Basin may represent an intermediate region between the two realms. Note that the extremities of ranges with horizontal bars represent true range bases and tops (i.e. inceptions and apparent extinctions respectively) as appropriate. The range extremities which lack horizontal bars represent interruptions to known stratigraphical ranges.

6. The Pliensbachian and Toarcian dinoflagellate cyst provincialism of the northern hemisphere

6.1. Overview of provincialism during the Pliensbachian and Toarcian

In the Mesozoic of Europe, two palaeogeographical realms are recognised; these are the northerly Boreal Realm and the Tethyan Realm to the south (Arkell, 1956; Hallam, 1969; Reid, 1973). An intermediate area, the Sub-Boreal region, separates these major biotic provinces. This transitional area comprises southern France, Hungary, Portugal and Spain, and it exhibits faunal/floral characteristics of both the Boreal and Tethyan realms (Figs. 2.16, 2.17; Bucefalo Palliani and Riding, 1997a; 2003).

There are major differences between Pliensbachian and early Toarcian dinoflagellate cyst assemblages from the Boreal and Tethyan realms. In northern Europe, *Luehndea spinosa*, *Mancodinium semitabulatum* and several species of *Nannoceratopsis* are dominant within relatively diverse assemblages which may also include *Scriniocassis* and *Valvaeodinium* (Figs. 2.16, 2.17; Morgenroth, 1970; Riding, 1984c; Riding and Thomas, 1992; Riding et al., 1999; Bucefalo Palliani and Riding, 2000; 2003). However, *Nannoceratopsis* is the most prominent genus throughout the Boreal Realm (e.g. Riding et al., 1991; Bucefalo Palliani et al., 2002). The typically late Toarcian *Parvocysta* suite (including *Susadinium scrofoides*) of Riding (1984) had its inception in the *Hildoceras bifrons* AB, and significantly diversified during the remainder of the Toarcian and the early Aalenian (Wille, 1982a,b; Riding et al., 1991; 1999; Butler et al., 2005; Feist-Burkhardt and Pross, 2010).

The Tethyan counterparts are significantly different. The dinoflagellate cysts from Pliensbachian and lower Toarcian successions in this more southerly region, which includes Greece, central Italy and surrounding regions, are relatively low in diversity. *Mancodinium semitabulatum* is present, together with *Umbriadinium mediterraneense* and relatively common and diverse *Mendicodinium* spp. and *Valvaeodinium* spp. (Figs. 2.16, 2.17; Bucefalo Palliani et al., 1997b; Bucefalo Palliani and Riding, 1997a; 1999a; 2003, figs. 3, A2.1). While *Mancodinium semitabulatum*, *Mendicodinium* spp. and *Valvaeodinium* spp. are all cosmopolitan, their occurrence, especially when the latter two genera are diverse and prominent, is characteristically Tethyan. The former is a circum-Tethyan genus (Mantle and Riding, 2012). The *Parvocysta* complex is effectively absent, and genera such as *Luehndea* and *Nannoceratopsis* are relatively scarce and sporadic.

6.2. The Pliensbachian and Toarcian dinoflagellate cysts of the Sub-Boreal Realm

Dinoflagellate cysts from the Pliensbachian and Toarcian of the Sub-Boreal region have been studied in southern France, Hungary and Portugal. The palynology of the upper Pliensbachian of Quercy, southwest France was examined by de Vains (1988) and Bucefalo Palliani and Riding (1997a). De Vains (1988, fig. 8) provided presence/absence data for seven samples. She recorded *Luehndea spinosa*, *Mancodinium semitabulatum*, *Mancodinium* sp., *Mendicodinium* spp., *Nannoceratopsis* spp. and *Scriniocassis weberi*. Bucefalo Palliani and Riding (1997a) reported semi-quantitative data for the upper Pliensbachian of the Quercy area and a slightly more diverse assemblage. The flora is dominated by *Mendicodinium* spp. and *Nannoceratopsis* spp., together with a smaller contribution of *Luehndea spinosa* and *Mancodinium semitabulatum*.

The first study on the Jurassic dinoflagellate cysts of Hungary was by Baldanza et al. (1995). These authors worked on the phytoplankton from the upper Pliensbachian and lower Toarcian succession of Reka Valley in the Mecsek Mountains of southwest Hungary. They encountered a relatively diverse flora comprising the genera *Luehndea*, *Mancodinium*, *Mendicodinium*, *Nannoceratopsis*, *Umbriadinium* and *Valvaeodinium* (Baldanza et al., 1995, figs. 4, 6). The two assemblages from the uppermost Pliensbachian were totally dominated by *Luehndea cirilliae*, *L. spinosa*, *Nannoceratopsis gracilis* and *N. senex*, with low proportions (6%) of *Mendicodinium* spp. By contrast, the three lower Toarcian samples were more diverse. *Luehndea* spp. (56%) continued their dominance, but *Nannoceratopsis* spp. comprised 16% of the assemblage, considerably less than in the latest Pliensbachian (49%). Also present were *Mendicodinium* spp. (15%), *Valvaeodinium* spp. (10%) and *Umbriadinium mediterraneense* (3%). *Mancodinium semitabulatum* proved rare, and was only observed in the lowermost Toarcian (Baldanza et al., 1995, fig. 4). Bucefalo Palliani and Riding (2003, fig. A2.5) recorded a relatively diverse association from the lower Toarcian of Urkut, Hungary including *Luehndea cirilliae*, *L. spinosa*, *Mendicodinium* spp., *Nannoceratopsis gracilis*, *Scriniocassis* spp, *Umbriadinium mediterraneense* and *Valvaeodinium* spp. *Mendicodinium* and *Valvaeodinium* were by far the most common genera. Recently, Baranyi et al. (2016) examined 35 samples from the lower Toarcian (*Dactylioceras tenuicostatum* to *Hildoceras bifrons* ABs) of the Reka Valley. In this study, *Luehndea* and *Nannoceratopsis* totally dominated the *Dactylioceras tenuicostatum* AB (assemblages 1 and 2). *Luehndea* spp. were confined to assemblage

1, but *Nannoceratopsis* spp. reappeared in the *Hildoceras bifrons* AB, following the T-OAE.

6.3. Upper Pliensbachian and middle Toarcian marine palynofloras of the Lusitanian Basin in a regional context

The earliest research on the Jurassic marine palynology of Portugal was by Davies (1985). This author provided presence/absence data for several localities of the Lusitanian Basin and identified forms such as *Dapcodinium priscum, Luehndea* sp., *Mancodinium semitabulatum, Mendicodinium* spp., *Nannoceratopsis* spp. and *Scriniocassis* spp. Semiquantitative dinoflagellate cyst data were presented for the Pliensbachian to lower Toarcian succession of the Lusitanian Basin by Bucefalo Palliani and Riding (2003). *Luehndea* spp., *Mancodinium semitabulatum* and *Mendicodinium* spp. were reported.

Nevertheless, the most detailed work on the Lower Jurassic palynology of the Lusitanian Basin is the present contribution. The uppermost Pliensbachian and lower Toarcian dinoflagellate cyst floras recorded here in the Lusitanian Basin were relatively low in diversity with only five genera, *Luehndea*, *Mancodinium*, *Mendicodinium*, *Nannoceratopsis* and *Scriniocassis*. *Luehndea spinosa* was by far the dominant species. By comparison with elsewhere in Europe (Morgenroth, 1970; Riding, 1987; Bucefalo Palliani and Riding, 1997a,b; 2000; 2003; Bucefalo Palliani et al., 1997a,b), the youngest occurrence of *Luehndea spinosa* in the Lusitanian Basin is apparently slightly diachronous (Fig. 2.17). This is probably due to a slight miscorrelation of the Tethyan and Sub-Boreal ammonite zonations. *Mancodinium semitabulatum* and *Nannoceratopsis* spp. were distinctly subordinate but occasionally relatively common below the T-OAE. On the other hand, *Mendicodinium microscabratum*, *Nannoceratopsis ambonis* and *Scriniocassis weberi* all proved sporadic and rare. Other taxa which have been reported from coeval strata in the southern part of the Sub-Boreal Realm, such as *Umbriadinium mediterraneense* and *Valvaeodinium* spp. were not encountered here (e.g. Baldanza et al., 1995). The floras are broadly comparable with coeval biotas from northern Europe and Russia (e.g. Riding, 1987; Feist-Burkhardt and Wille, 1992; Riding et al., 1999). Hence, the dominance of *Luehndea spinosa*, *Mancodinium semitabulatum* and *Nannoceratopsis* spp. during the late Pliensbachian to early Toarcian appears to be relatively persistent from northern Siberia throughout

northern Europe to the Lusitanian Basin. Thus, the low species richness flora dominated by *Luehndea, Mancodinium* and *Nannoceratopsis* in the Lusitanian Basin appears to be more typical of the Boreal than the Tethyan Realm. However, *Nannoceratopsis* is more diverse in the Boreal Realm than further south. For example *Nannoceratopsis deflandrei* subsp. *anabarensis, N. spiculata, N. raunsgaardii* and *N. triceras* are confined to the Boreal Realm (Fig. 2.17; Bucefalo Palliani and Riding, 2003). Furthermore, high diversities of *Mendicodinium*, as *M. umbriense* and *M. brunneum*, together with characteristically Tethyan species such as *Umbriadinium mediterraneense* and *Valvaeodinium hirsutum*, do not appear to be present in the Lusitanian Basin.

Therefore, unsurprisingly, the Sub-Boreal region appears to be an intermediate area which exhibits biotic aspects of both the Boreal and Tethyan realms. For example, dinoflagellate cyst assemblages are typically more diverse than further southeast in the Tethys, but *Mendicodinium* and *Valvaeodinium* are more prominent than in the Boreal Realm (Bucefalo Palliani and Riding, 1999a). The prominence of *Luehndea spinosa* in the late Pliensbachian and earliest Toarcian of Hungary and Portugal may be geographically restricted to southern Europe, representing a slightly lower latitudinal assemblage than southern France, where it is less common. The floras from the uppermost Pliensbachian at Quercy are dominated by *Nannoceratopsis* (Bucefalo Palliani and Riding, 1997a, fig. 3), which is a typically Boreal phenomenon. An alternative, and probably more plausible, explanation of the striking relative abundance of *Luehndea spinosa* in the upper Pliensbachian to lowermost Toarcian strata, immediately underlying the T-OAE, in the Lusitanian Basin is that it migrated from the Boreal Realm, following southward expansion of cold water masses, and thrived in the western part of the Sub-Boreal Realm (Fig. 2.16). It is also possible that the relatively low diversity associations in the Lusitanian Basin reflect its relatively isolated position from the rest of the Sub-Boreal Realm and Tethys due to the emergent Iberian Massif (Fig. 2.16). This is supported by the absence of typically Tethyan taxa such as *Umbriadinium mediterraneense* and *Valvaeodinium* spp. This study has also highlighted the fact that *Mancodinium semitabulatum* occurs throughout the Pliensbachian and Toarcian of the northern hemisphere, and appears to have been an effective recoloniser following the T-OAE in the Lusitanian Basin (Fig. 2.17).

In conclusion, the Boreal dinoflagellate cysts *Luehndea spinosa*, *Nannoceratopsis senex, N. gracilis* and *Scriniocassis weberi*, and the Tethyan genus *Mendicodinium*, may have migrated at this time to the intermediate Sub-Boreal Realm,

where the Lusitanian Basin and the studied sections were located (Fig. 2.16). *Mancodinium semitabulatum* is interpreted as having a very wide biogeographical range. The dinoflagellate cyst assemblage described here from the Lusitanian Basin presents therefore a combination of the aforementioned taxa (Fig. 2.17).

7. Conclusions

The three uppermost Pliensbachian and lower Toarcian successions of Maria Pares, Vale das Fontes and Peniche in the Lusitanian Basin was extensively sampled for palynological analysis; 103 samples were collected from the *Emaciaticeras emaciatum*, *Dactylioceras polymorphum*, *Hildaites levisoni* and *Hildoceras bifrons* ABs.

Seven dinoflagellate cyst species were recognised: *Luehndea spinosa*, *Mancodinium semitabulatum*, *Mendicodinium microscabratum*, *Nannoceratopsis ambonis*, *Nannoceratopsis gracilis*, *Nannoceratopsis senex* and *Scriniocassis weberi*. They were largely present in the *Emaciaticeras emaciatum* and *Dactylioceras polymorphum* ABs, and the most abundant taxon was *Luehndea spinosa*. The stratigraphically highest occurrence of *Luehndea spinosa* was at the top of *Dactylioceras polymorphum* AB, immediately before the T-OAE. *Luehndea spinosa* was a cold water taxon. It appears to have tracked the southerly movement of cold water from the Boreal Realm, and thrived in the western Sub-Boreal Realm which was somewhat isolated at this time due to the emergent Iberian Massif. *Luehndea spinosa* is also biostratigraphically significant, and its presence confirms the age of the uppermost Lemede Formation and the MLLF and CC1 members as established by ammonite faunas. The remainder of the palynoflora is entirely compatible with a latest Pliensbachian to early Toarcian age.

In terms of biotic provincialism, the dinoflagellate cyst floras from Lusitanian Basin, which is in the Sub-Boreal Realm, unsurprisingly exhibit some characteristics of the Boreal Realm to the north and the Tethyan Realm to the south. The associations from Lusitanian Basin most closely resemble coeval floras from elsewhere in the Sub-Boreal Realm such as Hungary, but not southern France.

The principal aim of this work was to analyse the response of marine palynoflora to the T-OAE. Prior to the T-OAE, in the *Emaciaticeras emaciatum* and *Dactylioceras polymorphum* ABs dinoflagellates thrived throughout the Lusitanian Basin with the exception of the relatively warm earliest Toarcian period. The recovery from this event

was relatively rapid, and cool temperatures were re-established. This interval was dominated by the cool water dinoflagellate cyst *Luehndea spinosa*.

The TNL and MMLHH members ate Maria Pares and Vale das Fontes, and the CC2 and lowermost CC3 members at Peniche, sampled here represent the T-OAE and the immediately overlying strata. This succession is characterised by a virtual 'blackout' of dinoflagellate cysts, which were largely replaced by opportunistic prasinophytes. Calcareous nannofossils were also badly disrupted at this time. The massive reduction in relative abundance of dinoflagellate cysts, and the rise of prasinophytes, in this interval reflects the effects of the T-OAE, and is termed the plankton crisis. The bottom water and water column anoxia, significantly elevated temperatures, and reduced salinities, badly affected the dinoflagellate life cycle which includes a benthic resting cyst. The prasinophytes do not necessarily need a benthic phase during their life cycle. Of these factors, anoxia was possibly most important as this entirely inhibits the excystment of dinoflagellates. Temperature was also a highly important factor, at least in the specific case of the *Luehndea spinosa* extinction, as the correlation between its relative abundance and seawater temperature changes is clearly show by our data. By contrast to *Luehndea spinosa*, *Mancodinium semitabulatum* was a successful recoloniser. The low numbers of dinoflagellate cysts following the T-OAE strongly indicates a long recovery phase, probably caused by especially stressful environmental conditions during the T-OAE in the Lusitanian Basin, enhanced by the relative enclosed position of this depocentre.

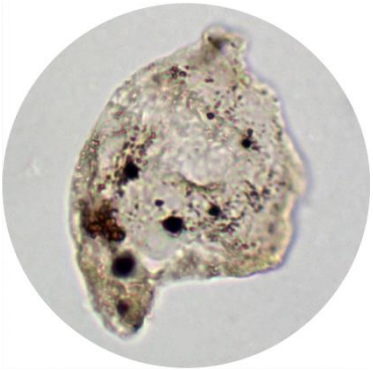

CHAPTER III

Early Jurassic palynostratigraphy

Chapter III cover:

Nannoceratopsis gracilis Alberti 1961. Peniche section, lower Toarcian (*Dactylioceras polymorphum* AB), sample P6.

Chapter III. Early Jurassic palynostratigraphy

Adapted from paper 3:

Correia, V.F., Riding, J.B., Duarte, L.V., Fernandes, P., Pereira, Z. 2018. The Early Jurassic palynostratigraphy of the Lusitanian Basin, western Portugal. *Geobios*, in press. https://doi.org/10.1016/j.geobios.2018.03.001

Abstract

A comprehensive investigation of the Early Jurassic stratigraphical palynology of the Lusitanian Basin in western Portugal was undertaken, with most emphasis placed on dinoflagellate cysts. A total of 214 samples, from an upper Sinemurian to upper Toarcian composite section based on six successions, were examined. The Sinemurian material examined was barren of dinoflagellate cysts, however the Pliensbachian and Toarcian successions are characterised by relatively low diversities. *Luehndea spinosa*, *Mancodinium semitabulatum*, *Mendicodinium microscabratum*, *Nannoceratopsis gracilis, Nannoceratopsis senex* and *Scriniocassis priscus* were relatively common, and are biostratigraphically significant. *Luehndea spinosa* dominates the lowermost Toarcian, at *Dactylioceras polymorphum* ammonite biozone (AB), and is an index species. At the base of *Hildaites levisoni* AB, the effects of the Toarcian-Oceanic Anoxic Event (T-OAE) caused *Luehndea spinosa* to become extinct. At the same time, dinoflagellate cyst abundance and diversity markedly decreased. After the T-OAE, during the middle and late Toarcian, phytoplankton recovery was prolonged and slow in the Lusitanian Basin. The *Luehndea spinosa* and *Mendicodinium microscabratum* dinoflagellate cyst biozones were defined, both of which are subdivided into two dinoflagellate cyst subbiozones.

Keywords

Biostratigraphy; Palynomorphs; Dinoflagellate cysts; Lower Jurassic; Lusitanian Basin; Portugal.

1. Introduction

The Lusitanian Basin of central western Portugal is an important Mesozoic depocentre, and the calcareous microfossil biostratigraphy of the Lower Jurassic succession has been well studied recently (e.g., Perilli and Duarte, 2006; Oliveira et al., 2007b; Pinto, 2008; Reggiani et al., 2010; Henriques and Canales, 2013; Mattioli et al., 2013; Cabral et al., 2014, 2015; Henriques et al., 2014; Ferreira et al., 2015; Rita et al., 2016). By contrast, the Jurassic palynology of this significant sedimentary basin has received relatively little attention. Previous studies on the Jurassic palynobiotas of the Lusitanian Basin are Davies (1985), Mohr and Schmidt (1988), van Erve and Mohr (1988), Smelror et al. (1991), Bucefalo Palliani and Riding (1999a; 2003), Barrón and Azerêdo (2003), Oliveira et al. (2007a), Barrón et al. (2013) and Correia et al. (2017a,b). Davies (1985) is a reconnaissance biostratigraphical study, and Oliveira et al. (2007a) and Barrón et al. (2013) are mainly on pollen and spores. Correia et al. (2017a,b) discussed the palynology of the uppermost Pliensbachian to middle Toarcian interval at Maria Pares, Peniche and Vale das Fontes.

The present contribution is a detailed study of the Lower Jurassic palynology of key Sinemurian, Pliensbachian and Toarcian reference sections in the Lusitanian Basin (e.g., Duarte, 2007; Duarte et al., 2014a,b), with emphasis on dinoflagellate cysts because they are of the greatest regional biostratigraphical significance (Riding and Thomas, 1992; Poulsen and Riding, 2003). Specifically, the main aims are to document the upper Sinemurian to upper Toarcian palynomorphs from São Pedro de Moel, Brenha, Peniche, Fonte Coberta, Maria Pares and Vale das Fontes (Fig. 3.1), and to erect a dinoflagellate cyst biozonation.

2. Geological background

The Lusitanian Basin is located in central western Portugal and is oriented NE–SW (Fig. 3.1). It is 300 km long and 150 km wide, with a maximum basin fill of 5 km (Kullberg et al., 2013). The origin and evolution of this sedimentary basin are related to the breakup of Pangaea and the opening of the North Atlantic Ocean. The fill is mainly composed of marine Jurassic sediments, ranging from Middle? –Upper Triassic to uppermost part of Lower Cretaceous (Wilson et al., 1989; Kullberg et al., 2013). A clear Atlantic influence is evident from the ammonite faunas throughout most of the Lower

Jurassic succession of the Lusitanian Basin (Mouterde et al., 1979). However, mixed Boreal and Tethyan faunas in the upper Pliensbachian to Toarcian interval indicate intermittent communication between the two realms (Elmi et al., 1989; Terrinha et al., 2002).

The lithostratigraphy of the Lower Jurassic of the Lusitanian Basin is summarised in Figure 3.2. During the Early Jurassic, marine carbonate ramps formed rapidly in the Lusitanian Basin (Soares et al., 1993; Azerêdo et al., 2003, 2014; Duarte, 2007). The upper Sinemurian, especially in the western area, at Figueira da Foz, Peniche and São Pedro de Moel, mainly comprises marl-limestone couplets with ammonite-bearing black shales of the Água de Madeiros Formation (Duarte et al., 2010, 2012). The type section is at São Pedro de Moel in the central western part of the basin (Fig. 3.1; Duarte and Soares, 2002; Duarte et al., 2014a,b). The overlying Pliensbachian and Toarcian hemipelagic deposits are rich in benthic and nektonic faunas; these are the Vale das Fontes, Lemede, São Gião, base of Cabo Carvoeiro and Póvoa da Lomba formations (Fig. 3.2; e.g., Duarte and Soares, 2002; Duarte et al., 2001, 2010, 2014b; Duarte, 2007). The Vale das Fontes Formation is Pliensbachian in age, ranges from the *Uptonia jamesoni* to *Amaltheus margaritatus* AB and is subdivided into three informal members, the last one particularly enriched in organic mater (e.g., Silva et al., 2015; Silva and Duarte, 2015; Fig. 3.2). The succeeding Lemede Formation is upper Pliensbachian to lowermost Toarcian and spans the upper *Amaltheus margaritatus* to the lower *Dactylioceras polymorphum* ABs. The Toarcian of the Lusitanian Basin largely comprises the São Gião Formation, that spans the *Dactylioceras polymorphum* to the lower *Dumortieria meneghinii* ABs, and is subdivided into five informal members (Fig. 3.2; Duarte and Soares, 2002; Duarte, 2007). The type section of the São Gião Formation is at Maria Pares in the northern part of the Lusitanian Basin (Fig. 3.1). This locality exposes a continuous ammonite-bearing upper Pliensbachian to Aalenian succession (Mouterde et al., 1964-65; Henriques, 1992, 1995).

At Peniche, in the southwest of the Lusitanian Basin, a thick succession of Pliensbachian limestone-marl alternations is overlain by the Toarcian Cabo Carvoeiro Formation which comprises at the top ooidal limestone-siliciclastic interbeds (Wright and Wilson, 1984; Duarte, 1997; Duarte et al., 2017). The type sections of the Vale das Fontes and Lemede formations are at Peniche, and this succession was recently formalised as the Toarcian Global boundary Stratotype Section and Point (GSSP) (Rocha et al., 2016).

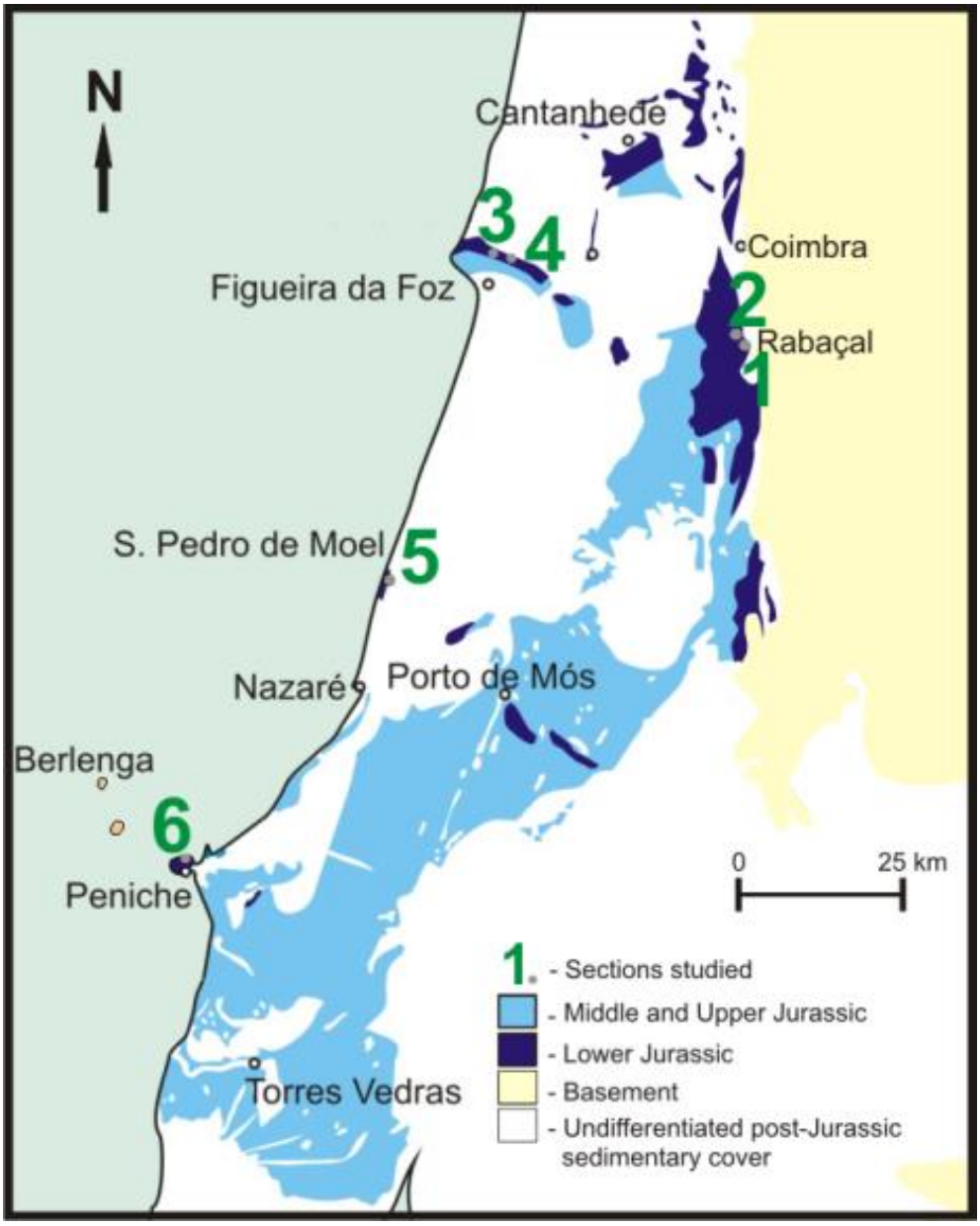

Figure 3.1. The geological setting of the Lusitanian Basin (adapted from Duarte et al., 2010) and the location of the six successions studied herein. Successions 1 and 2 are the sections at Maria Pares (40° 3' 10"N; 8° 27' 25"W) and Fonte Coberta (40° 3' 44"N; 8° 27' 31"W) respectively; both are close to Rabaçal village. Sections 3 and 4 are Vale das Fontes (40° 12' 10"N; 8° 51' 31"W) and Brenha (40° 11' 49"N; 8° 49' 55"W) respectively; both are located north of Figueira da Foz. The São Pedro de Moel composite section (Polvoeira section: 39° 43' 18"N; 9° 02' 56"W) is near the village of São Pedro de Moel and is the section number 5. The Peniche section (39° 22' 15"N; 9° 23' 07"W) is indicated by the number 6.

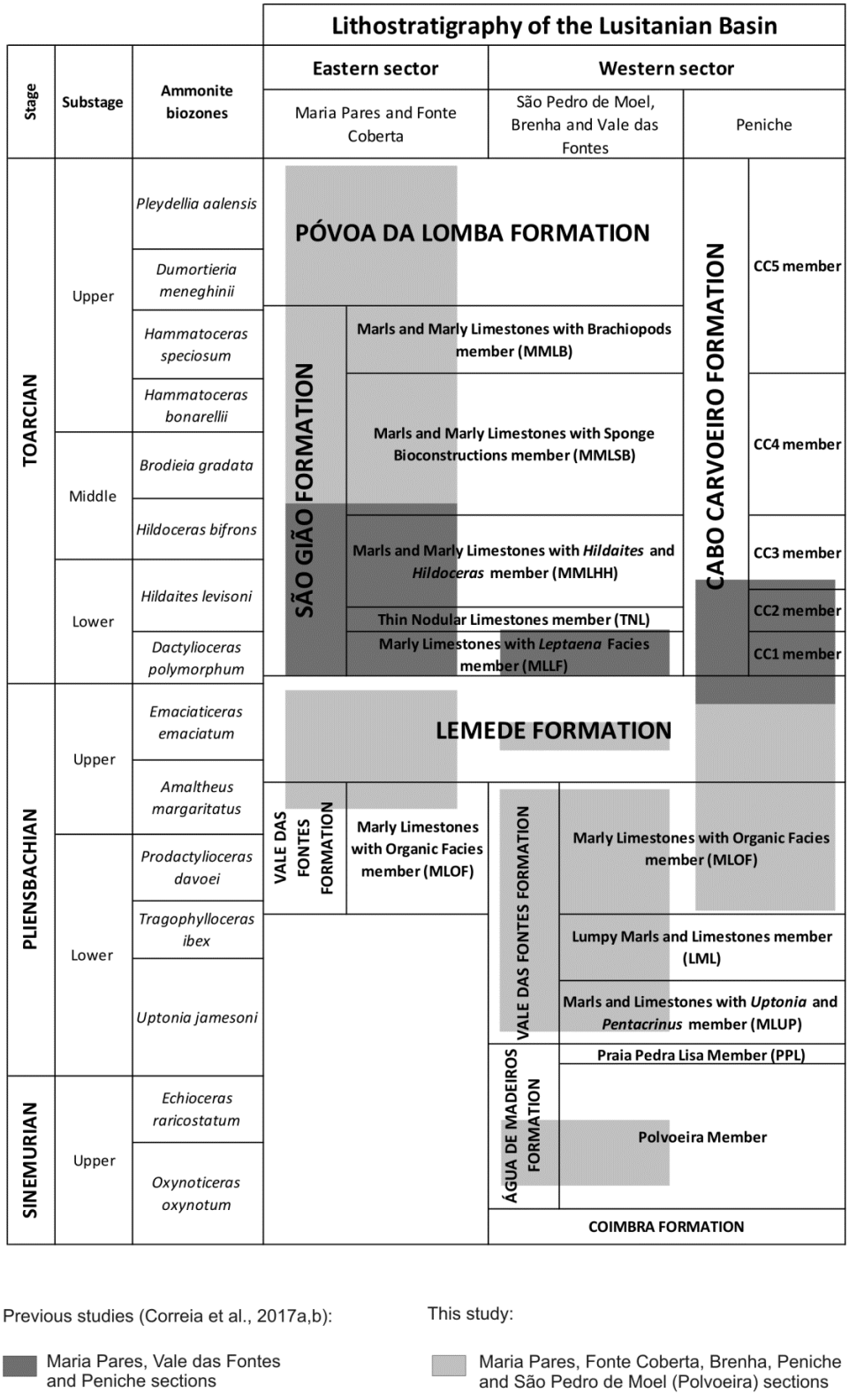

Figure 3.2. The ammonite biostratigraphy and lithostratigraphy of the Lower Jurassic (upper Sinemurian to upper Toarcian) of the eastern and western sectors of the Lusitanian Basin, central-western Portugal, based on Duarte and Soares (2002), Duarte (2007) and Duarte et al. (2014a,b). The light grey shading indicates the lithostratigraphical units studied in the present work, and the dark grey shading indicates material studied by Correia et al. (2017a,b).

3. Material and methods

In this work, 214 samples collected from six Lower Jurassic successions in the Lusitanian Basin were analysed, involving the lithostratigraphical units described above. The localities are São Pedro de Moel, Brenha, Peniche, Fonte Coberta, Maria Pares and Vale das Fontes (Fig. 3.1). Twelve samples (prefixed PM) were collected from the upper Sinemurian Polvoeira Member of the Água de Madeiros Formation at Polvoeira, which forms the lowest part of the São Pedro de Moel composite section (Figs. 3.3, 3.4). Herein, we refer to this section as "São Pedro de Moel", although the succession studied corresponds to the Polvoeira section of Duarte et al. (2012, 2014a). At Brenha, 22 samples were taken from a Pliensbachian composite section. The lower part of this section comprises the Vale das Fontes Formation (samples prefixed Br), and the upper part is the Lemede Formation (samples prefixed BrLem). The succession between these two formations is not continuous (Figs. 3.2, 3.5, 3.6). These two lithostratigraphical units and the Cabo Carvoeiro Formation were also sampled at Peniche, where 72 samples (numbered P-34 to P38) were collected (Fig. 3.7, 3.8; Table S3.1; Correia et al., 2017b). At Fonte Coberta, in the Rabaçal area, five samples (prefixed FC) from the upper Pliensbachian Vale das Fontes and Lemede formations were collected (Figs. 3.9, 3.10). The section at Maria Pares comprises the lower, middle and upper Toarcian São Gião and Póvoa da Lomba formations. Eighty-nine samples (numbered PZ1 to PZ89) were collected (Figs. 3.11–3.14; Table S1; Correia et al., 2017a). The type section of the São Gião Formation is at Maria Pares, and the lower Toarcian was previously studied by Correia et al. (2017a). The latter authors also examined 14 samples (numbered PVF1 to PVF14) from the lower Toarcian part of the São Gião Formation at Vale das Fontes (Table S2; Correia et al., 2017a).

The samples were all prepared using standard palynological techniques (Wood et al., 1996; Riding and Warny 2008), but the organic residues were not oxidised. All the residues were sieved using a 15 µm mesh. The palynomorph concentrates were stained with Safranin to enhance the visibility of morphological features. If possible, a minimum of 300 palynomorphs were counted for each sample; if not, the maximum number of specimens from two microscope slides were used. The samples, aqueous residues, microscope slides and figured specimens are all curated in the collections of the LNEG (Portuguese Geological Survey), São Mamede de Infesta, Portugal.

4. Palynology

In this section, new reports on the Lower Jurassic palynofloras of the five sections studied are described. The data from 14 samples from the São Gião Formation at Vale das Fontes section were included in Correia et al. (2017a). The data presented by Correia et al. (2017a,b) on Maria Pares and Peniche are also considered here. Most emphasis is placed on the dinoflagellate cysts, due to their biostratigraphical significance. The lithological log with the dinoflagellate cyst occurrences and the relative abundances of the six main palynomorph groups for each section are plotted in Figs. 3.3–3.14. Selected palynomorphs are pictured in Plates 3.1–3.5. The overall percentages of all taxa from each section are depicted in Tables S1–S6 (Digital Supplementary Data, Supplement B). The palynomorph taxa that were recorded herein, or mentioned in the text, are listed in the Appendix 1.

4.1. São Pedro de Moel

Twelve samples, PM1 to PM12, were studied from the upper Sinemurian Polvoeira Member of the Água de Madeiros Formation at São Pedro de Moel area. These horizons span the *Oxynoticeras oxynotum* and *Echioceras raricostatum* ABs (Figs. 3.2, 3.3). All the 12 samples proved productive, but the palynomorphs were generally poorly preserved and no dinoflagellate cysts were observed. The assemblages are low in diversity and are dominated (normally >95%) by the gymnosperm pollen *Classopollis classoides* (Plate 3.5(7)). The prasinophyte genus *Tasmanites* (Plate 3.3(6)) is present throughout, reaching 19% of the palynoflora in PM12. Other palynomorphs are present in low abundances and include acritarchs (*Micrhystridium* spp.), foraminiferal test linings, pollen (*Alisporites* spp. and *Cerebropollenites macroverrucosus*) and spores (*Cyathidites* spp. and *Kraeuselisporites reissingeri*) (Fig. 3.4; Table S4).

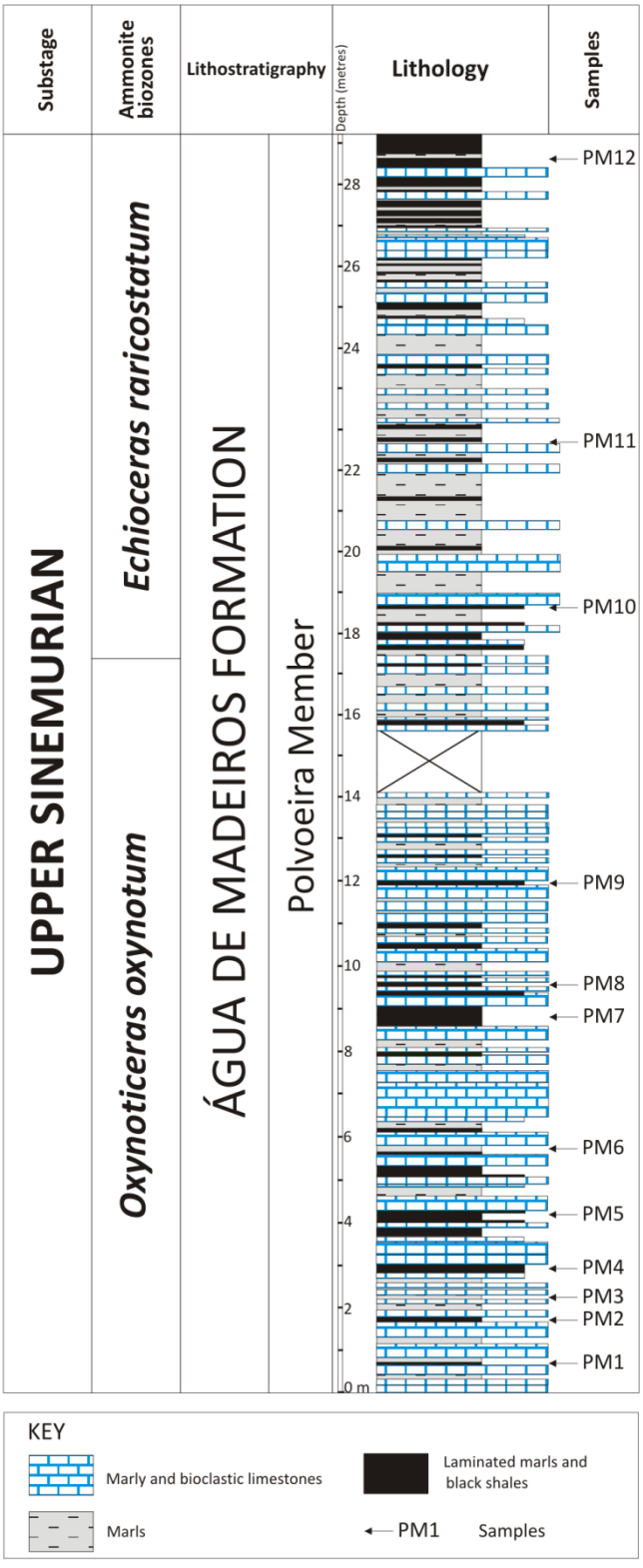

Figure 3.3. The stratigraphical log of the upper Sinemurian succession in the São Pedro de Moel composite section (= the Polvoeira section of Duarte et al. (2012, 2014a)), adapted from Duarte et al. (2014a), with the positions of the palynomorph samples PM1 to PM12 indicated. No dinoflagellate cyst taxa were identified throughout this succession.

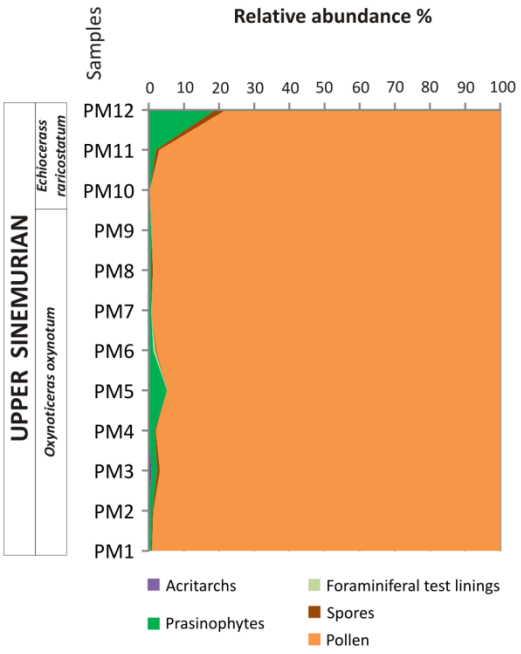

Figure 3.4. The relative abundances, expressed as percentages, of the five main palynomorph groups recorded from the upper Sinemurian (*Oxynoticeras oxynotum* and *Echioceras raricostatum* ABs) succession of the São Pedro de Moel section (samples PM1 to PM12). Note the overwhelming dominance of pollen.

4.2. Brenha

The Lower Jurassic composite section at Brenha spans the Pliensbachian and all five ammonite biozones are represented (Fig. 3.5). Twenty two samples (Br 1–20 and BrLem 1 and 2) were collected, and all except Br6 proved to be palynologically productive. The palynomorph assemblages are moderately well preserved, and exhibit higher diversites than the Sinemurian of São Pedro de Moel (Tables S4, S5).

Three dinoflagellate cyst species were encountered in the upper Pliensbachian; these are *Mancodinium semitabulatum*, *Nannoceratopsis gracilis* and *Nannoceratopsis senex* (Fig. 3.5). These species are present in both the *Amaltheus margaritatus* and the *Emaciaticeras emaciatum* ABs, corresponding to the MLOF member of the Vale das Fontes Formation, and the middle part of the Lemede Formation. *Luehndea spinosa* was not found in this succession. Dinoflagellate cysts in samples Br14 to Br20, within the *Amaltheus margaritatus* AB, are present in very low proportions, dominantly less than 1% of the palynoflora. However, the relative proportions of dinoflagellate cysts increased markedly in the Lemede Formation (*Emaciaticeras emaciatum* AB). All three species are present in significant numbers in samples BrLem1 and BrLem2; they represent 22.5% of the overall palynoflora in the latter sample (Table S5).

Other marine palynomorphs present at Brenha comprise foraminiferal test linings, *Halosphaeropsis liassica*, indeterminate acritarchs and prasinophytes, *Micrhystridium* spp., *Polygonium jurassicum* (Plate 3.3(4)) and *Tasmanites* spp.

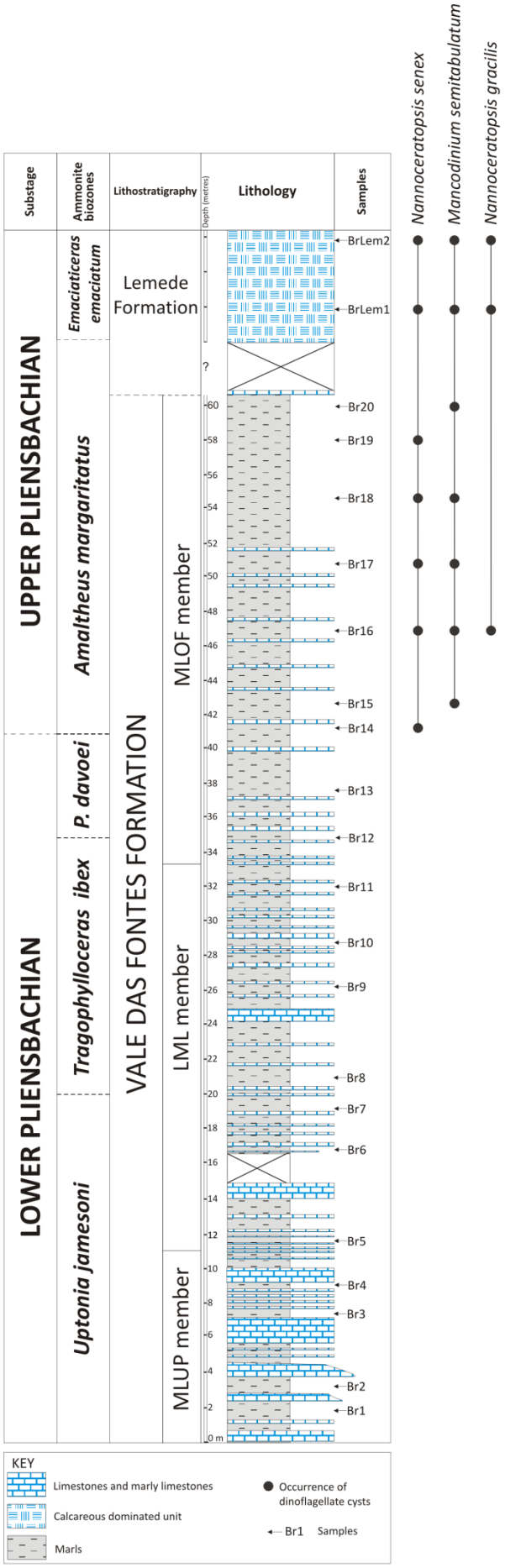

Figure 3.5. The lithological log of the lower and upper Pliensbachian succession in the composite section at Brenha, adapted from Silva et al. (2006), with the positions of the palynomorph samples Br1 to Br20 indicated. The uppermost part of this section, the Lemede Formation (samples BrLem1 and BrLem2), was not described by Silva et al. (2006). The ammonite biozones are based on, and modified from, Mouterde et al. (1978) and Elmi et al. (1988).The dinoflagellate cyst occurrences are indicated by black dots.

Foraminiferal test linings were only present in the upper Pliensbachian succession. However overall, these miscellaneous marine palynomorphs, like the dinoflagellate cysts, are most common in the *Emaciaticeras emaciatum* AB. Clearly, samples BrLem1 and BrLem2 exhibit the greatest marine influence in this succession (Fig. 3.6; Table S5).

The pollen grain *Classopollis classoides* is the most abundant palynomorph species throughout, with relative abundances between 27.0% and 94.5%. The bisaccate pollen genus *Alisporites* is also sporadically common, and other pollen present, normally in low proportions, are *Araucariacites australis*, *Cerebropollenites macroverrucosus* (Plate 3.5(6)).and *Spheripollenites* spp. The spores *Cyathidites* spp. and *Kraeuselisporites reissingeri*, together with indeterminate forms, are present throughout the succession. *Leptolepidites* spp. and *Lycopodiacidites rugulatus* (Plate 3.4 (5)) were sporadically identified in the upper Pliensbachian samples (Table S5).

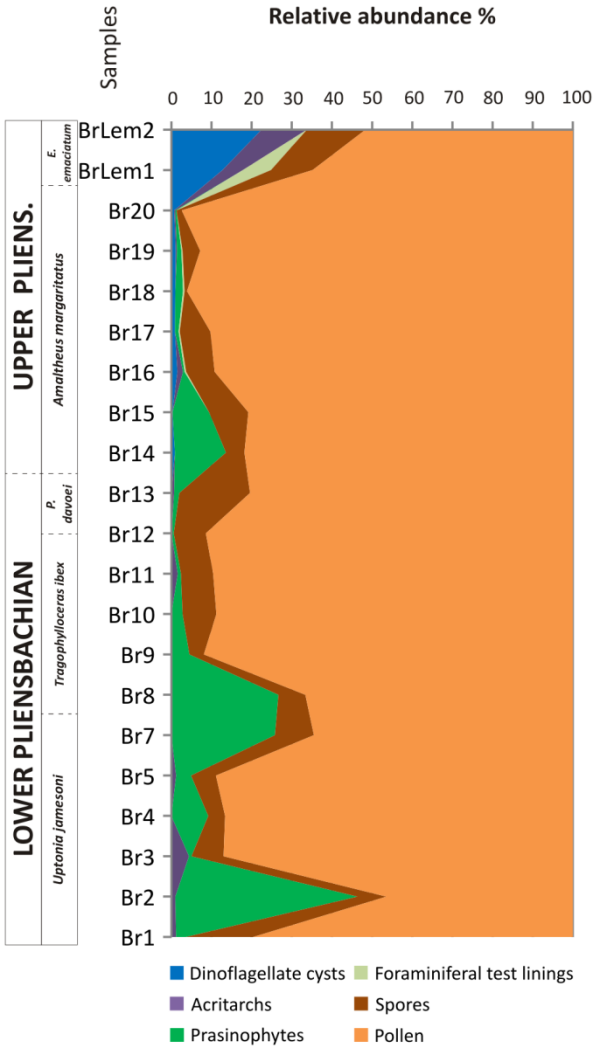

Figure 3.6. The relative abundances, expressed as percentages, of the six main palynomorph groups recorded from the Pliensbachian (*Uptonia jamesoni* to *Emaciaticeras emaciatum* ABs) succession of the Brenha section (samples Br1 to Br20 and BrLem1 and BrLem2). Note the overall dominance of pollen and the increase of dinoflagellate cysts in the *Emaciaticeras emaciatum* AB.

4.3. The Pliensbachian and lower Toarcian succession at Peniche

A total of 72 samples were collected from the lower Pliensbachian to lower Toarcian (*Tragophylloceras ibex* to *Hildaites levisoni* ABs) succession at Peniche (Fig. 3.1; Table S3.1). These were studied herein (Chapter III), and by Correia et al. (2017b)(see Chapter II). Twenty-seven samples, P-34 to P-8, were collected from the Pliensbachian Vale das Fontes and Lemede formations (Figs. 3.2, 3.7). Correia et al. (2017b) reported on 45 samples (P-7 to P38), from the overlying uppermost Lemede Formation and the lowermost Cabo Carvoeiro Formation (uppermost Pliensbachian–lower Toarcian). Fourteen samples from the upper Pliensbachian and lower Toarcian succession proved entirely devoid of palynomorphs (Table S3.1). The remaining 58 samples yielded reasonably abundant palynomorph assemblages which are moderately well preserved.

Eight forms of dinoflagellate cyst were recognised. The most stratigraphically extensive species are *Luehndea spinosa, Mancodinium semitabulatum, Nannoceratopsis gracilis* and *Nannoceratopsis senex. Mendicodiniuim microscabratum, Nannoceratopsis ambonis, Nannoceratopsis* sp. and *Scriniocassis weberi* occurred sporadically, and in low numbers (Figs. 3.7; Table S3.1). In the Pliensbachian part of this succession, between the upper *Prodactylioceras davoei* to lower *Emaciaticeras emaciatum* ABs (samples P-29 to P-13,) dinoflagellate cysts are especially sparse and comprise only *Luehndea spinosa*, *Mancodinium semitabulatum*, *Nannoceratopsis senex* and *Nannoceratopsis* sp. The latter form represents a single specimen found in sample P-20 in the *Amaltheus margaritatus* AB. It has two subequal antapical horns, and does not precisely conform to any of the formalised species of this genus (Plate 3.1(4)). The lowermost occurrence of *Mancodinium semitabulatum* is at the top of *Prodactylioceras davoei* AB, in sample P-29, where it is relatively sparse. *Luehndea spinosa* is only present, again in very low proportions, in samples P-26 and P-23 from the *Amaltheus margaritatus* AB. Stratigraphically above these records, *Mancodinium semitabulatum*, reappeared in the *Emaciaticeras emaciatum* AB (samples P-12 to P-10) in significantly greater proportions, up to 5.9% of the overall palynoflora. A similar occurrence pattern was exhibited by *Nannoceratopsis senex*. This species is rare in the *Amaltheus margaritatus* AB (samples P-28 to P-21), and became more frequent in the *Emaciaticeras emaciatum* AB (samples P-12 and P-10).

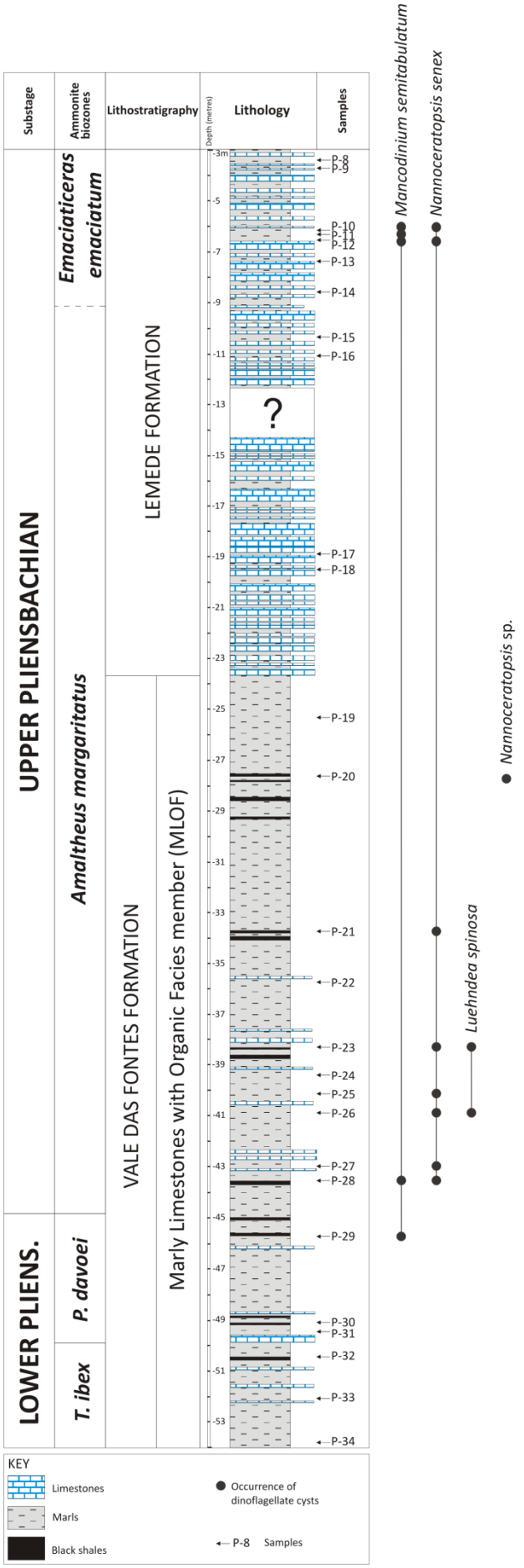

Figure 3.7. The stratigraphical log of the lower and upper Pliensbachian succession in the Peniche section, adapted from Phelps (1985), Duarte et al. (2010), Silva et al. (2011), Bárron et al. (2013) and Comas-Rengifo et al. (2016), with the positions of the palynomorph samples P-34 to P-8 indicated. The dinoflagellate cyst occurrences are indicated by black dots.

Therefore, the consistent occurrence of relatively common *Mancodinium semitabulatum* is in sample P-12. From this horizon in the *Emaciaticeras emaciatum* AB to the top of *Dactylioceras polymorphum* AB (sample P14, see Table S3.1), dinoflagellate cysts are abundant to common. *Luehndea spinosa* has two prominent acmes in the *Emaciaticeras emaciatum* and *Dactylioceras polymorphum* ABs (Correia et al., 2017b). *Mancodinium semitabulatum* is also common at the *Emaciaticeras emaciatum-Dactylioceras polymorphum* AB transition. *Nannoceratopsis* spp. were also prominent in sample P6 in the *Dactylioceras polymorphum* AB (Table S3.1). In the Lusitanian Basin, the beginning of the Toarcian Oceanic Anoxic Event (T-OAE) corresponds to the base of *Hildaites levisoni* AB (Hesselbo et al., 2007; Suan et al., 2008; Pittet et al., 2014; Correia et al., 2017a,b). This anoxic event (samples P15 to P24) badly affected the dinoflagellates due to profound benthic palaeoenvironmental stress (Correia et al., 2017b), and the assemblages had not recovered at the level of sample P38 in the *Hildaites levisoni* AB. The only survivors were sparse and sporadic *Mancodinium semitabulatum* and *Mendicodiniuim microscabratum* (Table S3.1).

Miscellaneous marine palynomorphs were recorded throughout this succession. They include acritarchs (indeterminate forms, *Micrhystridium* spp. and *Polygonium jurassicum*), foraminiferal test linings and prasinophytes (mostly *Halosphaeropsis liassica*, indeterminate forms and *Tasmanites* spp.). Generally, these occurrences are in small proportions (<1–2% of the palynoflora); foraminiferal test linings and *Tasmanites* spp. are the most consistently observed (Fig. 3.8; Table S3.1). Foraminiferal test linings and *Tasmanites* spp. are sporadically relatively frequent between samples P-32 and P-26 (*Tragophylloceras ibex* to *Amaltheus margaritatus* ABs), and in the productive part of the *Emaciaticeras emaciatum* AB (samples P-12 to P-10, see Table S3). The interval between samples P-25 and P-7 is relatively sparse in miscellaneous microplankton. Unlike dinoflagellate cysts, miscellaneous microplankton is present in relatively moderate proportons in the T-OAE interval (samples P15 to P24). Foraminiferal test linings are most prominent in this interval, and these dominate the palynobiotas above the T-OAE. In sample P36, these palynomorphs attain 71.9% of the assemblage (Table S3.1).

All the palynologically productive samples yielded terrestrially-derived palynomorphs in substantial proportions. The pollen grains *Alisporites* spp., *Araucariacites australis*, *Cerebropollenites macroverrucosus*, *Classopollis classoides*, *Exesipollenites* spp. and *Spheripollenites* spp. were recognised. *Classopollis classoides*

(Plate 3.5(9)) is normally the most abundant palynomorph below sample P5 in the lowermost Toarcian, with overall percentages up to 97.4% in sample P-21. The bisaccate genus *Alisporites* was relatively frequent in the upper Pliensbachian. Most pollen declined at the T-OAE, however *Exesipollenites* spp. and *Spheripollenites* spp. are more frequent in this succession than below the T-OAE (Table S3.1). Pteridophyte spores were recorded in relatively low numbers throughout the succession. *Cyathidites* spp., indeterminate spores, *Kraeuselisporites reissingeri* and *Leptolepidites* spp. were the most consistently present. Other forms were encountered rarely; these include *Concavisporites granulosus*, *Ischyosporites variegatus*, *Lycopodiacidites rugulatus* and *Plicifera delicata*. Unlike most pollen taxa, spores generally were slightly more frequent during the T-OAE and above it (Fig. 3.8; Table S3.1).

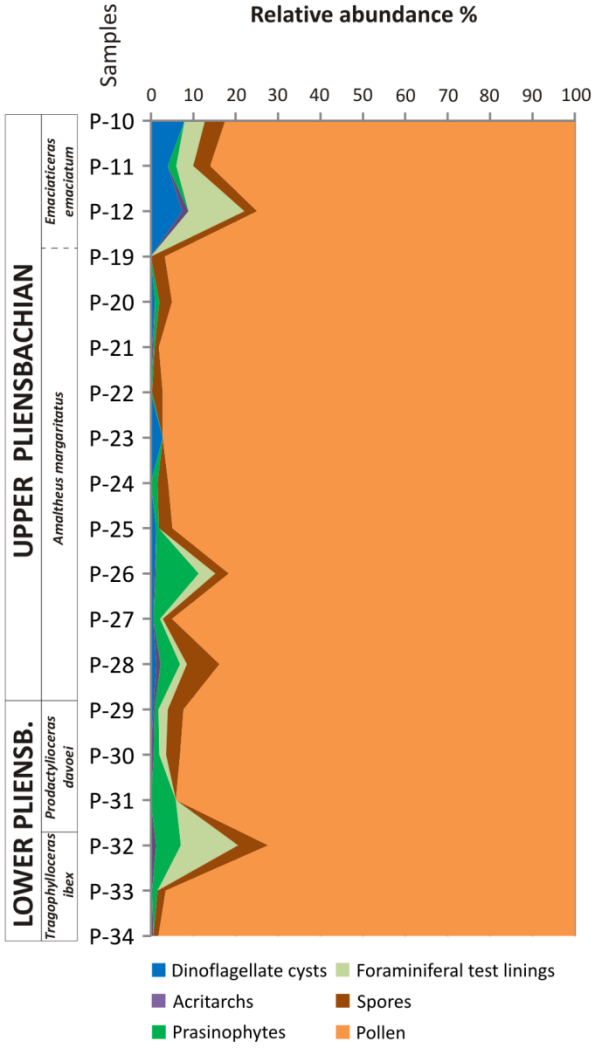

Figure 3.8. The relative abundances, expressed as percentages, of the six main palynomorph groups recorded from the Pliensbachian (*Tragophylloceras ibex* to *Emaciaticeras emaciatum* ABs) succession of the Peniche section (samples P-34 to P-10). Note the overwhelming dominance of gymnosperm pollen and the increase of dinoflagellate cysts in the *Emaciaticeras emaciatum* AB.

4.4. Fonte Coberta

Five palynologically productive samples, FC1 to FC5, were collected from the upper Pliensbachian section at Fonte Coberta, near Rabaçal in the northern part of the Lusitanian Basin (Fig. 3.1, Table S6). The samples are from the top of the Vale das Fontes and Lemede formations, and span the *Amaltheus margaritatus* and *Emaciaticeras emaciatum* ABs (Figs. 3.2, 3.9).

The palynomorphs from Fonte Coberta are of low diversity and are moderately well preserved. Three dinoflagellate cysts, *Luehndea spinosa*, *Mancodinium semitabulatum* and *Nannoceratopsis senex*, were identified (Fig. 3.9). The latter occurred in low numbers throughout the succession. By contrast, *Mancodinium semitabulatum* and *Luehndea spinosa* are confined to the *Emaciaticeras emaciatum* AB. The former was recorded in low proportions, but *Luehndea spinosa* was the most abundant palynomorph in samples FC3 (85.2%) and FC5 (62.4%) (Fig. 3.10; Table S6). This abundance of *Luehndea spinosa* at the Pliensbachian-Toarcian transition in the Lusitanian Basin was also observed by Correia et al. (2017a,b).

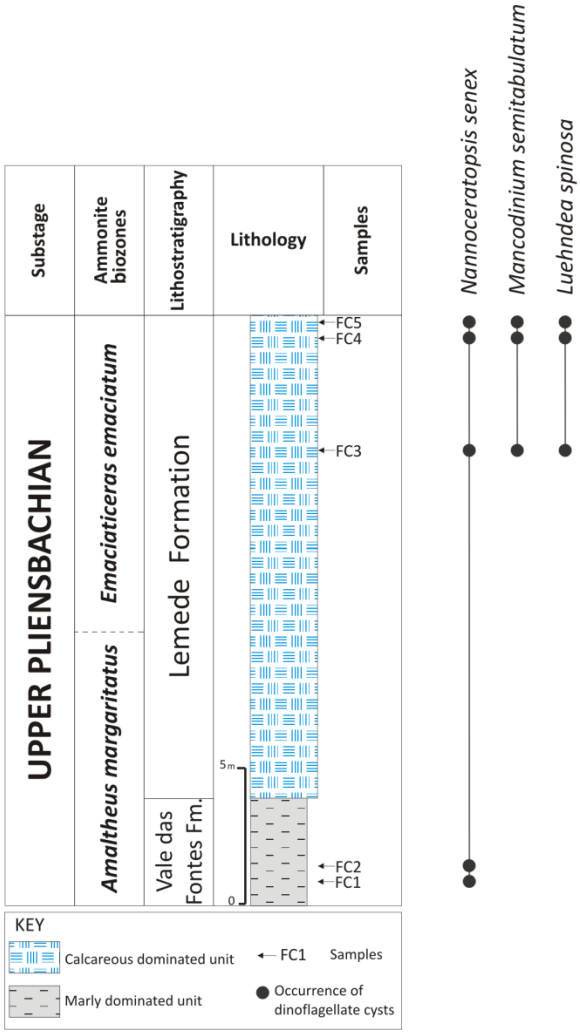

Figure 3.9. A simplified lithological log of the upper Pliensbachian succession in the Fonte Coberta section. The positions of the palynomorph samples FC1 to FC5 are indicated. The ammonite biozones are based on, and modified from, Mouterde et al. (1964-1965) and Paredes et al. (2016).
The dinoflagellate cyst occurrences are indicated by black dots.

Miscellaneous marine palynomorphs are present in relatively low numbers in all the samples except FC4. These comprise acritarchs (indeterminate forms and *Micrhystridium* spp.), foraminiferal test linings and prasinophytes (indeterminate forms and *Tasmanites* spp.). The most significant occurrence is the relatively high levels of foraminiferal test linings in the *Emaciaticeras emaciatum* AB (Table S6).

In samples FC1, FC2 and FC4, by the most abundant palynomorph was the pollen grain *Classopollis classoides*; it is also abundant in FC5. It represented >90% of the palynoflora in samples FC1 and FC4. There is an apparently inverse relationship between the abundances of *Classopollis classoides* and the dinoflagellate cyst *Luehndea spinosa* (Fig. 3.10; Table S6). Other pollen grains present in low proportions are *Alisporites* spp., *Araucariacites australis* and *Cerebropollenites macroverrucosus.* The spores recorded were *Cyathidites* spp., indeterminate forms and *Kraeuselisporites reissingeri* (Table S6).

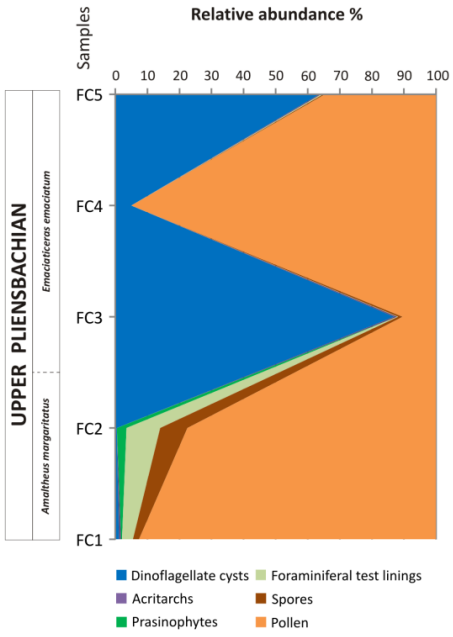

Figure 3.10. The relative abundances, expressed as percentages, of the six main palynomorph groups recorded from the upper Pliensbachian (*Amaltheus margaritatus* and *Emaciaticeras emaciatum* ABs) succession of the Fonte Coberta section (samples FC1 to FC5). Note the dominance of gymnosperm pollen in *Amaltheus margaritatus* AB and dinoflagellate cysts in *Emaciaticeras emaciatum* AB.

4.5. The lower to upper Toarcian succession at Maria Pares

Eighty-nine samples were taken from the lower, middle and upper Toarcian at Maria Pares, in the Rabaçal area of the eastern sector of the basin (Fig. 3.1; Table S1). This material is from the São Gião and Póvoa da Lomba formations, and the samples span the *Dactylioceras polymorphum* to the *Pleydellia aalensis* ABs (Figs. 3.2, 3.11–3.13). This material was studied herein, and also by Correia et al. (2017a) who reported

on the lowermost 54 samples PZ-1 to PZ54 from the São Gião Formation, lower and middle Toarcian (see Chapter II). The overlying 35 samples PZ55 to PZ89, from the middle and upper Toarcian were part of this study (Chapter III) only. All but five of the samples proved palynologically productive, with moderately well presered palynobiotas. Three samples from the upper Toarcian *Pleydellia aalensis* AB proved entirely devoid of palynomorphs (Table S1).

Thirteen dinoflagellate cyst forms were identified. These are: *Dapsilidinium*? *deflandrei*; *Luehndea spinosa*; *Mancodinium semitabulatum*; *Maturodinium*? *inornatum*; *Mendicodinium microscabratum*; *Mendicodinium spinosum* subsp. *spinosum*; *Mendicodinium* sp.; *Nannoceratopsis ambonis*; *Nannoceratopsis gracilis; Nannoceratopsis senex*; *Scriniocassis priscus*; *Sentusidinium* sp.; and *Valvaeodinium* sp. (Fig 3.11–3.13; Table S1). As in other sections, the most consistently occurring dinoflagellate cyst throughout is *Mancodinium semitabulatum,* the range top of which is in the *Dumortieria meneghinii* AB. *Luehndea spinosa* is dominant in the upper part of the *Dactylioceras polymorphum* AB. *Mancodinium semitabulatum* is also common in this AB and around the lower-middle Toarcian transition (samples PZ27 and PZ51, see Table S1). The lowest record of *Mendicodinium microscabratum* and *Scriniocassis priscus* is PZ55 in the *Hildoceras bifrons* AB. The stratigraphically highest record of *Scriniocassis priscus* is in the *Hammatoceras speciosum* AB. The maximum abundance of *Mendicodinium microscabratum* is 27.3% in sample PZ56 in the *Hildoceras bifrons* AB, with the stratigraphically highest record in *Hammatoceras speciosum* AB. *Nannoceratopsis* spp. did not recover following the T-OAE, but *Nannoceratopsis senex* is sporadically present in the *Dumortieria meneghinii* and *Pleydellia aalensis* ABs. In the *Pleydellia aalensis* AB, *Nannoceratopsis senex* was the only dinoflagellate cyst species present, with 10.3% of the overall palynoflora in sample PZ88. *Dapsilidinium*? *deflandrei, Maturodinium*? *inornatum, Mendicodinium spinosum* subsp. *spinosum, Mendicodinium* sp., *Nannoceratopsis ambonis, Sentusidinium* sp. and *Valvaeodinium* sp. were extremely rare (Table S1). For example, only one and two specimens each, respectively of *Dapsilidinium*? *deflandrei* (samples PZ57) and *Maturodinium*? *inornatum* (samples PZ58 and PZ77), were encountered (Table S1).

Other marine palynomorphs encountered throughout this succession were foraminiferal test linings, *Halosphaeropsis liassica,* indeterminate acritarchs and prasinophytes, *Micrhystridium* spp. and *Tasmanites* spp. These palynomorphs were dominated by acanthomorph acritarchs, foraminiferal test linings and prasinophytes.

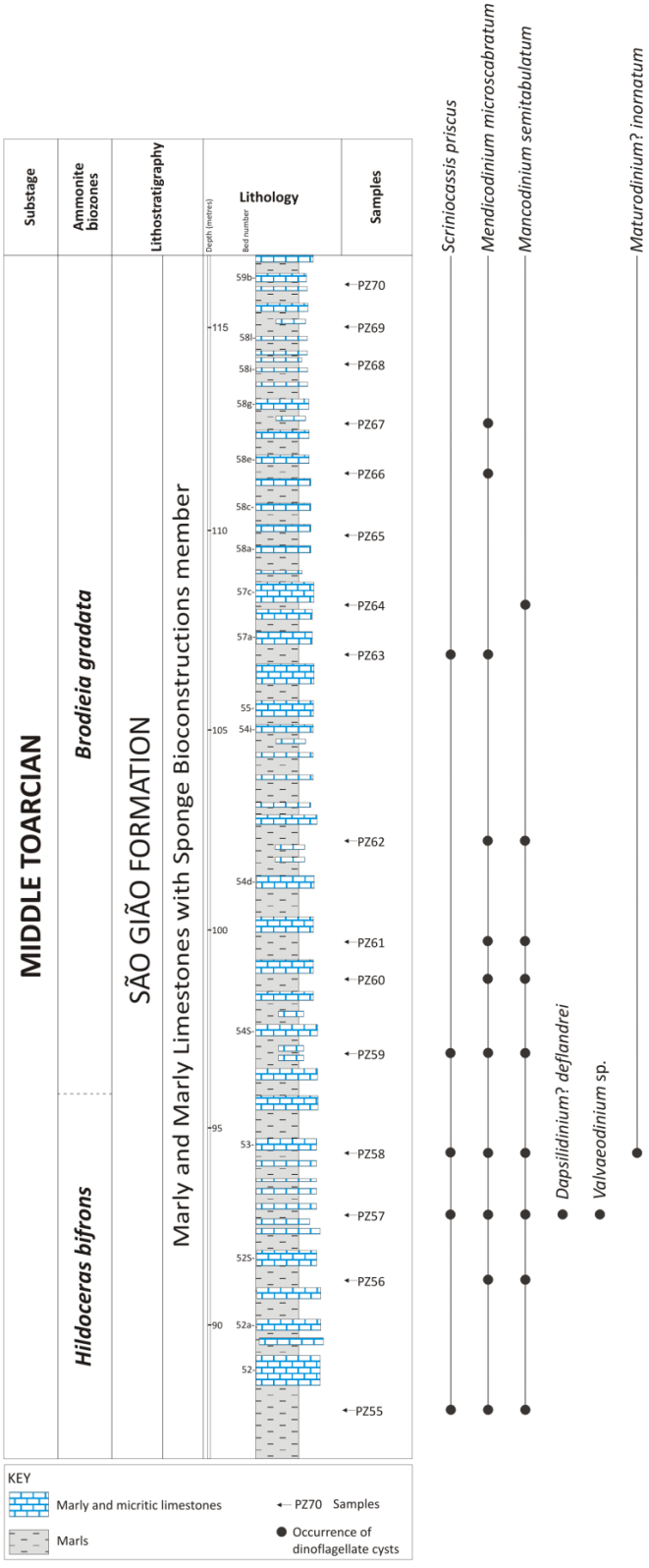

Figure 3.11. The lithological log of the middle Toarcian part of the São Gião Formation in the Maria Pares section, adapted from Duarte (1995), with the positions of the palynomorph samples PZ55 to PZ70 indicated. The ammonite biozones are based on, and modified from, Mouterde et al. (1964-1965) and Elmi et al. (1989). Standard bed numbers 52–59b are given immediately to the left of the lithological ornament. The dinoflagellate cyst occurrences are indicated by black dots.

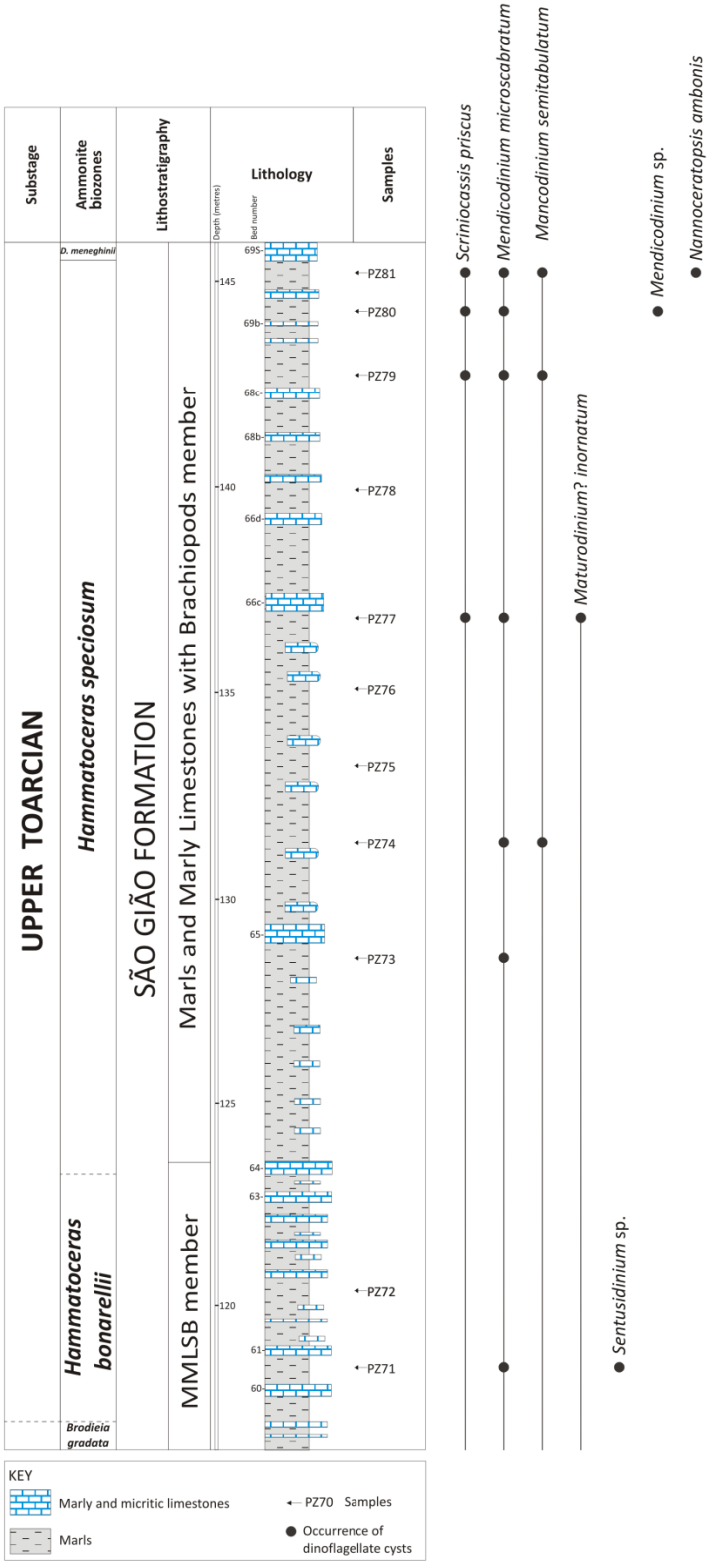

Figure 3.12. The lithological log of the upper Toarcian part of the São Gião Formation in the Maria Pares section, adapted from Duarte (1995), with the positions of the palynomorph samples PZ71 to PZ81 indicated. The ammonite biozones are based on, and modified from, Mouterde et al. (1964-1965) and Elmi et al. (1989). MMLSB = Marls and Marly Limestones with Sponge Bioconstructions member. Standard bed numbers 60–69S are given immediately to the left of the lithological ornament. The dinoflagellate cyst occurrences are indicated by black dots.

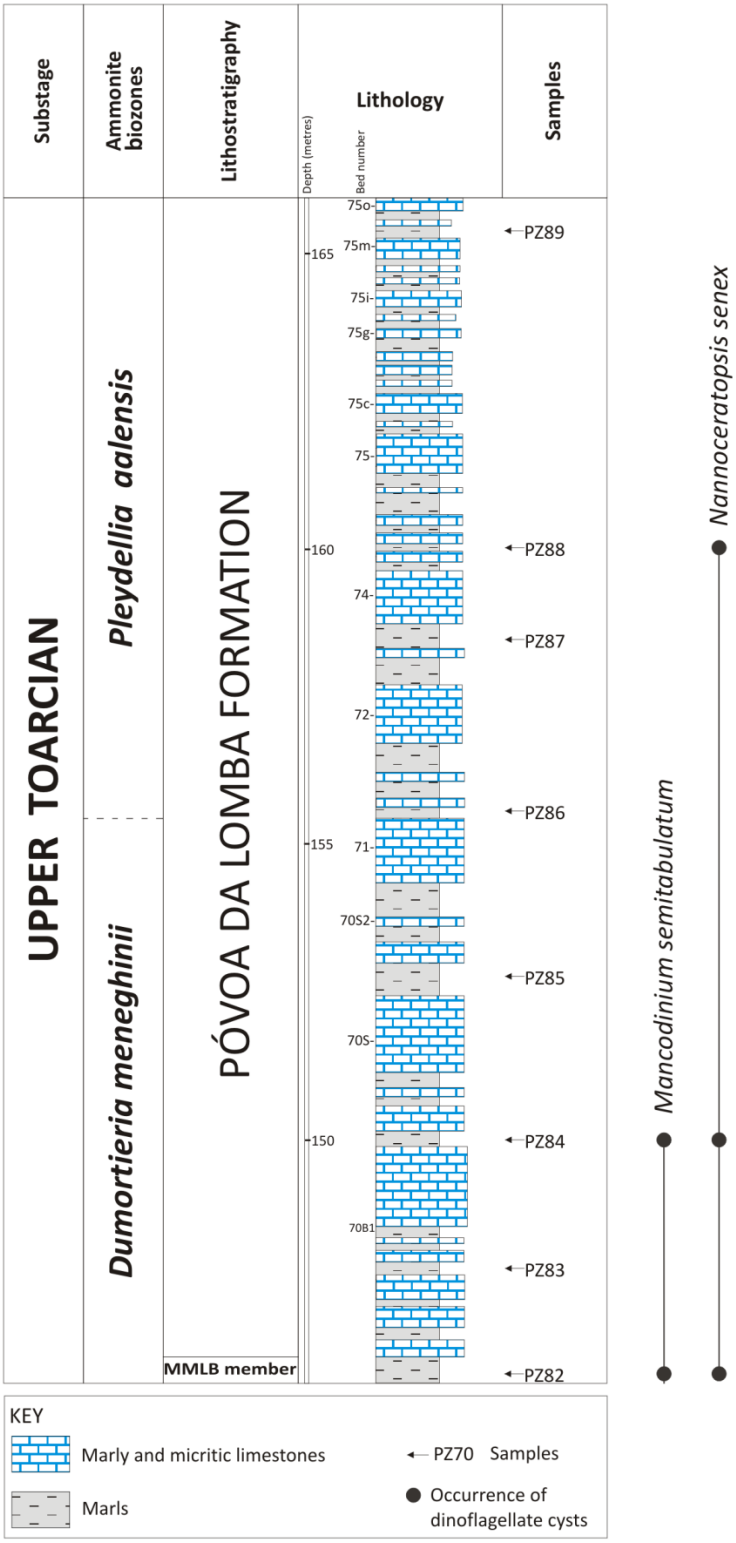

Figure 3.13. The lithological log of the upper Toarcian Póvoa da Lomba Formation in the Maria Pares section, adapted from Duarte (1995), with the positions of the palynomorph samples PZ82 to PZ89 indicated. The ammonite biozones are based on, and modified from, Mouterde et al. (1964-1965), Elmi et al. (1989) and Henriques (1992). MMLB = Marls and Marly Limestones with Brachiopods member. Standard bed numbers 70B1–75o are given immediately to the left of the lithological ornament. The dinoflagellate cyst occurrences are indicated by black dots.

Indeterminate acritarchs and *Micrhystridium* spp. (Plate 3.3(1–3)) are normally most prevalent in the lower and lowermost middle Toarcian, and foraminiferal test linings and indeterminate prasinophytes are most abundant in the upper Toarcian samples (Fig. 3.14). Clumps of *Halosphaeropsis liassica* (Plate 3.3(5)) increased their abundance from the *Hildaites levisoni* AB (sample PZ9, 89.7%, Table S1; Fig. 3.14).

All the palyniferous samples produced pollen-spore floras in significant numbers. The pollen comprises *Alisporites* spp., *Araucariacites australis*, *Callialasporites dampieri*, *Callialasporites turbatus*, *Cerebropollenites macroverrucosus*, *Classopollis classoides*, *Classopollis* sp. (Plate 3.5(10)), *Cycadopites* follicularis (Plate 3.5(3)). *Exesipollenites* spp., *Inaperturopollenites* sp., indeterminate forms and *Spheripollenites* spp. The diversity is greatest in the uppermost middle and upper Toarcian, and the dominant and consistent elements are *Alisporites* spp., *Araucariacites australis* and *Classopollis classoides* (Table S1). The latter is present throughout, and is the most abundant species, reaching a maximum of 50% of the palynoflora in sample PZ85 (*Dumortieria meneghinii* AB). The range top of *Araucariacites australis* and the inception of *Callialasporites* spp. (Plate 3.5(4,5)), are in the middle Toarcian (*Brodieia gradata* AB). The spores were relatively high in diversity, but only *Cyathidites* spp., indeterminate spores, *Ischyosporites variegatus* (Plate 3.4(1)) and *Leptolepidites spp.* were consistent and relatively frequent.

5. Palynostratigraphy

In this section, the palynological data outlined in section 4 are discussed and interpreted, primarily in terms of their biostratigraphical significance. A biostratigraphical scheme for the Pliensbachian and Toarcian of the Lusitanian Basin based on key dinoflagellate cysts bioevents, and a formal biozonation is outlined in Fig. 3.15.

5.1. Upper Sinemurian palynological overview

The upper Sinemurian succession at São Pedro de Moel proved entirely devoid of dinoflagellate cysts, confirming the findings of Duarte et al. (2012) and Poças Ribeiro et al. (2013). The late Sinemurian marker dinoflagellate cyst *Liasidium variabile* was not recovered. This distinctive species is characteristic of the upper Sinemurian of northwest Europe, and is a proven thermophilic taxon (Riding and

Hubbard, 1999; Brittain et al., 2010; Riding et al., 2013). *Liasidium variabile* thrived, and *Classopollis classoides* was extremely abundant, during a brief palaeoenvironmental perturbation in the late Sinemurian (~194 Ma) of northwest Europe. This was characterised by a significant oceanic and atmospheric injection of isotopically-light carbon, global warming and organic shale deposition (Riding et al., 2013). Organic-rich facies, resulting from anoxic/dysoxic intervals, occurred during the late Sinemurian in the western sectors of the Lusitanian Basin (Duarte et al., 2010, 2012; Boussaha et al., 2014; Plancq et al., 2016). *Classopollis classoides* was extremely abundant in the upper Sinemurian of São Pedro de Moel, and this represents the acme for the entire succession examined. The absence of *Liasidium variabile* at São Pedro de Moel may indicate that this species had specific palaeoenvironmental preferences, and did not migrate south of ~30° latitude at this time (Riding et al., 2013, fig. 1).

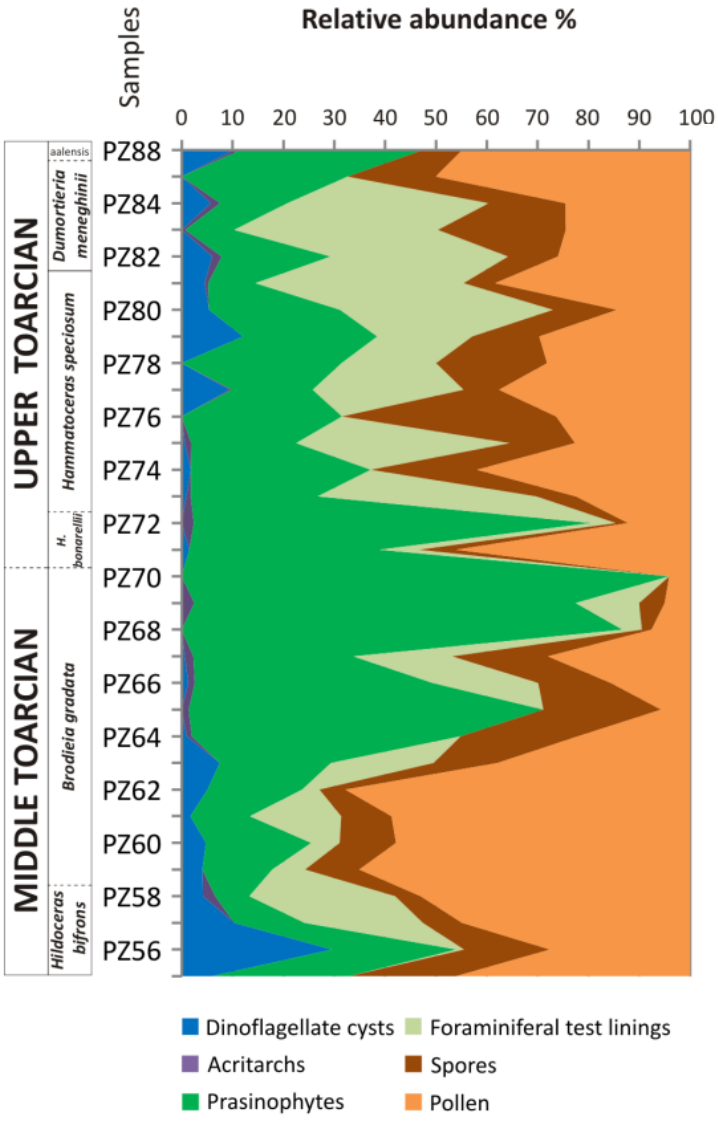

Figure 3.14. The relative abundances, expressed as percentages, of the six main palynomorph groups recorded from the middle and upper Toarcian (*Hildoceras bifrons* to *Pleydellia aalensis* ABs) succession of the Maria Pares section (samples PZ56 to PZ88). Note the dominance of gymnosperm pollen and prasinophytes.

5.2. Pliensbachian and Toarcian palynological overview

The five Pliensbachian and Toarcian successions studied herein are Brenha, Peniche, Fonte Coberta, Maria Pares and Vale das Fontes (Figs. 3.1–3.14); all these sections produced dinoflagellate cyst assemblages. Fifteen forms were recorded; these are: *Dapsilidinium*? *deflandrei*; *Luehndea spinosa*; *Mancodinium semitabulatum*; *Maturodinium*? *inornatum*; *Mendicodinium microscabratum*; *Mendicodinium spinosum* subsp. *spinosum*; *Mendicodinium* sp.; *Nannoceratopsis ambonis*; *Nannoceratopsis gracilis*; *Nannoceratopsis senex*; *Nannoceratopsis* sp.; *Scriniocassis priscus*; *Scriniocassis weberi*; *Sentusidinium* sp.; and *Valvaeodinium* sp. (Tables S1, S2, S3.1, S5, S6).

Other aquatic palynomorphs observed comprise acanthomorph acritarchs, foraminiferal test linings and prasinophytes (Tables S1, S2, S3.1, S5, S6). Pollen and spores are also present in relatively high relative proportions. The gymnospermous pollen species *Classopollis classoides* is the most abundant terrestrially-derived palynomorph in the Lower Jurassic of the Lusitanian Basin. Other pollen taxa present in significant numbers are *Alisporites* spp., *Araucariacites australis* and *Cerebropollenites macroverrucosus*. The spores *Cyathidites* spp., *Ischyosporites variegatus*, *Leptolepidites* spp. and *Kraeuselisporites reissingeri* were also frequently encountered throughout. The miscellaneous marine microplankton, pollen and spores are relatively conservative in their occurrences through this composite Sinemurian to Toarcian succession, and are consistent with an Early Jurassic age (Srivastava, 1987; 2011; Weiss, 1989; Ziaja, 2006; Quattrocchio et al., 2011; Bomfleur et al., 2014).

These relative low diversity dinoflagellate cyst assemblages are broadly typical of upper Pliensbachian to Toarcian successions throughout Europe and adjacent areas (Riding, 1984a; Riding et al., 1991; 1999; Koppelhus and Nielsen, 1994; Bucefalo Palliani and Riding, 1997a,b; 1999a; 2000; 2003; Baranyi et al., 2016; Goryacheva, 2017). Furthermore, the dinoflagellate cyst association reported herein is consistent with previous research on the Lower Jurassic palynology of the Lusitanian Basin (Davies, 1985; Oliveira et al., 2007a; Barrón et al., 2013). For example, Davies (1985), Oliveira et al. (2007a) and Barrón et al. (2013) also recorded *Luehndea spinosa*, *Mancodinium semitabulatum*, *Mendicodinium* sp., *Nannoceratopsis senex*, *Nannoceratopsis gracilis*, *Nannoceratopsis* sp. *Scriniocassis weberi* and *Scriniocassis priscus* from this area.

The dinoflagellate cyst diversity in the upper Pliensbachian of the Lusitanian Basin is relatively low, with only *Luehndea spinosa*, *Mancodinium semitabulatum*,

Mendicodinium microscabratum, *Nannoceratopsis senex*, *Nannoceratopsis gracilis* and *Nannoceratopsis* sp. present. In terms of abundances, dinoflagellate cysts are relatively rare in the *Amaltheus margaritatus* AB, but increased markedly within the *Emaciaticeras emaciatum* AB (Tables S3.1, S5). Both abundances and diversity increased in the earliest Toarcian *Dactylioceras polymorphum* AB. *Luehndea spinosa* dominates the palynofloras at the uppermost Pliensbachian – lower Toarcian interval (upper *Emaciaticeras emaciatum* and *Dactylioceras polymorphum* ABs), at Peniche, Fonte Coberta, Maria Pares and Vale das Fontes. For example, this species attained a maximum of 96.2% of the overall palynoflora in sample P11 at Peniche (Table S3.1). At Peniche, Maria Pares and Vale das Fontes, the abundance curves of *Luehndea spinosa* in the *Dactylioceras polymorphum* AB exhibit a characteristic double peak signature (see Fig. 2.14; Correia et al., 2017a,b). These acmes may reflect pulses of an early Toarcian transgressive event prior to the start of the T-OAE in the lowermost *Hildaites levisoni* AB (Duarte et al., 2004, 2007; Pittet et al., 2014).

The Toarcian dinoflagellate cyst assemblages above the base of *Hildaites levisoni* AB are dominated by *Mancodinium semitabulatum* and *Mendicodinium* spp. During the Toarcian, *Dapsilidinium*? *deflandrei*, *Maturodinium*? *inornatum*, *Mendicodinium spinosum* subsp. *spinosum*, *Mendicodinium* sp., *Nannoceratopsis ambonis*, *Scriniocassis priscus*, *Scriniocassis weberi*, *Sentusidinium* sp. and *Valvaeodinium* sp. had their inceptions (Tables S1, S3.1). Despite the somewhat moderate increase in diversity in the Toarcian, above the *Dactylioceras polymorphum* AB, overall dinoflagellate cyst abundances are markedly reduced due to the palaeoenvironmental perturbations caused by the T-OAE and the recovery from this event (Correia et al., 2017a,b). Only *Mancodinium semitabulatum* is consistently relatively common. *Mendicodinium microscabratum* and *Nannoceratopsis senex* were only sporadically present in reasonable proportions, and other forms were extremely rare (Tables S1, S3.1).

Hence the recovery of dinoflagellates after the T-OAE at Maria Pares and Peniche was extremely slow and somewhat indistinct (Tables S1, S3.1). A good example is the reappearance of *Nannoceratopsis senex* following the T-OAE. In northwest Europe, this species was typically suppressed only for part of the *Harpoceras exaratum* ammonite Subbiozone of the *Harpoceras serpentinum* AB in the early Toarcian (Bucefalo Palliani and Riding, 2000, fig. 3; Bucefalo Palliani et al., 2002, figs. 3, 13). In northern Siberia, this species was apparently unaffected by the T-OAE

(Riding et al., 1999, fig. 11). By contrast, in the Lusitanian Basin, *Nannoceratopsis senex* reappeared in the late Toarcian (*Dumortieria meneghinii* AB, Table S1).

This slow dinoflagellate recovery in southern Europe is illustrated by Correia et al. (2017a, fig. 10) (see also Fig. 2.17). The apparently unaffected dinoflagellate cyst associations of the high northerly latitudes and a slow recovery in southern Europe, with an intermediate region (northwest Europe) intercalated between these, appears to be a coherent trend. Despite extensive early Toarcian anoxia in northwest Europe, the palaeoenvironment in Italy and Portugal was far slower to recovery (Bucefalo Palliani et al., 2002; van de Schootbrugge et al., 2005; Jenkyns, 2010; Correia et al., 2017a,b). This may have been linked to the reestablishment of marine circulation patterns at this time.

In northwest Europe and in the Boreal Realm, part of the dinoflagellate recovery following the T-OAE in the mid Toarcian to earliest Aalenian is a minor radiation of a plexus of small genera placed in the Family Heterocapsaceae and termed the '*Parvocysta* complex' (Riding, 1984a; Riding et al., 1991; 1999; Butler et al., 2005; Feist-Burkhardt and Pross, 2010). This association is absent throughout the Lusitanian Basin, where the only significant dinoflagellate cyst inceptions in the middle Toarcian are those of *Mendicodinium microscabratum* and *Scriniocassis priscus* (Fig. 3.15). Furthermore, typical Tethyan species, such as *Mendicodinium brunneum*, *Mendicodinium umbriense*, *Umbriadinium mediterraneense* and *Valvaeodinium hirsutum* are also absent in central western Portugal (Bucefalo Palliani and Riding, 1997a, c; 1999a,b; 2003; Bucefalo Palliani et al., 1997a).

5.3. Pliensbachian and Toarcian palynomorph biostratigraphy of the Lusitanian Basin

In this subsection, the biostratigraphical significance of the principal palynomorphs, with the emphasis on dinoflagellate cyst taxa, are discussed. *Dapsilidinium*? *deflandrei* (Plate 3.2(2)) was found in the *Hildoceras bifrons* AB at Maria Pares (Fig. 3.11; Table S1). This species is very rare in the Middle Jurassic of northwest Europe (Valensi, 1947; Davey and Riley, 1978), and this is the first report from the Early Jurassic.

Luehndea spinosa (Plate 3.1(1–3)) ranges from the upper Pliensbachian to the lowermost Toarcian (*Amaltheus margaritatus* to *Dactylioceras polymorphum* ABs) in the Lusitanian Basin (Fig. 3.15). This range is consistent with the extent of this

distinctive and widespread species in Europe and elsewhere (Morgenroth, 1970; Riding, 1987; Bucefalo Palliani and Riding, 1997a,b; 2000; 2003; Bucefalo Palliani et al., 1997b). The range base of *Luehndea spinosa* in the Lusitanian Basin is represented by sparse and sporadic occurrences close to the base of the *Amaltheus margaritatus* AB at Peniche (Fig. 3.7; Table S3.1). These occurrences of *Luehndea spinosa* in the *Amaltheus margaritatus* AB, together with *Mancodinium semitabulatum*, *Nannoceratopsis gracilis* and *Nannoceratopsis senex*, confirms the late Pliensbachian age of the uppermost MLOF member of the Vale das Fontes Formation. *Luehndea spinosa* was not recorded in the coeval strata at Brenha (Fig. 3.5), possibly because the Brenha section is more proximal than Peniche (Fig. 3.1). *Luehndea cirilliae* is present in the upper Pliensbachian and lower Toarcian of Hungary (Baldanza et al., 1995; Bucefalo Palliani et al., 1997b; Baranyi et al., 2016). This species was also reported in the Pliensbachian of Brenha by Bucefalo Palliani and Riding (2003), but this taxon was not found in this study, or by Correia et al. (2017a,b).

Mancodinium semitabulatum (Plate 3.2(11,12)) is present in the Pliensbachian-Toarcian successions at Brenha, Peniche, Fonte Coberta, Maria Pares and Vale das Fontes (Tables S1, S2, S3.1, S5, S6). This species has a consistent range of late Pliensbachian to early Bajocian (Riding, 1984b; Feist Burkhardt and Wille 1992; Riding and Thomas 1992; Wiggan et al., 2017). The stratigraphically lowest record of *Mancodinium semitabulatum* in the Lusitanian Basin is at the top of *Prodactylioceras davoei* AB at Peniche (sample P-29, see Fig. 3.7; Table S3.1). At Brenha, *Mancodinium semitabulatum* was identified at the base of the *Amaltheus margaritatus* AB, in the MLOF member of the Vale das Fontes Formation (Fig. 3.5; Table S5). This species became much more common and consistent in the uppermost Pliensbachian and lowermost Toarcian (*Emaciaticeras emaciatum* and *Dactylioceras polymorphum* ABs) throughout the Lusitanian Basin (Tables S3.1, S4). *Mancodinium semitabulatum* was significantly suppressed by the T-OAE, and is sparse for the remainder of the Toarcian in the Lusitanian Basin, between the *Hildaites levisoni* and the *Dumortieria meneghinii* ABs (Fig. 3.15; Table S1). Rare, questionable specimens of *Maturodinium inornatum* (Plate 3.2(10)) were observed in the middle and upper Toarcian at Maria Pares (Table S1). This species was previously believed to be confined to the upper Pliensbachian (Morgenroth, 1970; Feist-Burkhardt and Wille, 1992).

At Peniche and Maria Pares, *Mendicodinium microscabratum* (Plate 3.2 (8)) was recorded between the *Hildaites levisoni* and the *Hammatoceras speciosum* ABs (Fig.

3.15; Tables S1, S3.1). This is inconsistent with the range of *Mendicodinium* spp., including *Mendicodinium microscabratum*, in the *Dactylioceras polymorphum* AB equivalent of central Italy reported by Bucefalo Palliani et al. (1997b). Thus, the records of *Mendicodinium microscabratum* in the middle and upper Toarcian in the Lusitanian Basin are the youngest known occurrences.

The oldest occurrences of the genus *Nannoceratopsis* (Plate 3.1(4–12)) in the Lusitanian Basin are the records of *Nannoceratopsis gracilis* and *N. senex* at the base of the *Amaltheus margaritatus* AB at Brenha and Peniche (Figs. 3.5, 3.7). This range base is consistent with records from northwest Europe (Morgenroth, 1970; Woollam and Riding, 1983; Bucefalo Palliani and Riding, 2003; Poulsen and Riding, 2003). The range tops of consistent occurrences of *Nannoceratopsis gracilis* and *N. senex* are in the lower Bajocian *Stephanoceras humphriesianum* AB (Poulsen and Riding, 2003, p. 124; Wiggan et al., 2017, table 2a). *Nannoceratopsis ambonis* is present in the *Dactylioceras polymorphum* AB at Maria Pares, Peniche and Vale das Fontes, and an isolated occurrence in the upper Toarcian (*Hammatoceras speciosum* AB) at Maria Pares (Tables S1, S2, S3.1).

Nannoceratopsis gracilis and *N. senex* occur consistently, and in relatively high proportions, throughout the *Dactylioceras polymorphum* AB at Maria Pares, Peniche and Vale das Fontes. The genus disappeared at the base of *Hildaites levisoni* AB in these three lower Toarcian successions. This event is interpreted to be a result of the palaeoenvironmental perturbations associated with the T-OAE in the Lusitanian Basin (e.g., Duarte et al., 2004; Hesselbo et al., 2007; Suan et al., 2008, 2010; Pittet et al., 2014; Correia et al., 2017a,b). *Nannoceratopsis ambonis* and *N. senex* reappeared in the upper Toarcian (*Hammatoceras speciosum* to *Pleydellia aalensis* ABs) at Maria Pares (Table S1).

The distinctive gonyaulacacean species *Scriniocassis weberi* and *S. priscus* were encountered, normally in low proportions, in the Toarcian of the Lusitanian Basin (Fig. 3.15; Tables S1, S3.1). *Scriniocassis weberi* ranges throughout the late Pliensbachian to early Aalenian, and *Scriniocassis priscus* is confined to the middle Toarcian to Aalenian, in northwest Europe (Riding, 1984a,b; Prauss, 1989; Feist-Burkhardt, 1990; Feist-Burkhardt and Wille, 1992; Feist-Burkhardt and Pross, 2010). At Peniche, *Scriniocassis weberi* (Plate 3.2(7)) was found in small numbers in the middle part of the *Dactylioceras polymorphum* AB (Table S3.1). By contrast, *Scriniocassis priscus* (Plate 3.2(4–6)) was sporadic, yet relatively common where present, between the Toarcian

Hildoceras bifrons and *Hammatoceras speciosum* ABs at Maria Pares, and apparently can be used as a marker for this interval in the Lusitanian Basin (Fig. 3.15).

The pollen-spore floras are generally not as biostratigraphically important as the dinoflagellate cysts. However, there are several miospore datums in the Maria Pares section which are noteworthy. The range base of *Callialasporites* spp. (Plate 3.5(4,5)) is in the *Brodieia gradata* AB of the middle Toarcian (Table S1). This biovent is consistent with other reports that the inception of this distinctive pollen genus is in the latest early Toarcian (Riding et al., 1991).

Apparently, the range top of the spore *Kraeuselisporites reissingeri* (Plate 3.4(3)) is in sample P33, within the *Hildaites levisoni* AB. This bioevent is broadly consistent with the findings of Morbey (1978, fig. 1). The distinctive spore *Kekryphalospora distincta* was encountered in sample PZ82 (*Dumortieria meneghinii* AB) at Maria Pares (Plate 3.4(2); Table S1). This occurrence is well within the known range of late Pliensbachian to early Bajocian (Fenton and Riding, 1987).

Plate 3.1. Selected dinoflagellate cysts from the Pliensbachian and Toarcian strata of the Lusitanian Basin, western Portugal. All specimens are housed in the collections of the LNEG (Portuguese Geological Survey), S. Mamede de Infesta, Portugal. The sample number, slide number and England Finder coordinates are provided. All the scale bars represent 20 μm.

1. *Luehndea spinosa* Morgenroth 1970. Fonte Coberta section, upper Pliensbachian (*Emaciaticeras emaciatum* AB), sample FC5, slide 1, L25/4. Ventral view, high focus.
2. *Luehndea spinosa* Morgenroth 1970. Fonte Coberta section, upper Pliensbachian (*Emaciaticeras emaciatum* AB), sample FC3, slide 1, T32/1. Ventral view, high focus. Note the epicystal archaeopyle.
3. *Luehndea spinosa* Morgenroth 1970. Peniche section, upper Pliensbachian (*Amaltheus margaritatus* AB), sample P-26, slide 1, M35/1.
4. *Nannoceratopsis* sp. Peniche section, upper Pliensbachian (*Amaltheus margaritatus* AB), sample P-20, slide 1, T35/4. Left lateral view. Note the two antapical horns of almost equal length.
5. *Nannoceratopsis gracilis* Alberti 1961. Brenha section, upper Pliensbachian (*Emaciaticeras emaciatum* AB), sample BrLem1, slide 1, G34/1. Right lateral view. Note the dorsal horn, which is larger than the ventral horn.
6. *Nannoceratopsis senex* van Helden 1977. Brenha section, upper Pliensbachian (*Emaciaticeras emaciatum* AB), sample BrLem1, slide 1, K41/2. Left lateral view. Note the single (dorsal) antapical horn, the subpentagonal lateral outline and the somewhat asymmetrical shape.
7. *Nannoceratopsis senex* van Helden 1977. Fonte Coberta section, upper Pliensbachian (*Emaciaticeras emaciatum* AB), sample FC3, slide 1, L31/4. Left lateral view.
8. *Nannoceratopsis senex* van Helden 1977. Brenha section, upper Pliensbachian (*Amaltheus margaritatus* AB), sample Br14, slide 1, G49/3. Left lateral view. Note the symmetrical and very rounded outline; the cingular archaeopyle is visible in the top right of the specimen.
9. *Nannoceratopsis senex* van Helden 1977. Peniche section, upper Pliensbachian (*Amaltheus margaritatus* AB), sample P-25, slide 1, O48/4. Right lateral view. Note the symmetrical lateral outline; the cingular archaeopyle is visible in the top left of the specimen.
10. *Nannoceratopsis senex* van Helden 1977. Maria Pares section, upper Toarcian (*Dumortieria meneghinii* AB), sample PZ82, slide 1, P41/3. Left lateral view. Note the single antapical horn and the asymmetrical lateral outline.
11. *Nannoceratopsis ambonis* Drugg 1978. Maria Pares section, upper Toarcian (*Hammatoceras speciosum* AB), sample PZ81, slide 1, U62/2. Left lateral view. Note the prominent dark sagittal rim.
12. *Nannoceratopsis ambonis* Drugg 1978. Maria Pares section, upper Toarcian (*Hammatoceras speciosum* AB), sample PZ81, slide 1, X63/1. Right lateral view. Note the prominent dark sagittal rim.

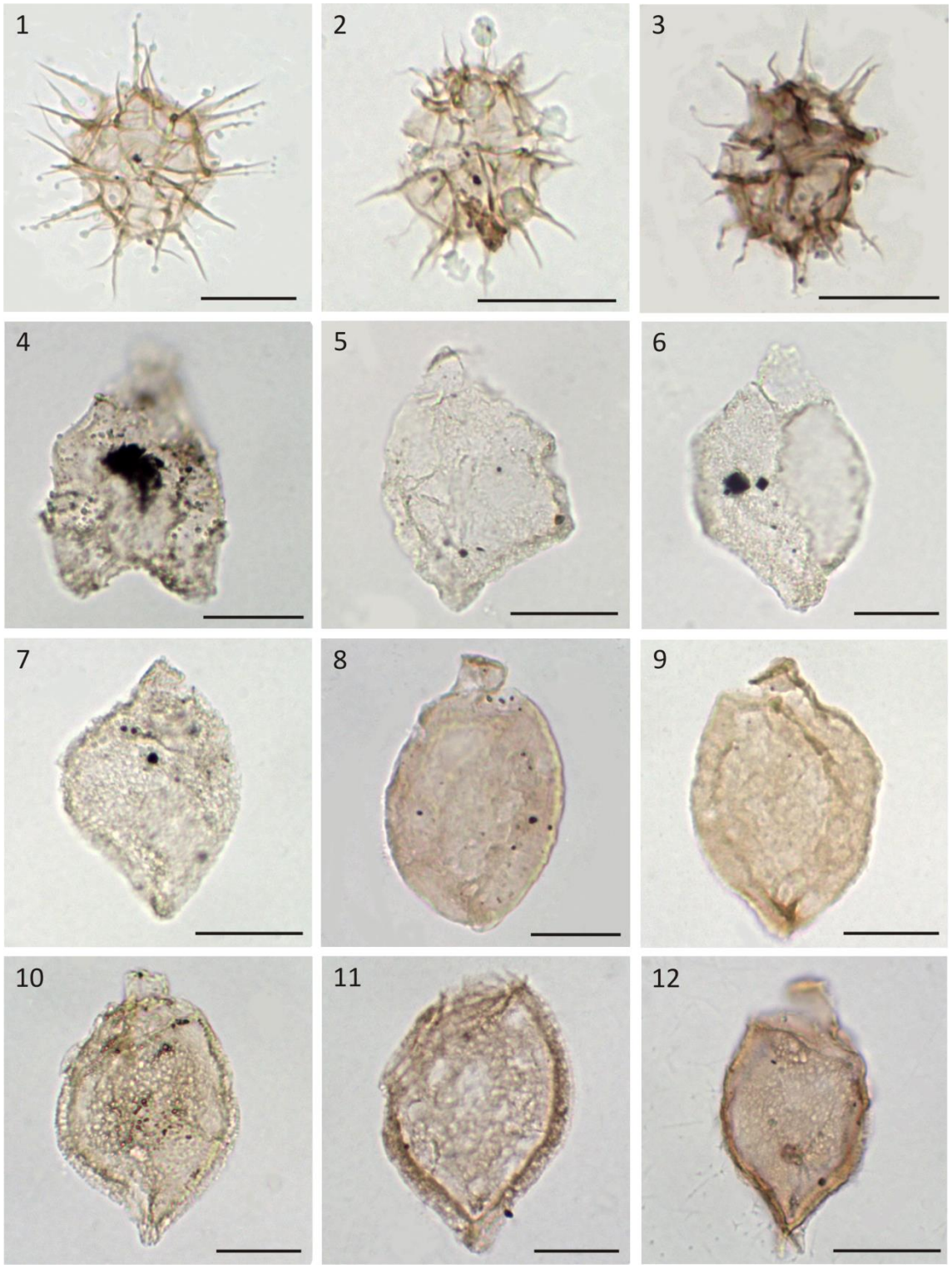

Plate 3.1 (caption on previous page)

Plate 3.2. Selected dinoflagellate cysts from the Pliensbachian and Toarcian strata of the Lusitanian Basin. All specimens are housed in the collections of the LNEG (Portuguese Geological Survey), S. Mamede de Infesta, Portugal. The sample number, slide number and England Finder coordinates are provided. All the scale bars represent 20 μm.

1. *Valvaeodinium* sp. Maria Pares section, middle Toarcian (*Hildoceras bifrons* AB), sample PZ57, slide 1, Q27/3. Note the relatively sparse cover of short, capitate processes and the combination (apical/intercalary) archaeopyle.
2. *Dapsilidium*? *deflandrei* (Valensi 1947) Lentin & Williams 1981. Maria Pares section, middle Toarcian (*Hildoceras bifrons* AB), sample PZ57, slide 1, R70/3. Note the covering of short distally-blunt processes.
3. *Sentusidinium* sp. Maria Pares section, upper Toarcian (*Hammatoceras bonarellii* AB), sample PZ71, slide 1, M52/2. Note the apical archaeopyle with deep accessory archaeopyle sutures.

4, 5. *Scriniocassis priscus* (Gocht 1979) Below 1990. **4, 5.** Maria Pares section, upper Toarcian (*Hammatoceras speciosum* AB), sample PZ77, slide 1, C32. **4.** - ventral view, high focus. **5.** - ventral view, low focus illustrating the dorsal surface. Note the rounded, subhexagonal cyst outline and the infrareticulate wall sculpture which is coarser near the sutures. The distinctive, strongly curved sutures surrounding the sulcus are evident in 4. In 5, the two plate (2" and 3") precingular archaeopyle, the large, middorsal 4''' plate and the sutural crests are clearly visible.

6. *Scriniocassis priscus* (Gocht 1979) Below 1990. Maria Pares section, upper Toarcian (*Hammatoceras speciosum* AB), sample PZ79, slide 1, W43/2. Dorsal view, high focus. Note the two plate precingular archaeopyle and the sulcus.
7. *Scriniocassis weberi* Gocht 1964. Peniche section, lower Toarcian (*Dactylioceras polymorphum* AB), sample P10, slide 1, N27/4. Dorsal view, high focus. Note the coarse reticulum and the precingular archaeopyle.
8. *Mendicodinium microscabratum* Bucefalo Palliani et al. 1997. Maria Pares section, upper Toarcian (*Hammatoceras speciosum* AB), sample PZ79, slide 1, G49/2. Ventral view; note the epicystal archaeopyle and the microscabrate autophragm.
9. *Mendicodinium* sp. Maria Pares section, upper Toarcian (*Hammatoceras speciosum* AB), sample PZ80, slide 1, H47/2. Oblique left lateral view.
10. *Maturodinium*? *inornatum* Morgenroth 1970. Maria Pares section, upper Toarcian (*Hammatoceras speciosum* AB), sample PZ77, slide 1, X52/1. Note the hypocystal tabulation and the faint cingulum.
11. *Mancodinium semitabulatum* Morgenroth 1970. **11.** Maria Pares section, upper Toarcian (*Dumortieria meneghinii* AB), sample PZ82, slide 1, X54/3. Note the well-preserved, partly separated, small epicystal plates which are involved in the formation of the 'disintegration' type archaeopyle, in which all the epicystal plates are individually lost.
12. *Mancodinium semitabulatum* Morgenroth 1970. Peniche section, lower Pliensbachian (*Prodactylioceras davoei* AB), sample P-29, slide 1, O37/1. Ventral view, median focus. Note the anterior sulcal plate (the sulcal tongue).

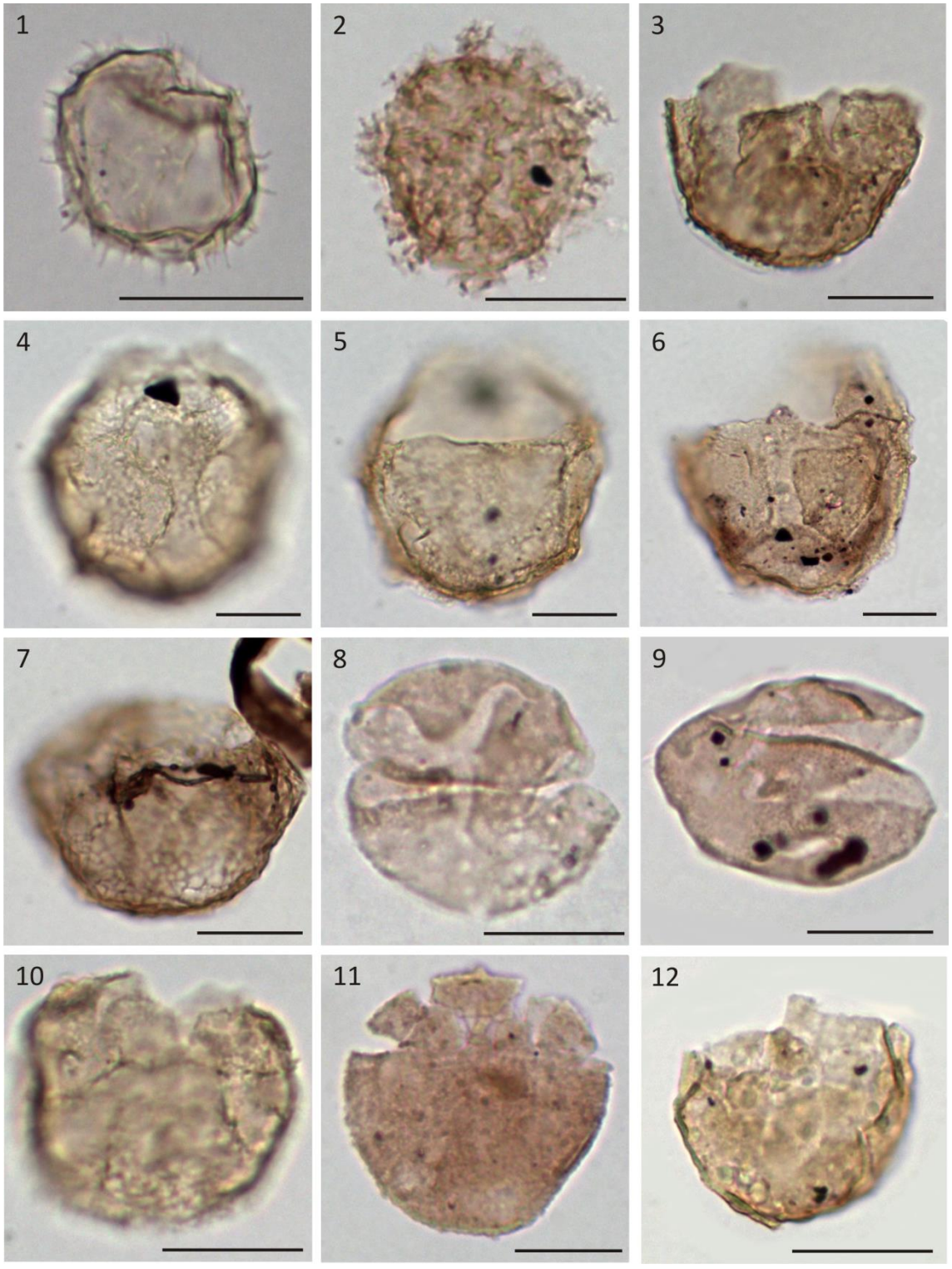

Plate 3.2 (caption on previous page)

Plate 3.3. Selected aquatic and terrestrially-derived palynomorphs from the Sinemurian to Toarcian strata of the Lusitanian Basin. All specimens are housed in the collections of the LNEG (Portuguese Geological Survey), S. Mamede de Infesta, Portugal. The sample number, slide number and England Finder coordinates are provided. All the scale bars represent 20 μm.

1. *Micrhystridium* sp. (acanthomorph acritarch). Peniche section, lower Pliensbachian (*Tragophylloceras ibex* AB), sample P-34, slide 1, R37.
2. *Micrhystridium* sp. (acanthomorph acritarch). Maria Pares section, upper Toarcian (*Hammatoceras speciosum* AB), sample PZ79, slide 1, G46/1.
3. Acanthomorph acritarch indeterminate. Maria Pares section, upper Toarcian (*Dumortieria meneghinii* AB), sample PZ82, slide 1, N30.
4. *Polygonium jurassicum* Bucefalo Palliani et al. 1996 (acanthomorph acritarch). Brenha section, upper Pliensbachian (*Amaltheus margaritatus* AB), sample Br20, slide 1, P33/1.
5. *Halosphaeropsis liassica* Mädler 1968 (prasinophyte). Maria Pares section, middle Toarcian (*Brodieia gradata* AB), sample PZ64, slide 1, K24/3.
6. *Tasmanites* sp. (prasinophyte). São Pedro de Moel section, upper Sinemurian (*Oxynoticeras oxynotum* AB), sample PM2, slide 1, S33.
7. Foraminiferal test lining. Maria Pares section, middle Toarcian (*Hildoceras bifrons* AB), sample PZ57, slide 1, P36.
8. *Calamospora tener* (Leschik 1955) Mädler 1964 (spore). Peniche section, lower Toarcian (*Dactylioceras polymorphum* AB), sample P13, slide 1, K24/4.
9. *Cibotiumspora jurienensis* (Balme1957) Filatoff 1975 (spore). Maria Pares section, lower Toarcian (*Hildaites levisoni* AB), sample P19, slide 1, V22.
10. *Conbaculatisporites* sp. (spore). Maria Pares section, lower Toarcian (*Hildaites levisoni* AB), sample P20, slide 1, D43.
11. *Concavisporites granulosus* Tralau 1968 (spore). Maria Pares section, lower Toarcian (*Hildaites levisoni* AB), sample P16, slide 1, G71/2.
12. *Cyathidites minor* Couper 1953 (spore). Vale das Fontes section, lower Toarcian (*Dactylioceras polymorphum* AB), sample PVF 11, slide 1, S33.

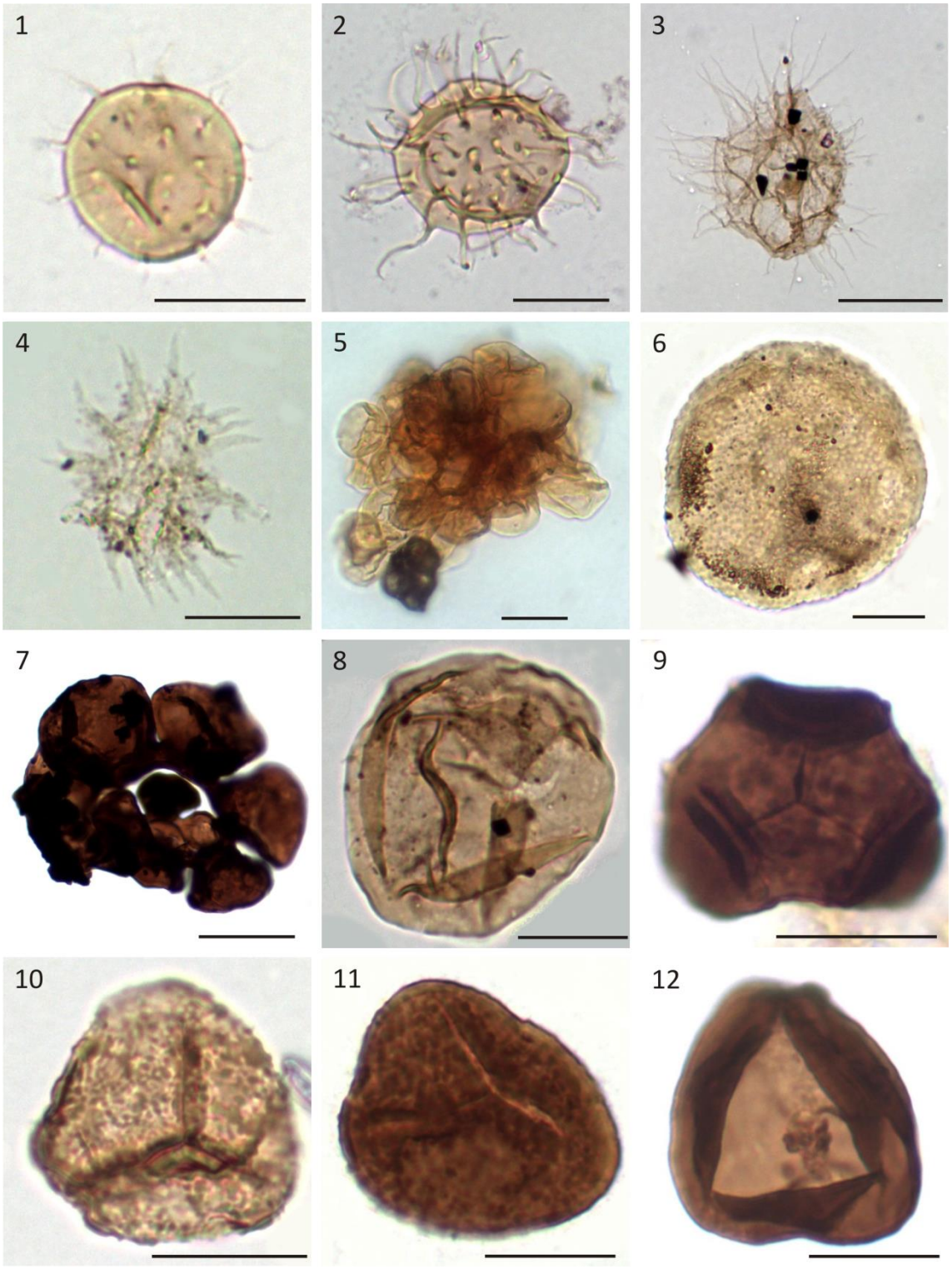

Plate 3.3 (caption on previous page)

Plate 3.4. Selected spores and pollen from the Pliensbachian and Toarcian strata of the Lusitanian Basin. All specimens are housed in the collections of the LNEG (Portuguese Geological Survey), S. Mamede de Infesta, Portugal. The sample number, slide number and England Finder coordinates are provided. All the scale bars represent 20 μm.

1. *Ischyosporites variegatus* (Couper 1958) Schulz 1967 (spore). Maria Pares section, lower Toarcian (*Hildaites levisoni* AB), sample PZ19, slide 1, V32/2.
2. *Kekryphalospora distincta* Fenton & Riding 1987 (spore). Maria Pares section, upper Toarcian (*Dumortieria meneghinii* AB), sample PZ82, slide 2, C36/1.
3. *Kraeuselisporites reissingeri* (Harris 1957) Morbey 1975 (spore). Vale das Fontes section, lower Toarcian (*Dactylioceras polymorphum* AB), sample PVF4, slide 1, R53/3.
4. Tetrad of *Leptolepidites* sp. (spore). Vale das Fontes section, lower Toarcian (*Dactylioceras polymorphum* AB), sample PVF13, slide 1, M27.
5. *Lycopodiacidites rugulatus* (Couper 1958) Schulz 1967 (spore). Brenha section, upper Pliensbachian (*Amaltheus margaritatus* AB), sample Br16, slide 2, U63.
6. *Osmundacidites wellmanii* Couper 1953 (spore). Maria Pares section, lower Toarcian (*Hildaites levisoni* AB), sample P19, slide 1, S36/2.
7. *Plicifera delicata* (Bolchovitina 1953) Bolchovitina 1966 (spore). Maria Pares section, lower Toarcian (*Hildaites levisoni* AB), sample PZ19, slide 1, N24.
8. *Retitriletes* sp. (spore). Vale das Fontes section, lower Toarcian (*Hildaites levisoni* AB), sample PV14, slide 1, K12/4.
9. *Striatella* sp. (spore). Maria Pares section, middle Toarcian (*Brodieia gradata* AB), sample PZ59, slide 1, K41/1.
10. *Todisporites granulatus* Tralau 1968 (spore). Peniche section, lower Toarcian (*Hildaites levisoni* AB), sample P17, slide 1, S36.
11. *Todisporites* sp. (spore). Maria Pares section, lower Toarcian (*Hildaites levisoni* AB), sample PZ19, slide 1, F49/3.
12. *Alisporites* sp. *sensu lato* (pollen). Brenha section, upper Pliensbachian (*Amaltheus margaritatus* AB), sample Br17, slide 1, V46/2.

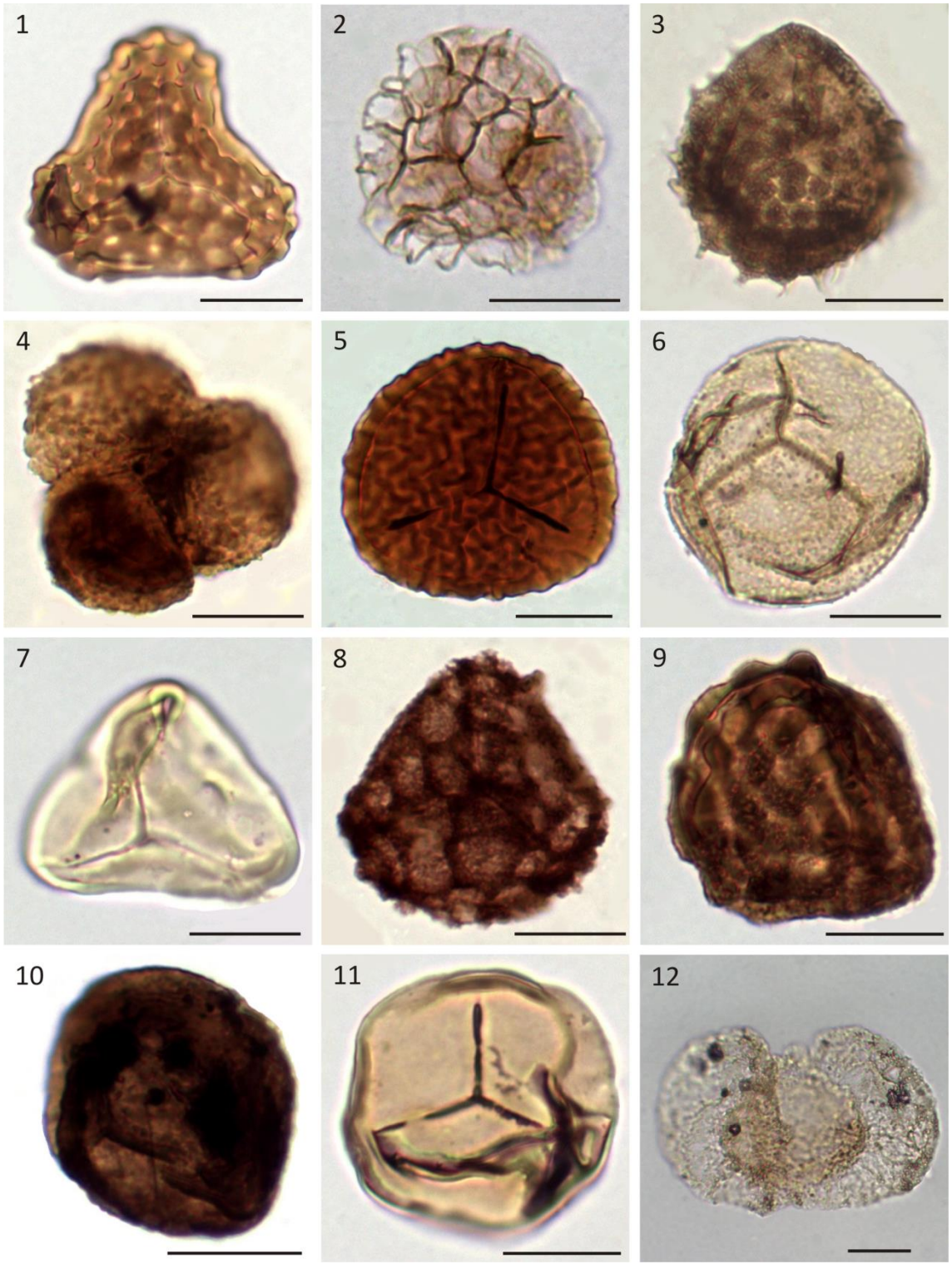

Plate 3.4 (caption on previous page)

Plate 3.5. Selected pollen grains from the Sinemurian to Toarcian strata of the Lusitanian Basin. All specimens are housed in the collections of the LNEG (Portuguese Geological Survey), S. Mamede de Infesta, Portugal. The sample number, slide number and England Finder coordinates are provided. All the scale bars represent 20 μm.

1. *Araucariacites australis* Cookson 1947 ex Couper 1958. Vale das Fontes section, lower Toarcian (*Dactylioceras polymorphum* AB), sample PVF3, slide 1, N30/1.
2. *Inaperturopollenites* sp. Vale das Fontes section, lower Toarcian (*Dactylioceras polymorphum* AB), sample PVF3, slide 1, O30/1.
3. *Cycadopites follicularis* Wilson & Webster 1946. Maria Pares section, middle Toarcian (*Hildoceras bifrons* AB), sample PZ57, slide 1, X62/1.
4. *Callialasporites dampieri* (Balme 1957) Dev 1961. Maria Pares section, upper Toarcian (*Hammatoceras speciosum* AB), sample PZ81, slide 3, K29/4.
5. *Callialasporites turbatus* (Balme 1957) Schulz 1967. Maria Pares section, upper Toarcian (*Hammatoceras speciosum* AB), sample PZ81, slide 3, N54.
6. *Cerebropollenites macroverrucosus* (Thiergart 1949) Schulz 1967. Brenha section, upper Pliensbachian (*Amaltheus margaritatus* AB), sample Br14, slide 1, E54.
7. *Classopollis classoides* (Pflug 1953) Pocock & Jansonius 1961. São Pedro de Moel section, upper Sinemurian (*Oxynoticeras oxynotum* AB), sample PM2, slide 1, Q36.
8. *Classopollis classoides* (Pflug 1953) Pocock & Jansonius 1961Vale das Fontes section, lower Toarcian (*Dactylioceras polymorphum* AB), sample PVF2, slide 1, H30/2.
9. Tetrad of *Classopollis classoides* (Pflug 1953) Pocock & Jansonius 1961. Peniche section, lower Pliensbachian (*Tragophylloceras ibex* AB), sample P-34, slide 1, Q32/2.
10. Tetrad of *Classopollis* sp. Maria Pares section, middle Toarcian (*Brodieia gradata* AB), sample PZ59, slide 1, Q38/4.
11. *Exesipollenites* sp. Maria Pares section, middle Toarcian (*Hildoceras bifrons* AB), sample PZ57, slide 1, M35/2.
12. Tetrad of *Spheripollenites* sp. Maria Pares section, middle Toarcian (*Hildoceras bifrons* AB), sample PZ58, slide 1, L51/1.

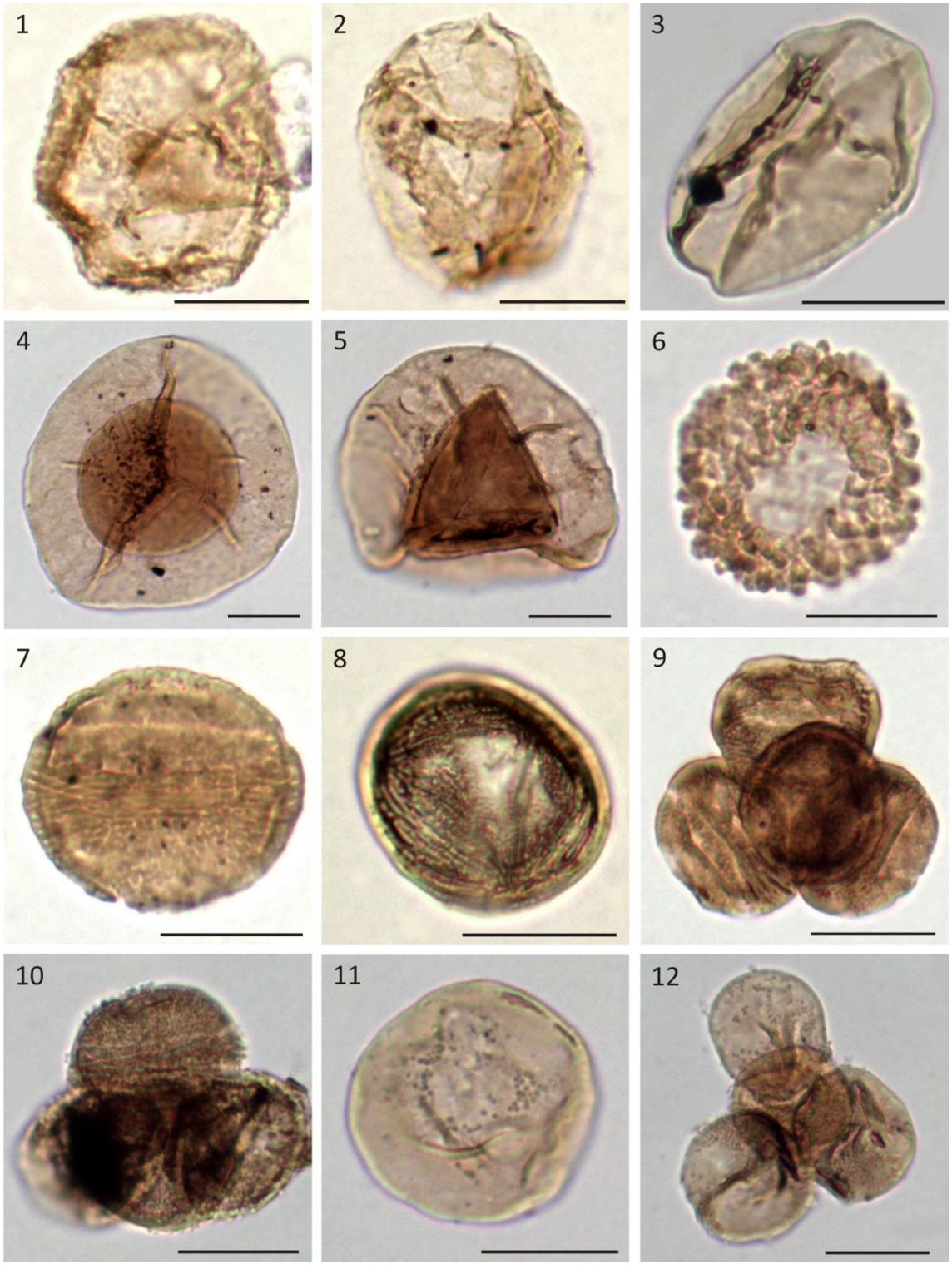

Plate 3.5 (caption on previous page)

5.4. The Pliensbachian–Toarcian dinoflagellate cyst biozonation of the Lusitanian Basin

Due their relatively short ranges, many Jurassic dinoflagellate cysts are reliable stratigraphical markers, and several biozonation schemes have been defined based on them (Woollam and Riding, 1983; Helby et al., 1987; Riding and Thomas, 1992; Poulsen and Riding, 2003; Riding et al., 2010). A new dinoflagellate cyst biozonation for the upper Pliensbachian to upper Toarcian of the Lusitanian Basin is summarised in Fig. 3.15, and compared with the schemes of Riding and Thomas (1992) and Poulsen and Riding (2003).

5.4.1. The Luehndea spinosa dinoflagellate cyst Biozone

Definition: The interval from the range bases of *Luehndea spinosa, Nannoceratopsis gracilis* and *Nannoceratopsis senex*, to the range top of *Luehndea spinosa*.

Age: Late Pliensbachian (base of *Amaltheus margaritatus* AB) to earliest Toarcian (top of the *Dactylioceras polymorphum* AB).

Characteristics: The dominance of *Luehndea spinosa* and the relatively consistent and frequent presence of *Mancodinium semitabulatum*, *Nannoceratopsis gracilis* and *Nannoceratopsis senex*. The inception of abundant *Luehndea spinosa* allows the consistent subdivision of this biozone.

Remarks: The *Luehndea spinosa* dinoflagellate cyst Biozone in the Lusitanian Basin is coeval with the *Luehndea spinosa* Total Range Biozone of Riding and Thomas (1992, p. 20–21) and the *Luehndea spinosa* Biozone of Poulsen and Riding (2003), both of northwest Europe (Fig. 3.15). All these three biozones are defined by the range base of *Luehndea spinosa* and other taxa, such as *Nannoceratopsis senex* or *Nannoceratopsis gracilis* at the base, to the range top of *Luehndea spinosa* at the top. The *Nannoceratopsis senex* and *Luehndea spinosa* subbiozones are broadly equivalent to subbiozones *a* and *b* of Riding and Thomas (1992), respectively (Fig. 3.15).

5.4.1.1. The Nannoceratopsis senex dinoflagellate cyst Subbiozone

Definition: The interval from the range base of *Luehndea spinosa,* to the range base of the abundant presence of this species.

Age: Late Pliensbachian (base of *Amaltheus margaritatus* AB) to latest Pliensbachian (close to the top of the *Emaciaticeras emaciatum* AB).

Characteristics: *Luehndea spinosa* is typically present in relatively low abundances in this Subbiozone.

5.4.1.2. The Luehndea spinosa dinoflagellate cyst Subbiozone

Definition: The interval from the range base of the abundant presence of *Luehndea spinosa*, to the range top of this species.

Age: Latest Pliensbachian (close to the top of the *Emaciaticeras emaciatum* AB) to earliest Toarcian (top of the *Dactylioceras polymorphum* AB).

Characteristics: *Luehndea spinosa* is consistently present, and largely in high abundances.

5.4.2. The Mendicodinium microscabratum dinoflagellate cyst Biozone

Definition: The interval from the range top of *Luehndea spinosa*, to the apparent range top of *Mendicodinium microscabratum*.

Age: Early Toarcian (base of the *Hildaites levisoni* AB) to late Toarcian (top of the *Hammoteceras speciosum* AB).

Characteristics: This biozone typically exhibits low abundances and diversities of dinoflagellate cysts. *Mancodinium semitabulatum*, *Mendicodinium microscabratum* and *Scriniocassis priscus* may be present (Fig. 3.15).

Remarks: This biozone is partially equivalent to the *Nannoceratopsis gracilis* Interval Biozone of Riding and Thomas (1992, p. 21–25), but the latter extends into the early Bajocian in northwest Europe. In the Lusitanian Basin, the top of this biozone is presently not well defined. *Nannoceratopsis gracilis* subbiozones *a* and *b* of Riding and Thomas (1992) are correlated with the *Mancodinium semitabulatum* and *Mendicodinium microscabratum* subbiozones herein respectively. Furthermore, the *Mancodinium semitabulatum* and *Mendicodinium microscabratum* subbiozones herein, correspond to the *Mancodinium semitabulatum* and *Parvocysta nasuta* biozones of Poulsen and Riding (2003).

This study represents the youngest record of *Mendicodinium microscabratum* in the middle and upper Toarcian (Fig. 3.15). Bucefalo Palliani et al. (1997b) reported this species from the lower Toarcian of Italy. Other coeval sections, and younger strata, should be studied in the Lusitanian Basin and adjacent regions in order to confirm if the range top of this species is at the top of *Hammoteceras speciosum* AB.

Using the apparent range top of *Mendicodinium microscabratum*, and the reappearance of *Nannoceratopsis senex*, the base of another dinoflagellate cyst biozone could possibly be defined at, or close to, the base of the *Dumortieria meneghinii* AB. Due the lack of information on the latest Toarcian of the Lusitanian Basin, we opted not to erect another dinoflagellate cyst biozone until more information becomes available.

5.4.2.1. The Mancodinium semitabulatum dinoflagellate cyst Subbiozone

Definition: The interval from the range top of *Luehndea spinosa*, to the range base of *Scriniocassis priscus*.

Age: Early Toarcian (base of the *Hildaites levisoni* AB) to middle Toarcian (close to the top of the *Hildoceras bifrons* AB).

Characteristics: The only dinoflagellate cysts present are rare *Mancodinium semitabulatum* and *Mendicodinium microscabratum*.

5.4.2.2. The Mendicodinium microscabratum dinoflagellate cyst Subbiozone

Definition: The interval from the range base of *Scriniocassis priscus,* to the apparent range top of *Mendicodinium microscabratum*.

Age: Middle Toarcian (close to the top of the *Hildoceras bifrons* AB) to late Toarcian (top of the *Hammoteceras speciosum* AB).

Characteristics: *Mendicodinium microscabratum* is the dominant dinoflagellate cyst species in a very low diversity flora.

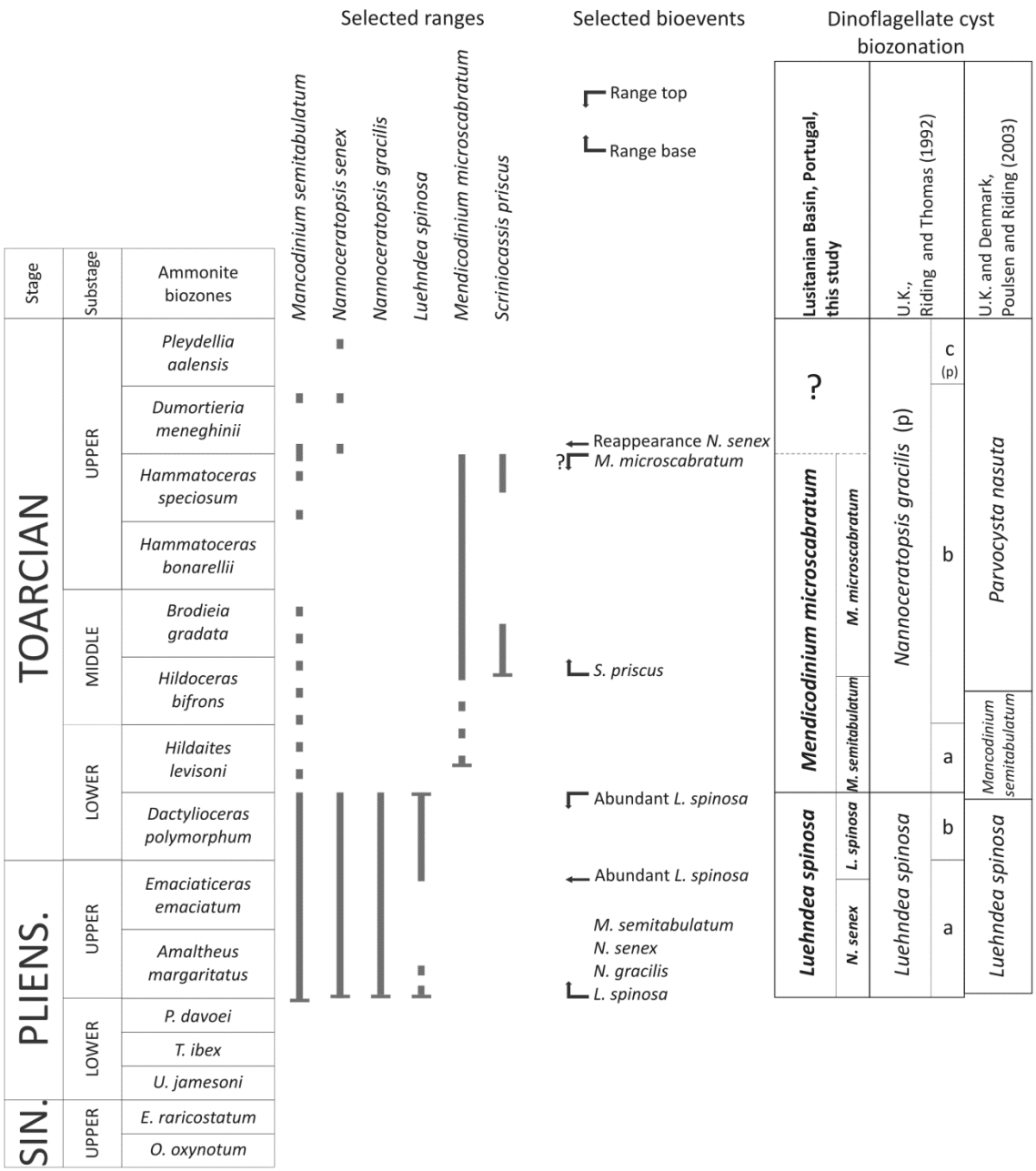

Figure 3.15. A composite dinoflagellate cyst range chart for the Lower Jurassic of the Lusitanian Basin based on selected bioevents. The database supporting this chart are the those herein, and those in Correia et al. (2017a,b). The proposed dinoflagellate cyst biozonation is also depicted on the right, and is compared to two northwest European zonal schemes (Riding and Thomas, 1992 and Poulsen and Riding, 2003).

6. Conclusions

The Lower Jurassic palynology of the Lusitanian Basin of western Portugal was comprehensively investigated, with the principal emphasis on dinoflagellate cysts. A Sinemurian to Toarcian composite succession from six sections throughout this important depocentre was constructed. The Sinemurian proved entirely devoid of dinoflagellate cysts, but the overlying Pliensbachian and Toarcian succession is characterised by relatively low dinoflagellate cyst diversity; fifteen taxa were encountered. Only seven genera were recorded with certainty, these are *Luehndea, Mancodinium, Mendicodinium, Nannoceratopsis, Scriniocassis, Sentusidinium* and *Valvaeodinium.*

The dinoflagellate cyst succession in the Lusitanian Basin is broadly consistent with other Lower Jurassic sedimentary basins in Europe. However, the reliable upper Sinemurian dinoflagellate cyst *Liasidium variabile* appears not to have migrated south into the Lusitanian Basin from northwest Europe. *Luehndea spinosa* is the dominant palynomorph in the lowermost Toarcian (*Dactylioceras polymorphum* AB), and is the most age-diagnostic species. At the base of *Hildaites levisoni* AB, *Luehndea spinosa* became extinct, probably due to the effects of the T-OAE. Also at this time, dinoflagellate cyst abundance and diversity sharply decreased. The recovery of phytoplankton during the middle and late Toarcian was relatively slow, following the T-OAE.

Other palynomorph groups such as acanthomorph acritarchs, foraminiferal test linings, pollen and spores, and prasinophytes were also documented. The pollen species *Classopollis classoides* is the most common and abundant palynomorph throughout the Lower Jurassic strata of the Lusitanian Basin. The non-dinoflagellate cyst taxa encountered exhibit no discernible trend, or stratigraphical succession.

By contrast, the dinoflagellate cysts *Luehndea spinosa*, *Mancodinium semitabulatum*, *Mendicodinium microscabratum*, *Nannoceratopsis gracilis*, *Nannoceratopsis senex* and *Scriniocassis priscus* were relatively frequent and proved to have biostratigraphical significance. Two dinoflagellate cyst biozones were defined for the succession studied. These are the *Luehndea spinosa* and the *Mendicodinium microscabratum* biozones which are of late Pliensbachian–earliest Toarcian, and earliest–late Toarcian age respectively. These two dinoflagellate cyst biozones are each subdivided into two subbiozones.

CHAPTER IV

Middle (Aalenian–Bathonian) Jurassic palynostratigraphy

Chapter IV cover:

Gonyaulacysta pectinigera (Gocht 1970) Fensome 1979. Cabo Mondego section, lower Bathonian (*Zigzagiceras zigzag* AB), sample Bt200.

Chapter IV. Middle Jurassic (Aalenian–Bathonian) palynostratigraphy

Adapted from paper 4:

Correia, V.F., Riding, J.B., Henriques, M.H., Fernandes, P., Pereira, Z. Wiggan, N. J. The Middle Jurassic palynostratigraphy of the northern Lusitanian Basin, Portugal. *Newsletters on Stratigraphy*, submitted.

Abstract

A composite largely Middle Jurassic succession spanning the Toarcian–Aalenian transition to the lowermost Bathonian exposed at Cabo Mondego and São Gião in the northern Lusitanian Basin, western Portugal, was examined palynologically. The 129 samples are correlated to ammonite biozones spanning *Pleydellia aalensis* to *Zigzagiceras zigzag*. The Cabo Mondego succession comprises the type section of the Cabo Mondego Formation and spans virtually the entire interval studied. This is a significant interval because it includes the Global Stratotype Section and Point (GSSP) and the Auxiliary Stratigraphical Section and Point (ASSP) for the Bajocian and Bathonian stages respectively. The Cabo Mondego Formation largely yielded relatively abundant palynomorph associations in the 68 productive samples recovered. By contrast, the Póvoa da Lomba Formation at São Gião only includes the Toarcian–Aalenian transition; the 21 productive horizons produced sparse assemblages. The uppermost Toarcian to lowermost Bajocian is characterised by a low diversity dinoflagellate cyst association, typified by *Nannoceratopsis*. Above this is a markedly more diverse assemblage. This influx, in the *Witchellia laeviuscula* AB, represents a global evolutionary radiation which may be linked to sea level rise. The trend of increasing dinoflagellate cyst diversity continued at the Bajocian–Bathonian transition. Nevertheless, the Middle Jurassic dinoflagellate cyst assemblages of the Lusitanian Basin are significantly less diverse than coeval palynobiotas from eastern and northern Europe, and the Arctic. The Toarcian Oceanic Anoxic Event (T-OAE) profoundly inhibited cyst-forming dinoflagellates in this depocentre, and the recovery was protracted. Hence the T-OAE may have suppressed dinoflagellate cyst diversity well into the Middle Jurassic. This phenomenon may have been exacerbated by the absence of typically Arctic taxa through latitudinal controls and/or global cooling during the early Aalenian. These low levels of dinoflagellate cyst species richness may also be

related to the palaeogeography of the Lusitanian Basin. This relatively isolated deepwater depocentre close to the Proto Atlantic, may have precluded extensive biotal exchange with the widespread shelfal areas of the western Tethys. The absence of *Dissiliodinium giganteum* in the Lusitanian Basin is consistent with this scenario. The pollen and spores observed in this study are typical of Middle Jurassic assemblages worldwide. Araucarian pollen, largely *Callialasporites*, diversified and became prominent during the Aalenian.

Keywords

Biostratigraphy; Dinoflagellate cysts; Cabo Mondego and São Gião; Lusitanian Basin; Middle Jurassic; Palaeobiology.

1. Introduction

This study documents the marine and terrestrial palynology of the uppermost Lower and Middle Jurassic (uppermost Toarcian to lowermost Bathonian) strata at Cabo Mondego and São Gião near Figueira da Foz in the northern part of the Lusitanian Basin, central western Portugal (Figs. 4.1, 4.2). The principal aim of this work is to investigate the biostratigraphy of these palynofloras, especially the dinoflagellate cysts, and to compare them with coeval biotas largely from Europe. The Cabo Mondego section at Murtinheira Beach was ratified as the Global Stratotype Section and Point (GSSP) for the Bajocian Stage in 1996 (Henriques et al., 1994, Pavia and Enay 1997). This succession also includes the Auxiliary Stratigraphical Section and Point (ASSP) for the Bathonian Stage (Fernández-López et al., 2009a, b).

The Middle Jurassic ammonite faunas at both Cabo Mondego and São Gião have been intensively researched (Henriques 1995, Fernández-López et al. 2006, 2009a, b, Sandoval et al. 2012, Henriques and Canales 2013, Henriques et al. 2016). These studies have provided a framework for many works on other fossil groups such as brachiopods (Andrade et al. 2016), calcareous nannofossils (Suchéras-Marx et al. 2012, 2015) and benthic foraminifera (Canales and Henriques 2008, 2013). This is the first detailed investigation throughout the Middle Jurassic palynology of the Lusitanian Basin. However, this topic has been previously studied by Davies (1985), Smelror et al. (1991), Barrón et al. (1999) and Barrón and Azerêdo (2003).

Davies (1985) examined four existing sample collections from outcrops of the Lower to Upper Jurassic (Sinemurian to Oxfordian) at Brenha, Peniche and Zambujal in

the Lusitanian Basin. However, the main emphasis of this author was on the Lower Jurassic, this study lacks stratigraphical resolution, and the stratigraphy of the Lusitanian Basin was not well established at that time. Of the Middle Jurassic, only the Aalenian to Callovian at Brenha and the Aalenian at Zambujal were studied (Davies 1985, figs. 8, 9). Smelror et al. (1991) described a relatively diverse marine palynoflora from 21 samples from the uppermost Bathonian and lowermost Callovian (*Macrocephalites herveyi* ammonite biozone - AB) of Cabo Mondego. Barrón and Azerêdo (2003) is a study which built on Barrón et al. (1999). The former work is on the Callovian to Oxfordian succession at Pedrógão, south of Cabo Mondego, and the emphasis was mainly on pollen and spores. These authors only recovered three dinoflagellate cysts (Barrón and Azerêdo 2003, p. 285). Other substantial contributions on the Jurassic palynology of Portugal include Mohr and Schmidt (1988), Bucefalo Palliani and Riding (2003), Oliveira et al. (2007a), Borges et al. (2011, 2012), Barrón et al. (2013), Rocha et al. (2016), Correia et al. (2017a, 2017b, 2018) and Turner et al. (2017).

The fossil record of dinoflagellates is based on their decay-resistant organic (and more rarely calcareous or siliceous) benthic resting cysts (Evitt, 1985). The oldest unequivocal fossil dinoflagellate cysts are known from the Middle Triassic (Riding et al. 2010). The group underwent a major evolutionary radiation during the Early–Middle Jurassic, and became abundant and diverse during the rest of Mesozoic and Cenozoic (Fensome et al. 1996, MacRae et al. 1996, Wiggan et al. 2017). Many dinoflagellate cyst taxa had relatively short ranges and therefore are used as biostratigraphical markers (e.g. Poulsen and Riding 2003). It is hoped that this study on the uppermost Toarcian to lowermost Bathonian palynomorph floras of the Lusitanian Basin will further characterise the biostratigraphy of this important depocentre.

2. Geographical and geological setting

The Lusitanian Basin is located on the western central coastal margin of Portugal; the basin trends NE-SW and is approximately 300 km long and 150 km wide (Fig. 4.1). The basin fill is up to 5 km thick; most of this is Jurassic but it ranges from the Middle?–Upper Triassic to the uppermost Lower Cretaceous (Wilson et al. 1989). The breakup of Pangaea and the opening of the North Atlantic initiated the development of the Lusitanian Basin and controlled its development (Rasmussen et al. 1998, Kullberg et al. 2013). Middle Jurassic strata are very well developed in the Lusitanian

Basin, especially in the coastal area at Cabo Mondego near the city of Figueira da Foz (Figs. 4.1, 4.2). These coastal outcrops include the Cabo Mondego Formation, which is late Toarcian to Callovian in age. The GSSP for the Bajocian, and the ASSP for the Bathonian are both within the Cabo Mondego Formation (Pavia and Enay 1997, Fernández-López et al., 2009a, b). This unit comprises almost 500 m of alternating interbeds of fossiliferous grey marls and marly limestones/limestones. It represents a distal platform setting which was established during the Toarcian (Azerêdo et al. 2003). The abundant and diverse molluscan faunas have enabled the establishment of an accurate ammonite-based biostratigraphy for this unit (e.g. Henriques 1995, Fernández-López et al. 2006, Sandoval et al. 2012). The São Gião section exposes the Póvoa da Lomba Formation. This unit is comprised of regularly-bedded marly limestones 10 to 30 cm thick, alternating with slightly thicker beds of grey marl. This succession is coeval with the lower part of Cabo Mondego Formation (Fig. 4.2, Azerêdo et al. 2003).

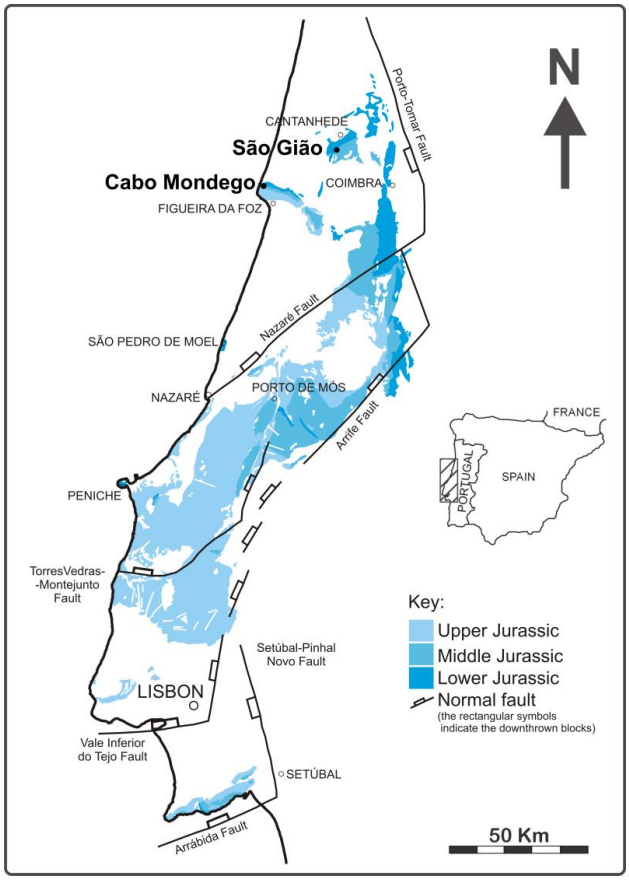

Figure 4.1. The Jurassic outcrops in the Lusitanian Basin of western Portugal, the major faults in this depocentre and the locations of the two sections studied herein. The Cabo Mondego succession is northwest of Figueira da Foz city at 40° 12' 1.26" N; 8° 54' 10.4" W (Murtinheira beach); the Bathonian Auxiliary Stratigraphical Section and Point (ASSP) is at 40° 11' 17.11" N; 8° 54' 32.17" W. The section at São Gião, south of Catanhede village, is at 40° 18' 12.63" N; 8° 37' 17.58" W. This figure is adapted from Figueiredo (2009) and Kullberg et al. (2013).

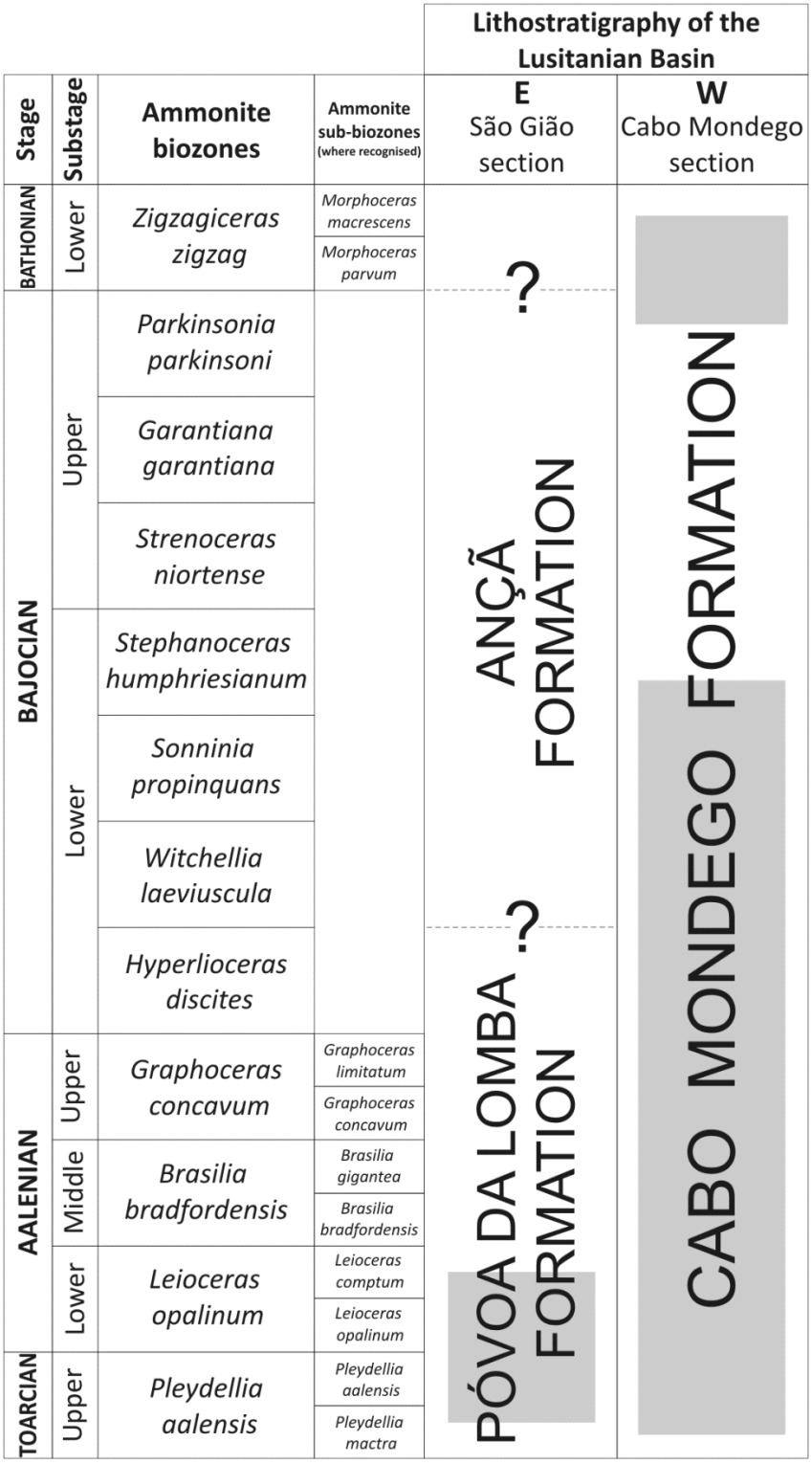

Figure 4.2. The ammonite biostratigraphy and the lithostratigraphy of the uppermost Toarcian to lowermost Bathonian successions at Cabo Mondego and São Gião in the northern Lusitanian Basin, western Portugal based on Azerêdo et al. (2003). The grey shading indicates the parts of the Cabo Mondego and Póvoa da Lomba formations which were studied herein.

3. Material and methods

The Cabo Mondego and São Gião sections are located in the northern Lusitanian Basin. Cabo Mondego is ~7 km northwest of Figueira da Foz and ~40 km west of Coimbra, and São Gião is situated about 5 km southwest of Cantanhede village (Fig. 4.1). Herein, 129 samples were collected from these two important reference sections which span the upper Toarcian *Pleydellia aalensis* ammonite biozone (AB) to the lower Bathonian *Zigzagiceras zigzag* AB (Figs. 4.2–4.7). The Cabo Mondego succession comprises the type section of the Cabo Mondego Formation, and spans virtually the entire interval studied except the upper Bajocian *Strenoceras niortense* and *Garantiana garantiana* ABs, which were not sampled (Figs. 4.3, 4.4) due to the absence of accurate biostratigraphical control. At São Gião, the Toarcian–Aalenian transition within the Póvoa da Lomba Formation was collected (Fig. 4.6).

The samples were prepared using traditional acid-digestion techniques (Riding and Warny 2008), but oxidation of macerated residues was not employed. All residues were screened using a 15 µm mesh sieve and the final palynomorph concentrates were stained with safranine. If possible, at least 300 palynomorphs were counted. However, if the material was sparse, as many specimens as possible from two microscope slides were counted. The unused sample material, aqueous residues, microscope slides and the figured specimens in Plates 4.1 to 4.3 are curated in the collections of LNEG (Portuguese Geological Survey), São Mamede de Infesta, Portugal.

4. Palynology

In this section, the palynomorph assemblages from Cabo Mondego and São Gião encountered in this study are described in three sections. These palynobiotas are fully documented in Tables S7 and S8 and Figs. 4.3–4.7. Selected specimens are illustrated in Plates 4.1–4.3. In the Appendix 1 are listed all the palynomorph taxa at and below the species level which were recovered from the material studied herein, or mentioned in the text, with full author citations.

4.1. The uppermost Toarcian to lower Bajocian part of the Cabo Mondego Formation at Cabo Mondego (samples M2 to AB192)

In the lower part of Cabo Mondego section at Murtinheira beach, 68 samples (numbered M2 to AB192), were collected from the Cabo Mondego Formation. The succession includes the Bajocian GSSP, and it spans the *Pleydellia aalensis* to *Stephanoceras humphriesianum* ABs (Figs. 4.2, 4.3). These samples were generally moderately well-preserved, however nine of the horizons samples proved barren of palynomorphs (Table S7).

This succession is dominated by foraminiferal test linings and gymnosperm pollen, with subordinate proportions of acritarchs, dinoflagellate cysts, prasinophytes and spores. Overall, pollen is the principal palynomorph type from the uppermost Toarcian to close to the top of the middle Aalenian (samples M2 to M237), with foraminiferal test linings and pollen exhibiting subequal proportions in the uppermost middle Aalenian to much of the lower Bajocian (samples M245 to AB178a) (Fig. 4.5).

Indeterminate pollen is prominent, and *Araucariacites australis*, *Classopollis* spp. and *Exesipollenites* spp. are relatively common. Bisaccate pollen (*Alisporites* spp.), *Callialasporites* spp., *Cerebropollenites macroverrucosus*, *Chasmatosporites* spp., *Cycadopites granulatus*, *Perinopollenites elatoides* and *Spheripollenites* spp. are relatively sparse. The overall diversity of pollen increased steadily up section. In sample M361, in the *Hyperlioceras discites* AB and above, the numbers of *Araucariacites australis* and the diversity of *Callialasporites* increased markedly. Moreover, *Exesipollenites* spp. was less prominent, and this genus became present only sporadically. Furthermore, the inception of *Chasmatosporites* spp. is in sample AB164, within the *Sonninia propinquan*s AB.

Like the pollen, the pteridophyte spore assemblages increased in diversity upsection in this interval. Most taxa recognised occur in relatively low proportions. *Anapiculalatisporites* spp., the smooth genus *Cyathidites*, indeterminate forms, *Leptolepidites* spp., *Lycopodiacidites rugulatus* and *Marattisporites* sp. were present consistently throughout. By contrast, *Kraeuselisporites reissingeri* is confined to the interval between samples M14 and M91 (uppermost Toarcian to lowermost Aalenian). The single occurrence of the distinctive spore *Kekryphalospora distincta* is in sample M24 (uppermost Toarcian). The lowest occurrences in this section of *Osmundacidites wellmanii*, *Ischyosporites variegatus*, *Striatella seebergensis*, *Todisporites* sp.,

Auritulinasporites triclavus and *Retitriletes austroclavatidites* are recorded in samples M34, M83t, M225, M305, M319 and M328 respectively (Table S7).

Foraminiferal test linings are consistently very common, and attained a maximum of 67.7% in sample M396. By contrast, dinoflagellate cysts are of low diversity and low abundance in the uppermost Toarcian and the lower Bajocian *Hyperlioceras discites* AB (samples M2 to M398). In this interval *Mancodinium semitabulatum*, *Nannoceratopsis gracilis*, *Nannoceratopsis senex* and *Scriniocassis priscus* were encountered reasonably consistently. All of these species, except *Nannoceratopsis gracilis*, are confined to this interval. By contrast, *Dissiliodinium* sp. 1, *Impletospheridium* sp., *Mendicodinium* spp., *Phallocysta elongata* and *Scriniocassis weberi* were observed extremely sporadically (Figs. 4.3, 4.5; Table S7).

However from sample AB55, at the top of the *Hyperlioceras discites* AB, and above (to sample AB192), the dinoflagellate cyst associations abruptly became substantially more common and diverse (Fig. 4.5; Table S7). In this part of the lower Bajocian, spanning the *Witchelluia laeviuscula* to *Stephanoceras humphriesianum* ABs, 17 forms have their range bases. These comprise *Acanthaulax* sp. cf. *A. crispa*, *Ctenidodinium sellwoodii*, *Dissiliodinium* sp. 2, *Dissiliodinium* spp., *Durotrigia daveyi*, *Durotrigia* sp., *Epiplosphaera gochtii*, *Kallosphaeridium*? sp., *Korystocysta* sp. cf. *K. aldridgeii*, *Meiourogonyaulax* spp., *Pareodinia* sp., *Rhynchodiniopsis* spp., *Sentusidinium* sp. cf. *S. asymmetrum*, *Sentusidinium* sp. cf. *S. explanatum*, *Sentusidinium* sp. 1, *Sentusidinium* spp. and *Wanaea* sp. Of these, *Acanthaulax* sp. cf. *A. crispa*, *Dissiliodinium* spp., *Durotrigia daveyi*, *Durotrigia* sp., *Epiplosphaera gochtii*, *Kallosphaeridium*? sp., *Korystocysta* sp. cf. *K. aldridgeii*, *Pareodinia* sp. and *Wanaea* sp. are sporadic and rare; the other forms are relatively consistently present (Fig. 4.3). Low diversity acritarch (largely *Micrhystridium* spp.) and prasinophytes (mainly large forms such as *Tasmanites*) assemblages were present throughout in relatively low numbers (Fig. 4.5; Table S7).

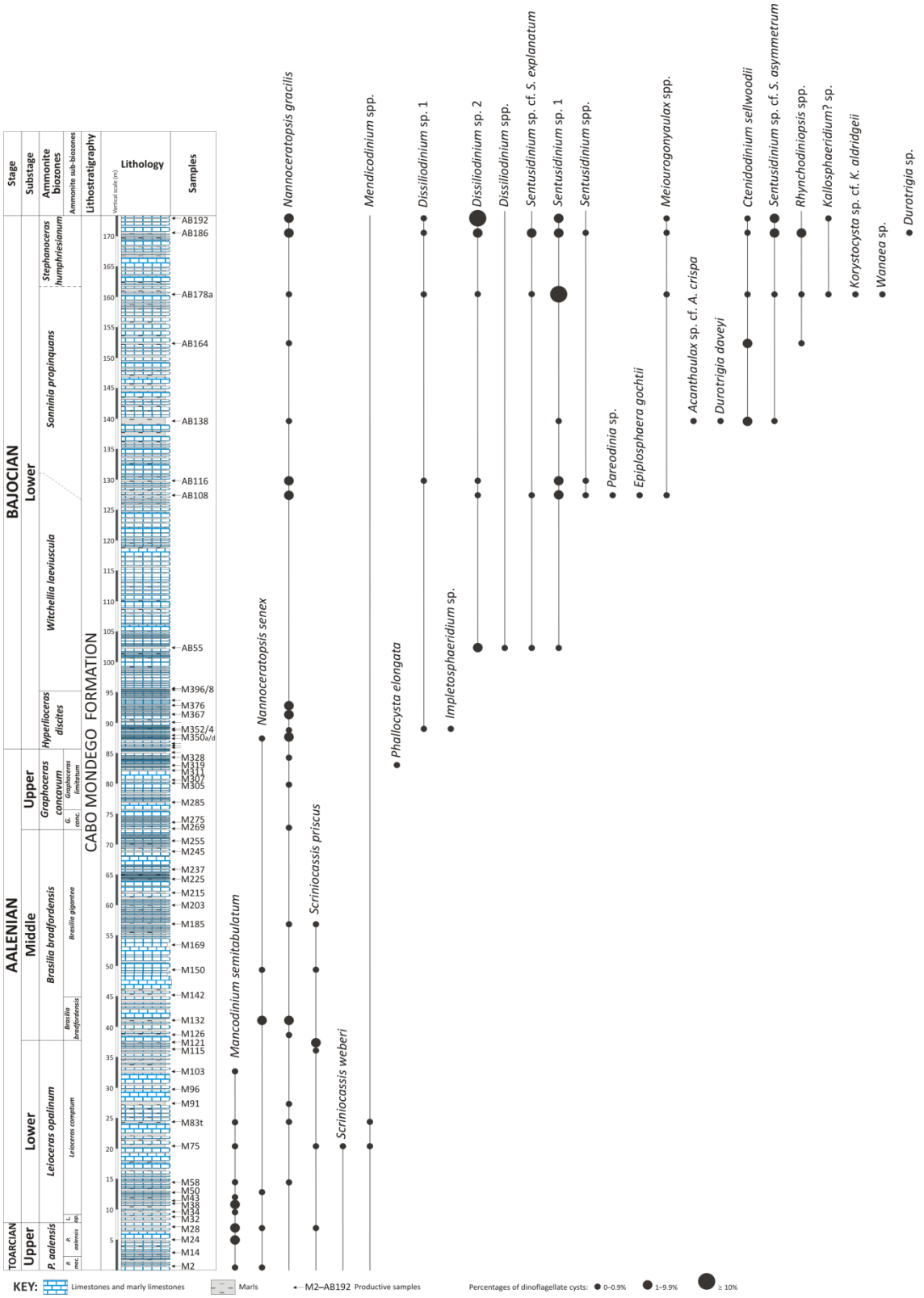

Figure 4.3. The lithological log of the lower part of Cabo Mondego Formation, spanning the uppermost Toarcian to lower Bajocian succession at Cabo Mondego, adapted from Fernández-López et al. (1988), and Canales and Henriques (2008, 2013). This succession includes the Global Stratotype Section and Point (GSSP) for the Bajocian Stage at Murtinheira Beach. The positions of the palynologically productive samples M2 through M398 and AB55 to AB192 are indicated. Semi-quantitative data for 26 selected dinoflagellate cysts are depicted.

4.2. The uppermost Bajocian and lowermost Bathonian part of the Cabo Mondego Formation at Cabo Mondego (samples Bt94 to Bt220)

The Bajocian–Bathonian transition in the Cabo Mondego Formation was sampled at Cabo Mondego section; 14 horizons were collected (numbers Bt94 to Bt220). This unit includes the Bathonian ASSP, and the succession comprises the *Parkinsonia parkinsoni* and *Zigzagiceras zigzag* ABs (Figs. 4.2, 4.4). Again, the preservation of palynomorphs proved moderately good, but one sample was barren (Table S7). This upper part of the Cabo Mondego succession is overwhelmingly dominated by gymnospermous pollen, with relatively abundant dinoflagellate cysts. The proportions of acritarchs, foraminiferal test linings, prasinophytes and spores are markedly subordinate. The most profound difference with the underlying succession at this locality is the significant diminution of foraminiferal test linings and prasinophytes, with the former group being most profoundly affected (Fig. 4.5; Table S7). An association between foraminiferal test linings and prasinophytes has not been previously noted. The foraminiferal test linings from the Toarcian to Lower Bajocian in this study are most likely to be benthic taxa. It is possible that the early planktonic foraminifera, which may not have produced these test linings, somehow suppressed their benthic counterparts (Hart et al. 2003).

Gymnosperm pollen is substantially more abundant than in the majority of the underlying succession at Cabo Mondego, and the relatively high diversity which developed in the Lower Bajocian is maintained. The pollen associations are largely similar to those from the underlying lower Bajocian (subsection 4.1). They are characterised by a dominance of *Araucariacites australis*; the saccate genus *Callialasporites*, *Cycadopites granulatus* and indeterminate pollen are also prominent. *Callialasporites segmentatus* and *Callialasporites* spp. are more common than in the underlying succession. Bisaccate pollen (*Alisporites* spp.) and *Chasmatosporites* spp. are consistently present throughout in very low proportions, and *Exesipollenites* spp. and *Spheripollenites* spp. were encountered somewhat intermittently. *Cerebropollenites macroverrucosus* and *Classopollis* spp. are both sporadic and relatively sparse, only being recorded in samples Bt 122 and Bt184 respectively. The inception of consistent *Perinopollenites elatoides* in sample Bt94 at the base of the *Parkinsonia parkinsoni* AB appears to be a notable local bioevent (Table S7).

The pteridophyte spore assemblages in the uppermost Bajocian and lowermost Bathonian succession are not prominent (Fig. 4.5). They are substantially similar in

relative proportions and taxonomic spectrum to those in the underlying Aalenian and Lower Bajocian part of the Cabo Mondego Formation. Diversity, however, is relatively low; the assemblages are largely comprised of *Cyathidites* spp., *Ischyosporites variegatus*, *Leptolepidites* spp and spores of indeterminate identification (Table S7).

The dinoflagellate associations in the *Parkinsonia parkinsoni* and *Zigzagiceras zigzag* ABs are highly variable in relative proportions, and exhibit several marked abundance peaks (Fig. 4.5). These associations are substantially higher in diversity than their counterparts in the underlying succession (Table S7); a total of 32 forms were recognised. *Chytroeisphaeridia chytroeides*, *Ctenidodinium sellwoodii*, *Dissiliodinium* spp., indeterminate forms, *Sentusidinium* spp. and *Valensiella ovulum* are present consistently and in significant numbers. The other taxa however, are present either sporadically, or have restricted ranges within this succession. For example *Gonyaulacysta pectinigera*, *Korystocysta pachyderma*, *Mendicodinium* spp., *Pareodinia ceratophora* are present intermittently, and *Bradleyella adela* and *Rhynchodiniopsis*? *regalis* are confined to sample Bt94 (*Parkinsonia parkinsoni* AB). *Meiourogonyaulax* spp. are confined to the *Parkinsonia parkinsoni* AB, and several taxa are confined to the overlying *Zigzagiceras zigzag* AB. The latter include *Ctenidodinium cornigerum*, *Gonyaulacysta jurassica* subsp. *adecta*, indeterminate complex chorate dinoflagellate cysts, ?*Korystocysta gochtii*, *Mendicodinium groenlandicum* and *Tubotuberella dangeardii* (Fig. 4.4; Table S7). The assemblage is overwhelmingly dominated by the gonyaulacacean lineage. However, many forms recognised in this interval are present in a single sample, or low numbers of horizons and are relatively rare. Furthermore, many of them are difficult to assign to existing species (Table S7).

Foraminiferal test linings dominate the miscellaneous marine palynomorphs, however these forms do not exceed 8.1% (sample Bt164). Acritarchs (largely *Micrhystridium* spp.) and large prasinophytes occur throughout this interval in relatively low proportions (Fig. 4.5; Table S7).

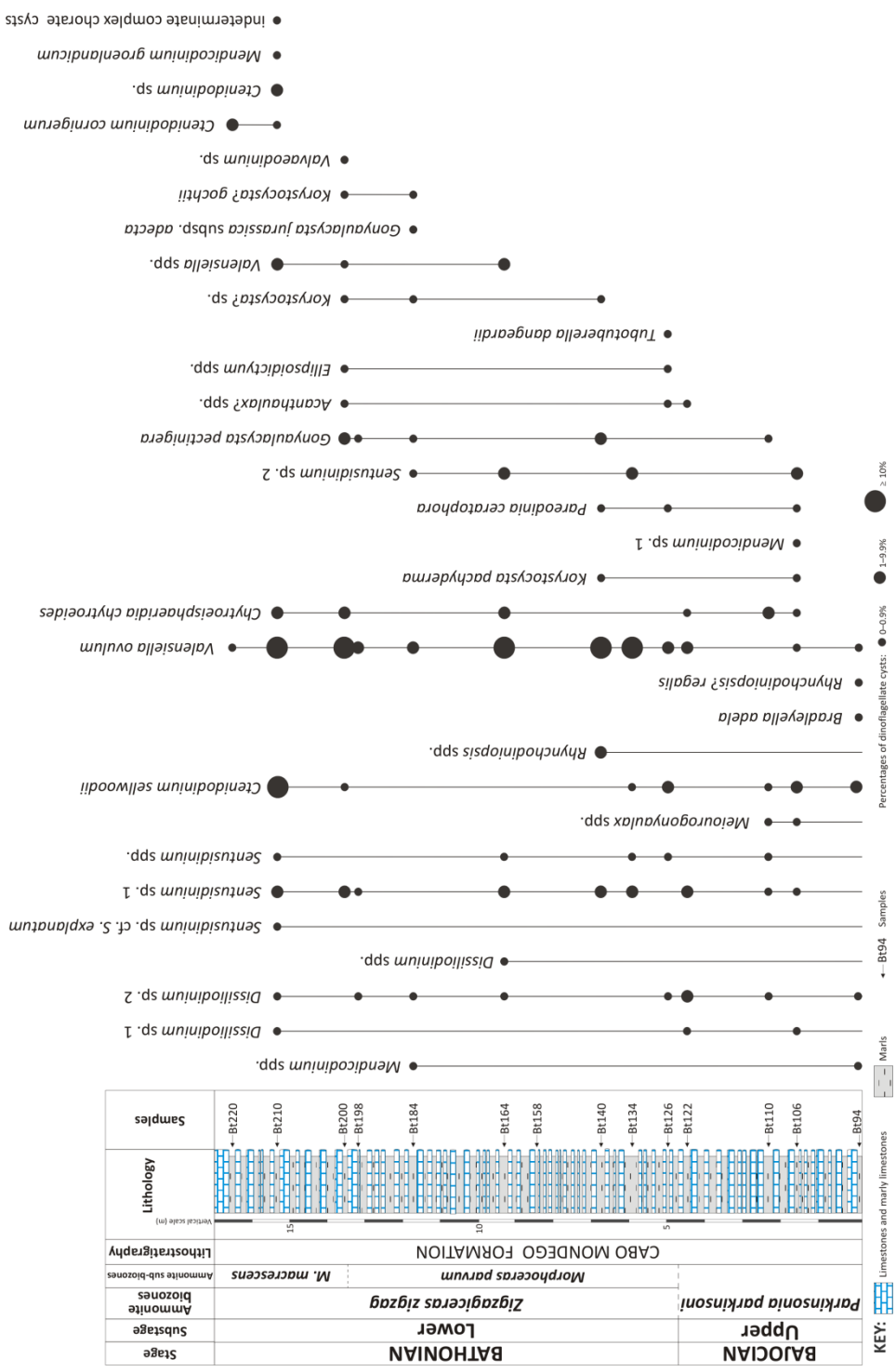

Figure 4.4. The lithological log of the upper part of Cabo Mondego Formation, spanning the uppermost Bajocian to lowermost Bathonian succession at Cabo Mondego, adapted from Fernández-López et al. (2006). This succession includes the Bathonian ASSP. The positions of the palynologically productive samples Bt94 through Bt220 are indicated, and semi-quantitative data for 31 selected dinoflagellate cysts are depicted.

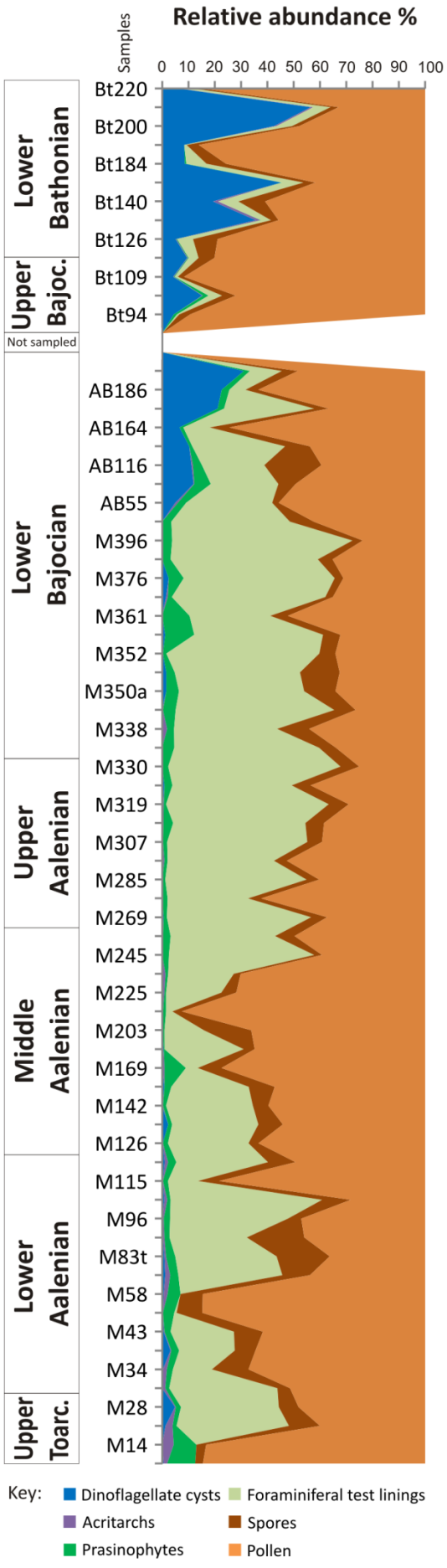

Figure 4.5. The relative abundances, expressed in percentages, of the six main palynomorph groups recorded from the uppermost Toarcian to lowermost Bathonian of the Cabo Mondego Formation at the type section at Cabo Mondego.

4.3. The uppermost Toarcian and lowermost Aalenian part of the Póvoa da Lomba Formation at São Gião (samples SG8 to SG102)

The Póvoa da Lomba Formation at São Gião section was also sampled herein. At this outcrop, 47 samples were collected from the Toarcian–Aalenian transition; the material is from the *Pleydellia aalensis* and *Leioceras opalinum* ABs (Figs. 4.2, 4.6). Overall the palynofloras from these samples were relatively sparse and poorly preserved, and 26 horizons proved entirely devoid of palynomorphs (Table S8).

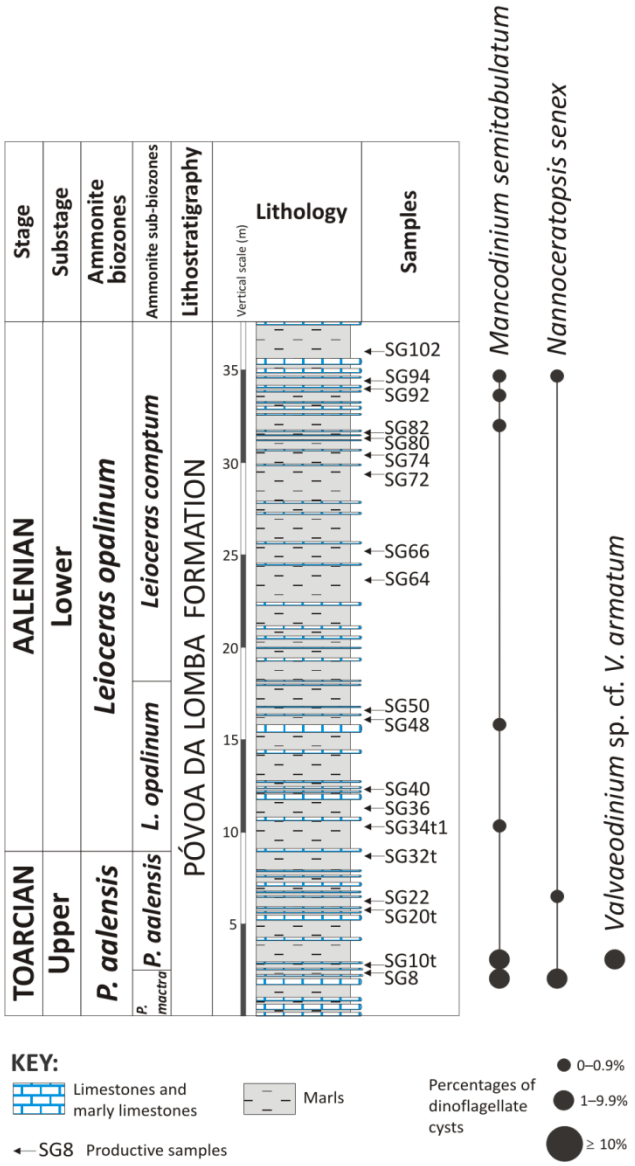

Figure 4.6. The lithological log of the Póvoa da Lomba Formation (uppermost Toarcian to lowermost Aalenian) at São Gião, adapted from Canales-Fernández et al. (2014), with the positions of the palynologically productive samples SG8 to SG102 indicated. Semi-quantitative data for three dinoflagellate cysts are illustrated.

The productive samples from the Póvoa da Lomba Formation are dominated by gymnospermous pollen (Fig. 4.7), largely tetrads of ?*Spheripollenites* spp. Bisaccate pollen (*Alisporites* spp.) is also present consistently, but in moderate to low proportions. *Classopollis* spp. is confined to the Upper Toarcian, and *Araucariacites australis* and *Callialasporites* spp. are restricted to the Lower Aalenian. *Cerebropollenites macroverrucosus* was present in the lower part of the succession sporadically in low numbers. The spore associations are also of low diversity. *Cyathidites* spp., indeterminate forms, *Kraeuselisporites reissingeri* and *Leptolepidites* spp. are present throughout. The proportions of these forms are generally relatively low, but indeterminate forms and *Leptolepidites* spp. intermittently attained significant numbers. *Ischyosporites variegatus* is confined to sample SG10t in the uppermost Toarcian *Pleydellia aalensis* AB (Table S8).

The marine microplankton are, like the terrestrially-derived palynomorphs, of low diversity. These associations are dominated by prasinophytes, with clumps of *Halosphaeropsis liassica* and large indeterminate types being especially prominent. These are both present throughout, but are most noticeable in the uppermost Toarcian and the *Leioceras opalinum* AB of the lowermost Aalenian (samples SG8 to SG50b). *Tasmanites* spp. are also present. Dinoflagellate cysts and acritarchs are both somewhat sporadic in occurrence and relatively rare (Fig. 4.7). Of the former, *Mancodinium semitabulatum and Nannoceratopsis senex* are present throughout the succession in very low numbers, and *Valvaeodinium* sp. cf. *V. armatum* was observed in sample SG10t in the uppermost Toarcian (*Pleydellia aalensis* AB). The acritarchs are largely referable to the genus *Micrhystridium.*

Foraminiferal test linings are entirely absent (Table S8). The relatively scarce marine palynofloras from this section may be related with the relative palaeoshore proximal position of São Gião, compared with Cabo Mondego. This is also pointed by the palaeoecological analyses of the foraminiferal assemblages, which enabled the recognition of a regional gradient ranging from the distal part of the platform (Cabo Mondego and Serra da Boa Viagem) towards the transitional (São Gião and Maria Pares) and proximal parts of the shelf (Zambujal de Alcaria) (Canales et al. 2014; Figueiredo et al. 2014; Silva et al. 2014, 2015; Henriques et al. 2016).

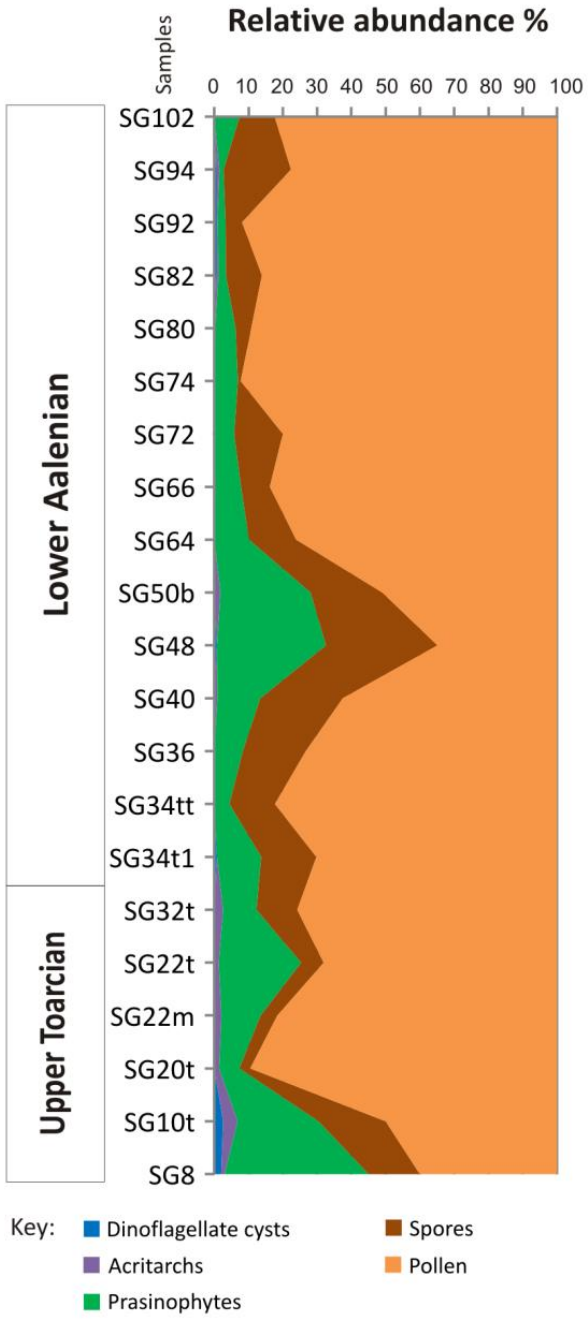

Figure 4.7. The relative abundances, expressed in percentages, of the six main palynomorph groups recorded from the uppermost Toarcian to lower Aalenian of the Póvoa da Lomba Formation at the São Gião section.

5. Palynostratigraphy

In this section, the dinoflagellate cyst and the pollen-spore biostratigraphy are discussed. The other palynomorphs groups, i.e. acritarchs, foraminiferal test linings and prasinophytes, do not exhibit significant evolutionary change throughout the succession studied.

5.1. Dinoflagellate cyst biostratigraphy

In this study a formal dinoflagellate cyst biozonation is not proposed, principally because much of the upper Bajocian succession was not sampled at Cabo Mondego. For example the *Strenoceras niortense* and *Garantiana garantiana* ABs were not studied here (Fig. 4.2, 4.8) due to the lack of comprehensive ammonite (or other group) biostratigraphical control. Furthermore, above the lower Aalenian, only one section is studied, at Cabo Mondego. Therefore, the recommended lateral comparison with, at least two successions, is inexistent above this horizon. The stratigraphical extents of selected dinoflagellate cysts at Cabo Mondego and São Gião plotted against the samples are depicted in Figs. 4.3, 4.4 and 4.6. Ranges of the most biostratigraphically significant dinoflagellate cysts are depicted in Fig. 4.8. A low diversity association, typified by the genus *Nannoceratopsis*, is present between the uppermost Toarcian (*Pleydellia aalensis* AB) and the lowermost Bajocian (*Hyperlioceras discites* AB). Above this is a substantially more diverse flora, between the lower Bajocian (*Witchellia laeviuscula* AB) and the lower Bathonian (*Zigzagiceras zigzag* AB) (Fig. 4.8).

*5.1.1. Uppermost Toarcian to lowermost Bajocian (*Pleydellia aalensis *to* Hyperlioceras discites *ABs)*

The older, uppermost Toarcian to lowermost Bajocian, assemblage at Cabo Mondego and São Gião only yielded 10 taxa. These are *Dissiliodinium* sp. 1, *Impletosphaeridium* sp., *Mancodinium semitabulatum, Mendicodinium* spp., *Nannoceratopsis gracilis, Nannoceratopsis senex, Phallocysta elongata, Scriniocassis priscus, Scriniocassis weberi* and *Valvaeodinium* sp. cf. *V. armatum* (Plate 4.1; Tables S7, S8).This low diversity association is prior to the major, geographically extensive, diversification of dinoflagellate cysts of the family Gonyaulacaceae in the Bajocian documented by Wiggan et al. (2017).

The range top of *Mancodinium semitabulatum* is in the lowermost Aalenian (*Leioceras opalinum* AB) at both Cabo Mondego and São Gião (Fig. 4.8; Tables S7, S8). The consistent range top is in the *Stephanoceras humphriesianum* AB of northwest Europe (Riding et al. 1991, Feist-Burkhardt and Wille 1992, Riding and Thomas 1992, Feist-Burkhardt and Götz 2016). Hence this bioevent is apparently substantially older in the Lusitanian Basin than further north.

The range top of *Scriniocassis priscus* is within the middle Aalenian (*Brasilia bradfordensis* AB) (Fig. 4.8). This is consistent with records from Germany (Prauss 1989, Feist-Burkhardt and Wille 1992, Feist-Burkhardt and Pross 2010), but not the UK where this datum has been placed in the lower Bajocian *Otoites sauzei* AB (equivalent of the *Sonninia propinquans* AB) (e.g. Riding and Thomas 1992). In the Lusitanian Basin, *Nannoceratopsis senex* apparently became extinct in the lowermost Bajocian (*Hyperlioceras discites* AB). This bioevent may be highly significant as there are few records of this species in northwest Europe. Also in the *Hyperlioceras discites* AB, the oldest representatives of *Dissiliodinium* were observed (Fig. 4.8). This is consistent with the records of Prauss (1989) and Riding et al. (1991) from further north, although Feist-Burkhardt (1990), Feist-Burkhardt and Wille (1992) and Feist-Burkhardt and Pross (2010) recorded this genus from the Aalenian in Germany.

*5.1.2. Lower Bajocian (*Witchellia laeviuscula *to* Stephanoceras humphriesianum *ABs)*

The diversity of dinoflagellate cysts increased markedly within the *Witchellia laeviuscula* AB, and the taxonomic richness rose further throughout the remainder of the lower Bajocian which was studied herein, up to the *Stephanoceras humphriesianum* AB (Table S7). This diversity increase in the *Witchellia laeviuscula* AB at Cabo Mondego appears to represent a significant influx, and the transition between this and the underlying *Hyperlioceras discites* AB is far less incremental than in northwest Europe (Riding et al. 1991, Feist-Burkhardt and Monteil 1997, Wiggan et al. 2017). Range bases in the lower Bajocian above the *Hyperlioceras discites* AB include those of *Acanthaulax* sp. cf. *A. crispa*, *Ctenidodinium sellwoodii*, *Durotrigia* spp., *Epiplosphaera gochtii*, *Meiourogonyaulax* spp., *Pareodinia* sp., *Sentusidinium* spp. and *Wanaea* sp (Plates 4.1, 4.2). The range top of *Nannoceratopsis gracilis* is in the *Stephanoceras humphriesianum* AB (Fig. 4.8).

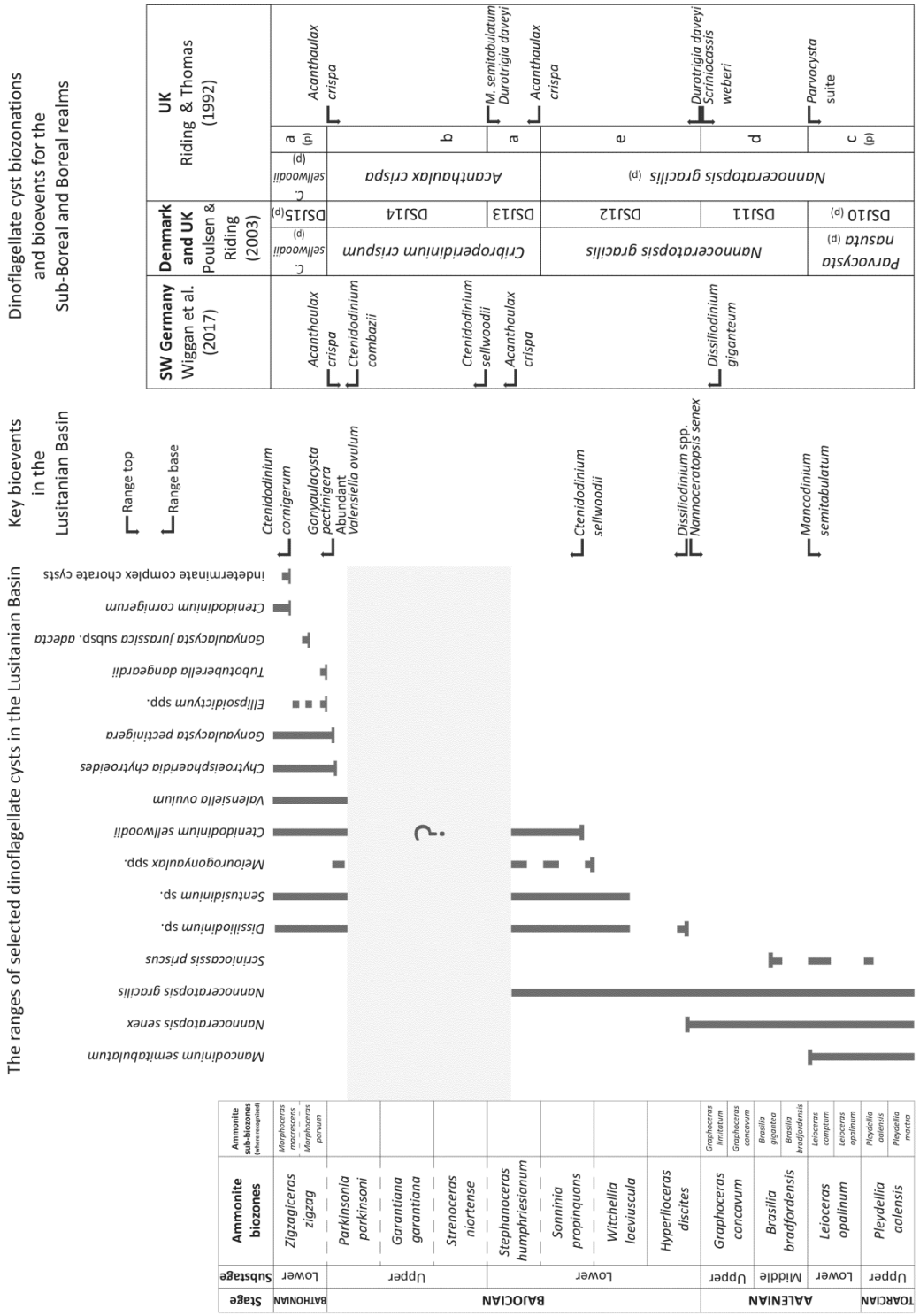

Figure 4.8. The ranges of 16 stratigraphically significant dinoflagellate cysts and selected bioevents from the uppermost Toarcian to lowermost Bathonian of the Lusitanian Basin are compared with bioevent successions and zonal schemes from Denmark, Germany and the UK.

This assemblage and richness increment is typical of the Bajocian of Europe. Fensome et al. (1996) reported a significant evolutionary radiation during the Bajocian and Wiggan et al. (2017) linked this event to significant and widespread increases in sea level. *Dissiliodinium giganteum*, a species characteristically abundant in the lower Bajocian is entirely absent in the Lusitanian Basin (section 6).

The inception of *Ctenidodinium sellwoodii* in the *Sonninia propinquans* AB herein precedes this bioevent further north in Europe. Most reports place this in the upper Bajocian (e.g. Riding and Thomas 1992), but Wiggan et al. (2017) recorded this range base in the *Stephanoceras humphriesianum* AB of Germany. The trend of earlier range bases in the Lusitanian Basin is continued with *Meiourogonyaulax* spp. In this study, this genus emerged in the *Sonninia propinquans* AB, and in northern Europe the earliest representatives are recorded in the *Stephanoceras humphriesianum* AB of France and Germany (Prauss 1989, Feist-Burkhardt and Monteil 1997, Wiggan et al. 2017). *Durotrigia daveyi* has a similar range base in the lower Bajocian throughout Europe. In this study, this species was recorded in the *Sonninia propinquans* AB, and it occurs elsewhere in the *Hyperlioceras discites* to *Stephanoceras humphriesianum* ABs (Bailey 1987, Riding et al. 1991, Butler et al. 2005, Wiggan et al. 2017). The records of *Acanthaulax* sp. cf. *A. crispa, Korystocysta* sp. cf. *K. aldridgei* and *Wanaea* sp. within the *Sonninia propinquans* AB in this study may represent ‘precursor forms’ which appeared prior to the *sensu stricto* representatives (Wiggan et al. 2017). This concept was previously explored in the context of the Bajocian of Europe by Feist-Burkhardt and Götz (2016).

The most significant range top in the lower Bajocian of the Lusitanian Basin is that of *Nannoceratopsis gracilis* in the *Stephanoceras humphriesianum* AB (Fig. 4.8). This may be an artefact due to the intra-Bajocian sampling gap here, but it is consistent with other European records (Prauss 1989, Gowland and Riding 1991, Riding et al. 1991, Feist-Burkhardt and Monteil 1997, Wiggan et al. 2017).

*5.1.3. Uppermost Bajocian and lowermost Bathonian (*Parkinsonia parkinsoni *and* Zigzagiceras zigzag *ABs)*

The trend of increasing dinoflagellate cyst diversity, instigated in the lower Bajocian, continued in the uppermost Bajocian and lowermost Bathonian at Cabo Mondego. Many inceptions were observed, several of which are biostratigraphically

significant (Fig. 4.8). This tendency is entirely consistent with the Bajocian–Bathonian transition elsewhere in the world (Mantle and Riding 2012, Wiggan et al. 2017). By contrast, no regionally significant apparent extinctions were noted.

There are several inceptions in sample Bt94 (*Parkinsonia parkinsoni* AB); these are those of *Bradleyella adela, Rhynchodiniopsis*? *regalis* and *Valensiella ovulum.* The holotype of *Bradleyella adela* is from the *Parkinsonia parkinsoni* AB of southern England (Fenton et al. 1980, p. 156). It is a characteristically Bajocian species with a range from the *Hyperlioceras discites* to *Parkinsonia parkinsoni* ABs (Prauss 1989, Riding and Thomas 1992). It is never common, but is most characteristic of the upper Bajocian. Similarly, the oldest range base reported for *Rhynchodiniopsis*? *regalis* is the *Stephanoceras humphriesianum* AB in northwest Europe (e.g. Feist-Burkhardt and Monteil 1997), but this species is most prevalent in the upper Bajocian and Bathonian (Riding et al. 1985, Prauss 1989).

Other range bases in the *Parkinsonia parkinsoni* AB include those of *Chytreoisphaeridia chytroeides*, *Gonyaulacysta pectinigera*, *Korystocysta pachyderma* and *Pareodinia ceratophora* (Fig. 4.8; Plate 4.2; Table S7). *Chytreoisphaeridia chytroeides* was been reported from the lower Bajocian *Witchellia laeviuscula* AB by Wiggan et al. (2017) but the range base is most frequently observed in the upper Bajocian (e.g. Prauss 1989). Prauss (1989) also noted the inception of *Korystocysta pachyderma* in the *Parkinsonia parkinsoni* AB in Germany.

Finally in this study, more inceptions occurred in the lowermost Bathonian. These include those of *Ctenidodinium cornigerum, Gonyaulacysta jurassica* subsp. *adecta,* indeterminate complex chorate dinoflagellate cysts, ?*Korystocysta gochtii*, *Mendicodinium groenlandicum* and *Tubotuberella dangeardii*. *Ctenidodinium cornigerum* is a characteristic Tethyan species, the range base of which is typical of the Bajocian–Bathonian transition (Jan du Chêne et al. 1985, Feist-Burkhardt and Monteil 1997, Wiggan et al. 2017). The range bases of *Gonyaulacysta jurassica* subsp. *adecta* and *Tubotuberella dangeardii* are consistently recorded in the lowermost Bathonian (e.g. Fenton et al. 1980, Feist-Burkhardt and Wille 1992, Wiggan et al. 2017). This study confirms that the inception of complex chorate dinoflagellate cysts lies in the lowermost Bathonian (Riding et al. 1985, Feist-Burkhardt and Wille 1992). The earliest records of these forms are frequently difficult to adequately assign to genera or species, however this morphostratigraphical bioevent clearly has significant regional significance.

Plate 4.1. Selected dinoflagellate cysts from the Lower and Middle Jurassic (uppermost Toarcian to Bajocian) of the Lusitanian Basin. All specimens are housed in the collections of LNEG (S. Mamede de Infesta). The sample number, slide number and England Finder coordinates are provided. All the scale bars represent 20 μm.

1. *Mancodinium semitabulatum* Morgenroth 1970. Cabo Mondego, upper Toarcian (*Pleydellia aalensis* AB), sample M28, slide 1, F35.
2. *Nannoceratopsis senex* van Helden 1977. São Gião, upper Toarcian (*Pleydellia aalensis* AB), sample SG22m, slide 1, W38/4.
3. *Nannoceratopsis gracilis* Alberti 1961. Cabo Mondego, lower Bajocian (*Witchellia laeviuscula–Sonninia propinquans* ABs) sample AB116, slide 1, H40.
4. *Scriniocassis priscus* (Gocht 1979) Below 1990. Cabo Mondego, middle Aalenian (*Brasilia bradfordensis* AB), sample M150, slide 1, W28.
5. *Dissiliodinium* sp. 1. Cabo Mondego, lower Bajocian (*Stephanoceras humphriesianum* AB), sample AB192, slide 1, R42. Note the psilate autophragm.
6. *Dissiliodinium* sp. 2. Cabo Mondego, lower Bajocian (*Stephanoceras humphriesianum* AB), sample AB192, slide 1, W29. Note the granulate autophragm.
7. *Sentusidinium* sp. cf. *S. explanatum* (Bujak in Bujak et al. 1980) Wood et al. 2016. Cabo Mondego, lower Bajocian (*Witchellia laeviuscula–Sonninia propinquans* ABs), sample AB108, slide 1, J32. Note the psilate autophragm.
8. *Sentusidinium* sp. 1. Cabo Mondego, lower Bajocian (*Witchellia laeviuscula–Sonninia propinquans* ABs) sample AB116, slide 1, W51/2. Note the scabrate to granulate autophragm.
9. *Sentusidinium* sp. 2. Cabo Mondego, upper Bajocian (*Parkinsonia parkinsoni* AB), sample Bt106, slide 1, W28. Note the scabrate autophragm with dense short spines.
10. *Kallosphaeridium*? sp. Cabo Mondego, lower Bajocian (*Sonninia propinquans–Stephanoceras humphriesianum* ABs), sample AB178a, slide 1, N25. The arrow points to what appears to be the attached apical operculum.
11. *Korystocysta* sp. cf. *K. aldridgeii* Wiggan et al. 2017. Cabo Mondego, lower Bajocian (*Sonninia propinquans–Stephanoceras humphriesianum* ABs), sample AB178a, slide 1, J37/4. This specimen is slightly smaller (width: 78 μm; length: 65 μm) compared with those of Wiggan et al. (2017). Photomicrograph taken using differential interference contrast.
12. *Rhynchodiniopsis* sp. Cabo Mondego, lower Bajocian (*Sonninia propinquans–Stephanoceras humphriesianum* ABs), sample AB178a, slide 2, L37/1. Photomicrograph taken using differential interference contrast.

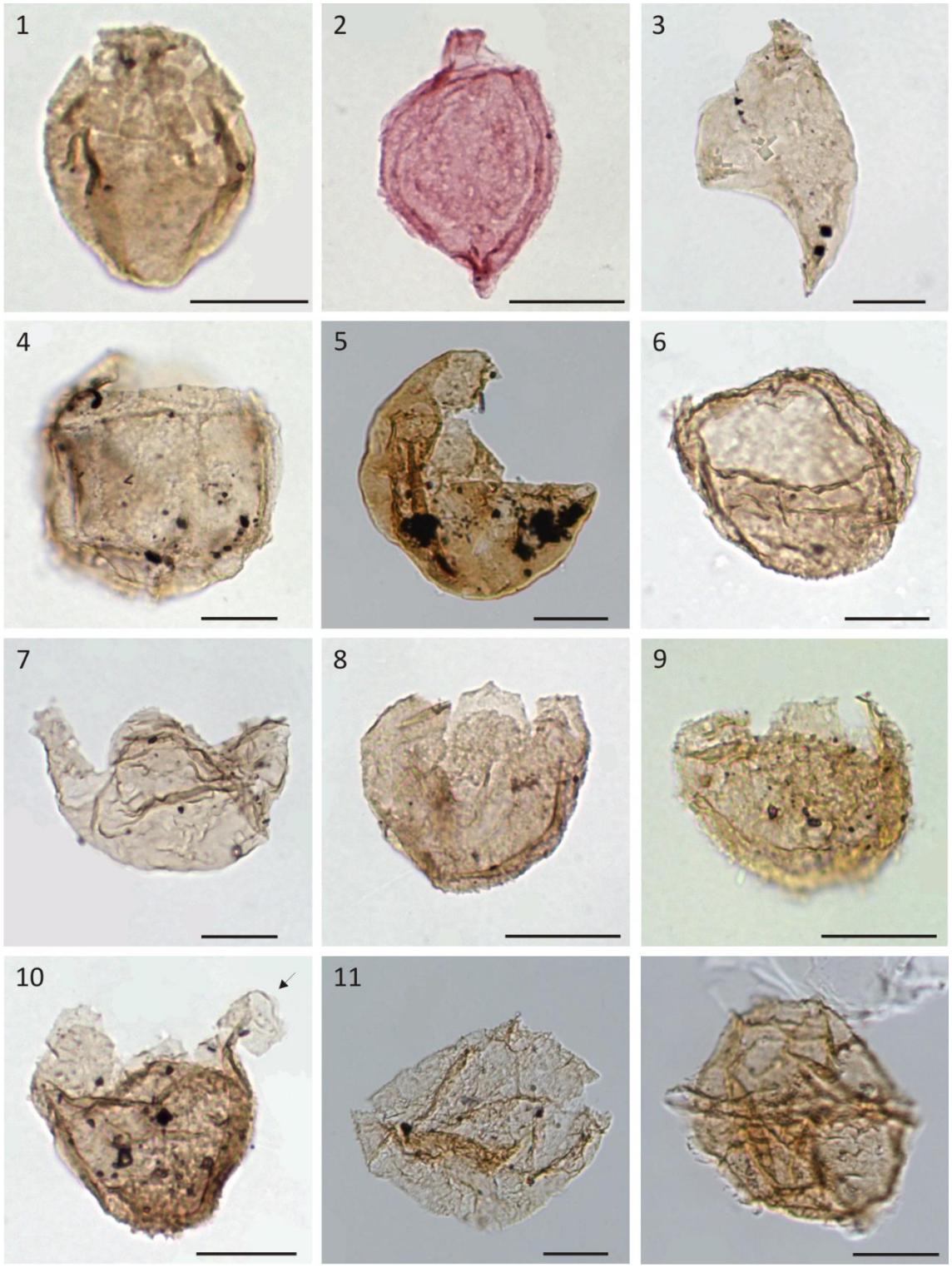

Plate 4.1 (caption on previous page)

Plate 4.2. Selected dinoflagellate cysts from Middle Jurassic (Bajocian and Bathonian) of the Lusitanian Basin. All specimens are housed in the collections LNEG (S. Mamede de Infesta). The sample number, slide number and England Finder coordinates are provided. All the scale bars represent 20 μm.

1. *Durotrigia daveyi* Bailey 1987. Cabo Mondego, lower Bajocian (*Sonninia propinquans* AB), sample AB138, slide 2, S47/3.
2. *Meiourogonyaulax* sp. Cabo Mondego, upper Bajocian (*Parkinsonia parkinsoni* AB), sample Bt110, slide 1, N24/1.
3. *Pareodinia ceratophora* Deflandre 1947. Cabo Mondego, upper Bajocian (*Parkinsonia parkinsoni* AB), sample Bt106, slide 1, R31.
4. *Epiplosphaera gochtii* (Fensome 1979) Brenner 1988. Cabo Mondego, lower Bajocian (*Witchellia laeviuscula–Sonninia propinquans* ABs), sample AB108, slide 1, J45/4. Note the short, capitate processes and the cingulum.
5. *Ellipsoidictyum* sp. Cabo Mondego, lower Bathonian (*Zigzagiceras zigzag* AB), sample Bt200, slide 1, P44. Note the strongly reticulate ornamentation and the cingulum.
6. *Valensiella ovulum* (Deflandre 1947) Eisenack 1963. Cabo Mondego, lower Bathonian (*Zigzagiceras zigzag* AB), sample Bt134, slide 1, H33.
7. *Ctenidodinium sellwoodii* (Sarjeant 1975) Stover & Evitt 1978. Cabo Mondego, upper Bajocian (*Parkinsonia parkinsoni* AB), sample Bt106, slide 1, R25/1.
8. *Ctenidodinium cornigerum* Valensi 1953. Cabo Mondego, lower Bathonian (*Zigzagiceras zigzag* AB), sample Bt220, slide 1, H24.
9. *Gonyaulacysta pectinigera* (Gocht 1970) Fensome 1979. Cabo Mondego, lower Bathonian (*Zigzagiceras zigzag* AB), sample Bt200, slide 1, J25/3.
10. *Chytroeisphaeridia chytroeides* (Sarjeant 1962) Downie & Sarjeant 1965. Cabo Mondego section, lower Bathonian (*Zigzagiceras zigzag* AB), sample Bt164, slide 1, N35. Note the precingular (1P) archaeopyle.
11. *Tubotuberella dangeardii* (Sarjeant 1968) Stover & Evitt 1978. Cabo Mondego, lower Bathonian (*Zigzagiceras zigzag* AB), sample Bt126, slide 1, O25/1.
12. *Mendicodinium* sp. Cabo Mondego, upper Bajocian (*Parkinsonia parkinsoni* AB), sample Bt106, slide 1, V29/1. Note the autophragm with short spines and baculae.

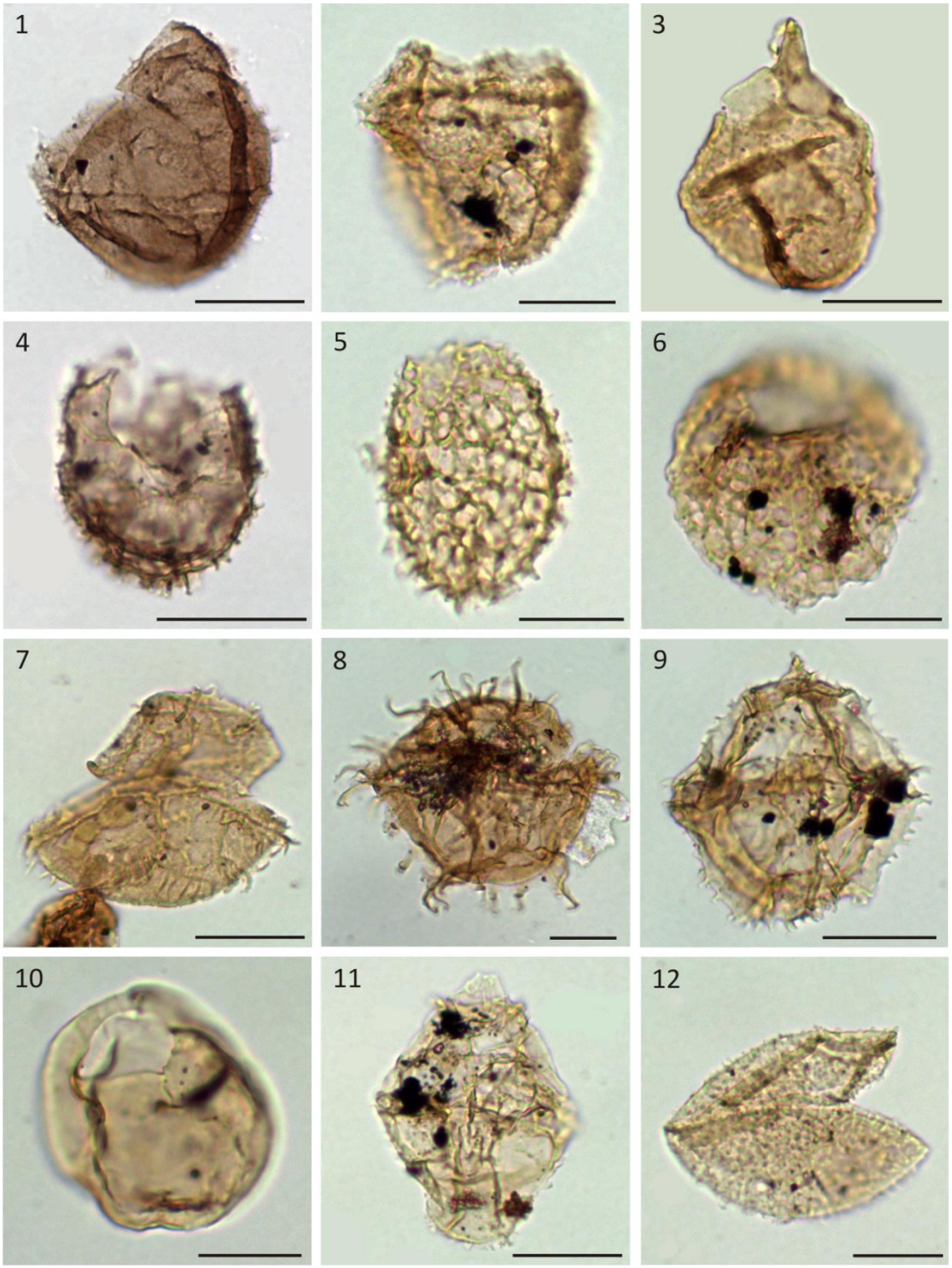

Plate 4.2 (caption on previous page)

Plate 4.3. Selected indigenous marine and terrestrially-derived palynomorphs from the Lower and Middle Jurassic (uppermost Toarcian to Bathonian) of the Lusitanian Basin. All specimens are housed in the collections of collections LNEG (S. Mamede de Infesta). The sample number, slide number and England Finder coordinates are provided. All the scale bars represent 20 μm.

1. *Micrhystridium* sp. 1 (acanthomorph acritarch). São Gião, upper Toarcian (*Pleydellia aalensis* AB), sample SG8, slide 1, G40. Note the long and slender spines and the unusual equatorial pylome.
2. *Cymatiosphaera* sp. cf. *C. pachytheca* Eisenack 1957 (prasinophyte). Cabo Mondego, lower Aalenian (*Leioceras opalinum* AB), sample M38, slide 1, O27/3.
3. *Tasmanites* sp. (prasinophyte). São Gião, lower Aalenian (*Leioceras opalinum* AB), sample SG94, slide 1, M40.
4. *Ischyosporites variegatus* (Couper 1958) Schulz 1967 (spore). Cabo Mondego, lower Bathonian (*Zigzagiceras zigzag* AB), sample Bt184, slide 1, H49.
5. *Striatella seebergensis* Mädler 1964 (spore). Cabo Mondego, middle Aalenian (*Brasilia bradfordensis* AB), sample M237, slide 1, U26.
6. *Auritulinasporites triclavus* Nilsson 1958 (spore). Cabo Mondego, upper Aalenian (*Graphoceras concavum* AB), sample M319, slide 1, L33/2.
7. *Callialasporites dampieri* (Balme 1957) Dev 1961 (pollen). Cabo Mondego, lower Bathonian (*Zigzagiceras zigzag* AB), sample Bt184, slide 1, U55/2.
8. *Callialasporites turbatus* (Balme 1957) Schulz 1967 (pollen). Cabo Mondego, lower Bajocian (*Hyperlioceras discites* AB) sample M341, slide 1, N23/2.
9. *Callialasporites segmentatus* (Balme 1957) Srivastava 1963 (pollen). Cabo Mondego, lower Bathonian (*Zigzagiceras zigzag* AB), sample Bt184, slide 1, H29/2.
10. *Araucariacites australis* Cookson 1947 ex Couper 1958 (pollen). Cabo Mondego, lower Bajocian (*Sonninia propinquans* AB), sample AB178a, slide 1, Q23/2.
11. *Perinopollenites elatoides* Couper 1958 (pollen). Cabo Mondego, lower Aalenian (*Leioceras opalinum* AB), sample M121, slide 1, V32/3.
12. *Cycadopites granulatus* (de Jersey 1962) de Jersey 1964 (pollen). Cabo Mondego, lower Bathonian (*Zigzagiceras zigzag* AB), sample Bt126, slide 1, Q23/4.

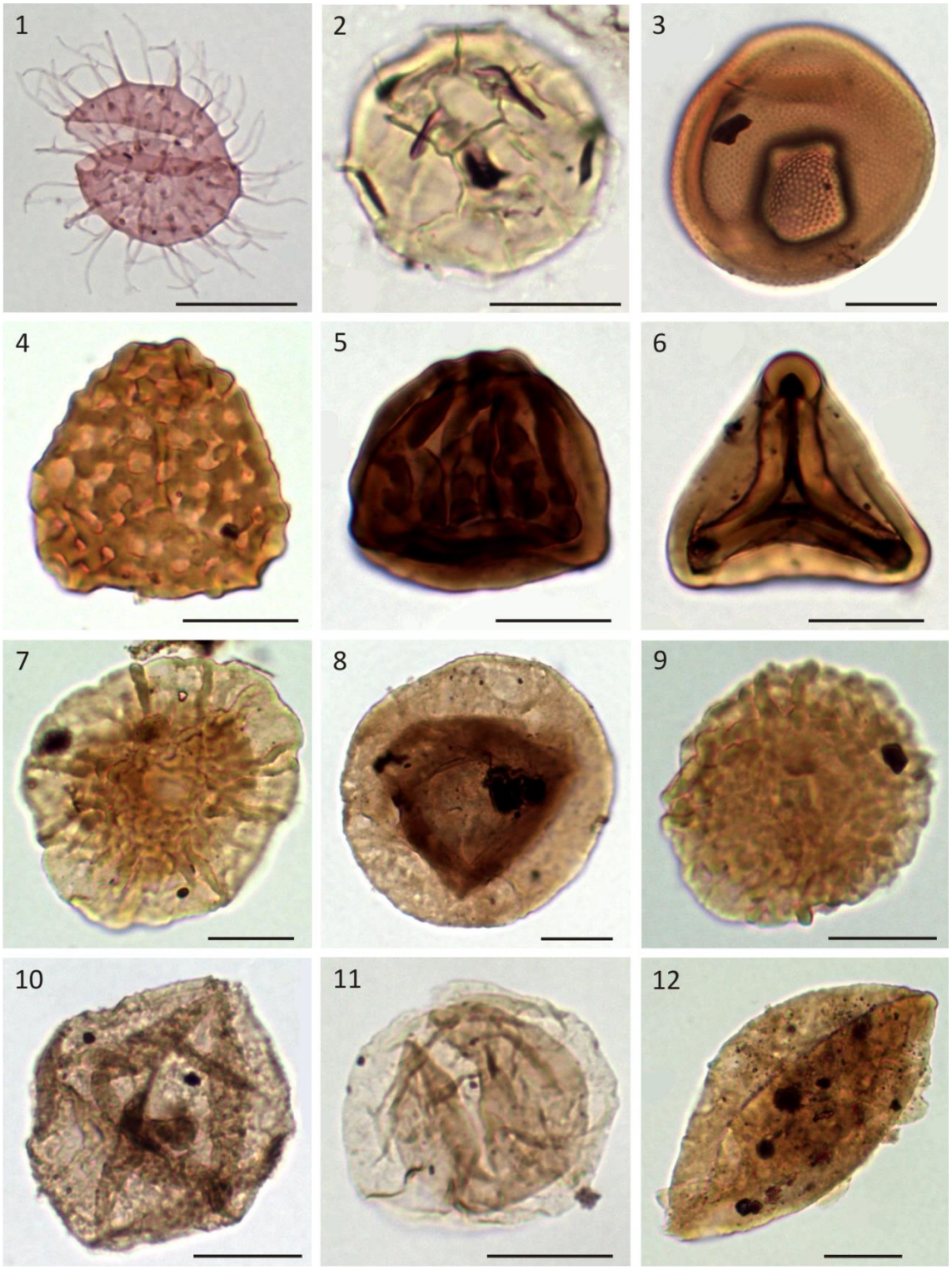

Plate 4.3 (caption on previous page)

5.2. Pollen and spore biostratigraphy

The pollen and spores observed in this study are typical of the Toarcian to Bathonian interval in Europe (e.g. Srivastava 1987, Guy-Ohlson 1989). In terms of species turnover they are substantially more conservative than the dinoflagellate cysts. Despite this, there are several notable pollen and spore bioevents in the succession studied. Moreover, significant shifts in abundance are observed which may have local biostratigraphical significance. For example, *Exesipollenites* is common and consistent throughout the Aalenian and lower Bajocian, but *Cycadopites granulatus* is more prominent at the Bajocian–Bathonian transition at Cabo Mondego (Table S7).

The inception and diversification of the characteristic monosaccate pollen genus *Callialasporites* (Plate 4.3), and an increase in the relative proportions of the closely related *Araucariacites australis,* are significant. The oldest records of *Callialasporites* are the somewhat isolated and rare specimens of *Callialasporites dampieri* and *Callialasporites turbatus* in the uppermost Toarcian of Cabo Mondego. The genus then substantially increased in diversity and relative abundance throughout the Aalenian of Cabo Mondego and São Gião (Tables S7, S8). These records confirm that this araucarian genus expanded significantly close to the base of the Middle Jurassic (Guy-Ohlson 1988a, Riding et al. 1991). The rise of *Callialasporites*, and the relative demise of *Classopollis*, close to the Early–Middle Jurassic transition is a global phenomenon (Helby et al. 1997, fig. 13), and appears to be related to the marked decrease in the palaeotemperatures at this time (Korte et al. 2015, fig. 2).

The cavate spore *Kraeuselisporites reissingeri* is present at the Toarcian–Aalenian transition at Cabo Mondego and São Gião (Tables S7, S8). This spore is also common in the Lower Jurassic of the Lusitanian Basin (Correia et al., 2018). In northern Europe, the range of this species is latest Triassic to Early Jurassic (Rhaetian–Pliensbachian) according to Morbey (1978). There is an isolated occurrence of the spore *Kekryphalospora distincta* in the uppermost Toarcian of Cabo Mondego. This form ranges from the upper Pliensbachian to lower Bajocian in northwest Europe (Fenton and Riding 1987) and the Toarcian of Australia (Riding and Helby 2001). The range base of *Chasmatosporites* spp. is in the lower Bajocian (*Sonninia propinquan*s AB) of Cabo Mondego. Elsewhere in Europe, this genus ranges from the uppermost Triassic to the Middle Jurassic (Rhaetian–Bathonian) (Guy-Ohlson 1988b, fig. 2).

6. Dinoflagellate cyst palaeobiology

The uppermost Toarcian to lowermost Bathonian dinoflagellate cyst assemblages of the Lusitanian Basin described herein are consistently and substantially less diverse than their counterparts further east and north in Europe. For example, relatively diverse dinoflagellate cyst floras are present throughout the Aalenian and Bajocian of Germany and Poland (e.g. Feist-Burkhardt 1990, Prauss 1989, Feist-Burkhardt and Pross 2010, Feist-Burkhardt and Götz 2017, Gedl 2008, Segit et al. 2015 and Wiggan et al. 2017). Moreover, Bathonian dinoflagellate cysts from northwest Europe typically exhibit substantially higher species richness than in the Lusitanian Basin (e.g. Riding et al., 1985). The causal factors for this phenomenon may include: amount and availability of nutrients; latitude/temperature controls; marine current regime; salinity, seawater depth; or a combination of these parameters.

The Toarcian Oceanic Anoxic Event (T-OAE) at ~183 Ma was a relatively short-lived environmental perturbation (e.g. Xu et al. 2017). Correia et al. (2017b) established that cyst-forming dinoflagellates were very slow to recover from the severe environmental pressures (principally anoxia, high temperatures and lowered salinities) caused by the T-OAE. It seems probable that the enclosed setting of the Lusitanian Basin intensified and prolonged these abiotical changes which developed in the water column at this time. This protracted recovery may have suppressed the diversity of dinoflagellate cyst associations throughout the Toarcian and well into the Aalenian. Moreover the lack of Arctic/Boreal forms, such as the diverse genera and species of the *Parvocysta* suite of Riding (1984), appears also to have contributed to the relatively low diversity of dinoflagellate cysts around the Toarcian–Aalenian transition in Portugal. The upper Toarcian to lower Aalenian successions of northern England, Scotland and the Arctic (Riding 1984c, Riding et al. 1991, Riding et al. 1999) are significantly more diverse than this interval in Portugal, largely due to the presence of the *Parvocysta* suite. The dinoflagellate cysts from the Toarcian–Aalenian transition in southwest France are also more diverse than in the Lusitanian Basin (de Vains 1988, Bucefalo Palliani and Riding 1997b). Notwithstanding the lack of the *Parvocysta* suite, the Lusitanian Basin floras also lack other typically European Toarcian–Aalenian dinoflagellate cysts such as *Mendicodinium spinosum*, *Nannoceratopsis dictyambonis*, *Nannoceratopsis plegas*, *Nannoceratopsis spiculata*, *Nannoceratopsis triceras*, *Pareodinia halosa* and *Sentusidinium* spp.

It is possible that the slow recovery of cyst-forming dinoflagellates following the T-OAE suppressed diversity until the earliest Aalenian. Subsequently, it is possible that the marked early Aalenian cooling (Korte et al. 2015) continued to suppress these planktonic biotas. The latter phenomenon, however, did not affect the high diversity in ammonite and benthic foraminifera assemblages recorded in the Lusitanian Basin (Henriques and Canales 2013) and is inconsistent with the expansion of diverse coldwater forms from the Boreal Realm, as envisaged for the Callovian–Oxfordian transition by Riding and Michoux (2013). The latter authors considered the Arctic region as a plankton diversity hotspot during the Jurassic. Moreover it is conceivable that, by the time the *Parvocysta* suite had become extinct in the earliest Aalenian, the Arctic floras could not have contributed many species to colonise further south.

Dinoflagellate cyst diversity continued to be relatively low in the Lusitanian Basin throughout the Aalenian and Bajocian, and into the earliest Bathonian (Table S7). The assemblages increased in species richness, but the major diversification of the family Gonyaulaceae, which is present throughout northwest Europe (Wiggan et al. 2017), is not manifested. Borges et al. (2011) and Borges et al. (2012) explained the relatively low Middle and Upper Jurassic dinoflagellate cyst assemblages in the Algarve Basin of Portugal by the fact that this depocentre was a relatively deep water and partially enclosed (restricted) setting. The Lusitanian Basin is very close to the relatively deep waters of the Proto Atlantic (Fig. 4.9). This relatively isolated position, well away from the widespread shelf settings of the northwest Tethys, prevented extensive mutual biotic exchange with southeast Europe and surrounding areas. Further evidence of the restricted nature of the Lusitanian Basin is that *Valensiella* is common and *Ctenidodinium* is relatively rare in the lowermost Bathonian (Table S7). The former genus is cosmopolitan and hence may represent a eurytopic taxon, whereas *Ctenidodinium* is abundant during maximum transgressions in open basins (Wiggan et al. 2017).

The large and distinctive dinoflagellate cyst species *Dissiliodinium giganteum* was not recorded herein. This taxon is extremely prominent in the lower Bajocian (*Witchellia laeviuscula* and *Sonninia propinquan*s ABs) of Germany and Eastern Europe (Gedl 2008, Gedl and Józsa 2015, Wiggan et al. 2017). This species apparently thrived in regions with high terrestrial runoff input, elevated nutrient levels and perhaps reduced salinities (Wiggan et al. 2017). By contrast, *Dissiliodinium giganteum* is rare in the lower Bajocian carbonate facies of southern England and northern France (Feist-

Burkhardt and Monteil 1997, unpublished data). As such, the absence of *Dissiliodinium giganteum* in the Lusitanian Basin is consistent with the deepwater environment, relatively far from sources of terrigenous input, of this region. This is further supported by the generally low abundances of spores throughout the successions studied.

Figure 4.9. The Middle Jurassic palaeogeography of the western Tethys region and the proto-Atlantic Ocean, modified from Gómez and Fernández-López (2006) and Korte et al. (2015). CM = Cabo Mondego; SG = São Gião.

7. Conclusions

The Lusitanian Basin of central western Portugal exposes an extremely important southern European Middle Jurassic reference section. This includes the GSSP and the ASSP for the Bajocian and Bathonian stages respectively within the type Cabo Mondego Formation. The palynology of the uppermost Toarcian to the lowermost Bathonian of Cabo Mondego and São Gião was studied herein. The composite Aalenian and Bajocian, and their lower and upper transitions, studied here from outcrops at Cabo Mondego and São Gião yielded 89 palynologically productive samples, all of which are correlated to the *Pleydellia aalensis* to *Zigzagiceras zigzag* ABs. The upper Bajocian *Strenoceras niortense* and *Garantiana garantiana* ABs were not studied.

The Cabo Mondego Formation generally produced abundant, well-preserved assemblages, but the Póvoa da Lomba Formation at São Gião yielded sparse assemblages with low levels of species richness. This may be due the distal position of Cabo Mondego compared with São Gião. A low diversity assemblage of dinoflagellate cysts, typified by the genus *Nannoceratopsis*, was recovered from the uppermost Toarcian to lowermost Bajocian (*Pleydellia aalensis* to *Hyperlioceras discites* ABs) interval. In the overlying succession, between the lower Bajocian and the lowermost Bathonian (*Witchellia laeviuscula–Zigzagiceras zigzag* ABs), a substantially more diverse biota was encountered. The principal influx of species is within the *Witchellia laeviuscula* AB, and is the manifestation of an evolutionary burst which may have been caused by increases in sea level. Dinoflagellate cyst diversity continued to increase at the Bajocian–Bathonian transition.

The dinoflagellate cysts exhibit significant species turnover and several bioevents have local and regional significance. For example, the lower Bajocian range top of *Nannoceratopsis gracilis* in the *Stephanoceras humphriesianum* AB is consistent with other European records (e.g. Prauss 1989). Furthermore, the range bases of complex chorate dinoflagellate cysts, *Gonyaulacysta jurassica* subsp. *adecta* and *Tubotuberella dangeardii* were recorded in the earliest Bathonian at Cabo Mondego. These datums are reliable biomarkers for the earliest Bathonian throughout Europe. (e.g. Wiggan et al. 2017). The pollen and spores recorded herein are characteristic of Middle Jurassic associations in both hemispheres. It is noticeable that araucarian pollen, such as *Araucariacites* and *Callialasporites*, diversified and became prominent during the Aalenian.

The Middle Jurassic dinoflagellate cyst floras of the Lusitanian Basin are markedly less diverse than their counterparts further north and east in the northern hemisphere. The T-OAE suppressed the early Toarcian dinoflagellate cysts in the Lusitanian Basin, and the recovery from it was extremely protracted. Hence the T-OAE may have inhibited early Middle Jurassic dinoflagellate cyst diversification in the Lusitanian Basin. This downward pressure on diversity may have been intensified by the absence of characteristic Boreal dinoflagellate cysts. Moreover, it is also possible that the sharp cooling of the seawater in the Laurasian Seaway during the early Aalenian further affected species richness at this time, although such cooling event was minimal in the Lusitanian Basin when compared to higher latitudes (Korte et al. 2015).

These low dinoflagellate cyst diversities in Portugal may also be as a result of the palaeogeography of the Lusitanian Basin. This was a relatively isolated, deepwater setting close to the Proto Atlantic, and this may have prevented large-scale biotic exchange with the widespread shelfal areas of the western Tethys to the east and northeast. The distinctive, large dinoflagellate cyst *Dissiliodinium giganteum* was not recovered from the Lusitanian Basin. This species is very abundant in the lower Bajocian of Europe (Wiggan et al. 2017), and appears to be characteristic of regions with high levels of terrestrial runoff and nutrients. Thus its absence in the deepwater environment of the Lusitanian Basin, relatively distant from sources of terrigenous input, is unsurprising.

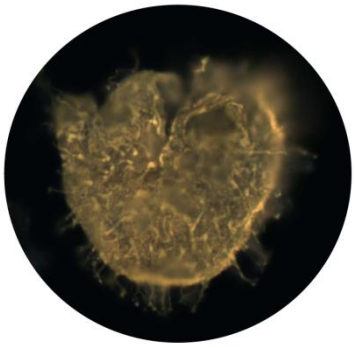

CHAPTER V

Palynomorph fluorescence

Chapter V cover:

Impletosphaeridium sp., Cabo Mondego section, lower Callovian, sample CM7. Fluorescence mode.

Chapter V. Palynomorph fluorescence

Paper in preparation:
Correia, V.F., Fernandes, P., Riding, J.B., Pereira, Z. The value of fluorescence microscopy in routine source-rock analysis: Lower–Middle Jurassic successions from the Lusitanian Basin, Portugal.

Abstract

Fluorescence microscopy, together with spore and pollen colours (Thermal Alteration Index-TAI) analyses is a fast and reliable technique to differentiate source rocks from non-source rocks, and to estimate the level of organic maturation. These methods were tested in 39 samples from the Lower and Middle Jurassic of the Lusitanian Basin, central western Portugal. The results suggest that most of these strata are within the main mature phase of liquid petroleum production. The exceptions are the upper Pliensbachian to lower Toarcian interval of the Rabaçal area, which corresponds to an organic thermal immature phase, and an overmature sediment in the Lower Bajocian succession at Cabo Mondego.

Keywords

Fluorescence; Jurassic; Lusitanian Basin; Organic matter; Palynomorphs; Spore–pollen colour.

1. Introduction

Fluorescence microscopy is used to differentiate hydrocarbon source rocks from non-source rocks and to estimate the level of maturation from fluorescence colours and spectra. Certain organic molecules and compounds have the property, when rays of short wavelength and higher energy excite them, to emit rays of greater wavelengths within the visible spectrum and even extend into the infrared field. The most common exciting light used in fluorescence microscopy of source rocks is blue light with a

wavelength of 447 nm and ultraviolet rays (UV). The organic compounds, which fluoresce in kerogen and hydrocarbons, are aromatic structures or chromophore groups. Pigments and carotene are examples of aromatic structures and are present, for instance, in chlorophyll. Chromophore groups are characteristic, and limited, to the exinite-liptinite maceral group (mainly sporinites and alginite, and algal-derived material including acritarchs and dinoflagellate cysts). Consequently; only the organic constituents of this maceral group exhibit primary fluorescence (Fernandes, 2000).

Fluorescence is variable in colour and intensity, and it depends on the composition and maturity level of the organic matter (Taylor et al., 1998). Organic maturation causes a gradual shift in fluorescence colours (red shift) from the shorter to the longer wavelengths, that is, blue and green to yellow, orange and finally red (Figure 5.1). Van Gijzel (1979) detected some significant differences in fluorescence colour and intensity, within the different components of the liptinite-exinite group going from immature to mature and overmature stages of oil generation.

Fresh spores and pollen have fluorescence colours ranging from blue to red, depending on the species. Algal material starts to fluoresce with greener colours than spores and, generally, shows more intense fluorescence than the spores of the same rank. From all the sub-macerals of liptinite-exinite group, sporinite shows the most consistent changes in fluorescence colour spectra and intensity with increasing organic maturation levels. Under fluorescence excitation, it changes colour from green through yellow to orange and finally red with increasing organic maturation to the top of the oil-window, after which is no longer fluoresces (Fig. 5.1; Fernandes, 2000).

Thus, the spore fluorescence is an important parameter of organic maturation for low rank material and it is suitable for evaluating maturation levels of very rich source rocks at low rank where vitrinite is virtually absent, or its values are less reliable. The main disadvantages of this technique are that there are some differences in fluorescence colours and intensity for different spore species, and there are no accepted international standards for spectral analysis, resulting in variations in the definition of spectral parameters (Suárez-Ruiz et al., 2012).

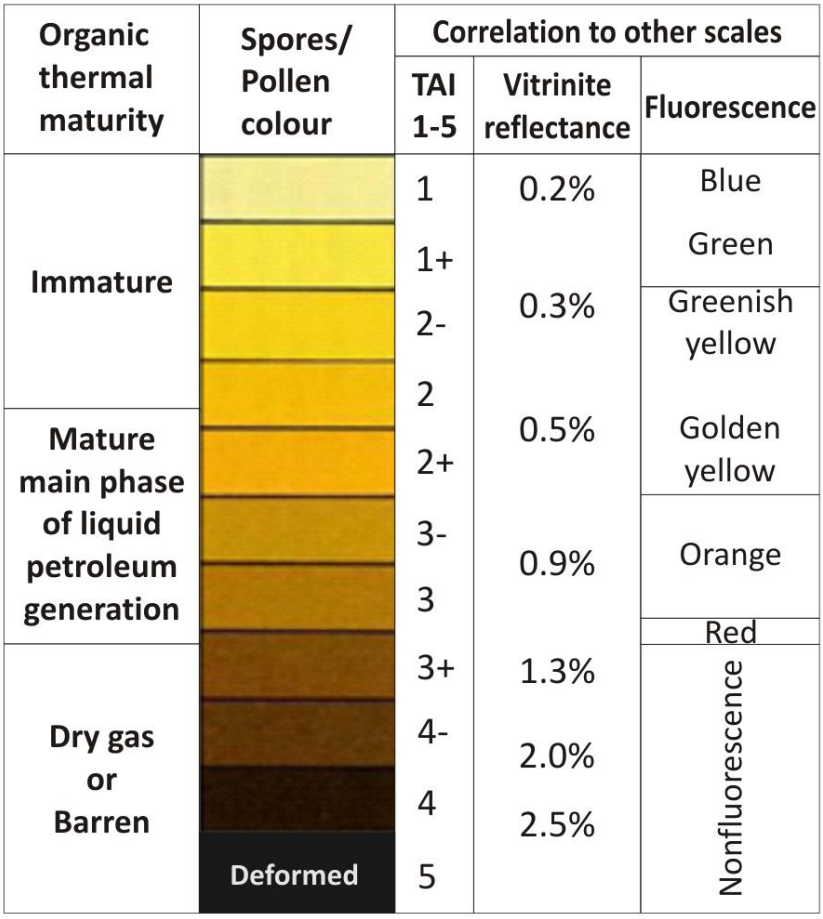

Figure 5.1. Correlation chart between the miospores colour, thermal alteration index (TAI) and fluorescence, used in assessing organic maturation (based and modified from the *Phillips Petroleum Colour Standard, version no. 2, 1984* and Stach et al., 1982).

Together with fluorescence, the palynomorphs colour can also be used as a useful technique for evaluating organic maturation levels. The palynomorphs colour, when observed under transmitted light, changes gradually and irreversibly with increasing temperatures related to burial depth, from light to dark. Using these colour changes of spores and pollen, Staplin (1969) developed the Thermal Alteration Index (TAI) as a relatively simple and rapid method for evaluating maturation levels in kerogen concentrates. The colour indices in Staplin's TAI scale range from 1 to 5 (Fig. 5.1) and represent kerogen colour changes from light yellow to dark yellow, light brown, brown, dark brown and finally to black. Kerogens with yellow colours represent immature source rocks with regard to oil. The light browns and brown are mature; dark browns and black indicate overmature source rocks. The designation of the colour is restricted to land plant material, such as spores, pollen, since exinite exhibits more consistent changes than other plant substances with increasing temperature during maturation. Not all miospore species are suitable for TAI determinations. Thin walled

or delicately ornamented spores should be avoided. Thick walled and heavily ornamented spores should also be avoided. The species best suited for TAI determinations are miospores with a smooth exine of medium thickness (Fernandes, 2000).

TAI, as with fluorescence, has the limitations of being a subjective maturation method which depends on the experience of the operator and is not a quantitative and objective method such as vitrinite reflectance. Spore colour charts also lack universally standardization. Numerous charts have been proposed, such as the Spore Colour Index (SCI) of Collins (1990), but none have been consensually accepted. Some alternative methods to measure the spore colour were reported, such as the Colour Image Analyses (CIA) that uses software incorporated with RGB (red, green, blue) colour format (Yule et al., 1998), to enhance accuracy and to avoid subjectivity. Recently, Goodhue and Clayton (2010) proposed the Palynomorph Darkness Index (PDI) as a new thermal maturity indicator. PDI is calculated from measurement of the RGB intensities of light transmitted through palynomorphs, using standard palynological microscopes and digital cameras. The TAI has the advantage of being quick, inexpensive and applicable to various sedimentary rock types (Fernandes, 2000).

The aim of the present work is to determine the fluorescence colours and TAIs of selected continental palynomorphs from Lower and Middle Jurassic sections in the Lusitanian Basin, in order to determine its vertical and lateral differences in organic maturation within this succession. The validity of this method in source-rock assessment and analysis will also be discussed.

2. Geological background

The Lusitanian Basin is an important sedimentary depocenter located in central western Portugal and is oriented NE–SW. It is 300 km long and 150 km wide, with a maximum basin fill of 5 km (Fig. 1.1; Kullberg et al., 2013). The fill deposits range from Middle?–Upper Triassic to uppermost part of Lower Cretaceous, however the majority comprises marine Jurassic sediments (Wilson et al., 1989; Kullberg et al., 2013). The Lower and Middle Jurassic series of the Lusitanian Basin are characterised by well developed marl and limestones alternations (Azerêdo et al., 3003), occasionally cyclic, and abundant and diverse nektonic, planktonic and benthic organisms (e.g. Henriques 1995; Fernández-López et al. 2006, 2009a,b; Oliveira et al., 2007a,b; Canales

and Henriques 2008, 2013; Sandoval et al. 2012; Mattioli et al., 2013; Comas-Rengifo et al., 2013, 2015; Figueiredo et al., 2014; Henriques et al., 2014; Cabral et al., 2011, 2013, 2014, 2015; Ferreira et al., 2015; Silva et al., 2015; Andrade et al. 2016; Rita et al., 2016; Correia et al., 2017a,b). The lithostratigraphy of the Lower and Middle Jurassic (upper Sinemurian to upper Callovian) of the Lusitanian Basin was described in detail in Duarte and Soares (2002), Azêredo et al. (2003), Duarte (2007) and Duarte et al. (2014a,b) and is summarized in Fig. 1.2. The Lower and Middle Jurassic successions studied herein are presented in detail in the previous Chapters I–IV (see also Correia et al., 2017a,b, 2018). The geological setting and the location of the studied sections are shown in Fig. 1.1.

3. Material and methods

For this study samples were selected from the eight sections (Maria Pares, Fonte Coberta, Brenha, Vale das Fontes, São Gião, Cabo Mondego, São Pedro de Moel and Peniche), studied in the previous chapters for their palynological content, corresponding to the upper Sinemurian–lower Bathonian succession, and also 15 extra samples from the ?middle Bathonian–upper Callovian of the Cabo Mondego section. The selected samples make a composite and complete stratigraphy of the Lower and Middle Jurassic sequence allowing, therefore, lateral and vertical comparisons between the different sections studied. The samples were prepared using standard palynological techniques (Wood et al., 1996; Riding and Warny 2008), however, the organic residues were not oxidised or stained. All the residues were sieved using a 15 µm mesh. A total of 39 samples were analysed for fluorescence and TAI.

The analysis of qualitative palynomorphs fluorescence colours was undertaken in the University of the Algarve using an Olympus BX 51 microscope equipped with a metal halide lamp fluorescence unit XCite Series 120Q and with a violet and Blue 12 filter block that yields a wavelength band of 390–490 nm. This system was allowed to stabilize for 15 minutes prior to any observation of the fluorescence of the samples. Initial analyses with all palynomorph groups and amorphous organic material were accessed in order to confirm the differences in colour and intensity, described in section 1. Although fluorescence and TAI analyses should be preferentially undertaken on spores, in this work that was not possible because most of the spores recorded have relatively thick and/or ornamented exine. For that reason, we used especially

Classopollis spp. and *Callialasporites* spp. as suitable miospores species for these analyses, which have smooth and medium thick exines and are abundant in the entire succession. The grains were subjected to 5 minutes of excitation, after which their fluorescence colours was recorded. The terminology used for describing fluorescence colours was blue (B), green (G), greenish yellow, yellow (Y), golden yellow, orange (O) and red (R). We also used three degrees of fluorescence intensity: low **(+)**, medium **(**++) and high **(+++)** (Table XX).

Miospore colours were recorded using the Phillips Petroleum Colour Standard, version no.2 (1984) (Figure 5.1), which is an adaptation of Staplin's initial TAI chart and includes more shades for the same colour index. In order to determine the true miospore colour for a sample, the dominant and palest (assuming no contamination) miospore colour, in this case from pollen was recorded and compared with the Phillips Petroleum Colour chart. The index number from this chart was then attributed to the remaining 39 samples. The results are presented together with fluorescence colour data.

4. Fluorescence and TAI analyses

In this section the fluorescence and TAI values of the Lower and Middle Jurassic of the Lusitanian Basin are described and discussed. Fig. 5.2 is an overview of the results of this work, where selected spores and pollen are pictured in chronological order. In Tables 5.1 and 5.2 the values of TAI and fluorescence for the Lower and Middle Jurassic, are presented respectively. In Plates 5.1–5.7 selected palynomorphs and AOM are figured in transmitted white light and in fluorescence mode.

In general, the fluorescence and TAI values of the Lower and Middle Jurassic of the Lusitanian Basin comprising the greenish yellow to orange and 2- to 3+ intervals, respectively, with the exception of sample AB108, which apparently has no fluorescence (Figs. 5.1, 5.2; Table 5.1). According with this fluorescence and TAI values, only samples FC3, PZ5 and PZ15 seems to characterize an immature stage in terms of organic thermal maturity (Figs. 5.1, 5.2; Tables 5.1, 5.2). These samples present a greenish yellow fluorescence and spores and pollen colour between 2- and 2. These horizons correspond to the upper Pliensbachian to lower Toarcian interval in the Rabaçal area (Fonte Coberta and Maria Pares sections). The rest of the samples are within the main mature phase of liquid petroleum generation, with fluorescence colours ranging between yellow and orange, and TAI between 2 to 3+ (Figs. 5.1, 5.2; Tables 5.1, 5.2).

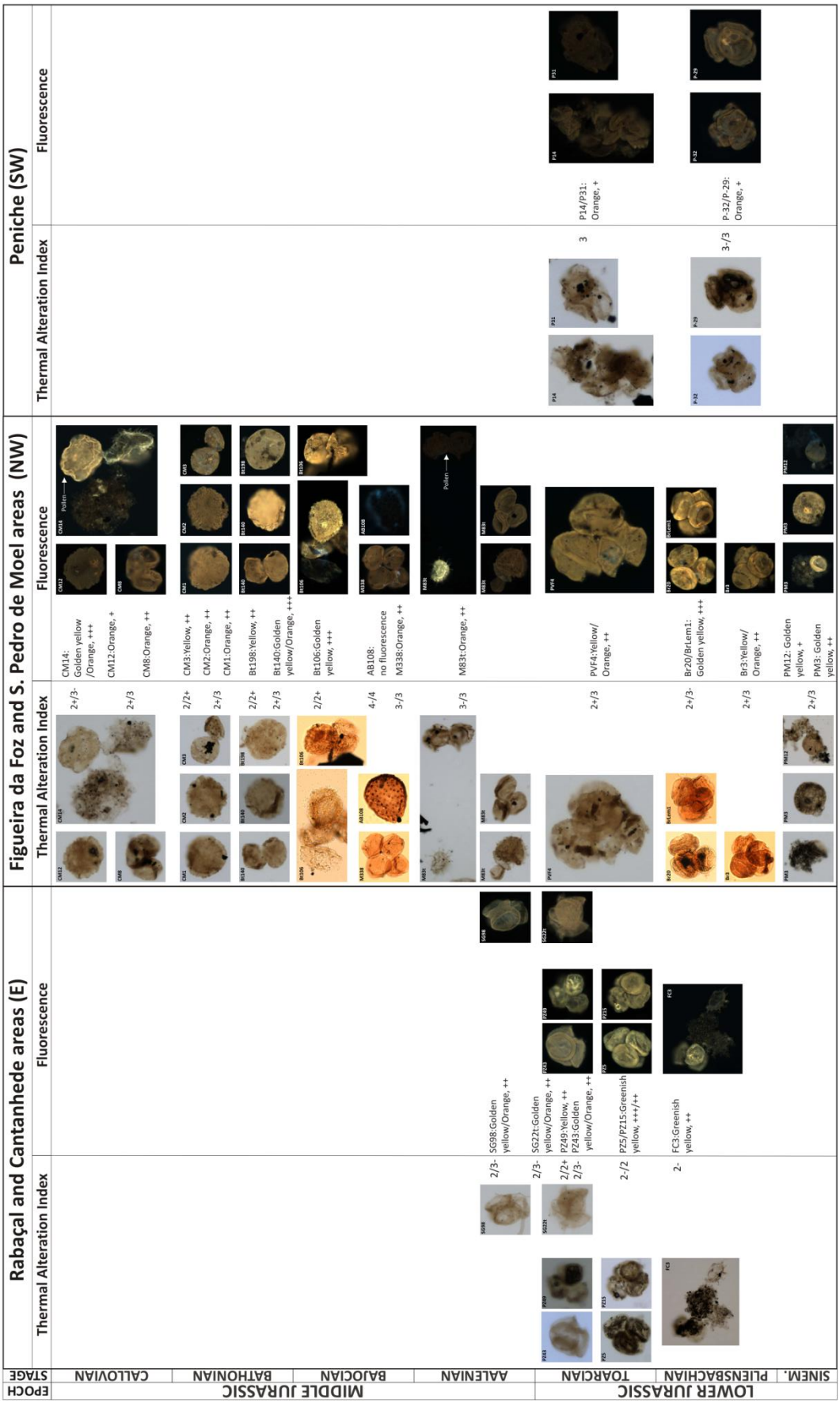

Figure 5.2. Overview of the TAI (Thermal Alteration Index) and fluorescence results (pollen, mainly *Classopollis* spp. and *Callialasporites* spp.) from the Lower and Middle Jurassic of the Lusitanian Basin, according with their stratigraphic position.

The lower Pliensbachian–lower Toarcian of the Peniche section show darker spores and pollen colours and orange fluorescence, comparing with the same interval in the Rabaçal and Brenha successions, for the same interval (Fig. 5.2; Table 5.1). This suggests that the Peniche sediments may have been exposed to higher burial temperatures, comparing to the northern Lusitanian Basin successions of the same age. Nevertheless, the lighter TAI colours and fluorescence of the lower Toarcian in Rabaçal, the middle and upper Toarcian of Maria Pares section give TAI and fluorescence values which are slightly darker, indicate mature sediments within the main petroleum production phase (the oil window). The upper Sinemurian of São Pedro de Moel succession is also within the oil window, with golden yellow fluorescence colours (Figs. 5.1, 5.2; Table 5.1).

Except for sample AB108 (lower Bajocian), the Middle Jurassic sediments of São Gião and Cabo Mondego successions are also in the early oil window. For the Middle Jurassic samples studied from the different locations, an increase in organic maturation levels for the younger samples was observed. The uppermost Bathonian and Callovian sediments show orange fluorescence colours. However, sample CM14, of upper Callovian age, has a slightly lighter fluorescence with golden yellow to orange colorations (Figs. 5.1, 5.2; Table 5.2). This suggests that subsidence rates and consequently, the burial depth were not uniform throughout the basin during Middle Jurassic times.

As was expected, each palynomorph group (i.e. dinoflagellate cysts, acritarchs, prasinophytes, spores and pollen) presented a different fluorescence colour, even in the same sample (Plates 5.1, 5.2). Acritarchs (e.g. *Micrhystridium* sp.) and prasinophytes (e.g. *Tasmanites*), in general, have always green fluorescence with medium or high intensity (Tables 5.1, 5.2; Plates 5.1, 5.2, 5.3). By contrary, the fluorescence of dinoflagellate cysts is highly variable, ranging between green to orange in the studied samples (Plates 5.1, 5.2, 5.5, 5.6, 5.7). This is depending mostly with the species (or genus), and not only with the chronological position. For example, in sample PZ5 (lower Toarcian of Maria Pares section), *Luehndea spinosa* presents an orange with very low intensity fluorescence and *Nannoceratopsis senex* has a green with medium/high intensity fluorescence (Plate 5.1). This may be explained by the differences in the outer wall (autophragm, periphragm or ectophragm) thickness and ornamentation of each dinoflagellate cyst species.

Table 5.1. TAI (Thermal Alteration Index) and fluorescence results from the Lower Jurassic of the Lusitanian Basin.

Sections	Substage	Samples	TAI	Fluorescence	
			Miospores	Miospores	Other
Rabaçal	Upper Toarcian	PZ85	2/2+	Yellow, ++	Prasinophytes: G, +++
	Middle Toarcian	PZ49	2/2+	Yellow, ++	Dinocysts: G/Y, +++ Acritarchs: G, ++, Prasinophytes: G, +++ AOM: G/O, ++
		PZ43	2/3-	Golden yellow/ Orange, ++	Prasinophytes: G/Y, +++
	Lower Toarcian	PZ15	2-/2	Greenish yellow, ++	Prasinophytes: G/Y, +++
		PZ5	2-/2	Greenish yellow, ++	Dinocysts: G/O, ++ Acritarchs: G, ++ AOM: G/O, ++
	Upper Pliensbachian	FC3	2-/2	Greenish yellow, ++	Dinocysts: O, + AOM: Y/O, ++
Vale das Fontes	Lower Toarcian	PVF4	2+/3	Yellow/ Orange, ++	Acritarchs: G, ++ AOM:Y, +
Peniche	Lower Toarcian	P31	3	Orange, +	Acritarchs: G/Y, ++ AOM: O, +
		P19	3	Orange, +	Acritarchs: O, +
		P14	3	Orange, +	Dinocysts: O, + Prasinophytes: G, +++ AOM: Y/O, +
	Upper Pliensbachian	P-23	3-/3	Orange, ++	Dinocysts: O, + Acritarchs: G, ++ AOM: G/O, +
	Lower Pliensbachian	P-29	3	Orange, +	Acritarchs: G, ++ Prasinophytes: G, +++
		P-32	3-/3	Orange, +	Acritarchs: G, ++ Prasinophytes: G, +++
Brenha	Upper Pliensbachian	BrLem1	2+/3-	Golden yellow, +++	AOM:Y, +
		Br20	2+/3-	Golden yellow, +++	AOM:Y, +
		Br15	3-/3	Orange, +	AOM:Y, +
	Lower Pliensbachian	Br9	2+/3	Golden yellow/ Orange, +	AOM:Y, ++
		Br3	2+/3	Yellow/ Orange, ++	AOM:Y, +
S. Pedro Moel	Upper Sinemurian	PM12	3-/3	Golden yellow, +	AOM: B/G
		PM3	2+/3-	Golden yellow, ++	Prasinophytes: G, ++ AOM: O, +

Table 5.2. TAI (Thermal Alteration Index) and fluorescence results from the Middle Jurassic of the Lusitanian Basin.

Sections	Substage	Samples	TAI	Fluorescence	
			Miospores	Miospores	Other
Cabo Mondego	Upper Callovian	CM14	2+/3-	Golden yellow/ Orange, +++	Dinocysts: Y/G, +++ AOM: O/Y, ++
		CM12	2+/3	Orange, +	Dinocysts: G/Y, ++
	Lower Callovian	CM8	2+/3	Orange, ++	AOM: Y/O, +
		CM7	2+/3	Orange, ++	Dinocysts: Y, ++
		CM6	2+/3	Orange, ++	AOM: Y/O, +
	Bathonian/ Callovian	CM5	3	Orange, +++	Dinocysts: G/Y, ++
	Upper Bathonian	CM4	2+/3	Orange, ++	Dinocysts: G/Y, ++
		CM3	2/2+	Yellow, ++	Dinocysts: G/Y, ++
	?Middle Bathonian	CM2	2+/3	Orange, ++	Dinocysts: G/Y, ++
		CM1	2+/3	Orange, ++	Dinocysts: G/Y, ++
	Lower Bathonian	Bt198	2/2+	Yellow, ++	AOM: Y/O, ++
		Bt140	2+/3	Golden yellow/ Orange, +++	Dinocysts: G/Y, ++
	Upper Bajocian	Bt106	2/2+	Golden yellow, +++	AOM: Y/O, +
	Lower Bajocian	AB108	4-/4	No fluorescence	AOM: Y/O, +
		M338	3-/3	Orange, ++	AOM: Y/O, +
	Lower Aalenian	M83t	3-/3	Orange, ++	Acritarch: G, ++ AOM: G/O, ++
São Gião	Lower Aalenian	SG98	2/3-	Golden yellow/ Orange, ++	Prasinophytes: G, ++ AOM: B/G, +
		SG48	2/3-	Golden yellow/ Orange, ++	Prasinophytes: G, ++ AOM: G/Y, +
	Upper Toarcian	SG22t	2/3-	Golden yellow/ Orange, ++	Prasinophytes: G, ++ AOM: G/Y, +

Spores show fluorescence colours ranging between greenish yellow to orange and, in some specimens, the orange intensity was very low (Plates 5.1, 5.2, 5.4). This also can be due the exine thickness and ornamentation of these spore species. Pollen exhibited always fluorescence within the yellow to orange colours (Fig. 5.1; Plates 5.1, 5.2, 5.4). In this Jurassic study, as in Fernandes et al. (2013), the pollen group revealed to be more consistent regarding the changes in fluorescence colour spectra and intensity (Plate 5.4) and, thus, more suitable to determine the fluorescence and TAI values, instead of spores. This is due to the relatively smooth and medium thickness of pollen exine, particularly the genera *Classopollis* and *Callialasporites,* compared to most of the Jurassic spores recorded in this study, such as *Cyathidites* spp. *Leptolepidites* spp. *Kraeuselisporites reissingeri* and *Ischyosporites variegatus* (Plate 5.4). Furthermore, the pollen were very abundant throughout the stratigraphic intervals of the Lusitanian Basin studied, especially *Classopollis* spp., *Callialasporites* spp. and *Araucariacites australis*, and thus, easily to be assessed and making also possible the correlation of fluorescence colours and TAI values between different sections. For these reasons, *Classopollis* spp. or *Callialasporites* spp. were used to evaluate the fluorescence colour and TAI values (Fig. 5.2; Tables 5.1, 5.2).

Although the limitations of these methods (fluorescence and TAI), especially the difficulties and subjectivity to attribute a number or colour/intensity scale to different pollen specimens, this method has the advantage to be inexpensive and a fast tool to evaluate the general maturation levels of potential source rocks. When possible, these techniques should be complemented with other organic maturation assessment methodologies, as vitrinite reflectance, (see also Suárez-Ruiz et al., 2012). Other advantage of fluorescence is the possibility to detect in detail microstructures of the palynomorphs wall, especially in Middle Jurassic dinoflagellate cysts, which have, in general, high relief ornamentation and/or complex processes (Plates 5.5–5.7). When the palynomorphs are not well preserved, in transmitted white light is difficult to observe specific morphological features of some taxa, but using fluorescence light these microstructures are made visible. This feature allows further morphological characterization of the studied specimens and an accurate taxonomical identification.

Plate 5.1. Selected palynomorphs from the Lusitanian Basin, Maria Pares section, lower Toarcian (*Dactylioceras polymorphum* AB), sample PZ5. **1, 3, 5, 7.** Transmitted white light; **2, 4, 6, 8.** Fluorescence (UV) mode.

1, 2. Association of an acritarch (*Micrhystridium* sp.), pollen and AOM.

3, 4. Association of a spore and a dinoflagellate cyst (*Luehndea spinosa*).

5, 6. Spore *Kraeuselisporites reissingeri.*

7, 8. Dinoflagellate cyst *Nannoceratopsis senex*.

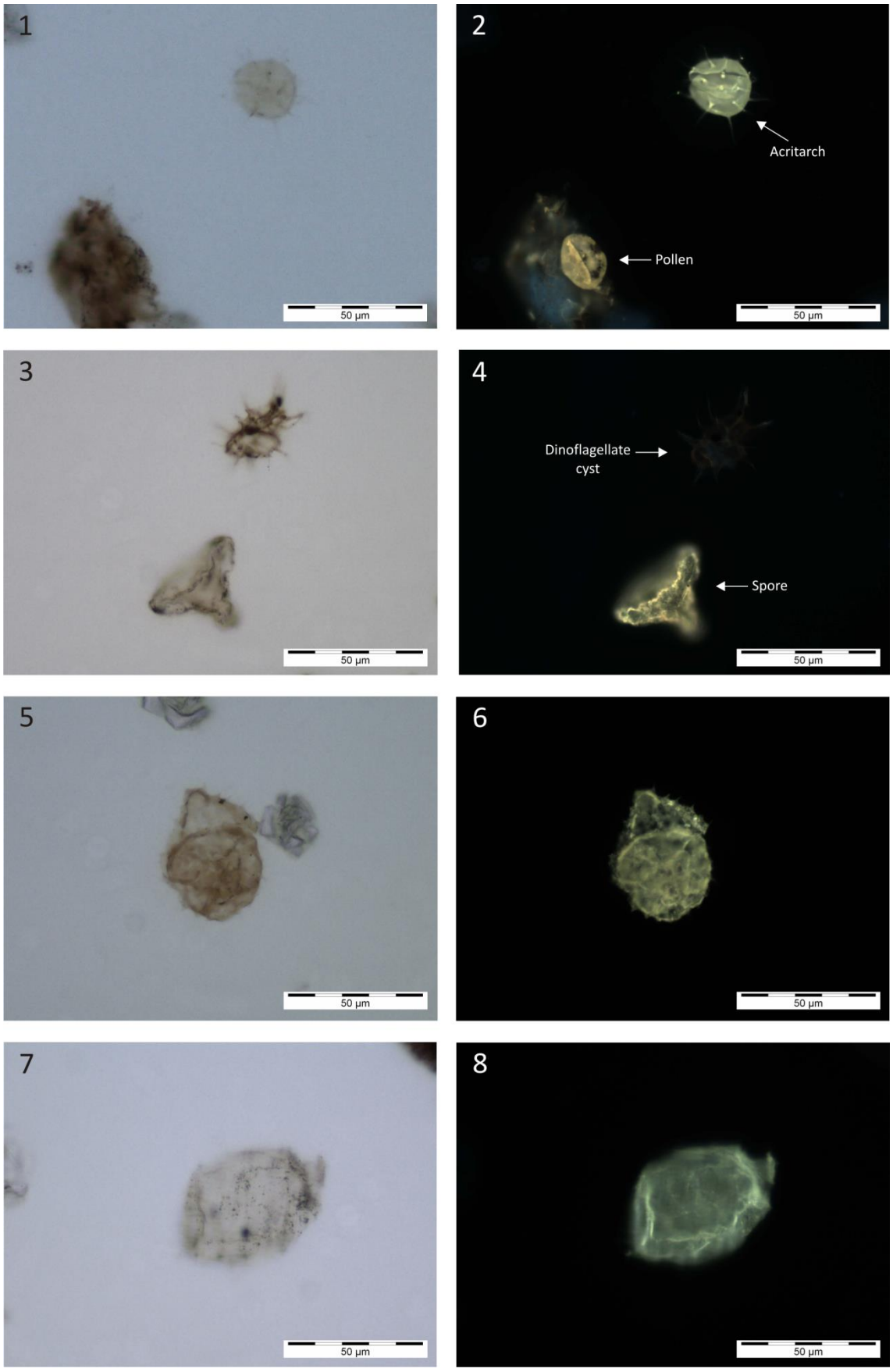

Plate 5.1 (caption on previous page)

Plate 5.2. Selected palynomorphs from the Lusitanian Basin. **1, 3, 5, 7.** Transmitted white light; **2, 4, 6, 8.** Fluorescence (UV) mode. **1-6.** Maria Pares section, middle Toarcian (*Hildoceras bifrons* AB), samples PZ43.

1, 2. Tetrad of pollen *Classopollis* sp.

3, 4. Spore *Cyathidites* sp.

5, 6. Prasinophyte *Tasmanites* sp.

7, 8. Association of a dinoflagellate cyst (*Ctenidodinium cornigerum*) and a pollen (*Callialasporites sp*.), Cabo Mondego section, ?middle Bathonian, sample CM1.

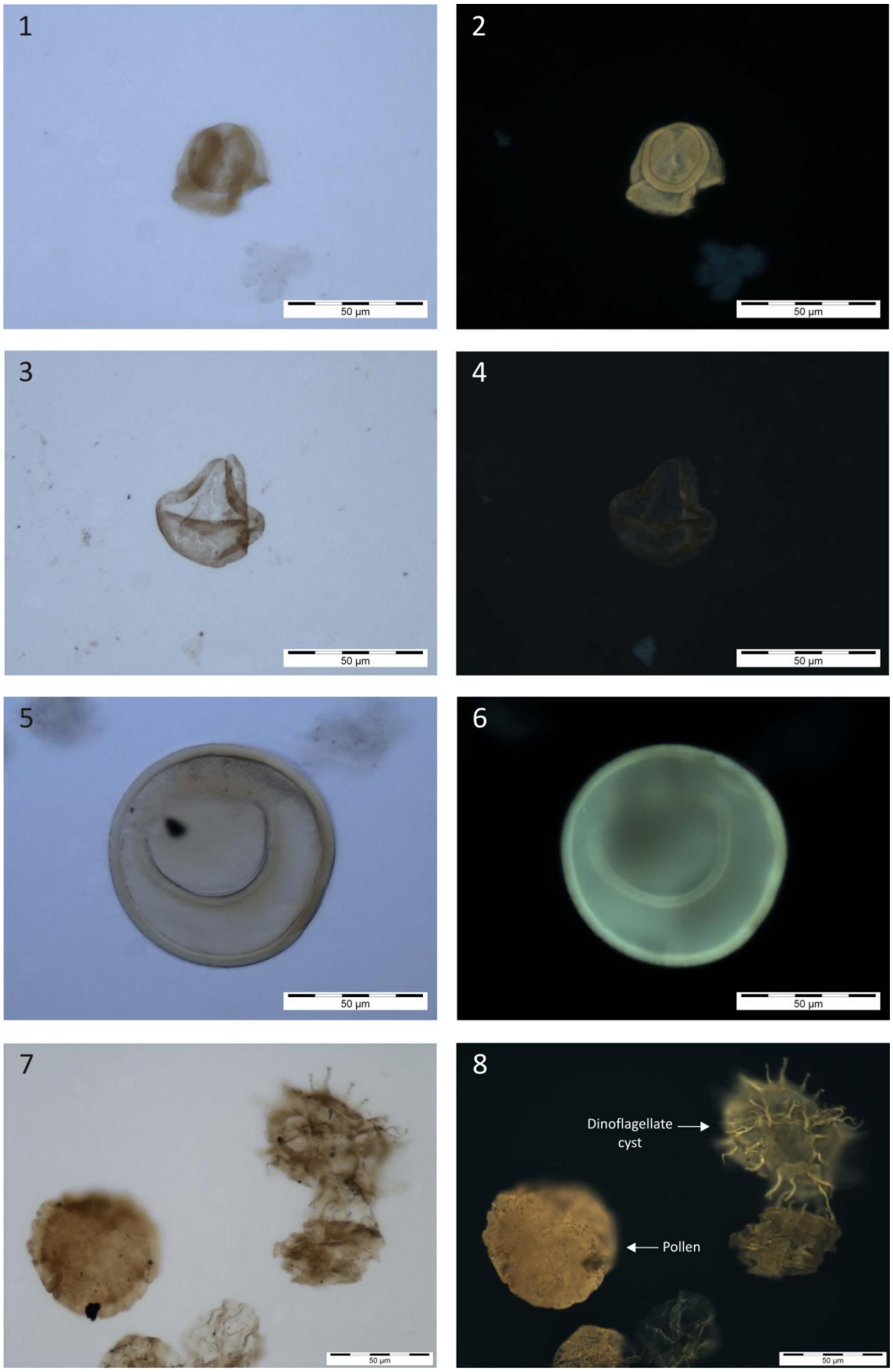

Plate 5.2 (caption on previous page)

Plate 5.3. Selected marine palynomorphs and amorphous organic matter (AOM) from the Lusitanian Basin. **1, 2, 3, 4, 6, 7, 8.** Fluorescence (UV) mode; **5.** Transmitted white light.

1. Prasinophyte *Tasmanites* sp., Peniche section, lower Toarcian (*Dactylioceras polymorphum* AB), sample P14.
2. Prasinophyte *Halosphaeropsis liassica* (clump), Maria Pares section, middle Toarcian (*Hildoceras bifrons* AB), samples PZ43.
3. Prasinophyte *Tasmanites* sp., Cabo Mondego section, lower Aalenian (*Leioceras opalinum* AB), sample M83t.
4. Acritarch *Micrhystridium* sp., Cabo Mondego section, lower Aalenian (*Leioceras opalinum* AB), sample M83t.
5, 6. Acritarch and AOM, Peniche section, upper Pliensbachian (*Amaltheus margaritatus* AB), sample P-23.
7. AOM, Maria Pares section, lower Toarcian (*Dactylioceras polymorphum* AB), sample PZ5.
8. AOM, Cabo Mondego section, lower Aalenian (*Leioceras opalinum* AB), sample M83t.

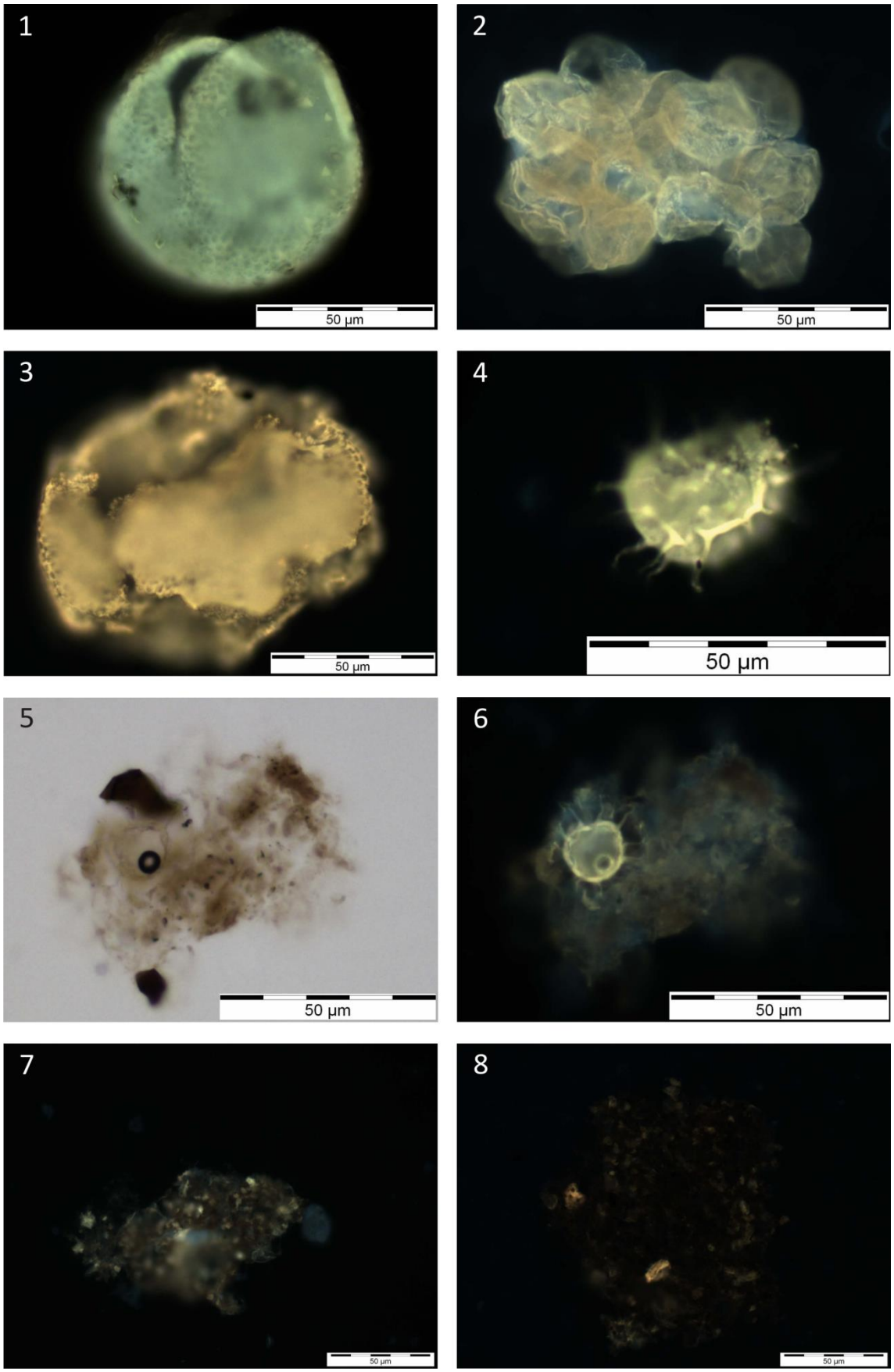

Plate 5.3 (caption on previous page)

Plate 5.4. Selected pollen and spores from the Lusitanian Basin. **5, 7.** Transmitted white light; **1, 2, 3, 4, 6, 8.** Fluorescence (UV) mode.

1. Pollen *Alisporites* sp., Peniche section, lower Pliensbachian (*Tragophylloceras ibex* AB), sample P-32.
2. Tetrad of pollen *Classopollis classoides*, Maria Pares section, lower Toarcian (*Dactylioceras polymorphum* AB), sample PZ5.
3. Pollen *Araucariacites australis*, Cabo Mondego section, lower Bathonian (*Zigzagiceras zigzag* AB), sample Bt140.
4. Pollen *Callialasporites segmentatus,* Cabo Mondego section, Bathonian-Callovian transition, sample CM5.
5, 6.Spore *Ischyosporites variagatus,* Maria Pares section, lower Toarcian (*Dactylioceras polymorphum* AB), sample PZ5.
7, 8. Tetrad of spore *Kraeuselisporites reissingeri,* Cabo Mondego section, lower Aalenian (*Leioceras opalinum* AB), sample M83t.

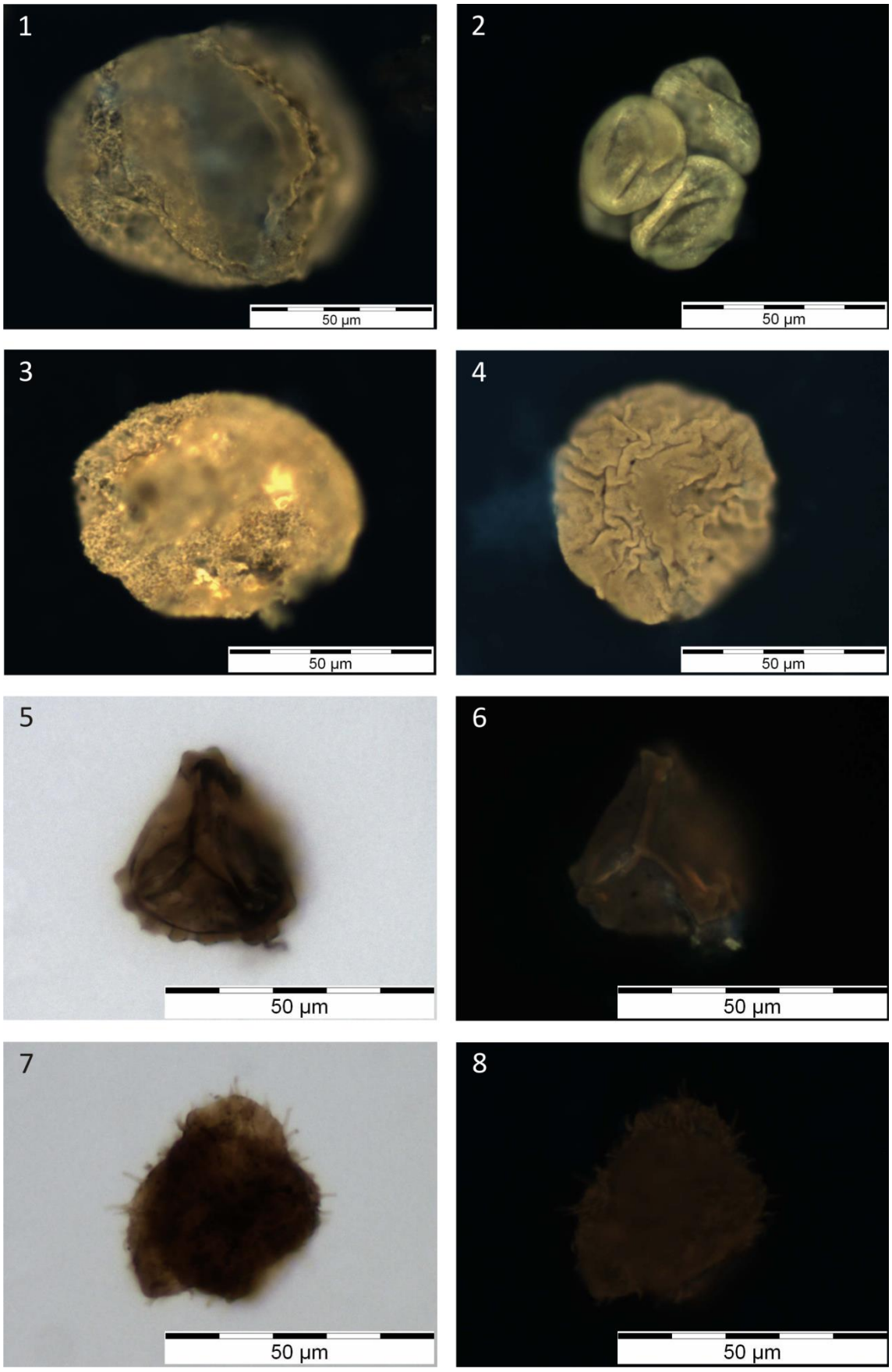

Plate 5.4 (caption on previous page)

Plate 5.5. Selected dinoflagellate cysts from the Lusitanian Basin. **1, 3, 5, 7.** Transmitted white light; **2, 4, 6, 8.** Fluorescence (UV) mode.

1, 2. *Mancodinium semitabulatum*, Maria Pares section, middle Toarcian (*Hildoceras bifrons* AB), samples PZ49.

3-8. *Ctenidodinium cornigerum*, Cabo Mondego section, ?middle Bathonian, sample CM1.

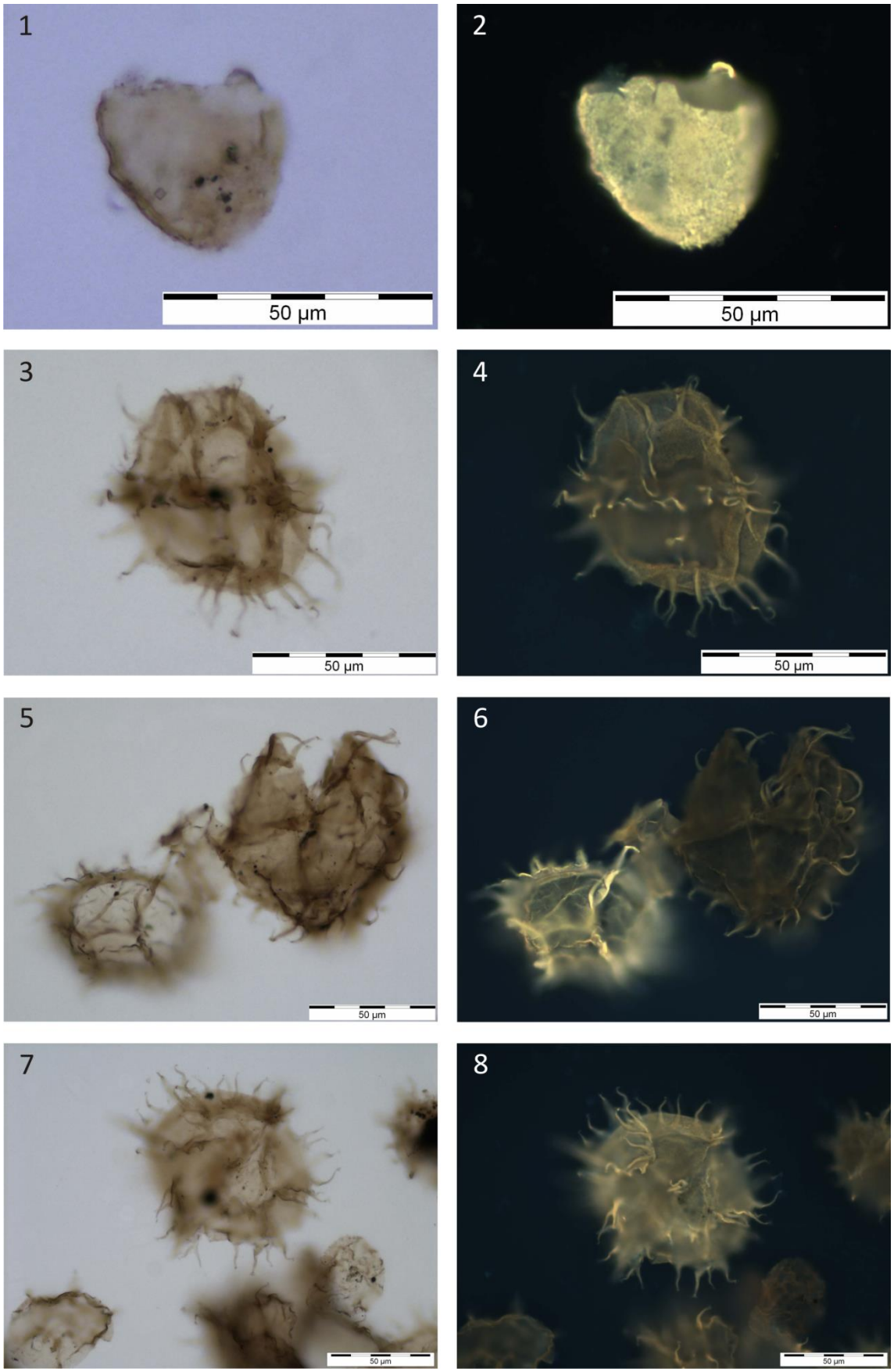

Plate 5.5 (caption on previous page)

Plate 5.6. Selected dinoflagellate cysts from the Lusitanian Basin. **1, 3, 5, 7.** Transmitted white light; **2, 4, 6, 8.** Fluorescence (UV) mode.

1, 2. *Ctenidodinium sellwoodii,* Cabo Mondego section, lower Bathonian (*Zigzagiceras zigzag* AB), sample Bt140.

3, 4. *Adnatosphaeridium*? *caulleryi,* Cabo Mondego section, upper Bathonian, sample CM4.

5, 6. *Chytroeisphaeridia chytroeides*, Cabo Mondego section, upper Bathonian, sample CM4.

7, 8. *Ellipsoidictyum* sp., Cabo Mondego section, upper Bathonian, sample CM4.

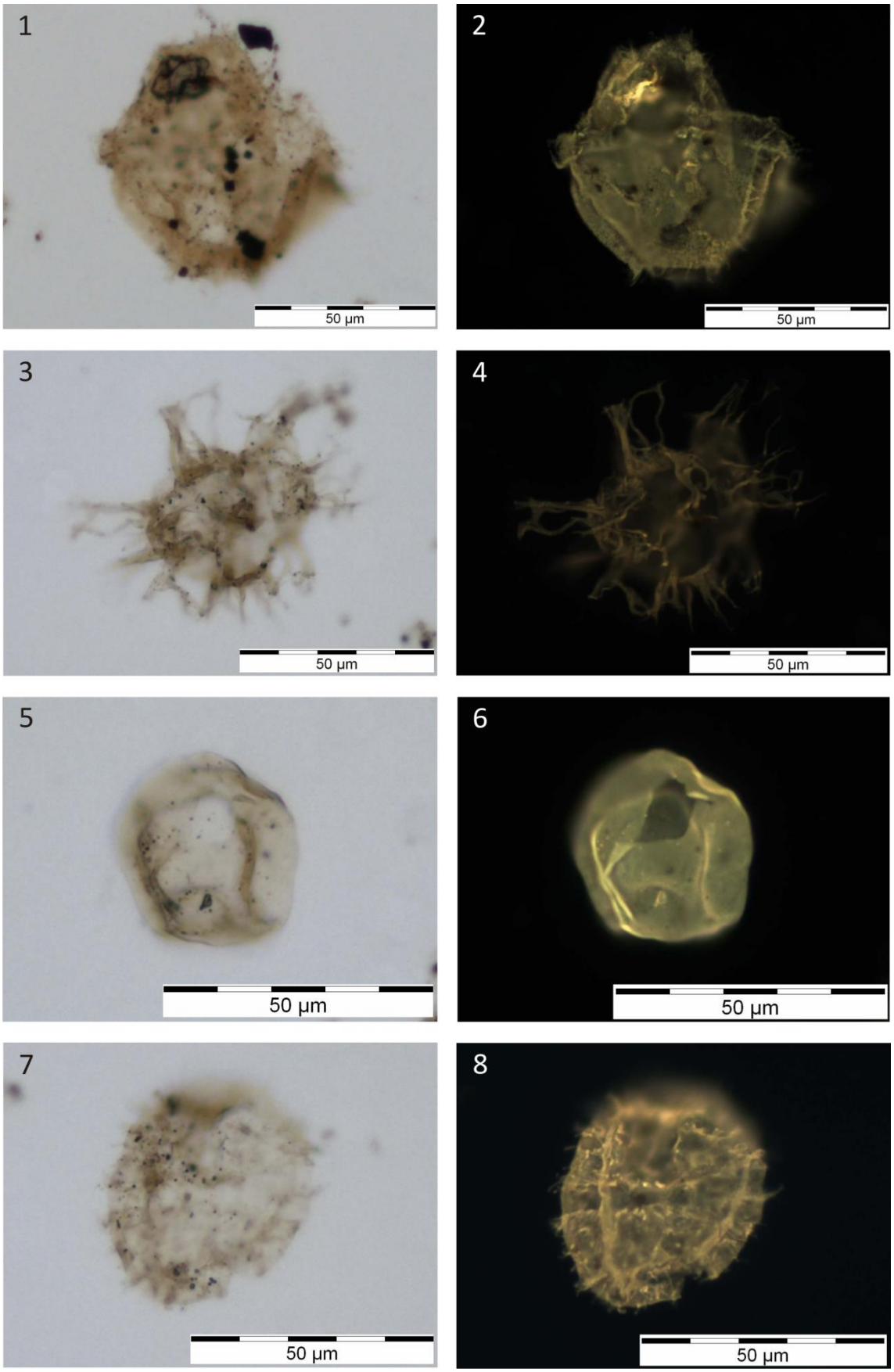

Plate 5.6 (caption on previous page)

Plate 5.7. Selected dinoflagellate cysts from the Lusitanian Basin. **1, 3, 5, 7.** Transmitted white light; **2, 4, 6, 8.** Fluorescence (UV) mode.

1, 2. *Gonyaulacysta jurassica* subsp. *adecta,* Cabo Mondego section, Bathonian-Callovian transition, sample CM5.

3, 4. *Impletosphaeridium* sp., Cabo Mondego section, lower Callovian, sample CM7.

5, 6. *Gonyaulacysta jurassica* subsp. *adecta,* Cabo Mondego section, upper Callovian, sample CM12.

7, 8**.** *Adnatosphaeridium caulleryi,* Cabo Mondego section, upper Callovian, sample CM12.

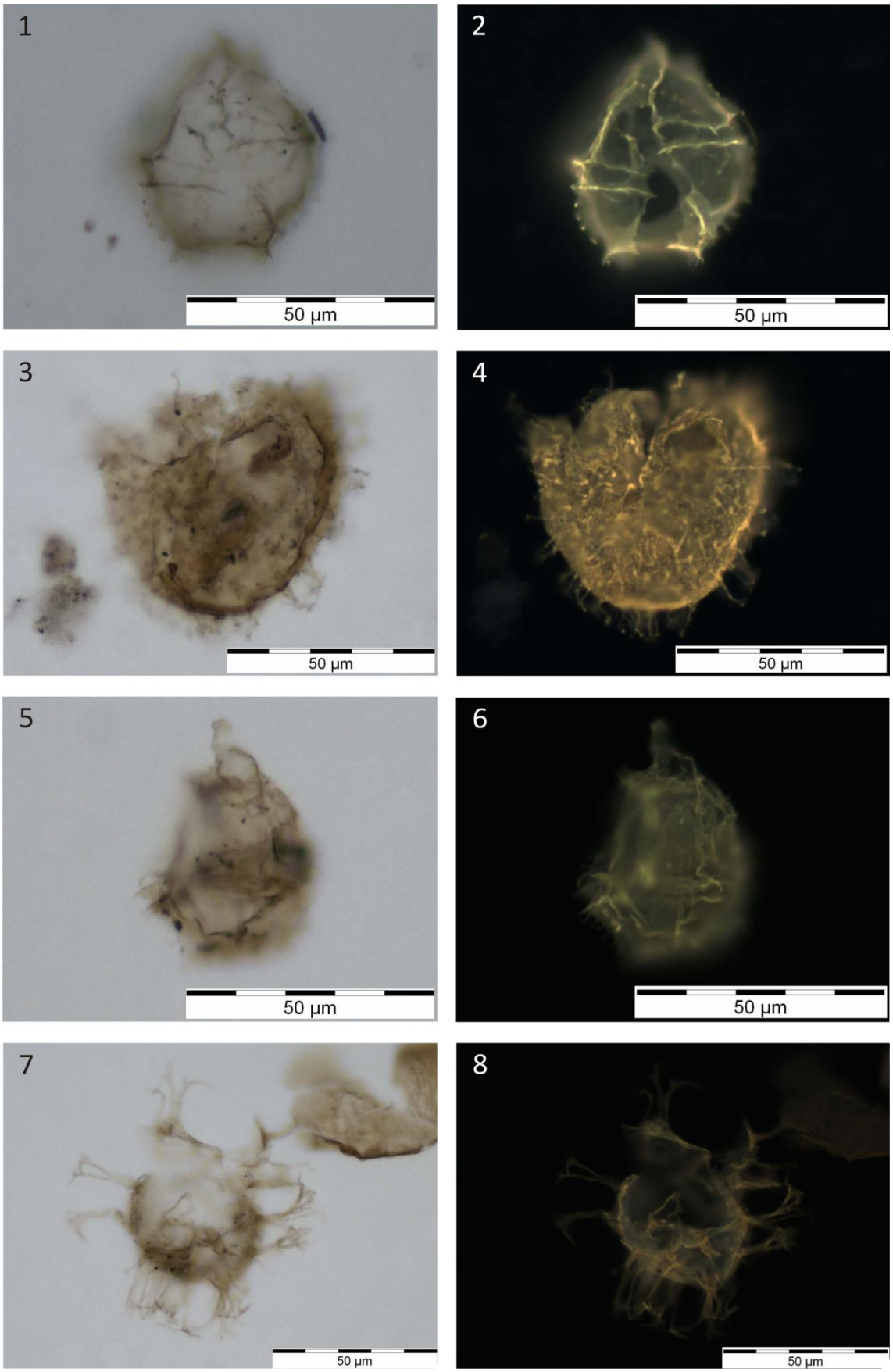

Plate 5.7 (caption on previous page)

5. Conclusions

The fluorescence and TAI values of the Lower and Middle Jurassic of the Lusitanian Basin suggests that most part of these sediments are mature and within the oil window, showing yellow to orange fluorescene colours and 2 to 3+ TAI values, respectively. Exceptions are, samples FC3, PZ5 and PZ15, which probably characterize an organic thermal immature interval ranging the upper Pliensbachian to lower Toarcian in the Rabaçal area, and sample AB108, which is regard as overmature regarding the oil window. This study highlighted the importance of fluorescence microscopy technique, together with TAI analyses, as rapid and inexpensive tool for general characterization of the organic maturation of potential hydrocarbon source rocks. Complementary analyses are required for a more comprehensive organic maturation study, e.g. the measurement of vitrinite reflectance, since it was also observed that different palynomorphs groups have different fluorescence colours for the same maturation level. In this study the fluorescence of pollen grains of *Classopollis* spp., *Callialasporites* spp. were selected to describe the organic maturation levels of the stratigraphic successions studied, due to its abundance, exine features and consistence in fluorescence colour. It was also observed that spore fluorescence colours overestimated organic maturation levels, whereas dinoflagellates, acritarch and prasinophytes tend to underestimated maturation levels, assessed by the observation of pollen fluorescence. Other advantage of this practice for biostratigraphic palynology, is the possibility to observe in detail some microstructures in the outer layers of the palynomorphs, which may not be visible in transmitted white light

CHAPTER VI

Final remarks

Chapter VI cover:

Cabo Mondego section, Bathonian ASSP (Middle Jurassic)

Chapter VI. Final remarks

1. General conclusions

This PhD project represents a comprehensive contribution on the palynology of the Lusitanian Basin. In this study, 358 samples were studied in detail, of which 57 proved barren, giving a general productivity of 84.1% (Table 6.1). The Lower Jurassic samples were more productive, with 90.7%, compared with Middle Jurassic horizons, with 74.3%. This lower percentage is related with the high number of barren samples of the São Gião section.

Table 6.1. Summary of the number of studied samples in each section and their productivity in percentage. The totals are also presented.

EPOCH	Stage	Sections	Nº studied samples	N º barren samples	Productivity %
LOWER JURASSIC	Sinemurian	S. Pedro de Moel	12	0	100.0
	Pliensbachian	Brenha	22	1	95.5
	Pliens.-Toarcian	Peniche (Toarcian GSSP)	72	14	80.6
	Toarcian	Vale das Fontes	14	0	100.0
	Pliens.-Toarcian	Rabaçal area: Maria Pares and Fonte Coberta	94	5	94.7
		Total	214	20	90.7
MIDDLE JURASSIC	Aalenian	São Gião	47	26	44.7
	Aalenian-Bajocian	Cabo Mondego (Murtinheira, Bajocian GSSP)	68	9	86.8
	Bajocian-Bathonian	Cabo Mondego (Bathonian ASSP)	14	1	92.9
	Bathonian, Callovian	Cabo Mondego (extra samples)	15	1	93.3
		Total	144	37	74.3
		TOTAL	**358**	**57**	**84.1**

Part of this work (Chapter II) was focused on the major palaeoenvironmental perturbation during the early Toarcian, the T-OAE. The high resolution dinoflagellate cyst record reflects well the dramatic changes occurring during this period in the marine organisms: extinctions and disappearance events. This work also highlighted the fact of not only anoxia caused these bioevents, but also changes in the paleotemperatures and salinity, in particular the rapid increase of seawater temperatures with the T-OAE. In the Lusitanian Basin, the beginning of this anoxic event occurred at the base of *Hildaites levisoni* AB and is marked by the extinction of *Luehndea spinosa*, the disappearance of *Nannoceratopsis* spp. and the general reduction of dinoflagellate cyst and increase of prasinophytes abundances. These bioevents are precisely equivalent with the negative

carbon ($\delta^{13}C_{carb)}$ and oxygen ($\delta^{18}O$) isotopes excursion records, previously established for the Lusitanian Basin, and correlate well with coeval European basins.

In this study, the Lower and Middle (Aalenian–lowermost Bathonian) Jurassic high resolution biostratigraphy of the Lusitanian Basin was documented, especially based on the dinoflagellate cyst records. These allow the establishment of palynostratigraphical charts for the Lower (Chapter III) and Middle (Chapter IV) Jurassic of this depocentre and a biozonation scheme for the Lower Jurassic is proposed. To create a Middle Jurassic biozonation scheme for the Lusitanian Basin is necessary study in detail, at least, the upper Bajocian of Cabo Mondego section and a lateral equivalent succession. In Fig. 6.1 is illustrate the summary of the palynostratigraphical results of this investigation, in which 23 biostratigraphical significant palynomorphs ranges and bioevents are schemed for the lower Pliensbachian–lower Bathonian interval. These stratigraphical key taxa are pictured in the catalogue of Appendix 3.

The T-OAE severely affected the chronological distribution of the early Jurassic dinoflagellate cysts. Due their abundance and short stratigraphical range (Fig. 6.1), *Luehndea spinosa* is an example of a dinoflagellate cyst as a reliable tool for biostratigraphy and paleoenvironmental interpretations. The increase of dinoflagellate cyst inceptions during the lower Bajocian to lower Bathonian interval, document the Middle Jurassic radiation of these planktonic group. The Jurassic spores and pollen have relatively long stratigraphical ranges and, thus, usually are not primarily used as biostratigraphical markers. Nevertheless, in the Lusitanian Basin the spore *Kraeuselisporites reissingeri* and the pollen *Classopollis* spp., *Araucariacites australis* and *Callialasporites* spp. are good additional stratigraphical indicators of the Lower to Middle Jurassic interval (Fig. 6.1).

The palynostratigraphical chart proposed in this project may be used in future hydrocarbon research of the onshore and offshore Lusitanian Basin. The fluorescence colour of palynomorphs and spore-pollen colours (TAI) analyses, suggest that most of the Lower and Middle Jurassic sediments of the Lusitanian Basin are between the immature and mature phases for oil generation, depending on their position within the basin structures. Immature sediments are common on the horst or basin high strutures, whereas mature successions are found in graben or basin trough structures suggesting burial under thicker sedimentary successions (Chapter V).

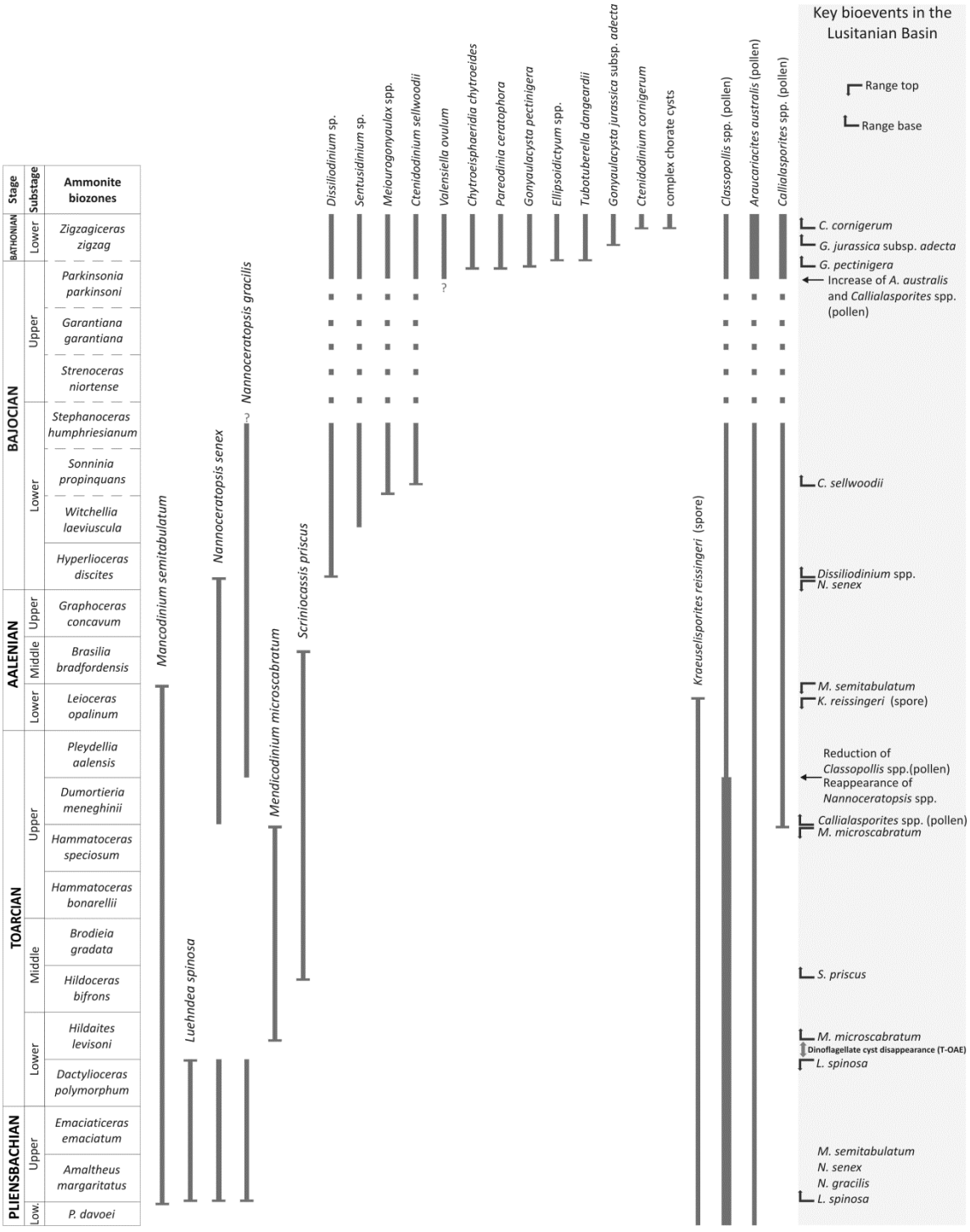

Figure 6.1. Overview of the stratigraphically significant ranges of 19 dinoflagellate cysts and 4 terrestrial palynomorphs, and selected bioevents from the lower Pliensbachian to lowermost Bathonian of the Lusitanian Basin. The spore-pollen taxa are identified and the rest are dinoflagellate cysts. The extremities of ranges with horizontal bars represent true range bases and tops (i.e. inceptions and apparent extinctions, respectively) as appropriate. The range extremities which lack horizontal bars represent interruptions to known stratigraphical ranges. The dotted ranges represent inferred occurrences in the non-studied interval (uppermost *Stephonoceras humphriesianum*–lower *Parkinsonia parkinsoni* ABs).

Hence, the initial objectives of this PhD project were substantially attained. The Lower and part of Middle Jurassic palynostratigraphy chart (Fig. 6.1) of the Lusitanian Basin, as well the Early Jurassic biozonal scheme (Fig. 3.15) proposed in this work, were correlated with other fossil groups, especially with nannofossils and ammonite biozones, and compared with coeval basins. This work can be a valuable instrument for hydrocarbon investigations of the Lusitanian Basin. In addition, high resolution palynostratigraphy based on dinoflagellate cysts and palaeoecological and palaeobiological interpretations of Jurassic key events were documented. These were the T-OAE, GSSPs for the Toarcian Stage at Peniche and the Bajocian Stage at Murtinheira, Cabo Mondego and the ASSP for the Bathonian stage at Cabo Mondego. The remaining upper Bajocian, Bathonian and Callovian sediments of Cabo Mondego succession were not studied for palynology. As was expected, the dinoflagellate cyst assemblages recorded in this investigation, suggest that the Lusitanian Basin is an intermediate area between the Boreal and Tethyan realms, with a mixture of taxa characteristic of each realm, and represented a transition between the northern and southern Europe during the early phases of the opening of the North Atlantic Ocean. With this work, we expect to present a significant contribution to the Lusitanian Basin background, especially for biostratigraphy, and to the general palaeoenvironmental knowledge of the Jurassic period.

2. Future perspectives

In this study, the palynological response to the T-OAE was investigated in three key sections of the Lusitanian Basin, i.e. Maria Pares, Vale das Fontes and Peniche. These results help to elucidate about the effects of this perturbation in the planktonic organisms, i.e. the dinoflagellate cysts in the case of this work, and what were the major abiotic factors that caused the extinctions and disappearance events. The same research could be established in other Lower Jurassic basins (e.g. Spain, France, Morocco) with relatively expanded lower Toarcian, in order to fully understand the global and local trends of this major Mesozoic palaeoenvironmental perturbation.

The Cabo Mondego succession is an exceptional well developed Middle Jurassic succession (uppermost Aalenian–upper Callovian). Due the lack of biostratigraphical control, part of the upper Bajocian, most of the Bathonian and Callovian horizons of

this section were not studied in this PhD project. Only preliminary results of the dinoflagellate cysts from the uppermost Bathonian–lower Callovian and upper Callovian of the Cabo Mondego were presented in an International Meeting (AASP 50th Annual Meeting, Nottingham 2017, see Supplement C). The relatively well preserved palynomorphs and high abundances of dinoflagellate cysts, are a promising indication of valuable data to continue the palynostratigraphical study of the Lusitanian Basin. Palaeoenvironmental interpretations, based on marine and terrestrial palynomorphs, and dinoflagellate cyst evolution assessments, could also be discussed with the study of upper Bajocian, Bathonian and Callovian sediments from Cabo Mondego section, as well in other Middle Jurassic successions from Lusitanian Basin).

References

Al-Suwaidi, A.H., Angelozzi, G.N., Baudin, F., Damborenea, S.E., Hesselbo, S.P., Jenkyns, H.C., Manceñido, M.O., Riccardi, A.C., 2010. First record of the Early Toarcian Oceanic Anoxic Event from the Southern Hemisphere, Neuquén Basin, Argentina. Journal of the Geological Society, London 167, 633–636.

Al-Suwaidi, A.H., Hesselbo, S.P., Damborenea, S.E., Manceñido, M.O., Jenkyns, H.C., Riccardi, A.C., Angelozzi, G.N., Baudin, F., 2016. The Toarcian Oceanic Anoxic Event (Early Jurassic) in the Neuquén Basin, Argentina: A reassessment of age and carbon isotope stratigraphy. The Journal of Geology 124, 171–193.

Anderson, D.M., Taylor, C.D., Armbrust, E.V., 1987. The effects of darkness and anaerobiosis on dinoflagellate cyst germination. Limnology and Oceanography 32, 340–351.

Andrade, B., Duarte, L.V., García Joral, F., Goy, A., Henriques, M.H., 2016. Palaeobiogeographic patterns of the brachiopod assemblages of the Iberian Subplate during the Late Toarcian–Early Aalenian (Jurassic). Palaeogeography, Palaeoclimatology, Palaeoecology 442, 12–22.

Arkell, W.J. 1956. Jurassic Geology of the World. Oliver and Boyd Limited, Edinburgh, 806 p.

Azerêdo, A.C., Duarte, L.V., Henriques, M.H., Manuppella, G., 2003. Da dinâmica continental no Triássico aos mares do Jurássico Inferior e Médio. Cadernos de Geologia de Portugal, Instituto Geológico e Mineiro, Lisboa, 43 pp.

Azerêdo, A.C., Duarte, L.V., Silva, R.L., 2014. Configuração sequencial em ciclos (2ª ordem) de fácies transgressivas-regressivas do Jurássico Inferior e Médio da Bacia Lusitânica (Portugal). Comunicações Geológicas 101 (Especial I), 383–386.

Bailey, D.A., 1987. *Durotrigia daveyi* gen. et sp. nov., an Early Bajocian dinocyst with a variable precingular archaeopyle. Journal of Micropalaeontology 6, 89–96.

Baker, S.J., Hesselbo, S.P., Lenton, T.M., Duarte, L.V., Belcher, C.M., 2017. Charcoal evidence that rising atmospheric oxygen terminated Early Jurassic ocean anoxia. Nature Communications, doi: 10.1038/ncomms15018.

Baldanza, A., Bucefalo Palliani, R., Mattioli, E., 1995. Calcareous nannofossils and dinoflagellate cysts from Late Liassic of Hungary and comparison with Central Italy assemblages. Paleopelagos 5, 161–174.

Baranyi, V., Pálfy J., Görög, A., Riding, J.B., Raucsik, B., 2016. Multiphase response of palynomorphs to early Toarcian (Early Jurassic) environmental changes in southwest Hungary. Review of Palaeobotany and Palynology 235, 51–70.

Barrón, E., Azerêdo, A.C., 2003. Palynology of the Jurassic (Callovian–Oxfordian) succession from Pedrógão (Lusitanian Basin, Portugal). Palaeoecological and palaeobiogeographical aspects. Neues Jahrbuch für Geologie und Paläontologie Abhandlungen 227, 259–286.

Barrón, E., Azerêdo, A.C., Cabral, M.C., Ramalho, M.M., Pereira, R., 1999. Palinomorfos del Jurásico de Pedrógão (Portugal). Descripción y comparación con otros elementos micropaleontológicos y sedimentológicos. Temas Geológico-Mineros, Instituto Tecnologico Geominero de España 26, 186–191.

Barrón, E., Ureta, S., Goy, A., Lassaletta, L., 2010. Palynology of the Toarcian-Aalenian Global Boundary Stratotype Section and Point (GSSP) at Fuentelsaz (Lower-Middle Jurassic, Iberian Range, Spain). Review of Palaeobotany and Palynology 162, 11–28.

Barrón, E., Comas-Rengifo, M.J., Duarte, L.V., 2013. Palynomorph succession of the Upper Pliensbachian–Lower Toarcian of the Peniche section (Portugal). Comunicações Geológicas 100 (Especial I), 55–61.

Batten, D.J., 1975. Wealden palaeoecology from the distribution of plant fossils. Proceedings of the Geologists' Association 85, 433–458.

Bjerrum, C.J., Surlyk, F., Callomon, J.H., Slingerland, R.L., 2001. Numerical paleoceanographic study of the early transcontinental Laurasian Seaway. Paleoceanography 16, 390–404.

Bomfleur, B., Schöner, R., Schneider, J.W., Viereck, L., Kerp, H., McKellar, J.L., 2014. From the Transantarctic Basin to the Ferrar Large Igneous Province: New palynostratigraphic age constraints for Triassic–Jurassic sedimentation and magmatism in East Antarctica. Review of Palaeobotany and Palynology 207, 18–37.

Borges, M.E.N., 2012. Palinostratigrafia e isótopos estáveis do Jurássico da Bacia Algarvia e da Carrapateira. Unpublished PhD Thesis, Faculdade de Ciências e Tecnologia, Universidade do Algarve, 473 pp.

Borges, M.E.N., Riding, J.B., Fernandes, P., Pereira, Z., 2011. The Jurassic (Pliensbachian to Kimmeridgian) palynology of the Algarve Basin and the Carrapateira outlier, southern Portugal. Review of Palaeobotany and Palynology 163, 190–204.

Borges, M.E.N., Riding, J.B., Fernandes, P., Matos, V., Pereira, Z., 2012. Callovian (Middle Jurassic) dinoflagellate cysts from the Algarve Basin, southern Portugal. Review of Palaeobotany and Palynology 170, 40-56.

Boussaha, M., Pittet, B., Mattioli, E., Duarte, L.V., 2014. Spatial characterization of the late Sinemurian (Early Jurassic) palaeoenvironments in the Lusitanian Basin. Palaeogeography, Palaeoclimatology, Palaeoecology 409, 320–339.

Bowman, V.C., Francis, J.E., Riding, J.B., 2013. Late Cretaceous winter sea ice in Antarctica? Geology 41, 1227–1230.

Bown, P.R., 1987. Taxonomy, evolution, and biostratigraphy of Late Triassic–Early Jurassic calcareous nannofossils. Special Paper Palaeontology 38, 1–118.

Brittain, J.M., Higgs, K.T., Riding, J.B., 2010. The palynology of the Pabay Shale Formation (Lower Jurassic) of SW Raasay, northern Scotland. Scottish Journal of Geology 46, 67–75.

Bucefalo Palliani, R., Riding, J.B., 1997a. Lower Toarcian palynostratigraphy of Pozzale, central Italy. Palynology 21, 91–103.

Bucefalo Palliani, R., Riding, J.B., 1997b. The influence of palaeoenvironmental change on dinoflagellate cyst distribution. An example from the Lower and Middle Jurassic of Quercy, southwest France. Bulletin des Centres de Recherches Exploration Production Elf-Aquitaine 21, 107–123.

Bucefalo Palliani, R., Riding, J.B., 1997c. *Umbriadinium mediterraneense* gen. et sp. nov. and *Valvaeodinium hirsutum* sp. nov.: two dinoflagellate cysts from the Lower Jurassic of the Tethyan Realm. Palynology 21, 197–206.

Bucefalo Palliani, R., Mattioli, E., 1998. High resolution integrated microbiostratigraphy of the Lower Jurassic (late Pliensbachian-early Toarcian) of central Italy. Journal of Micropalaeontology 17, 153–172.

Bucefalo Palliani, R., Riding, J.B., 1999a. Early Jurassic (Pliensbachian–Toarcian) dinoflagellate migrations and cyst paleoecology in the Boreal and Tethyan realms. Micropaleontology 45, 201–214.

Bucefalo Palliani, R., Riding, J.B., 1999b. Relationships between the early Toarcian anoxic event and organic-walled phytoplankton in central Italy. Marine Micropaleontology 37, 101–116.

Bucefalo Palliani, R., Riding, J.B., 2000. A palynological investigation of the Lower and lowermost Middle Jurassic strata (Sinemurian to Aalenian) from North Yorkshire, UK. Proccedings of the Yorkshire Geological Society 53, 1–16.

Bucefalo Palliani, R., Riding, J.B., 2003. Biostratigraphy, provincialism and evolution of European Early Jurassic (Pliensbachian to early Toarcian) dinoflagellate cysts. Palynology 27, 179–214.

Bucefalo Palliani, R., Riding, J.B., Torricelli, S., 1996. *Polygonium jurassicum* sp. nov., a polygonomorph acritarch from the lower Toarcian (lower Jurassic) of the Tethyan realm. Palynology 20, 157–161.

Bucefalo Palliani, R., Riding, J.B., Torricelli, S., 1997a. The dinoflagellate cyst *Luehndea* Morgenroth, 1970, emend. from the upper Pliensbachian (Lower Jurassic) of Hungary. Review of Palaeobotany and Palynology 96, 113–120.

Bucefalo Palliani, R., Riding, J.B., Torricelli, S., 1997b. The dinoflagellate cyst *Mendicodinium* Morgenroth, 1970, emend. from the lower Toarcian (Jurassic) of central Italy. Review of Palaeobotany and Palynology 96, 99–111.

Bucefalo Palliani, R., Mattioli, E., Riding, J.B., 2002. The response of marine phytoplankton and sedimentary organic matter to the early Toarcian (Lower Jurassic) oceanic anoxic event in northern England. Marine Micropaleontology 46, 223–245.

Butler, N., Charnock, M.A., Hager, K.O., Watkins, C.A., 2005. The Ravenscar Group: a coeval analogue for the Middle Jurassic reservoirs of the North Sea and offshore Mid-Norway, in: Powell, A.J., Riding, J.B. (Eds.), Recent Developments in Applied Biostratigraphy. The Micropalaeontological Society, Special Publications. The Geological Society, London, U.K., pp. 43–53.

Cabral, M.C., Loureiro, I.M., Pinto, S., Duarte, L.V., Azerêdo, A.C., 2011. New light on the Metacopina (Crustacea, Ostracoda) Toarcian Extinction Event: integrated data from the Lusitanian Basin, Portugal. EGU General Assembly 2011. Geophysical Research Abstracts 13, EGU2011-3607-1.

Cabral, M.C., Loureiro, I.M., Duarte, L.V., Azerêdo, A.C., 2013. The record of the Matacopina (Ostracoda, Crustacea) extinction in the Toarcian of Rabaçal, Coimbra region. Comunicações Geológicas 100 (Especial I), 63–68.

Cabral, M.C., Lord, A., Boomer, I., Loureiro, I., Malz, H., 2014. *Tanycithere* new genus and its significance for Jurassic ostracoda diversity. Journal of Palaeontology 88 (3), 519–530.

Cabral, M.C., Colin, J.P., Azerêdo, A.C., Silva, R.L., Duarte, L.V., 2015. Brackish and marine ostracode assemblages from the Sinemurian of western Portugal, with descriptions of new species. Micropaleontology 61 (1-2), 3–24.

Canales, M.L., Henriques, M.H., 2008. Foraminifera from the Aalenian and the Bajocian GSSP (Middle Jurassic) of Murtinheira section (Cabo Mondego, West Portugal): Biostratigraphy and paleoenvironmental implications. Marine Micropaleontology 67, 155–179.

Canales, M.L., Henriques, M.H., 2013. Foraminiferal assemblages from the Bajocian Global Stratotype Section and Point (GSSP) at Cabo Mondego (Portugal). Journal of Foraminiferal Research 43, 182–206.

Canales-Férnandez, M.L., Gárcia-Baquero, G., Henriques, M.H., Figueiredo, V.L., 2014. Palaeoecological distribution pattern of Early–Middle Jurassic benthic foraminifera in the Lusitanian Basin (Portugal) based on multivariate analysis. Palaeogeography, Palaeoclimatology, Palaeoecology 410, 14–26.

Castro, L.N.S.P., 2006. Dinoflagelados e outros palinomorfos do Miocénico do sector distal da Bacia do Baixo-Tejo. Unpublished PhD Thesis, Faculdade de Ciências e Tecnologia da Universidade Nova Lisboa, 380 pp.

Caswell, B.A., Coe, A.L., 2012. A high-resolution shallow marine record of the Toarcian (Early Jurassic) Oceanic Anoxic Event from the East Midlands Shelf, UK. Palaeogeography, Palaeoclimatology, Palaeoecology 365, 124–135.

Caswell, B.A., Coe, A.L., 2013. Primary productivity controls on opportunistic bivalves during Early Jurassic oceanic deoxygenation. Geology 41, 1163–1166.

Caswell, B.A., Coe, A.L., Cohen, A.S., 2009. New range data for marine invertebrate species across the early Toarcian (Early Jurassic) mass extinction. Journal of the Geological Society 166, 859–872.

Cohen, A.S., Coe, A.L., Kemp, D.B., 2007. The Late Palaeocene–Early Eocene and Toarcian (Early Jurassic) carbon isotope excursions: a comparison of their time scales, associated environmental changes, causes and consequences. Journal of the Geological Society, London 164, 1093–1108.

Collins, A., 1990. The 1-10 Spore Colour Index (SCI) scale: a universally applicable colour maturation scale, based on graded, picked palynomorphs. Mededelingen Rijks Geologische Dienst., 45, pp. 39–47.

Comas-Rengifo, M.J., Duarte, L.V., Félix, F.F., García Joral, F., Goy, A., Rocha, R.B., 2015. Latest Pliensbachian-Early Toarcian brachiopod assemblages from the Peniche section (Portugal) and their correlation. Episodes 38, 2–8.

Comas-Rengifo, M.J., Duarte, L.V., García Joral, F., Goy, A., 2013. Los braquiópodos del Toarciense Inferior (Jurássico) en el área de Rabaçal-Condeixa (Portugal): distribución estratigráfica y paleobiogeografia. Comunicações Geológicas 100 (Especial I), 37–42.

Comas-Rengifo, M.J., Duarte, L.V., Felix, F.F., Goy, A., Paredes, R., Silva, R. L., 2016. Amaltheidae e Hildoceratidae (ammonitina) del Pliensbachiense Superior (Cronozona Spinatum) en las cuencas septentrionales de la Península Ibérica, in: Meléndez, G., Núñez, A., Tomás, M. (Eds.), Actas de las XXXII Jornadas de la Sociedad Española de Paleontología. Cuadernos del Museo Geominero nº 20. Instituto Geológico y Minero de España, Madrid, pp. 47-52.

Correia, V.F., Riding, J.B., Fernandes, P., Duarte, L.V., Pereira, Z. 2017a. The palynology of the lower and middle Toarcian (Lower Jurassic) in the northern Lusitanian Basin, western Portugal. Review of Palaeobotany and Palynology 237, 75–95.

Correia, V.F., Riding, J.B., Duarte, L.V., Fernandes, P., Pereira, Z. 2017b. The palynological response to the Toarcian Oceanic Anoxic Event (Early Jurassic) at Peniche, Lusitanian Basin, western Portugal. Marine Micropaleontology, 137, 46-63.

Correia, V.F., Riding, J.B., Duarte, L.V., Fernandes, P., Pereira, Z. 2018. The Early Jurassic palynostratigraphy of the Lusitanian Basin, western Portugal. Geobios, in press.

Dale, B., 1983. Dinoflagellate resting cysts: ‘benthic plankton’. In: Fryxell, G.A. (Ed.), Survival strategies of the algae. Cambridge University Press, pp. 69–136.

Dale, B., 1996. Dinoflagellate cyst ecology: modeling and geological applications. In: Jansonius, J., McGregor, D.C. (Eds.), Palynology: Principles and Applications, 3. American Association of Stratigraphic Palynologists Foundation, Dallas, pp. 1249–1275.

Danise, S., Twitchett, R.J., Little, C.T.S., Clémence, M.E., 2013. Marine benthic community dynamics through the Early Toarcian (Early Jurassic) global warming event. PLoS One 8, e56255, http://dx.doi.org/10.1371/journal.pone.0056255.

Davey, R.J., Riley, L.A. 1978. Late and Middle Jurassic dinoflagellate cysts, in: Thusu, B. (Ed.), Distribution of biostratigraphically diagnostic dinoflagellate cysts and miospores from the northwest European continental shelf and adjacent areas. Continental Shelf Institute Publication 100, pp. 51–45.

Davies, E.H., 1985. The miospore and dinoflagellate cyst Oppel-Zonation of the Lias of Portugal. Palynology 9, 105–132.

de Vains, G., 1988. Étude palynologique préliminaire de l'Hettangien à l'Aalénien du Quercy (France). Bulletin des Centres de Recherches Exploration-Production Elf-Aquitaine 12, 451–469.

Duarte, L.V., 1995. O Toarciano da Bacia Lusitaniana. Estratigrafia e Evolução Sedimentogénica. Unpublished PhD thesis, Universidade de Coimbra, Portugal, 349 pp.

Duarte, L.V., 1997. Facies analysis and sequential evolution of the Toarcian-Lower Aalenian series in the Lusitanian Basin (Portugal). Comunicações do Instituto Geológico e Mineiro 83, 65-94.

Duarte, L.V., 2007. Lithostratigraphy, sequence stratigraphy and depositional setting of the Pliensbachian and Toarcian series in the Lusitanian Basin, Portugal. In: Rocha, R.B. (Ed.), The Peniche Section (Portugal). Contributions to the Definition of the Toarcian GSSP. International Subcommission on Jurassic Stratigraphy. ISBN: 978972-8893-14-9, pp. 17–23.

Duarte, L.V., Soares, A.F., 2002. Litostratigrafia das séries margo-calcárias do Jurássico inferior da Bacia Lusitânica (Portugal). Comunicações do Instituto Geológico e Mineiro 89, 135–154.

Duarte, L. V., Krautter, M., Soares, A. F., 2001. Bioconstructions à spongiaires siliceux dans le Lias terminal du Bassin lusitanien (Portugal): stratigraphie, sédimentologie et signification paléogéographique. Bulletin Société Géologique de France 172(5), 637-646.

Duarte, L.V., Perilli, N., Dino, R., Rodrigues, R., Paredes, R., 2004. Lower to Middle Toarcian from the Coimbra region (Lusitanian Basin, Portugal): sequence

stratigraphy, calcareous nannofossils and stable-isotope evolution. Rivista Italiana di Paleontologia e Stratigrafia 100, 115–127.

Duarte, LV., Oliveira, L.C., Rodrigues, R., 2007. Carbon isotopes as a sequence stratigraphic tool: examples from Lower and Middle Toarcian marly limestones of Portugal. Boletim Geologico Minero de España, 118, 3-17.

Duarte, L.V., Silva,. RL., Oliveira, L.C.V., Comas-Rengifo, M.J., Silva, F., 2010. Organic-rich facies in the Sinemurian and Pliensbachian of the Lusitanian Basin, Portugal: total organic carbon distribution and relation to transgressive–regressive facies cycles. Geologica Acta 8, 325–340.

Duarte, L.V., Silva, R.L., Mendonça Filho, J.G., Poças Ribeiro, N., Chagas, R.B.A., 2012. High resolution stratigraphy, palynofacies and source rock potential of the Água de Madeiros Formation (Lower Jurassic), Lusitanian Basin, Portugal. Journal of Petroleum Geology 35 (2), 105–126.

Duarte, L.V., Comas-Rengifo, M.J., Silva, R.L., Paredes, R., Goy, A., 2014a. Carbon isotope stratigraphy and ammonite biochronostratigraphy across the Sinemurian-Pliensbachian boundary in the western Iberian margin. Bulletin of Geosciences 89, 719–738.

Duarte, L. V., Silva, R. L., Mendonça Filho, J. G., Azerêdo, A. C., Cabral, M. C., Comas-Rengifo, M. J., Correia, G., Ferreira, R., Loureiro, I. M., Paredes, R., Pereira, A., Ribeiro, N. P., 2014b. Advances in the Stratigraphy and Geochemistry of the Organic-Rich Lower Jurassic Series of the Lusitanian Basin (Portugal), in: Rocha, R.B., Pais, J., Kullberg, J.C., Finney, S. (Eds.), STRATI 2013. Springer International Publishing, pp. 841 - 846., doi: 10.1007/978-3-319-04364-7_158.

Duarte, L.V, Silva, R.L., Félix, F., Comas-Rengifo. M.J., Rocha, R.B., Mattioli, E., Paredes, R., Mendonça Filho, J. G., Cabral, M.C., 2017. The Jurassic of the Peniche Peninsula (Portugal): scientific, educational and science popularization relevance. Revista de la Sociedad Geológica de España 30(1), 55–70.

Elmi, S., 2006. Pliensbachian/Toarcian boundary: the proposed GSSP of Peniche (Portugal). Volumina Jurassica 4, 5–16.

Elmi, S., Rocha, R.B., Mouterde, R., 1988. Sédimentation pelagique et encroûtements cryptalgaires: les calcaires grumeleux du Carixien portugais. Ciências da Terra 9, 69–90.

Elmi, S., Goy, A., Mouterde, R., Rivas, P., Rocha, R., 1989. Correlaciones bioestratigráficas en el Toarciense de la Peninsula Iberica. Cuadernos de Geologia Iberica 13, 265–277.

Eshet, Y., Rampino, M.R., Visscher, H., 1995. Fungal event and palynological record of ecological crisis and recovery across the Permian-Triassic boundary. Geology 23, 967–970.

Evitt, W.R., 1962. Dinoflagellate synonyms: *Nannoceratopsis deflandrei* Evitt junior to *N.? gracilis* Alberti. Journal of Paleontology 36, 1129–1130.

Evitt, W.R., 1985. Sporopollenin dinoflagellate cysts. Their morphology and interpretation. American Association of Stratigraphic Palynologists, Dallas, 333 p.

Falkowski, P.G., Katz, M.E., Knoll, A.H., Quigg, A., Raven, J.A., Schofield, O., Taylor, F.J.R., 2004. The evolution of modern eukaryotic phytoplankton. Science 305, 354–360.

Feist-Burkhardt, S., 1990. Dinoflagellate cyst assemblages from the Hausen coreholes (Aalenian to early Bajocian), southwest Germany. Bulletin des Centres de Recherches Exploration-Production Elf-Aquitaine 14, 611–633.

Feist-Burkhardt, S., Wille, W., 1992. Jurassic palynology in southwest Germany - state of the art. Cahiers de Micropaléontologie N.S. 7, 141–156.

Feist-Burkhardt, S., Monteil, E., 1997. Dinoflagellate cysts from the Bajocian stratotype (Calvados, Normandy, western France). Bulletin des Centres de Recherches Exploration-Production Elf-Aquitaine 21, 3–105.

Feist-Burkhardt, S., Pross, J., 2010. Dinoflagellate cyst biostratigraphy of the Opalinuston Formation (Middle Jurassic) in the Aalenian type area in southwest Germany and north Switzerland. Lethaia 43, 10–31.

Feist-Burkhardt, S., Götz, A.E., 2016. Ultra-high-resolution palynostratigraphy of the Early Bajocian Sauzei and Humphriesianum Zones (Middle Jurassic) from outcrop sections in the Upper Rhine Area, southwest Germany. In: Montenari, M. (editor), Stratigraphy and Timescales, First Edition, Academic Press, 325–392.

Fensome, R.A., Williams, G.L., 2004. The Lentin and Williams index of fossil dinoflagellates 2004 edition. American Association of Stratigraphic Palynologists, Contributions Series 42, 909 pp.

Fensome, R.A., Riding, J.B., Taylor, J.R., 1996. Dinoflagellates. In: Jansonius, J. & McGregor, D.C. (Eds.). Palynology: Principles and Applications; American Association of Stratigraphic Palynologists Foundation, Salt Lake City Foundation 1, 107-169 pp.

Fenton, J.P.G., Riding, J.B., 1987. *Kekryphalospora distincta* gen. et sp. nov., a trilete spore from the Lower and Middle Jurassic of north-west Europe. Pollen et Spores 29, 427–434.

Fenton, J.P.G., Neves, R., Piel, K.M., 1980. Dinoflagellate cysts and acritarchs from the Upper Bajocian to Middle Bathonian strata of central and southern England. Palaeontology 23, 151–170.

Fernandes, P.M.C. 2000. Investigation of the stratigraphy, maturation and source-rock potential of Carboniferous black shales in the Dublin Basin. Unpublished PhD thesis, University of Dublin, Trinity College**,** Ireland, 218 pp.

Fernandes, P., Rodrigues B., Borges, M., Matos, V., Clayton, G., 2013. Organic maturation of the Algarve Basin (southern Portugal) and its bearing on thermal history and hydrocarbon exploration. Marine and Petreoleum Geology 46, 210–233.

Fernández-López, S., Henriques, M.H.P., Mouterde, R., Rocha, R., Sadki, D., 1988. Le Bajocien inférieur du Cap Mondego (Portugal). Essai de biozonation. In: Rocha, R.B., Soares, A.F. (Eds.), Second International Symposium on Jurassic Stratigraphy, Lisbon, Proceedings, 301–313.

Fernández-López, S., Henriques, H., Mangold, C., 2006. Ammonite succession at the Bajocian/Bathonian boundary in the Cabo Mondego region (Portugal). Lethaia 39, 253–264.

Fernández-López, S., Pavia, G., Erba, E., Guiomar, M., Henriques, M.H., Lanza, R., Mangold, C., Olivero, D., Tiraboschi, D., 2009a. Formal proposal for the Bathonian GSSP (Middle Jurassic) in the Ravin du Bès (Bas-Auran, SE France). Swiss Journal of Geosciences 102, 271–295.

Fernández-López, S., Pavia, G., Erba, E., Guiomar, M., Henriques, M.H., Lanza, R., Mangold, C., Olivero, D., Tiraboschi, D., 2009b. The Global Boundary Stratotype Section and Point (GSSP) for base of the Bathonian Stage (Middle Jurassic), Ravin du Bès Section, SE France. Episodes 32, 222–248.

Ferreira, J., Mattioli, E., Pittet, B., Cachão, M., Spangenberg, J.E., 2015. Palaeoecological insights on Toarcian and lower Aalenian calcareous nannofossils from the Lusitanian Basin (Portugal). Palaeogeography, Palaeoclimatology, Palaeoecology, 436, 245–262.

Figueiredo, V. 2009. Foraminíferos da passagem Jurássico Inferior–Médio do Sector Central da Bacia Lusitânica: o perfil de Zambujal de Alcaria. Unpublished M.Sc. thesis, Universidade de Coimbra, Portugal, 88 pp.

Figueiredo, V., Canales, M.L.,. Henriques, M.H. 2014. Foraminifera of the Toarcian-Aalenian boundary from the Lusitanian Basin (Portugal): a paleoecological analysis. Journal of Iberian Geology 40 (3), 409-450.

Filatoff, J., 1975. Jurassic palynology of the Perth Basin, Western Australia. Palaeontographica Abteilung B 154, 1–120.

Fraguas, A., Comas-Rengifo, M.J., Gómez, J.J., Goy, A., 2012. The calcareous nannofossil crisis in Northern Spain (Asturias province) linked to the Early Toarcian warming-driven mass extinction. Marine Micropaleontology 94–95, 58–71.

Francis, J.E., 1983. The dominant conifer of the Jurassic Purbeck Formation, England. Palaeontology 26, 277–294.

Gedl, P., 2008. Organic-walled dinoflagellate cyst stratigraphy of dark Middle Jurassic marine deposits of the Pieniny Klippen Belt, West Carpathians. Studia Geologica Polonica 131, 7–227.

Gedl, P., Józsa, Š., 2015. Early?–Middle Jurassic dinoflagellate cysts and foraminifera from the dark shale of the Pieniny Klippen Belt between Jarabina and Litmanová (Slovakia): age and palaeonvironment. Annales Societatis Geologorum Poloniae 85, 91–122.

Gómez, J.J., Fernández-López, S.R., 2006. The Iberian Middle Jurassic carbonate-platform system: Synthesis of the palaeogeographic elements of its eastern margin (Spain). Palaeogeography, Palaeoclimatology, Palaeoecology 236, 190–205.

Gómez, J.J., Arias, C., 2010. Rapid warming and ostracods mass extinction at the Lower Toarcian (Jurassic) of central Spain. Marine. Micropaleontology 74, 119–135.

Goodhue, R., Clayton, G., 2010. Palynomorph Darkness Index (PDI) – a new technique for assessing thermal maturity. Palynology 34, 147–156.

Goryacheva, A. A., 2017.Lower Jurassic Palynostratigraphy of Eastern Siberia. Stratigraphy and Geological Correlation, 25(3), 265–295.

Gowland, S., Riding, J.B., 1991. Stratigraphy, sedimentology and palaeontology of the Scarborough Formation (Middle Jurassic) at Hundale Point, North Yorkshire. Proceedings of the Yorkshire Geological Society 48, 375–392.

Guy-Ohlson, D., 1988a. Toarcian palynostratigraphical correlations within and between different biogeographical provinces. Second International Symposium on Jurassic Stratigraphy, Lisbon, Proceedings, 807–820.

Guy-Ohlson, D., 1988b. The use of dispersed palynomorphs referable to the formgenus Chasmatosporites (Nilsson) Pocock et Jansonius in Jurassic biostratigraphy. Actas IV Congresso Argentino de Paleontologia y Bioestratigraphica, Mendoza, Noviembre 1986 3:5–13.

Guy-Ohlson, D., 1989. Spore and pollen assemblage zonation of Swedish Bajocian and Bathonian sediments. In: Batten, D.J., Keen, M.C. (Eds), Northwest European micropalaeontology and palynology. British Micropalaeontological Society Series. Ellis Horwood Limited, Chichester, p. 70–91.

Hallam, A., 1969. Faunal realms and facies in the Jurassic. Palaeontology 12, 1–12.

Harries, P.J., Little, C.T.S., 1999. The early Toarcian (Early Jurassic) and the Cenomanian–Turonian (Late Cretaceous) mass extinctions: similarities and contrasts. Palaeogeography, Palaeoclimatology, Palaeoecology 154, 39–66.

Hart, M.B., Hylton, M.D., Oxford, M.J., Price, G.D., Hudson, W., Smart, C.W., 2003. The search for the origin of the planktic foraminifera. Journal of the Geological Society 160, 341–343.

Head, M.J., Harland, R., Matthiessen, J., 2001. Cold marine indicators of the late Quaternary: The new dinoflagellate cyst genus *Islandinium* and related morphotypes. Journal of Quaternary Science 16, 621–636.

Heimhofer, U.,Hochuli, P.A., Burla, S. and Weissert, H., 2007. New records of Early Creteaceous angiosperm pollen from Portuguese coastal deposits: Implications for the timing of the early angiosperm radiation. Review of Paleobotany and Palynology 144, 39-76.

Heimhofer, U.,Hochuli, P.A., Burla, S., Oberli, F., Adatte, T., Dinis, J., Weissert, H., 2012. Climate and vegetation history of Western Portugal inferred from Albian near-shore deposits (Galé Formation, Lusitanian Basin). Geological Magazine 149, 1046-1064.

Helby, R., Morgan, R., Partridge, A.D., 1987. A palynological zonation of the Australian Mesozoic. Memoir of the Association of Australasian Palaeontologists 4, 1–94.

Hennissen, J.A.I., Head, M.J., De Schepper, S., Groeneveld, J., 2017. Dinoflagellate cyst paleoecology during the Pliocene–Pleistocene climatic transition in the North Atlantic. Palaeogeography, Palaeoclimatology, Palaeoecology 470, 81–108.

Henriques, M.H., 1992. Biostratigrafia e paleontologia (Ammonoidea) do Aaleniano em Portugal (Sector Setentrional da Bacia Lusitaniana). Unpublished PhD Thesis, Universidade de Coimbra, Portugal, 301 pp.

Henriques, M.H., 1995. Les faunes d'ammonites de l'Aalénien Portugais: composition et implications paléobiogéographiques. In: Gayet, M., Courtinat, B. (Eds.), First European Palaeontological Congress, Lyon, 1993. Geobios, Mémoire Spécial 18, 229–235.

Henriques, M.H., Canales, M.L., 2013. Ammonite-benthic foraminifera turnovers across the Lower-Middle Jurassic transition in the Lusitanian Basin (Portugal). Geobios 46, 395–408.

Henriques, M.H., Gardin, S., Gomes, C.R., Soares, A.F., Rocha, R.B., Marques, J.F., Lapa, M.R., Montenegro, J.D., 1994. The Aalenian–Bajocian boundary at Cabo Mondego (Portugal). Miscellanea del Servizio Geologico Nazionale 5, 63–77.

Henriques, M.H., Canales, M.L., Figueiredo, V., García-Frank, A., Hernández, L., Silva, S., Ureta, S., 2014. Biostratigrafia integrada (ammonoidea, foraminiferida) da passagem Jurássico Inferior-Médio na Península Ibérica: resultados preliminares. Comunicações Geológicas 101 (Especial I), 443–446.

Henriques, M.H., Canales, M.L., Silva, S.C., Figueiredo, V., 2016. Integrated biostratigraphy (Ammonoidea, Foraminiferida) of the Aalenian of the Lusitanian Basin (Portugal): A Synthesis. Episodes 39(3), 482-490.

Hesselbo, S.P., Pieńkowski, G., 2011. Stepwise atmospheric carbon-isotope excursion during the Toarcian Oceanic Anoxic Event (Early Jurassic, Polish Basin). Earth and Planetary Science Letters 301, 365–372.

Hesselbo, S.P., Gröcke, D.R., Jenkyns, H.C., Bjerrum, C.J., Farrimond, P., Morgans Bell, H.S., Green, O.R., 2000. Massive dissociation of gas hydrate during a Jurassic oceanic anoxic event. Nature 406, 392–395.

Hesselbo, S.P., Jenkyns, H.C., Duarte, L.V., Oliveira, L.C.V., 2007. Carbon-isotope record of the Early Jurassic (Toarcian) Oceanic Anoxic Event from fossil wood and marine carbonate (Lusitanian Basin, Portugal). Earth and Planetary Science Letters 253, 455–470.

Ilyina, V.I., Kul'kova, I.A., Lebedeva, N.K., 1994. Microphytofossils and detail stratigraphy of marine Mesozoic and Cenozoic of Siberia. Russian Academy of Sciences, Siberian Branch, United Institute of Geology, Geophysics and Mineralogy, Transactions 818, 192 pp.

Izumi, K., Miyaji, T., Tanabe, K., 2012. Early Toarcian (Early Jurassic) oceanic anoxic event recorded in the shelf deposits in the northwestern Panthalassa: Evidence from the Nishinakayama Formation in the Toyora area, west Japan. Palaeogeography, Palaeoclimatology, Palaeoecology 315–316, 100–108.

Jan du Chêne, R., Fauconnier, D.C., Fenton, J.P.G., 1985. Problèmes taxonomiques liés a la révision de l'espèce "*Gonyaulax*" *cornigera* Valensi, 1953, kyste fossile de dinoflagellé Revue de Micropaléontologie 28, 109–124.

Jenkyns, H.C., 2010. Geochemistry of oceanic anoxic events, Geochemistry Geophysics Geosystems 11, Q03004, doi:10.1029/2009GC002788.

Kemp, D.B., Coe, A.L., Cohen, A.S., Schwark, L., 2005. Astronomical pacing of methane release in the Early Jurassic period. Nature 437, 396–399.

Kender, S., Stephenson, M.H., Riding, J.B., Leng, M.J., Knox, R.W.O'B., Peck, V.L., Kendrick, C.P., Ellis, M.A., Vane, C.H., Jamieson, R., 2012. Marine and terrestrial environmental changes in NW Europe preceding carbon release at the Paleocene–Eocene transition. Earth and Planetary Science Letters 353–354, 108–120.

Koppelhus, E.B., Nielsen, L.H., 1994. Palynostratigraphy and palaeoenvironments of the Lower to Middle Jurassic Bagå Formation of Bornholm, Denmark. Palynology 18, 139–194.

Korte, C., Hesselbo, S.P., 2011. Shallow marine carbon and oxygen isotope and elemental records indicate icehouse-greenhouse cycles during the Early Jurassic. Paleoceanography 26, PA4219.

Korte, C., Hesselbo, S.P., Ullmann, C.V., Dietl, G., Ruhl, M., Schweigert, G., 2015. Jurassic climate mode governed by ocean gateway. Nature Communications 6:10015, doi: 10.1038/ncomms10015.

Kremp, A., Anderson, D.M., 2000. Factors regulating germination of resting cysts of the spring bloom dinoflagellate *Scrippsiella hangoei* from the northern Baltic Sea. Journal of Plankton Research 22, 1311–1327.

Kullberg, J.C., Rocha, R.B., Soares, A.F., Rey, J., Terrinha, P., Azerêdo, A.C., Callapez, P., Duarte, L.V., Kullberg, M.C., Martins, L., Miranda, J.R., Alves, C., Mata, J., Madeira, J., Mateus, O., Moreira, M., Nogueira, C.R., 2013. A Bacia Lusitaniana: estratigrafia, paleogeografia e tectónica. In: Geologia de Portugal 2, 195–347.

Littler, K., Hesselbo, S.P., Jenkyns, H.C., 2010. A carbon-isotope perturbation at the Pliensbachian–Toarcian boundary: evidence from the Lias Group, NE England. Geological Magazine 147, 181–192.

Loh, H., Maul, B., Prauss, M., Riegel, W., 1986. Primary production, maceral formation and carbonate species in the Posidonia Shale of NW Germany. Mitteilungen des Geologisch-Paläontologischen Institüts der Universität Hamburg 60, 397–421.

MacRae, R.A., Fensome, R.A., Williams, G.L., 1996. Fossil dinoflagellate diversity, originations, and extinctions and their significance. Canadian Journal of Botany 74, 1687–1694.

Mädler, K., 1968. Die figurierten organischen Bestandteile der Posidonienschiefer. Beihefte zum Geologischen Jahrbuch 58, 287–406.

Mantle, D.J., Riding, J.B., 2012. Palynology of the Middle Jurassic (Bajocian-Bathonian) *Wanaea verrucosa* dinoflagellate cyst zone of the North West Shelf of Australia. Review of Palaeobotany and Palynology 180, 41–78.

Martindale, R.C., Aberhan, M., 2017. Response of microbenthic communities to the Toarcian Oceanic Anoxic Event in northeastern Panthalassa (Ya Ha Tinda, Alberta, Canada). Palaeogeography, Palaeoclimatology, Palaeoecology 478, 103–120.

Mattioli, E., Pittet, B., 2004. Spatial and temporal distribution of calcareous nannofossils along a proximal-distal transect in the Lower Jurassic of the Umbria-Marche Basin (central Italy). Palaeogeography, Palaeoclimatology, Palaeoecology 205, 295–316.

Mattioli, E., Pittet, B., Suan, G., Mailliot, S., 2008. Calcareous nannoplankton changes across the early Toarcian oceanic anoxic event in the western Tethys. Paleoceanography 23, PA3208, doi:10.1029/2007PA001435.

Mattioli, E., Plancq, J., Boussaha, M., Duarte, L.V., Pittet, B., 2013. Calcareous nannofossil biostratigraphy: new data from the Lower Jurassic of the Lusitanian Basin. Comunicações Geológicas, 100 (Especial I), 69–76.

McElwain, J.C., Wade-Murphy, J., Hesselbo, S.P., 2005. Changes in carbon dioxide during an oceanic anoxic event linked to intrusion into Gondwana coals. Nature 435, 459–482.

Mendes, M.M., Dinis, J., Pais, J. & Friis, E.M., 2011. Early Cretaceous flora from Vale Painho (Lusitanian Basin, western Portugal): An integrated palynological and mesofossil study. Review of Palaeobotany and Palynology, 166, 152-162.

Mohr, B.A.R., Schmidt, D., 1988. The Oxfordian/Kimmeridgian boundary in the region of Porto de Mós (Central Portugal): stratigraphy, facies and palynology. Neus Jahrbuch für Geologie und Paläontologie Abhandlungen 176, 245–267.

Morbey, S.J., 1978. Late Triassic and Early Jurassic subsurface palynostratigraphy in northwestern Europe. Palinologia número extraordinario 1, 355–365.

Morbey, S.J., Dunay, R.E., 1978. Early Jurassic to Late Triassic dinoflagellate cysts and miospores. In: Thusu, B., (Ed.), Distribution of biostratigraphically diagnostic dinoflagellate cysts and miospores from the northwest European continental shelf and adjacent areas. Continental Shelf Institute Publication 100, 47–59.

Morgenroth, P., 1970. Dinoflagellate cysts from the Lias Delta of Lühnde/Germany. Neues Jahrbuch für Geologie und Paläontologie Abhandlungen 136, 345–359.

Mouterde, R., 1955. Le Lias de Peniche. Comunicações dos Serviços Geológicas de Portugal 37, 87–115.

Mouterde, R., Rocha, R.B., Ruget, 1978. Stratigraphie et faune du Lias et de la base du Dogger au Nord du Mondego (Quaios et Brenha). Comunicações dos Serviços Geológicas de Portugal 63, 83–103.

Mouterde, R., Rocha, R.B., Ruget, C., Tintan, H., 1979. Faciès, biostratigraphie et paléogéographie du Jurassique portugais. Ciências da Terra, Universidade Nova de Lisboa 5, 29–52.

Mouterde, R., Rocha, R.B., Ruget, Ch., 1980. Stratigraphie et faune du Lias et de la base du Dogger au Nord du Mondego (Quiaios et Brenha) (parties 2 à 4). Comunicações dos Serviços Geológicos de Portugal, 66, 79-97.

Mouterde, R., Ruget, C., Moitinho de Almeida, F., 1964-1965. Coupe du Lias au Sud de Condeixa. Comunicações dos Serviços Geológicas de Portugal 48, 61–91.

Oliveira, L.C.V., Dino, R., Duarte, L.V., Perilli, N., 2007a. Calcareous nannofossils and palynomorphs from Pliensbachian-Toarcian boundary in Lusitanian Basin, Portugal. Revista Brasileira de Paleontologia 10, 5–16.

Oliveira, L.C.V., Duarte, L.V., Lemos, V.B., Comas-Rengifo, M.J., Perilli, N., 2007b. Bioestratigrafia de nanofósseis calcários e correlação com as zonas de amonites do Pliensbaquiano–Toarciano basal (Jurássico inferior) de Peniche (Bacia Lusitânica, Portugal), in: Carvalho, I.S., Cassab, R.C.T., Schwanke, C., Carvalho, M.A., Fernandes, A.C.S., Rodrigues, M.A.C., Carvalho, M.S.S., Arai, M., Oliveira, M.E.Q. (Eds.), Paleontologia: Cenários de Vida. Proceedings of XIX Congresso Brasileiro de Paleontologia, Búzios (Brazil), Editora Interciência, pp. 411–420.

Page, K.N., 2003. The Lower Jurassic of Europe: its subdivision and correlation. Geological Survey of Denmark and Greenland Bulletin 1: 23–59.

Pavia, G., Enay, R., 1997. Definition of the Aalenian–Bajocian stage boundary. Episodes 20, 16–22.

Paredes, R., Comas-Rengifo, M.J., Duarte, L.V., 2016. Passagem Pliensbaquiano–Toarciano: a diversidade de macroinvertebrados antes da extinção, in: Duarte, L.V., Sêco, S. (Eds.), "O Jurássico da região de Penela: novos avanços no conhecimento estratigráfico", pp. 30-34. ISBN (digital): 978-989-97997-3-8.

Perilli, N., Duarte, L.V., 2006. Toarcian nannobiohorizons from Lusitanian Basin (Portugal) and their calibration against amonite zones. Revista Italiana di Paleontologia e Stratigrafia 112, 417–434.

Peti, L., Thibault, N., 2017. Abundance and size changes in the calcareous nannofossil *Schizosphaerella* — Relation to sea-level, the carbonate factory and palaeoenvironmental change from the Sinemurian to earliest Toarcian of the Paris Basin. Palaeogeography, Palaeoclimatology, Palaeoecology 485, 271–282.

Phelps, M., 1985. A refined ammonite biostratigraphy for the Middle and Upper Carixian (Ibex and Davoei zones, Lower Jurassic) in North-West Europe and stratigraphical details of the Carixian–Domerian boundary. Geobios 18, 321–362.

Piel, K.M., Evitt, W.R., 1980. Paratabulation in the Jurassic dinoflagellate genus *Nannoceratopsis* and a comparison with modern taxa. Palynology 4, 79–104.

Pinto, S., 2008. Ostracodos do Toarciano da Bacia Lusitânica (Peniche e Alvaiázare) – Sistemática, Aspectos biosestratigráficos, paleoecológicos e palaebiogeográficos. Unpublished Master's Thesis, Universidade de Lisboa, Portugal, 174 pp.

Pittet, B., Suan, G., Lenoir, F., Duarte, L.V., Mattioli, E., 2014. Carbon isotope evidence for sedimentary discontinuities in the Lower Toarcian of the Lusitanian Basin (Portugal): Sea level change at the onset of the Oceanic Anoxic Event. Sedimentary Geology 303, 1–14.

Plancq, J., Mattioli, E., Pittet, B., Baudin, F., Duarte, L.V., Boussaha, M., Grossi, V., 2016. A calcareous nannofossil and organic geochemical study of marine palaeoenvironmental changes across the Sinemurian/Pliensbachian (early Jurassic, 191 Ma) in Portugal. Palaeogeography, Palaeoclimatology, Palaeoecology 449, 1–12.

Poças Ribeiro, N., Mendonça Filho, J.G., Duarte, L.V., Silva, R.L., Mendonça, J.O., Silva, T.F., 2013. Palynofacies and organic geochemistry of the Sinemurian carbonate deposits in the western Lusitanian Basin (Portugal): Coimbra and Água de Madeiros formations. International Journal of Coal Geology 111, 37–52.

Pocock, S.J., Jansonius, J., 1961. The pollen genus *Classopollis* Pflug, 1953. Micropaleontology 7, 439–449.

Poulsen, N.E., 1996. Dinoflagellate cysts from marine Jurassic deposits of Denmark and Poland. American Association of Stratigraphic Palynologists Contributions Series 31, 227 pp.

Poulsen, N.E., Riding, J.B., 2003. The Jurassic dinoflagellate cyst zonation of Subboreal Northwest Europe. Geological Survey of Denmark and Greenland Bulletin 1, 115–144.

Prauss, M., 1989. Dinozysten-stratigraphie und Palynofazies im Oberen Lias und Dogger von NW-Deutschland. Palaeontographica Abteilung B 214, 1–124.

Prauss, M., 1996. The Lower Toarcian Posidonia Shale of Grimmen, Northeast Germany. Implications from the palynological analysis of a near-shore section. Neues Jahrbuch für Geologie und Paläontologie Abhandlungen 200, 107–132.

Prauss, M., 2006. The Cenomanian/Turonian Boundary Event (CTBE) at Wunstorf, north-west Germany, as reflected by marine palynology. Cretaceous Research 27, 872–886.

Prauss, M., Riegel, W., 1989. Evidence from phytoplankton associations for causes of black shale formation in epicontinental seas. Neues Jahrbuch für Geologie und Paläontologie Monatshefte 1989(11), 107–132.

Prauss, M., Ligouis, B., Luterbacher, H., 1991. Organic matter and palynomorphs in the 'Posidonienschiefer' (Toarcian, Lower Jurassic) of southern Germany. In: Tyson, R.V., Pearson, T.H., (editors), Modern and Ancient Continental Shelf Anoxia. Geological Society of London Special Publication 58, 335–351.

Quattrocchio, M.E., Volkheimer, W., Borromei, A.M., Martínez, M.A., 2011. Changes of the palynobiotas in the Mesozoic and Cenozoic of Patagonia: a review. Biological Journal of the Linnean Society 103, 380–396.

Rasmussen, E.S., Lomholt, S., Andersen, C., Vejbæk, O.V., 1998. Aspects of the structural evolution of the Lusitanian Basin in Portugal and the shelf and slope area offshore Portugal. Tectonophysics 300, 199–225.

Reggiani, L., Mattioli, E., Pittet, B., Duarte, L.V., Veiga de Oliveira, L.C., Comas-Rengifo, M.J., 2010. Pliensbachian (Early Jurassic) calcareous nannofossils from the Peniche section (Lusitanian Basin, Portugal): A clue for palaeoenvironmental reconstructions. Marine Micropaleontology 75, 1–16.

Reid, R.E.H., 1973. Origin of the Mesozoic 'Boreal' realm. Geological Magazine 110, 67–69.

Reis, R.P., Pimentel, N.L. & Garcia, A.J.V., 2010-2011. A Bacia Lusitânica (Portugal): análise estratigráfica e evolução geodinâmica. Boletim de Geociências da Petrobras, Rio de Janeiro 19(1/2), 23-52.

Reolid, M., Duarte, L.V., 2014. Sponge-microbialite buildups from the Toarcian of the Coimbra region (Northern Lusitanian Basin, Portugal): paleoecological and paleoenvironmental significance. Facies 60, 561–580.

Reolid, M., Nikitenko, B.L., Glinskikh, L., 2014. *Trochammina* as opportunist foraminifera in the Lower Jurassic from north Siberia. Polar Research 33, 21653.

Rey, J., Dinis, J.L., Callapez, P. & Cunha, P.P., 2006. Da rotura continental à margem passiva. Composição e evolução do Cretácico de Portugal. Lisboa: Ed. INETI, 75 pp.

Riding, J.B., 1984a. Dinoflagellate cyst range-top biostratigraphy of the uppermost Triassic to lowermost Cretaceous of northwest Europe. Palynology 8, 195–210.

Riding, J.B., 1984b. Observations on the Jurassic dinoflagellate cyst *Nannoceratopsis ambonis* Drugg, 1978. Journal of Micropalaeontology 3, 75–79.

Riding, J.B., 1984c. A palynological investigation of Toarcian to early Aalenian strata from the Blea Wyke area, Ravenscar, North Yorkshire. Proceedings of the Yorkshire Geological Society 46, 109–122.

Riding, J.B., 1987. Dinoflagellate cyst stratigraphy of the Nettleton Bottom Borehole (Jurassic: Hettangian to Kimmeridgian), Lincolnshire, England. Proceedings of the Yorkshire Geological Society 46, 231–266.

Riding, J.B., Thomas, J.E., 1992. Dinoflagellate cysts of the Jurassic System. In: Powell, A.J. (Ed.), A stratigraphic index of dinoflagellate cysts. British Micropalaeontological Society Publications Series. Chapman and Hall, London, pp. 7–97.

Riding, J.B., Hubbard, R.N.L.B., 1999. Jurassic (Toarcian to Kimmeridgian) dinoflagellate cysts and paleoclimates. Palynology 23, 15–30.

Riding, J.B., Helby, R., 2001. Early Jurassic (Toarcian) dinoflagellate cysts from the Timor Sea, Australia. Memoir of the Association of Australasian Palaeontologists 24, 1–32.

Riding, J.B., Warny, S. (Eds.), 2008. Palynological Techniques. Second Edition, American Association of Stratigraphic Palynologists Foundation, Dallas, Texas 137 p.

Riding, J.B., Michoux, D., 2013. Further observations on the Jurassic dinoflagellate cyst *Gonyaulacysta dentata* (Raynaud 1978) Lentin & Vozzhennikova 1990 emended Riding 2012. Review of Palaeobotany and Palynology 196, 51–56.

Riding, J.B., Penn, I.E., Woollam, R., 1985. Dinoflagellate cysts from the type area of the Bathonian Stage (Middle Jurassic; southwest England). Review of Palaeobotany and Palynology 45, 149–169.

Riding, J.B., Walton, W., Shaw, D., 1991. Toarcian to Bathonian (Jurassic) palynology of the Inner Hebrides, Northwest Scotland. Palynology 15, 115–179.

Riding, J.B., Fedorova, V.A., Ilyina, V.I., 1999. Jurassic and lowermost Cretaceous dinoflagellate cysts biostratigraphy of the Russian Platform and north Siberia, Russia. American Association of Stratigraphic Palynologists Contributions Series 36, 179 pp.

Riding, J.B., Mantle, D.J., Backhouse, J., 2010. A review of the chronostratigraphical ages of Middle to Late Jurassic dinoflagellate cyst biozones of the North West Shelf of Australia. Review of Palaeobotany and Palynology 162, 543–575.

Riding, J.B., Leng, M.J., Kender, S., Hesselbo, S.P., Feist-Burkhardt, S., 2013. Isotopic and palynological evidence for a new Early Jurassic environmental perturbation. Palaeogeography, Palaeoclimatology, Palaeoecology 374, 16–27.

Rita, P., Reolid, M., Duarte, L.V., 2016. Benthic foraminiferal assemblages record major environmental perturbations during the Late Pliensbachian–Early Toarcian interval in the Peniche GSSP, Portugal. Palaeogeography, Palaeoclimatology, Palaeoecology 454, 267–281.

Rocha, R.B., Mattioli, E., Duarte, L.V., Pittet, B., Elmi, S., Mouterde, R., Cabral, M.C., Comas-Rengifo, M.J., Gómez, J.J., Goy, A., Hesselbo, S.P., Jenkyns, H.C., Littler, K., Mailliot, S., de Oliveira, L.C.V., Osete, M.L., Perilli, N., Pinto, S., Ruget, C., Suan, G., 2016. Base of the Toarcian Stage of the Lower Jurassic defined by the Global Boundary Stratotype Section and Point (GSSP) at the Peniche section (Portugal). Episodes 39, 460–481.

Rodrigues, B., Duarte, L.V., Mendonça Filho, J.G., Santos, L.G., Oliveira, A.D., 2016. Evidence of terrestrial organic matter deposition across the early Toarcian recorded in the northern Lusitanian Basin, Portugal. International Journal of Coal Geology 168, 35–45.

Röhl, H.J., Schmid- Röhl, A., Wolfgang, O., Frimmel, A., Lorenz, S., 2001. The Posidonia Shale (Lower Toarcian) of SW-Germany: An oxygen-depleted ecosystem controlled by sea level and palaeoclimate. Palaeogeography, Palaeoclimatology, Palaeoecology 165, 27–52.

Sandoval, J., Henriques, M.H., Chandler, R.B., Ureta, S., 2012. Latest Toarcian–earliest Bajocian (Jurassic) Grammoceratinae (Hildoceratidae, Ammonitina) of the western Tethys: Their palaeobiogeographic and phylogenetic significance. Geobios 45, 109–119.

Segit, T., Matyja, B.A., Wierzbowski, A., 2015. The Middle Jurassic succession in the central sector of the Pieniny Klippen Belt (Sprzycne Creek): implications for the timing of the Czorsztyn Ridge development. Geologica Carpathica 66, 285–302.

Silva, R.L., Duarte, L. V., 2015. Organic matter production and preservation in the Lusitanian Basin (Portugal) and Pliensbachian climatic hot snaps. Global and Planetary Change 131, 24-34.

Silva, F., Duarte, L.V., Oliveira, L.C.V., Comas-Rengifo, M.J., Rodrigues, R., 2006. Vale das Fontes Formation in the northern sector of the Lusitanian Basin (Portugal): Characterization and preliminary evaluation of the Total Organic Carbon. Actas do VII Congresso Nacional de Geologia, Évora, 669–672.

Silva, R.L., Duarte, L.V., Comas-Rengifo, M.J., Mendonça Filho, J.G., Azerêdo, A.C., 2011. Update of the carbon and oxygen isotopic records of the Early–Late Pliensbachian (Early Jurassic, ~187 Ma): insights from the organic-rich hemipelagic series of the Lusitanian Basin (Portugal). Chemical Geology 283, 177–184.

Silva, R.L., Duarte, L.V., Comas-Rengifo, M.J., 2015. Facies and carbon isotope chemostratigraphy of lower Jurassic carbonate deposits, Lusitanian Basin (Portugal): implications and limitations to the application in sequence stratigraphic studies. in: Ramkumar, M. (Ed.), Chemostratigraphy: concepts, techniques, and applications. Elsevier, pp. 341-371, doi: 10.1016/B978-0-12-419968-2.00013-3

Silva, S., Henriques, M.H., Canales, M.L., 2014. Análise paleoecológica baseada em foraminíferos da passagem Aaleniano-Bajociano (Jurássico Médio) no perfil da Serra da Boa Viagem II (Portugal). Comunicações Geológicas 101, 573–576.

Silva, S., Henriques, M.H., Canales, M.L., 2015. High resolution ammonite-benthic foraminiferal biostratigraphy across the Aalenian-Bajocian boundary in the Lusitanian Basin (Portugal). Geological Journal 50(4), 477–496.

Simms, M.J., Chidlaw, N., Morton, N., Page, K.N., 2004. British Lower Jurassic Stratigraphy. Geological Conservation Review Series, No. 30, Joint Nature Conservation Committee, Peterborough, UK, 458 pp.

Sluijs, A., Pross, J., Brinkhuis, H., 2005. From greenhouse to icehouse; organic-walled dinoflagellate cysts as paleoenvironmental indicators in the Paleogene. Earth-Science Reviews 68, 281–315.

Smelror, M., Århus, N., Meléndez, G.L.M., Lardies, M.D., 1991. A reconnaissance study of Bathonian to Oxfordian (Jurassic) dinoflagellates and acritarchs from the Zaragoza region (NE Spain) and Figueira da Foz (Portugal). Revista Española de Micropaleontología 23, 47–82.

Soares, A.F., Rocha, R.B., Elmi, S., Henriques, M.H., Mouterde, R., Almeras, Y., Ruget, C., Marques, J., Duarte, L.V., Carapito, C., Kullberg, J.C., 1993. Le sous-bassin nord lusitanien (Portugal) du Trias au Jurassique moyen: histoire d'un "rift avorté". Comptes Rendus de l'Académie des Sciences de Paris 317, 1659–1666.

Srivastava, S.K., 1976. The fossil pollen genus *Classopollis*. Lethaia 9, 437–457.

Srivastava, S.K., 1987. Jurassic spore-pollen assemblages from Normandy (France) and Germany. Geobios 20, 5–79.

Srivastava, S.K., 2011. Spore-pollen biostratigraphy of the English Jurassic. Palaeontographica Abteilung B 285, 113–201.

Stach, E., Mackowsky, M. Th., Teichmuller, M., Taylor, G. H., Chandra, D. & Teichmuller, R., 1982. Stack's Textbook of Coal Petrology (3rd edition), Gebrüder Borntraeger (Berlin & Stuttgart), 535 pp.

Stancliffe, R.P.W., 1996. Microforaminferal linings. In: Jansonius, J., McGregor, D.C. (editors), Palynology: Principles and Applications. American Association of Stratigraphic Palynologists Foundation, Dallas 1, 373–379.

Staplin, F. L., 1969. Sedimentary organic matter, organic metamorphism and oil and gas occurrence. Bulletin of Canadian Petroleum Geology 17, 47–66.

Suárez-Ruiz, I., Flores, D. Mendonça Filho, J.G., Hackley, P.C. 2012. Review and update of the applications of organic petrology: Part 1, geological applications. International Journal of Coal Geology 99, 54–112.

Suan, G., Mattioli, E., Pittet, B., Mailliot, S., Lécuyer, C., 2008a. Evidence for major environmental perturbation prior to and during the Toarcian (Early Jurassic) oceanic anoxic event from the Lusitanian Basin, Portugal. Paleoceanography 23, PA1202, http://dx.doi.org/10.1029/2007PA001459.

Suan, G., Pittet, B., Bour, I., Mattioli, E., Duarte, L.V., Mailliot, S., 2008b. Duration of the Early Toarcian carbon isotope excursion deduced from spectral analysis: consequence for its possible causes. Earth and Planetary Science Letters 265, 666–679.

Suan, G., Mattioli, E., Pittet, B., Lécuyer, C., Suchéras-Marx, B., Duarte, L.V., Philippe, M., Reggiani, L., Martineau, F., 2010. Secular environmental precursors to Early Toarcian (Jurassic) extreme climate changes. Earth and Planetary Science Letters 290, 448–458.

Suan, G., Nikitenko, B.L., Rogov, M.A., Baudin, F., Spangenberg, J.E., Knyazev, V.G., Glinskikh, L.A., Goryacheva, A.A., Adatte, T., Riding, J.B., Föllmi, K.B., Pittet, B., Mattioli, E., Lécuyer, C., 2011. Polar record of Early Jurassic massive carbon injection. Earth and Planetary Science Letters 312, 102–113.

Suchéras-Marx, B., Guihou, A., Giraud, F., Lécuyer, C., Allemand, P., Pittet, B., Mattioli, E., 2012. Impact of the Middle Jurassic diversification of *Watznaueria* (coccolith-bearing algae) on the carbon cycle and $\delta^{13}C$ of bulk marine carbonates. Global and Planetary Change 86/87, 92–100.

Suchéras-Marx, B., Mattioli, E., Giraud, F., Escarguel, G., 2015. Paleoenvironmental and paleobiological origins of coccolithophorid genus *Watznaueria* emergence during the late Aalenian–early Bajocian. Palaios 41, 415–435.

Svensen, H., Planke, S., Chevallier, L., Malthe-Sorenssen, A., Corfu, F., Jamtvei, B., 2007. Hydrothemal venting of greenhouse gases triggering Early Jurassic global warming. Earth and Planetary Science Letters 256, 554–566.

Tappan, H., 1980. Green Algae: Prasinophyta, Chlorophyta, and Euglenophyta. In: The Paleobiology of Plant Protists. W.H. Freeman and Company, San Francisco, 804–912.

Taylor, F.J.R., Pollingher, U., 1987. Ecology of dinoflagellates. In: Taylor, F.J.R. (editor), The biology of dinoflagellates. Blackwell Scientific Publications, Oxford, 398–529.

Taylor, G.H., Teichmuller, M., Davis, A., Diessel, C.F.K., Littke, R., Robert, P., 1998. Organic Petrology. Gebrüder Borntraeger, Berlin. 704 pp.

Terrinha, P.A.G., Ribeiro, C., Kullberg, J.C., Lopes, C., Rocha, R.B., Ribeiro, A., 2002. Compressive episodes and faunal isolation during rifting in the Algarve and Lusitanian Basins, Southwest Iberia. Journal of Geology 110, 101–113.

Thierry, J., Barrier, E., 2000. Middle Toarcian. In: Dercourt, J., Gaetani, M., Vrielynck, B., Barrier, E., Biju-Duval, B., Brunet, M.F., Cadet, J.P., Crasquin, S., Sandulescu, M. (editors), Atlas Peri-Tethys, Palaeogeographic Maps. CCGM/CGMW, Paris, map 8.

Traverse, A., 2007. *Paleopalynology*, 2ª edição. In: Landman, N.H. & Jones, D.S. (eds.), Topics in Geobiology Series, American Association of Stratigraphic Palynologists Foundation, Springer, Dordrecht, 28, 814 pp.

Trincão, P.R., 1990. Esporos e polenes do Cretácico Inferior (Berriasiano – Aptiano). De Portugal: Paleontologia e Biostratigrafia. Unpublished PhD, Universidade Nova de Lisboa, 312 pp.

Turner, H.E., Gradstein, F.M., Gale, A.S., Watkins, D.K., 2017. The age of the Tojeira Formation (Late Jurassic, Early Kimmeridgian), of Montejunto, west-central Portugal. Swiss Journal of Palaeontology 136, 287–299.

Vakhrameev, V.A., 1981. Pollen *Classopollis*: indicator of Jurassic and Cretaceous climates. The Palaeobotanist 28–29, 301–307.

Valensi, L., 1947. Note préliminaire à une étude des microfossiles des silex jurassiques de la région de Poitiers. Comptes rendus hebdomadaires des séances de l'Académie des sciences 225, 816–818.

van de Schootbrugge, B., Bailey, T.R., Rosenthal, Y., Katz, M.E., Wright, J.D., Miller, K.G., Feist-Burkhardt, S., Falkowski, P.G., 2005. Early Jurassic climate change and the radiation of organic-walled phytoplankton in the Tethys Ocean. Paleobiology 31, 73–97.

van de Schootbrugge, B., Bachan, A., Suan, G., Richoz, S., Payne, J.L., 2013. Microbes, mud and methane: causes and consequences of recurrent Early Jurassic anoxia following the end-Triassic mass extinction. Palaeontology 56, 685–709.

van Erve, A., Mohr, B., 1988. Palynological investigations of the Late Jurassic microflora from the vertebrate locality at Guimarota coal mine (Leiria, Central

Portugal). Neues Jahrbuch für Geologie und Paläontologie Abhandlungen 4, 256–262.

Van Gizel, P., 1979. Manual of the techniques and some geological applications of fluorescence microscopy. American Association of Stratigraphical Palynologists Foundation, Dallas, 55 pp.

Van Helden, B.G.T., 1977. Correlation of microplankton assemblages with ammonite faunas from the Jurassic Wilkie Point Formation, Prince Patrick Island, District of Franklin. Geological Survey of Canada Paper 77-1B, 163–171.

Weiss, M., 1989. Die Sporenfloren aus Rät und Jura Südwest-Deutschlands und ihre Beziehung zur Ammoniten-Stratigraphie. Palaeontographica Abteilung B 215, 1–168.

Wiggan, N.J., Riding, J.B., Franz, M., 2017. Resolving the Middle Jurassic dinoflagellate radiation: The palynology of the Bajocian of Swabia, southwest Germany. Review of Palaeobotany and Palynology 238, 55–87.

Wille, W., 1982a. Evolution and ecology of Upper Liassic dinoflagellates from SW Germany. Neues Jahrbuch für Geologie und Paläontologie Abhandlungen 164, 74–82.

Wille, W., 1982b. Palynology of Upper Liassic bituminous shales (abstract). In: Einsele, G., Seilacher, A., (Eds.), Cyclic and event stratification. Springer-Verlag, Berlin, Heidelberg, New York, 505 pp.

Williams, G.L., Fensome, R.A., MacRae, R.A., 2017. The Lentin and Williams index of fossil dinoflagellates 2017 edition. American Association of Stratigraphic Palynologists, Contributions Series 48, 1097 pp.

Wilson, R.C.L., 1979. A Reconnaissance Study of Upper Jurassic Sediments of the Lusitanian Basin. Ciências da Terra 5, 53-84.

Wilson, R.C.L., Hiscott, R.N., Willis, M.G., Gradstein, F.M., 1989. The Lusitanian Basin of West-Central Portugal: Mesozoic and Tertiary tectonic, stratigraphic and subsidence history. AAPG Memoir 46, 341–362.

Wood, G.D., Gabriel, A.M., Lawson, J.C., 1996. Palynological techniques – processing and microscopy, in: Jansonius, J., McGregor, D.C., (Eds.), Palynology: Principles and Applications. American Association of Stratigraphic Palynologists Foundation, Dallas, 1, pp. 29–50.

Woollam, R., Riding, J.B., 1983. Dinoflagellate cyst zonation of the English Jurassic. Institute of Geological Sciences Report 83/2, 42 pp.

Wright, V.P., Wilson, R.C.L., 1984. A carbonate sub-marine fan sequence from the Jurassic of Portugal. Journal of Sedimentary Petrology 54, 394–412.

Xu, W., Ruhl, M., Jenkyns, H.C., Hesselbo, S.P., Riding, J.B., Selby, D., Naafs, B.D.A., Weijers, J.W.H., Pancost, R.D., Tegelaar, E.W., Idiz, E.F., 2017. Carbon sequestration in an expanded lake system during the Toarcian oceanic anoxic event. Nature Geoscience, doi: 10.1038/NGEO2871.

Yule, B., Roberts, S., Marshall, J.E.A., Milton, J.A., 1998. Quantitative spore colour measurement using colour image analysis. Organic Geochemistry 28 (3–4), 139–149.

Ziaja, J., 2006. Lower Jurassic spores and pollen grains from Odrowaz, Mesozoic margin of the Holy Cross Mountains, Poland. Acta Palaeobotanica 46, 3–83.

APPENDICES

Appendices

Appendix 1: list of palynomorphs

This is a list of all palynomorphs taxa which were recovered from the material studied herein, or mentioned in the text, with full author citations. The taxa are listed alphabetically in four groups. All dinoflagellate cyst taxa mentioned here, but not found in the material from the Lusitanian Basin are asterisked. References to the dinoflagellate cyst author citations can be found in Williams et al. (2017). Are also provided the reference to the plates where each taxon is illustrate in this work. Note the plates from the Appendix 3 are labelled with Roman numerals.

Dinoflagellate cysts:

Acanthaulax crispa (Wetzel 1967) Woollam & Riding 1983 [Plate XXI(4)]

Adnatosphaeridium? *caulleryi* (Deflandre 1939) Williams & Downie1969 [Plate XX(3,4)]

Bradleyella adela (Fenton et al. 1980) Woollam 1983 [Plate XXI(7)]

Chytroeisphaeridia chytroeides (Sarjeant 1962) Downie & Sarjeant 1965 [Plate 4.2(10), XIV]

**Ctenidodinium combazii* Dupin 1968

Ctenidodinium cornigerum (Valensi 1953) Jan du Chêne 1985 [Plate 4.2(8), XIX]

Ctenidodinium sellwoodii (Sarjeant 1975) Stover & Evitt 1978 [Plate 4.2(7), XII(1–4)]

Ctenidodinium spp. [Plate XII(5,6)]

**Dapcodinium priscum* Evitt 1961

Dapsilidinium? *deflandrei* (Valensi, 1947) Lentin & Williams 1981 [Plate 3.2(2)]

**Dissiliodinium giganteum* Feist-Burkhardt 1990

Dissiliodinium spp. [Plate IX]

Durotrigia daveyi Bailey 1987 [Plate 4.2(1)]

Ellipsoidictyum sp. [Plate XVII]

Epiplosphaera gochtii (Fensome 1979) Brenner 1988 [Plate 4.2(4)]

Gonyaulacysta jurassica (Deflandre 1938) Norris & Sarjeant 1965 subsp. *adecta* Sarjeant 1982 [Plate XVI (5,6)]

Gonyaulacysta pectinigera (Gocht 1970) Fensome 1979 [Plate 4.2(9), XVI (1–4)]

Kallosphaeridium? sp. [Plate 4.1(10)]

Korystocysta aldridgeii Wiggan et al. 2017 [Plate 4.1(11)]

Korystocysta? *gochtii* (Sarjeant 1976) Woollam 1983 [Plate XXI(12)]

Korystocysta pachyderma (Deflandre 1938) Woollam 1983 [Plate XXI(10,11)]

**Liasidium variabile* Drugg 1978

**Luehndea cirilliae* Bucefallo Palliani et al. 1997

Luehndea spinosa Morgenroth 1970 [Plates 2.1(7–9), 2.3(1–3), 3.1(1–3), II]

Mancodinium semitabulatum Morgenroth 1970 [Plates 2.1(10–12), 2.3(10), 3.2(11,12), 4.1(1), I]

Maturodinium? *inornatum* Morgenroth 1970 [Plate 3.2(10)]

Meiourogonyaulax spp. [Plate XI]

**Mendicodinium brunneum* Bucefalo Palliani et al. 1997

Mendicodinium groenlandicum (Pocock & Sarjeant 1972) Davey 1979 [Plate VII (3,4)]

Mendicodinium microscabratum Bucefalo Palliani et al. 1997 [Plates 2.1(5), 2.3(12), 3.2(8), VI (1–9)]

Mendicodinium spp. [Plate 2.1(6), 3.2(9), VII(1,2)]

Mendicodinium spinosum Bucefalo Palliani et al. 1997 subsp. *spinosum* (autonym) [Plate 2.1(4)]

**Mendicodinium umbriense* Bucefalo Palliani et al. 1997

Nannoceratopsis ambonis Drugg 1978 [Plates 2.1(3), 2.3(8), 3.1(11,12), V(1–4)]

**Nannoceratopsis deflandrei* Evitt 1961

**Nannoceratopsis deflandrei* Evitt 1961 subsp. *anabarensis* Ilyina et al. 1994

**Nannoceratopsis dictyambonis* Riding 1984

Nannoceratopsis gracilis Alberti 1961 [Plates 2.1(1), 2.3(4–7), 3.1(5), 4.1(3), IV]

**Nannoceratopsis magnicornis* Bucefalo Palliani & Riding 1997

**Nannoceratopsis plegas* Drugg 1978

**Nannoceratopsis raunsgaardii* Poulsen 1996

Nannoceratopsis senex van Helden 1977 [Plates 2.1(2), 2.3(9), 3.1(6–10), 4.1(2), III]

Nannoceratopsis sp. [Plate 3.1(4)]

**Nannoceratopsis spiculata* Stover 1966

**Nannoceratopsis symmetrica* Bucefalo Palliani & Riding 2000

**Nannoceratopsis triceras* Drugg 1978

Pareodinia ceratophora Deflandre 1947 [Plate 4.2(3), XV (2–4)]

Pareodinia sp. [Plate XV (1)]

**Pareodinia halosa* (Filatoff 1975) Prauss 1989

**Parvocysta nasuta* Bjaerke 1980

Phallocysta elongata (Beju 1971) Riding 1994 [Plate XXI(3)]

Rhynchodiniopsis ?*regalis* (Gocht 1970) Jan du Chêne 1985 [Plate XXI(8,9)]

Rhynchodiniopsis spp. [Plate 4.1(12)]

Scriniocassis priscus (Gocht 1979) Below 1990 [Plate 3.2(4–6), 4.1(4), VIII (4–12)]

Scriniocassis weberi Gocht 1964 [Plates 2.3(11), 3.2 (7), VIII (1–3)]

Sentusidinium asymmetrum (Fenton et al. 1980) Lentin & Williams 1981 [Plate X(11)]

Sentusidinium explanatum (Bujak in Bujak et al. 1980) Wood et al. 2016 [Plate 4.1(7)]

Sentusidinium spp. [Plate 3.2(3), X]

**Susadinium scrofoides* Dörhöfer & Davies 1980

Tubotuberella dangeardii (Sarjeant 1968) Stover & Evitt 1978 [Plate 4.2(11), XVIII]

**Umbriadinium mediterraneense* Bucefalo Palliani & Riding 1997

Valensiella ovulum (Deflandre 1947) Eisenack 1963 [Plate 4.2(6), XIII]

Valvaeodinium armatum Morgenroth 1970 [Plate XXI(1)]

**Valvaeodinium hirsutum* Bucefalo Palliani & Riding 1997

**Valvaeodinium koessenium* (Morbey 1975) Below 1987

**Valvaeodinium punctatum* (Wille & Gocht 1979) Below 1987

Valvaeodinium spp. [Plate 3.2(1), XXI(2)]

Wanaea sp. [Plate XXI(6)]

Miscellaneous microplankton:

Cymatiosphaera pachytheca Eisenack 1957 (prasinophytes) [Plate 2.4(6), 4.3(2)]

Halosphaeropsis liassica Mädler 1968 (prasinophyte) [Plates 2.2(12), 3.3(5)]

Micrhystridium spp. (acritarch) [Plates 2.2(10), 2.4(4), 3.3(1,2), 4.3(1)]

Polygonium jurassicum Bucefalo Palliani et al. 1996 (acritarch) [Plates 2.4(1–3), 3.3(4)]

Tasmanites spp. (prasinophyte) [Plates 2.2(11), 3.3(6), 4.3(3)]

Foraminiferal test linings [Plates 2.4(11,12), 3.3(7)]

Spores:

Anapiculatisporites spp.

Auritulinasporites triclavus Nilsson 1958 [Plate 4.3(6)]

Calamospora tener (Leschik 1955) Mädler 1964 [Plate 3.3(8)]

Cibotiumspora jurienensis (Balme1957) Filatoff 1975 [Plate 3.3(9)]

Cingutriletes sp.

Conbaculatisporites sp. [Plate 3.3(10)]

Concavisporites granulosus Tralau 1968 [Plates 2.4(9), 3.3(11)]

Concavisporites spp.

Cyathidites minor Couper 1953 [Plate 3.3(12)]

Cyathidites spp. [Plate 2.2(1)]

Ischyosporites variegatus (Couper 1958) Schulz 1967 [Plates 2.2(2), 3.4(1), 4.3(4)]

Kekryphalospora distincta Fenton & Riding 1987 [Plate 3.4(2)]

Kraeuselisporites reissingeri (Harris 1957) Morbey 1975 [Plates 2.2(3), 3.4(3), XXII]

Leptolepidites spp. [Plates 2.2(4), 3.4(4)]

Lycopodiacidites rugulatus (Couper 1958) Schulz 1967 [Plates 2.2(5), 3.4(5)]

Marattisporites sp.

Osmundacidites wellmanii Couper 1953 [Plates 2.4(7), 3.4(6)]

Plicifera delicata (Bolchovitina 1953) Bolchovitina 1966 [Plate 3.4(7)]

Retitriletes austroclavatidites (Cookson 1953) Doring et al. in Krutzsch 1963

Retitriletes spp. [Plate 3.4(8)]

Striatella seebergensis Madler 1964 [Plate 4.3(5)]

Striatella spp. [Plates 2.4(8), 3.4(9)]

Todisporites granulatus Tralau 1968 [Plate 3.4 (10)]

Todisporites spp. [Plate 3.4 (11)]

Pollen:

Alisporites spp. [Plates 2.2(6), 3.4(12)]

Araucariacites australis Cookson 1947 ex Couper 1958 [Plates 2.2(7), 3.5(1), 4.3(10), XXIV]

Callialasporites dampieri (Balme 1957) Dev 1961 [Plate 3.5(4), 4.3(7), XXV(1–3)]

Callialasporites microvelatus Schulz 1967 [Plate XXV(11)]

Callialasporites minus (Tralau 1968) Guy 1971 [Plate XXV(10)]

*Callialasporites segmentatu*s (Balme 1957) Srivastava 1963 [Plate 4.3(9), XXV(7–9)]

Callialasporites trilobatus (Balme 1957) Dev 1961 [Plate XXV(12)]

Callialasporites turbatus (Balme 1957) Schulz 1967 [Plate 3.5(5), 4.3(8), XXV(4–6)]

Cerebropollenites macroverrucosus (Thiergart 1949) Schulz 1967 [Plates 2.2(8), 2.4(10), 3.5(6)]

Chasmatosporites spp.

Classopollis classoides (Pflug 1953) Pocock & Jansonius 1961 [Plates 2.2(9), 3.5 (7–9), XXIII(1–8)]

Classopollis meyeriana (Klaus 1960) de Jersey 1973 [Plate XXIII(10–12)]

Classopollis sp. [Plate 3.5 (10)]

Cycadopites follicularis Wilson & Webster 1946 [Plate 3.5 (3)]

Cycadopites granulatus (de Jersey 1962) de Jersey 1964 [Plate 4.3(12)]

Exesipollenites spp. [Plate 3.5 (11)]

Inaperturopollenites sp. [Plate 3.5 (2)]

Perinopollenites elatoides Couper 1958 [Plate 4.3(11)]

Spheripollenites spp. [Plate 3.5 (12)]

Appendix 2: Nannoceratopsis senex remarks

In this study, we do not follow the taxonomic proposals of Ilyina et al. (1994) with regard to the dinoflagellate cyst species *Nannoceratopsis senex*. These authors changed the status of this taxon from a species to a subspecies of *Nannoceratopsis deflandrei*. Ilyina et al. (1994) placed the newly attributed subspecies *senex,* alongside two other subspecies, *Nannoceratopsis deflandrei* subsp. *anabarensis* and *Nannoceratopsis deflandrei* subsp. *deflandrei*. This strategy was on the basis that *Nannoceratopsis deflandrei* has a relatively untextured autophragm, in comparison to *Nannoceratopsis gracilis,* which has a rough, spongy wall. This difference between *Nannoceratopsis gracilis* and *Nannoceratopsis senex* was also discussed by Piel and Evitt (1980, p. 103).

In the present authors' view, the principal criteria for speciation in *Nannoceratopsis* should be the lateral outline and the number of hypocystal horns, not the fine-scale texture of the autophragm. Therefore we maintain the original contention of van Helden (1977), who established *Nannoceratopsis senex* as a distinctly tear-shaped form with a narrow antapical margin formed by the posterior part of the single hypocystal horn (see Plates 2.1(2), 2.3(9), 3.1(6–10)). This contrasts with *Nannoceratopsis gracilis,* which has a subtriangular lateral outline with a much wider antapical margin (see Plates 2.1(1), 2.3(4–7), 3.1(5)). *Nannoceratopsis gracilis* is therefore deemed to be the senior synonym of *Nannoceratopsis deflandrei,* as originally envisaged by Evitt (1962).

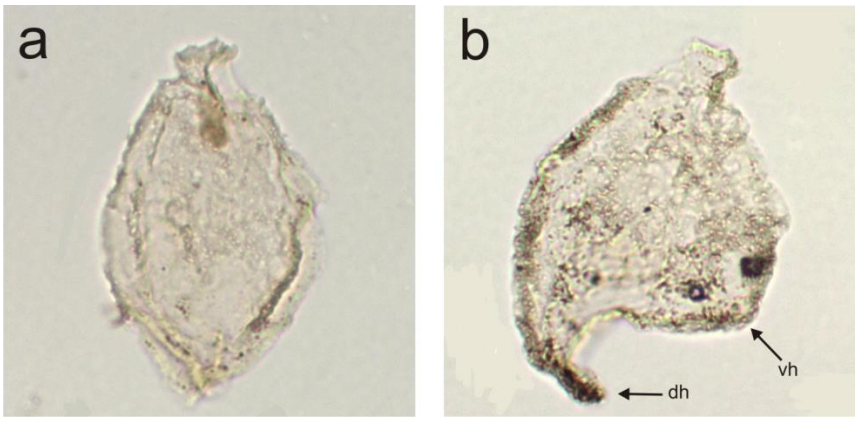

Figure I. *Nannoceratopsis senex* (a) and *Nannoceratopsis gracilis* (b), vh = ventral horn; dh = dorsal horn. Note the microtextured autophragm in both specimens but the differences in shape.

Appendix 3: catalogue with the biostratigraphical significant palynomorphs

Selected palynomorphs from the Lower and Middle Jurassic (Sinemurian to Callovian) of the Lusitanian Basin, in central western Portugal, are presented in the following plates and listed by biostratigraphical order, within each palynomorph group, i.e. dinoflagellate cysts (Plates I–XXI), spores (Plate XXII) and pollen (Plates XXIII–XXV). These illustrations intend to document the palynomorphs diversity, in particular of dinoflagellate cysts, throughout the studied succession, as well the intra-specific variability identified in some taxa.

All specimens are housed in the collections of LNEG (Portuguese Geological Survey), S. Mamede de Infesta, Portugal. The sample number, slide number and England Finder coordinates are provided. All the scale bars represent 20 μm. The references in the author citations are not listed in the bibliography herein, but may be found in Williams et al. (2017).

Plate I. *Mancodinium semitabulatum* Morgenroth 1970.

Note the anterior sulcal plate (the sulcal tongue) and the precingular plates (the 1" and 7") which are involved in the formation of the 'disintegration' style archaeopyle.

1. Peniche section, lower Pliensbachian (*Prodactylioceras davoei* AB), sample P-29, slide 1, O37/1. Ventral view, median focus.
2. Brenha section, upper Pliensbachian (*Amaltheus margaritatus* AB), sample Br15, slide 1, T47/4. Ventral view, high focus.
3. Peniche section, lower Toarcian (*Dactylioceras polymorphum* AB), sample P6, slide 1, O27/4. Dorsal view, high focus.
4. Vale das Fontes section, lower Toarcian (*Dactylioceras polymorphum* AB), sample PVF1, slide 1, H56/2. Oblique right lateral, ventral view.
5. Vale das Fontes section, lower Toarcian (*Dactylioceras polymorphum* AB), sample PVF1, slide 1, K29/4. Apical view.
6. Maria Pares section, lower Toarcian (*Hildaites levisoni* AB), sample PZ32, slide 1, D42. Oblique ventral-left lateral view.
7. Maria Pares section, lower Toarcian (*Hildaites levisoni* AB), sample PZ32, slide 1, K39. Slightly oblique dorsal view.
8. Maria Pares section, upper Toarcian (*Hammatoceras speciosum* AB), sample PZ74, slide 1, D44. Ventral view, high focus.
9. Maria Pares section, upper Toarcian (*Dumortieria meneghinii* AB), sample PZ82, slide 1, X54/3. Ventral view, high focus.
10. Maria Pares section, upper Toarcian (*Dumortieria meneghinii* AB), sample PZ82, slide 2, L45. Dorsal view, low focus.
11. Cabo Mondego section, upper Toarcian (*Pleydellia aalensis* AB), sample M24, slide 1, Y43. Ventral view, high focus.
12. Cabo Mondego section, upper Toarcian (*Pleydellia aalensis* AB), sample M28, slide 1, F35.Oblique apical view, high focus.

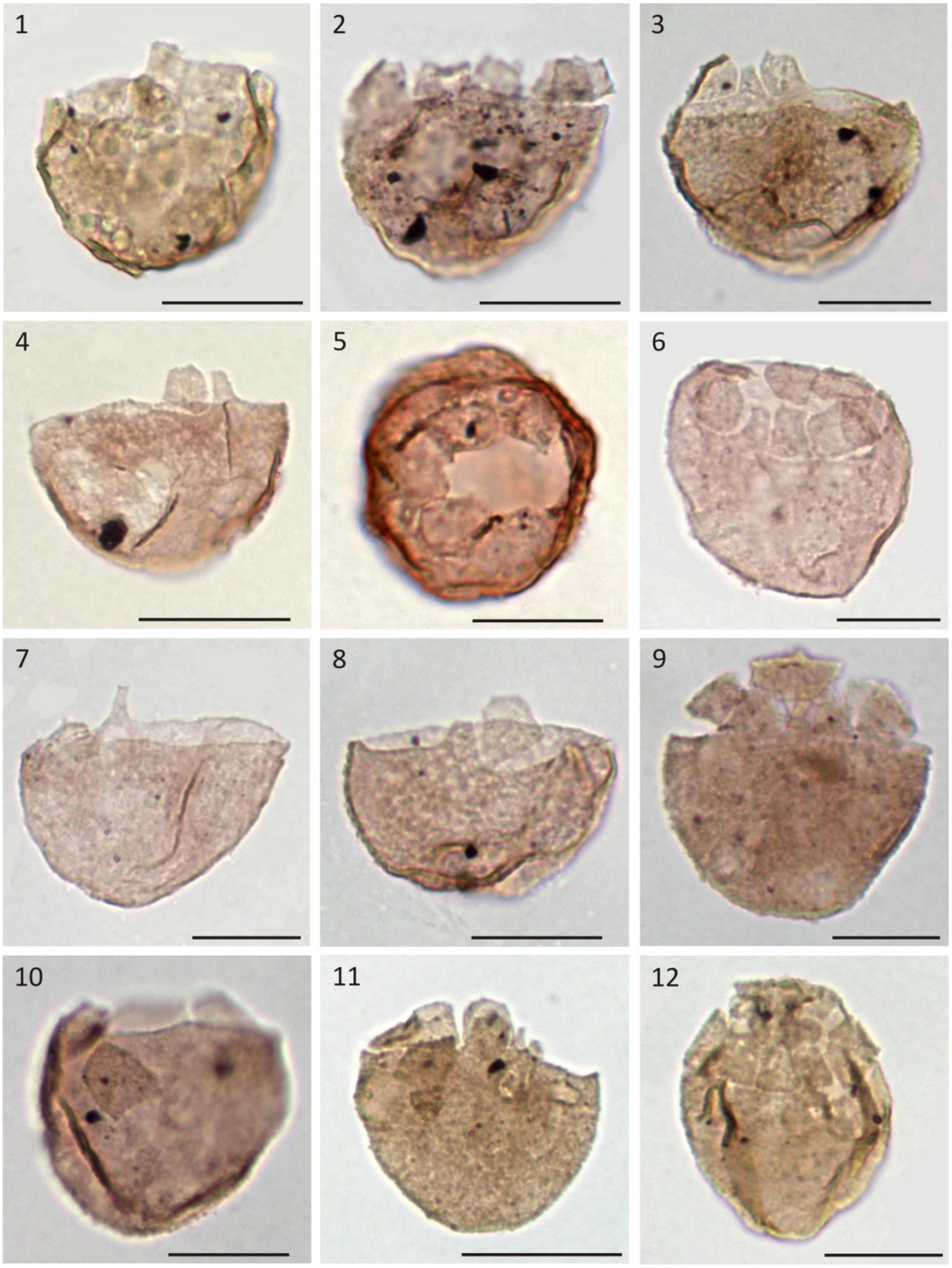
1
2
3
4
5
6
7
8
9
10
11
12

Plate II. *Luehndea spinosa* Morgenroth 1970.

Note the long and distally pointed spines, which arise from the suture junctions, and the epicystal archaeopyle.

1. Peniche section, upper Pliensbachian (*Amaltheus margaritatus* AB), sample P-26, slide 1, M35/1. Dorsal view, high focus.
2. Peniche section, lower Toarcian (*Dactylioceras polymorphum* AB), sample P9, slide 1, X37. Oblique lateral view, high focus.
3. Peniche section, lower Toarcian (*Dactylioceras polymorphum* AB), sample P12, slide 1, N27/4. Dorsal view, high focus.
4. Fonte Coberta section, upper Pliensbachian (*Emaciaticeras emaciatum* AB), sample FC5, slide 1, L25/4. Ventral view, high focus.
5. Maria Pares section, lower Toarcian (*Dactylioceras polymorphum* AB), sample PZ5, slide 1, O22/2. Oblique dorsal view.
6. Maria Pares section, lower Toarcian (*Dactylioceras polymorphum* AB), sample PZ7, slide 1, C28. Oblique antapical view.
7. Vale das Fontes section, lower Toarcian (*Dactylioceras polymorphum* AB), sample PVF3, slide 1, M34. Dorsal view, high focus.
8. Vale das Fontes section, lower Toarcian (*Dactylioceras polymorphum* AB), sample PVF4, slide 1, H37/3. Hypocyst.
9. Vale das Fontes section, lower Toarcian (*Dactylioceras polymorphum* AB), sample PVF8, slide 1, O24. Mid-ventral view, high focus. Note the prominent cingulum, interrupted by the sulcus.
10. Vale das Fontes section, lower Toarcian (*Dactylioceras polymorphum* AB), sample PVF10, slide 1, Y27/3. Dorsal view, high focus.
11. Vale das Fontes section, lower Toarcian (*Dactylioceras polymorphum* AB), sample PVF12, slide 1, G29/3. Ventral view, high focus.
12. Vale das Fontes section, lower Toarcian (*Dactylioceras polymorphum* AB), sample PVF12, slide 1, K40/4. Dorsal view, high focus.

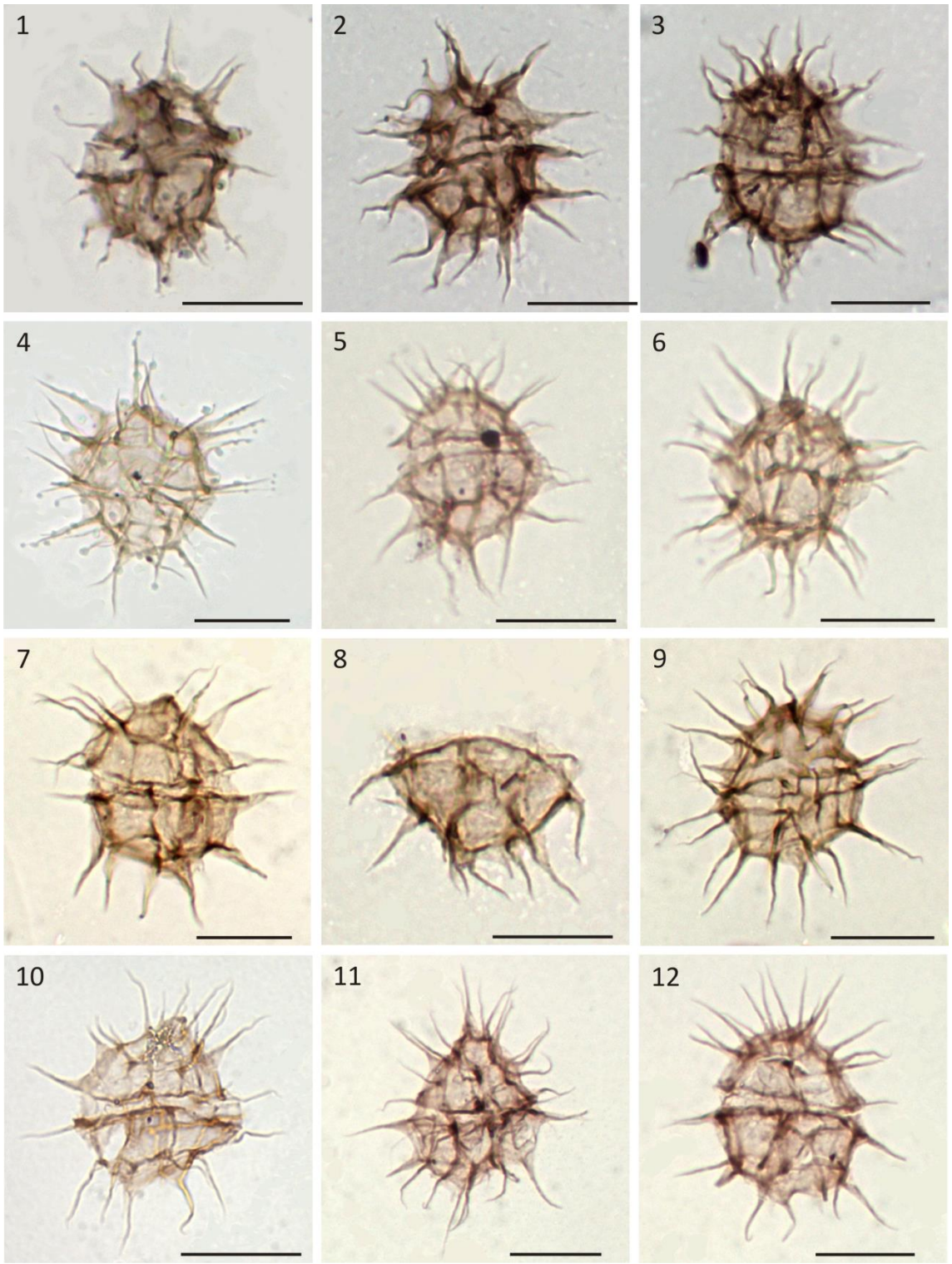
1
2
3
4
5
6
7
8
9
10
11
12

Plate III. *Nannoceratopsis senex* van Helden 1977.

Note the single antapical horn and the almost symmetric shape ("tear-shaped").

1. Peniche section, upper Pliensbachian (*Amaltheus margaritatus* AB), sample P-28, slide 1, N35. Right lateral view.
2. Peniche section, upper Pliensbachian (*Amaltheus margaritatus* AB), sample P-25, slide 1, O48/4. Right lateral view.
3. Peniche section, upper Pliensbachian (*Emaciaticeras emaciatum* AB), sample P-4, slide 1, M50/3. Left lateral view.
4. Brenha section, upper Pliensbachian (*Amaltheus margaritatus* AB), sample Br14, slide 1, G49/3. Left lateral view.
5. Brenha section, upper Pliensbachian (*Emaciaticeras emaciatum* AB), sample BrLem1, slide 1, K41/2. Left lateral view.
6. Fonte Coberta section, upper Pliensbachian (*Amaltheus margaritatus* AB), sample FC1, slide 1, K34/2. Left lateral view.
7. Fonte Coberta section, upper Pliensbachian (*Emaciaticeras emaciatum* AB), sample FC3, slide 1, L31/4. Left lateral view.
8. Vale das Fontes section, lower Toarcian (*Dactylioceras polymorphum* AB), sample PVF2, slide 1, Q57. Right lateral view.
9. Maria pares section, upper Toarcian (*Dumortieria meneghinii* AB), sample PZ82, slide 1, P41/3. Left lateral view.
10. São Gião section, upper Toarcian (*Pleydellia aalensis* AB), sample SG8, slide 2, P30. Oblique dorsal-right view.
11. São Gião section, upper Toarcian (*Pleydellia aalensis* AB), sample SG22m, slide 1, W38/4. Left lateral view.
12. Cabo Mondego section, middle Aalenian (*Brasilia bradfordensis* AB), sample M150, slide 1, C30. Right lateral view.

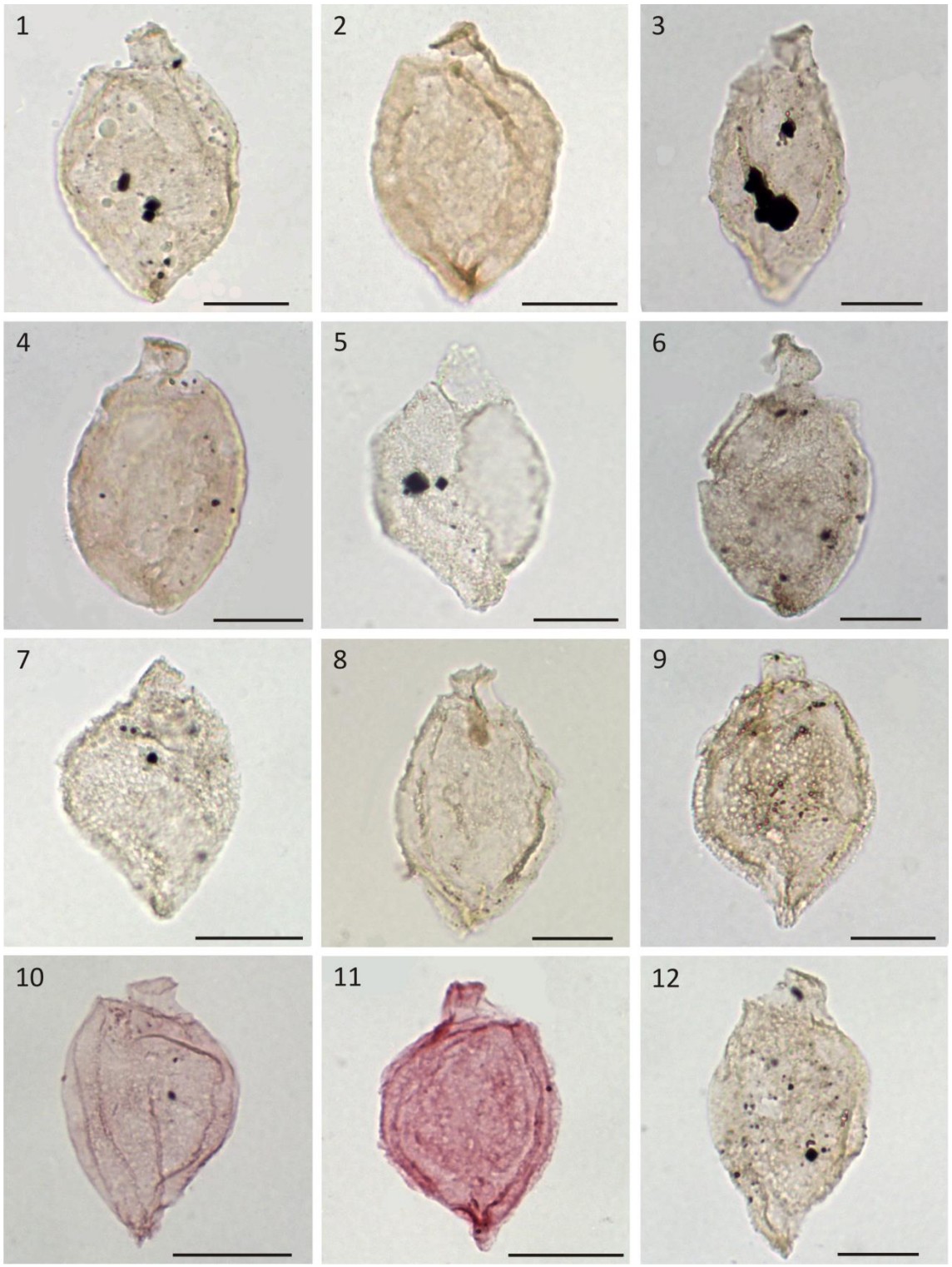
1
2
3
4
5
6
7
8
9
10
11
12

Plate IV. *Nannoceratopsis gracilis* Alberti 1961.

Note the dorsal antapical horn.

1. Brenha section, upper Pliensbachian (*Emaciaticeras emaciatum* AB), sample BrLem1, slide 1, G34/1. Right lateral view.
2. Vale das Fontes section, lower Toarcian (*Dactylioceras polymorphum* AB), sample PVF10, slide 1, R47/1. Right lateral view.
3. Peniche section, lower Toarcian (*Dactylioceras polymorphum* AB), sample P6, slide 1, G36. Left lateral view.
4. Peniche section, lower Toarcian (*Dactylioceras polymorphum* AB), sample P6, slide 1, D45/4. Left lateral view.
5. Peniche section, lower Toarcian (*Dactylioceras polymorphum* AB), sample P6, slide 1, G28/3. Right lateral view.
6. Peniche section, lower Toarcian (*Dactylioceras polymorphum* AB), sample P6, slide 1, G20/4. Right lateral view.
7. Peniche section, lower Toarcian (*Dactylioceras polymorphum* AB), sample P10, slide 1, Q20/4. Right lateral view.
8. Cabo Mondego section, lower Bajocian (*Witchellia laeviuscula–Sonninia propinquans* ABs), sample AB116, slide 1, H40. Left lateral view.
9. Cabo Mondego section, lower Bajocian (*Witchellia laeviuscula–Sonninia propinquans* ABs), sample AB116, slide 1, G36/4. Right lateral view.
10. Cabo Mondego section, lower Bajocian (*Witchellia laeviuscula–Sonninia propinquans* ABs), sample AB116, slide 1, S47. Left lateral view.
11. Cabo Mondego section, lower Bajocian (*Sonninia propinquans* AB), sample AB164, slide 1, C34. Right lateral view.
12. Cabo Mondego section, lower Bajocian (*Stephanoceras humphriesianum* AB), sample AB192, slide 1, O45/1. Left lateral view.

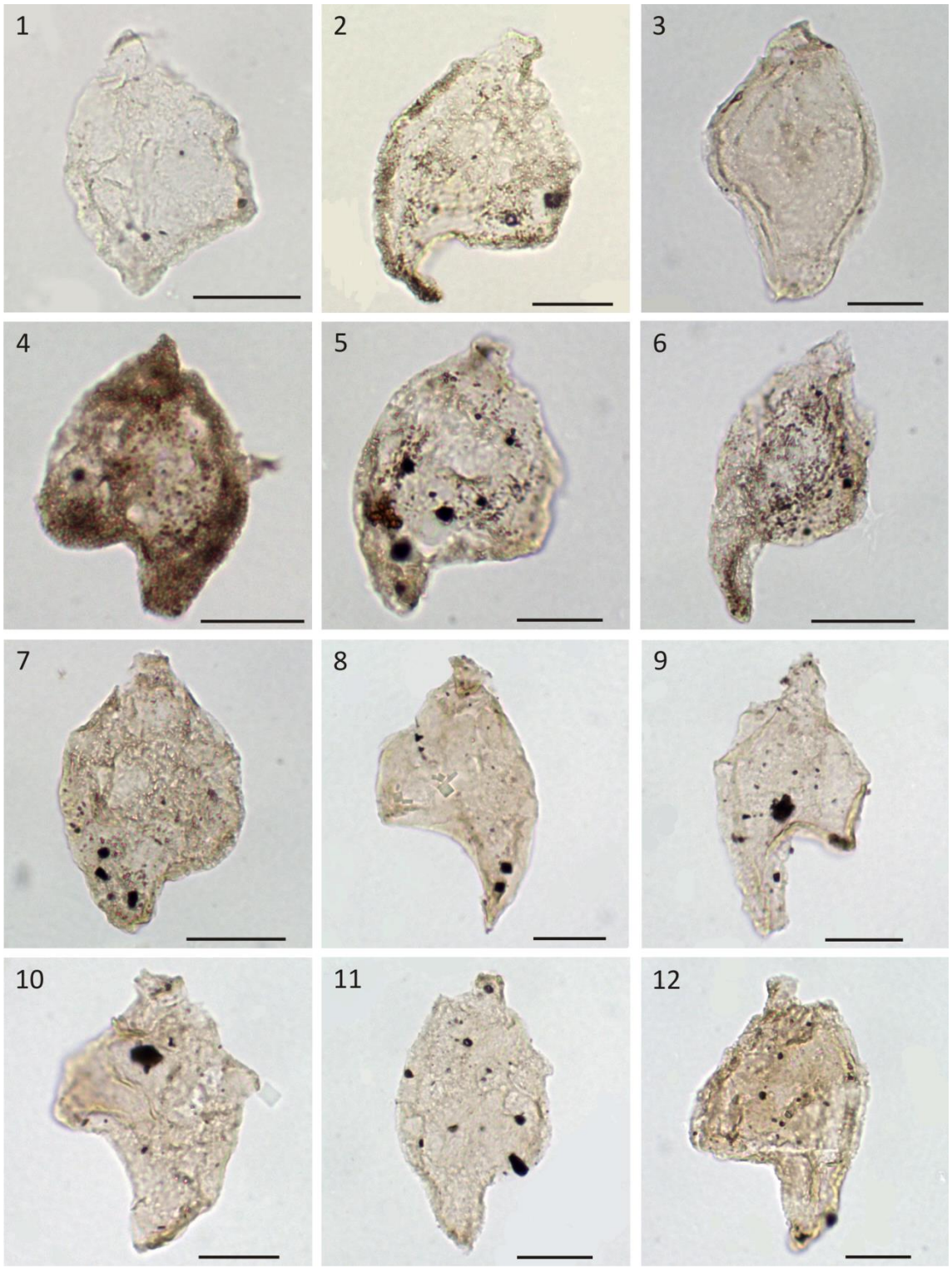
1
2
3
4
5
6
7
8
9
10
11
12

Plate V. *Nannoceratopsis* spp.

1–4. *Nannoceratopsis ambonis* Drugg 1978. Note the prominent dark sagittal rim.

1. Vale das Fontes section, lower Toarcian (*Dactylioceras polymorphum* AB), sample PVF2, slide 1, Y36/1. Left lateral view.
2. Peniche section, lower Toarcian (*Dactylioceras polymorphum* AB), sample P10, slide 1, T25/3. Left lateral view.
3. Maria Pares section, upper Toarcian (*Hammatoceras speciosum* AB), sample PZ81, slide 1, U62/2. Left lateral view.
4. Maria Pares section, upper Toarcian (*Hammatoceras speciosum* AB), sample PZ81, slide 1, X63/1. Right lateral view.
5. *Nannoceratopsis gracilis* Alberti 1961. Cabo Mondego section, lower Bajocian (*Witchellia laeviuscula–Sonninia propinquans* ABs), sample AB108, slide 1, D42/2. Left lateral view. Note that part of the saggital rim of this specimen is darker. It may be an intermediate form between *N. gracilis* and *N. ambonis*.
6. *Nannoceratopsis* sp. Peniche section, upper Pliensbachian (*Amaltheus margaritatus* AB), sample P-20, slide 1, T35/4. Left lateral view. Note the two antapical horns of almost equal length.

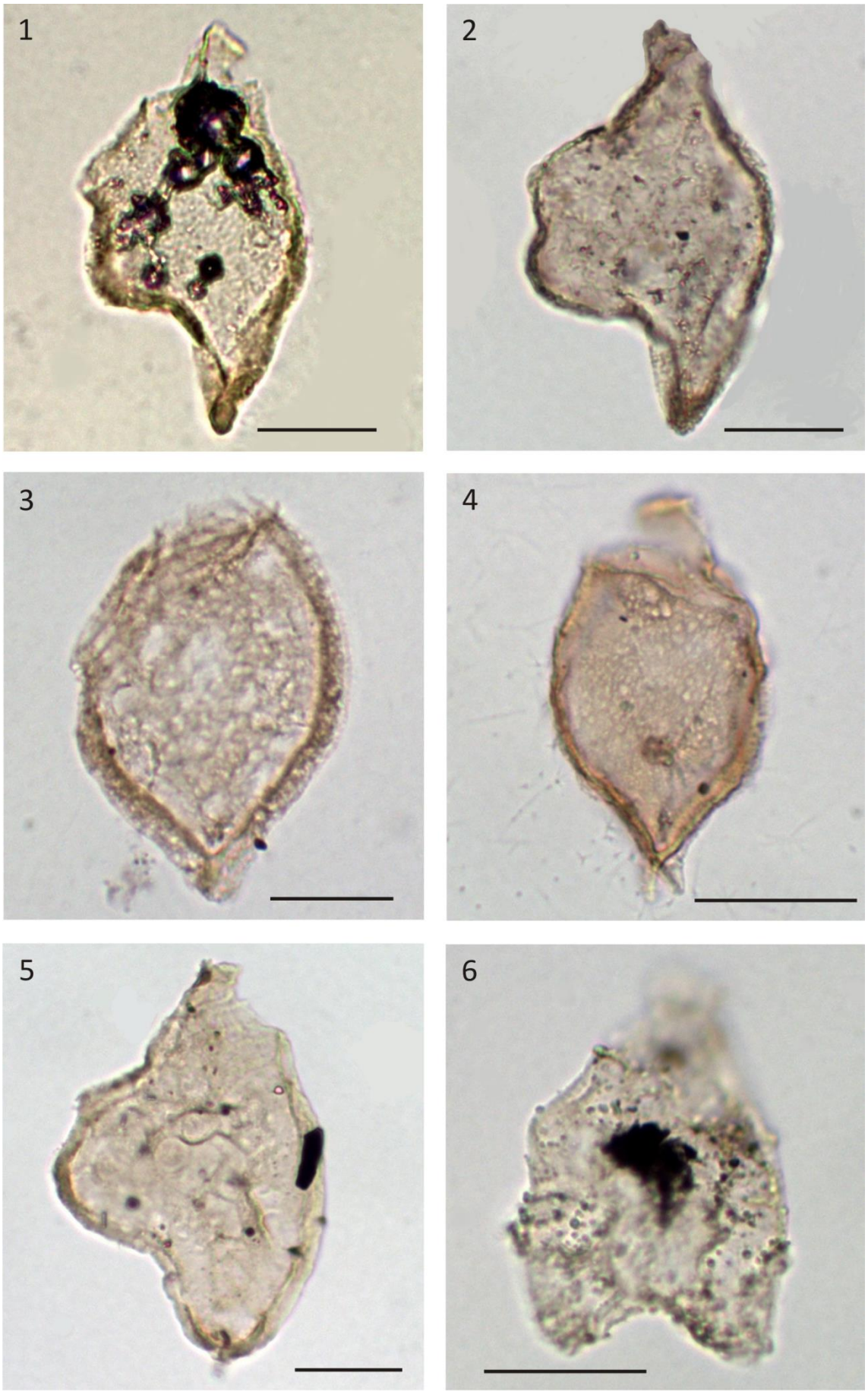
1
2
3
4
5
6

Plate VI. *Mendicodinium* spp. (lower Jurassic)

1–9. *Mendicodinium microscabratum* Bucefalo Palliani et al. 1997. Note the epicystal archaeopyle and the microscabrate autophragm.

1. Peniche section, lower Toarcian (*Hildaites levisoni* AB), sample P23, slide 1, L24/4. Dorsal view, high focus.
2. Maria Pares section, lower Toarcian (*Hildaites levisoni* AB), sample PZ16, slide 1, T36/1. Right lateral view.
3. Maria Pares section, lower Toarcian (*Hildaites levisoni* AB), sample PZ22, slide 1, T68/2. Dorsal view, high focus.
4. Maria Pares section, middle Toarcian (*Hildoceras bifrons* AB), sample PZ54, slide 1, T27. Left lateral view.
5. Maria Pares section, middle Toarcian (*Hildoceras bifrons* AB), sample PZ56, slide 1, G27/3. Ventral view, high focus.
6. Maria Pares section, middle Toarcian (*Hildoceras bifrons* AB), sample PZ56, slide 1, G53/4. Left lateral view.
7. . Maria Pares section, middle Toarcian (*Hildoceras bifrons* AB), sample PZ57, slide 1, O42. Dorsal view, high focus.
8. Maria Pares section, middle Toarcian (*Hildoceras bifrons* AB), sample PZ58, slide 1, Q33/4. Ventral view, high focus.
9. Maria Pares section, upper Toarcian (*Hammatoceras speciosum* AB), sample PZ79, slide 1, G49/2. Ventral view, high focus.
10. *Mendicodinium spinosum* Bucefalo Palliani et al. 1997 subsp. *spinosum* (autonym). Maria Pares section, lower Toarcian (*Hildaites levisoni* AB), sample PZ26, slide 1, F49/1. Oblique dorsal view. Note the spines and the smooth autophragm.
11. *Mendicodinium* sp. Maria Pares section, lower Toarcian (*Hildaites levisoni* AB), sample PZ29, slide 1, M33/3. Oblique left lateral view. Note that this form is larger than most Toarcian specimens of *Mendicodinium*; the width is 40 μm.
12. *Mendicodinium* sp. Maria Pares section, upper Toarcian (*Hammatoceras speciosum* AB), sample PZ80, slide 1, H47/2. Oblique left lateral view. The width is 42 μm.

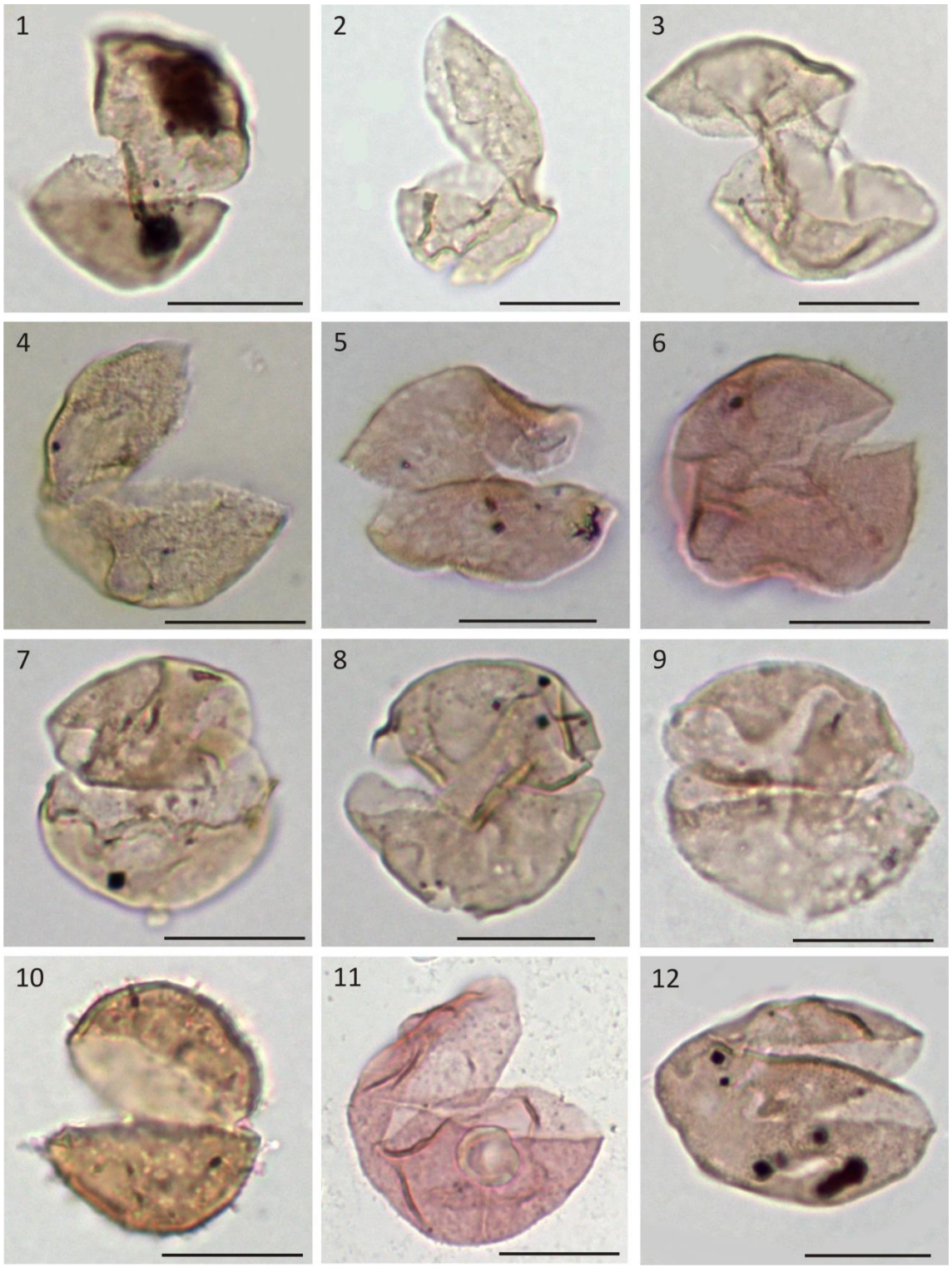
1
2
3
4
5
6
7
8
9
10
11
12

Plate VII. *Mendicodinium* spp. (middle Jurassic)

1. *Mendicodinium* sp. Cabo Mondego section, lower Aalenian (*Leioceras opalinum* AB), sample M75, slide 1, S33. Ventral view. The width is 40 μm.
2. *Mendicodinium* sp. 1. Cabo Mondego, upper Bajocian (*Parkinsonia parkinsoni* AB), sample Bt106, slide 1, V29/1. Left lateral view. Note the autophragm with short spines and baculae.

3, 4. *Mendicodinium groenlandicum* (Pocock & Sarjeant 1972) Davey 1979.

3. Cabo Mondego section, lower Bathonian (*Zigzagiceras zigzag* AB), sample Bt210, slide 1, Q25/2. Ventral view.
4. Cabo Mondego section, upper Bathonian (*Clydoniceras discus* AB) sample CM3, slide 1, O24. Ventral view.

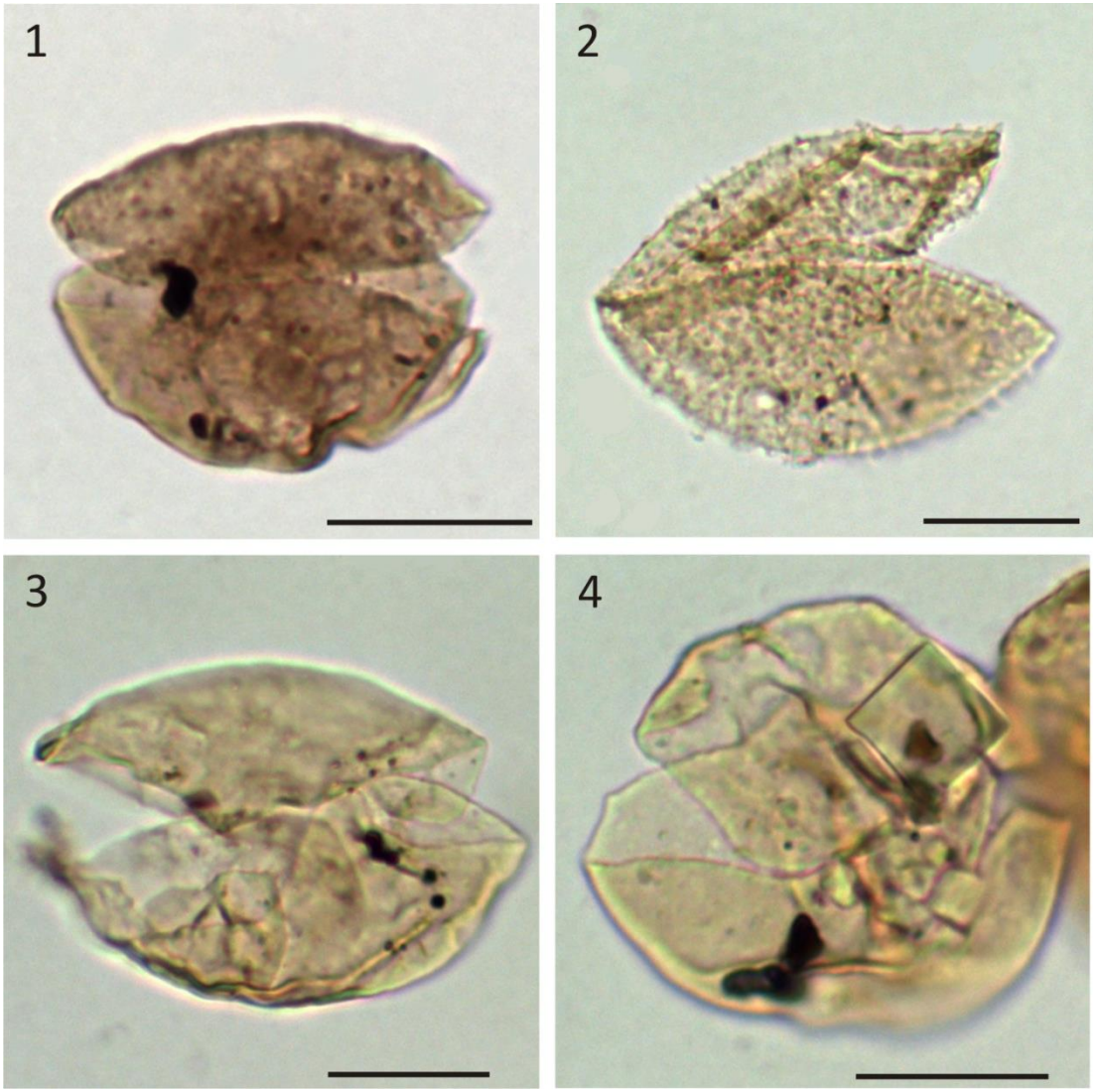
1
2
3
4

Plate VIII. *Scriniocassis* spp.

Note the reticulate wall sculpture and the two plate precingular (2P) archaeopyle.

1–3. *Scriniocassis weberi* Gocht 1964.

1. Peniche section, lower Toarcian (*Dactylioceras polymorphum* AB), sample P9, slide 1, R36/1. Dorsal view, high focus. Note the coarse reticulum and the 2P archaeopyle.

2, 3. Cabo Mondego section, lower Aalenian (*Leioceras opalinum* AB), sample M75, slide 1, J42/3. **2.** -ventral view, high focus; note the coarse reticulum and the sulcus. **3**. – dorsal view, low focus; note the sutural crests and the 2P archaeopyle.

4–12. *Scriniocassis priscus* (Gocht 1979) Below 1990.

4, 5. Maria Pares section, upper Toarcian (*Hammatoceras speciosum* AB), sample PZ77, slide 1, C32. **4.** - ventral view, low focus. **5.** - dorsal view, high focus. Note the rounded, subhexagonal cyst outline and the infrareticulate wall sculpture. The distinctive, strongly curved sutures surrounding the sulcus are evident in 4. In 5, the 2P (2" and 3") archaeopyle, the large middorsal postcingular (4"') plate and the sutural crests are clearly visible.

6. Maria Pares section, upper Toarcian (*Hammatoceras speciosum* AB), sample PZ79, slide 1, W43/2. Oblique lateral-dorsal view, high focus. Note the postcingular plates.

7, 8. Maria Pares section, upper Toarcian (*Hammatoceras speciosum* AB), sample PZ80, slide 1, E24/3. **7.** –ventral view, high focus; note the sulcus. **8.** – dorsal view, low focus.

9. Cabo Mondego section, upper Toarcian (*Pleydellia aalensis* AB), sample M28, slide 1, K30/2. Oblique left lateral view.

10, 11. Maria Pares section, upper Toarcian (*Hammatoceras speciosum* AB), sample PZ80, slide 1, N58. **10**. –ventral view, high focus. Note the sulcus and the sutural crests. **11.** – dorsal view, low focus.

12. Cabo Mondego section, middle Aalenian (*Brasilia bradfordensis* AB), sample M150, slide 1, W28. Oblique left lateral view.

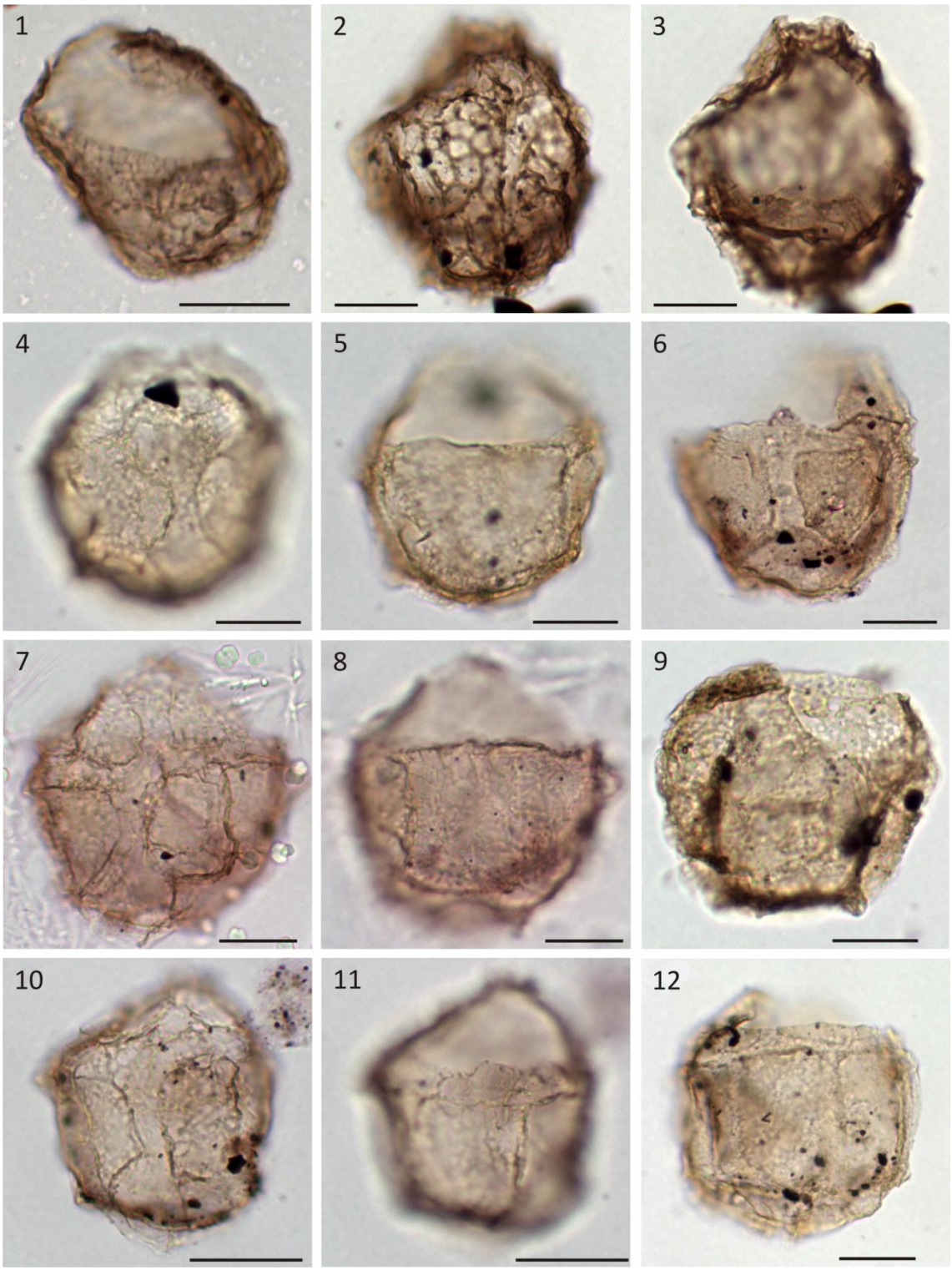
1
2
3
4
5
6
7
8
9
10
11
12

Plate IX. *Dissiliodinium* spp.

Note the multiplate precingular archaeopyle.

1. *Dissiliodinium* sp. 1. Cabo Mondego section, lower Bajocian, lower Bajocian (*Hyperlioceras discites* AB), M354, slide 1, O24. Oblique left lateral view. Note the psilate autophragm.
2. *Dissiliodinium* sp. 1. Cabo Mondego section, lower Bajocian (*Witchellia laeviuscula–Sonninia propinquans* ABs), sample AB116, slide 1, S26. Oblique left lateral view.
3. *Dissiliodinium* sp. 1. Cabo Mondego section, lower Bajocian (*Stephanoceras humphriesianum* AB), sample AB192, slide 1, R42. Left lateral view.
4. *Dissiliodinium* sp. 2. Cabo Mondego section, lower Bajocian (*Witchellia laeviuscula* AB), sample AB55, slide 1, Q29/2. Note the granulate autophragm.
5. *Dissiliodinium* sp. 2. Cabo Mondego section, lower Bajocian (*Stephanoceras humphriesianum* AB), sample AB186, slide 1, N42/4.
6. *Dissiliodinium* sp. 2. Cabo Mondego section, lower Bajocian (*Stephanoceras humphriesianum* AB), sample AB192, slide 1, W29.

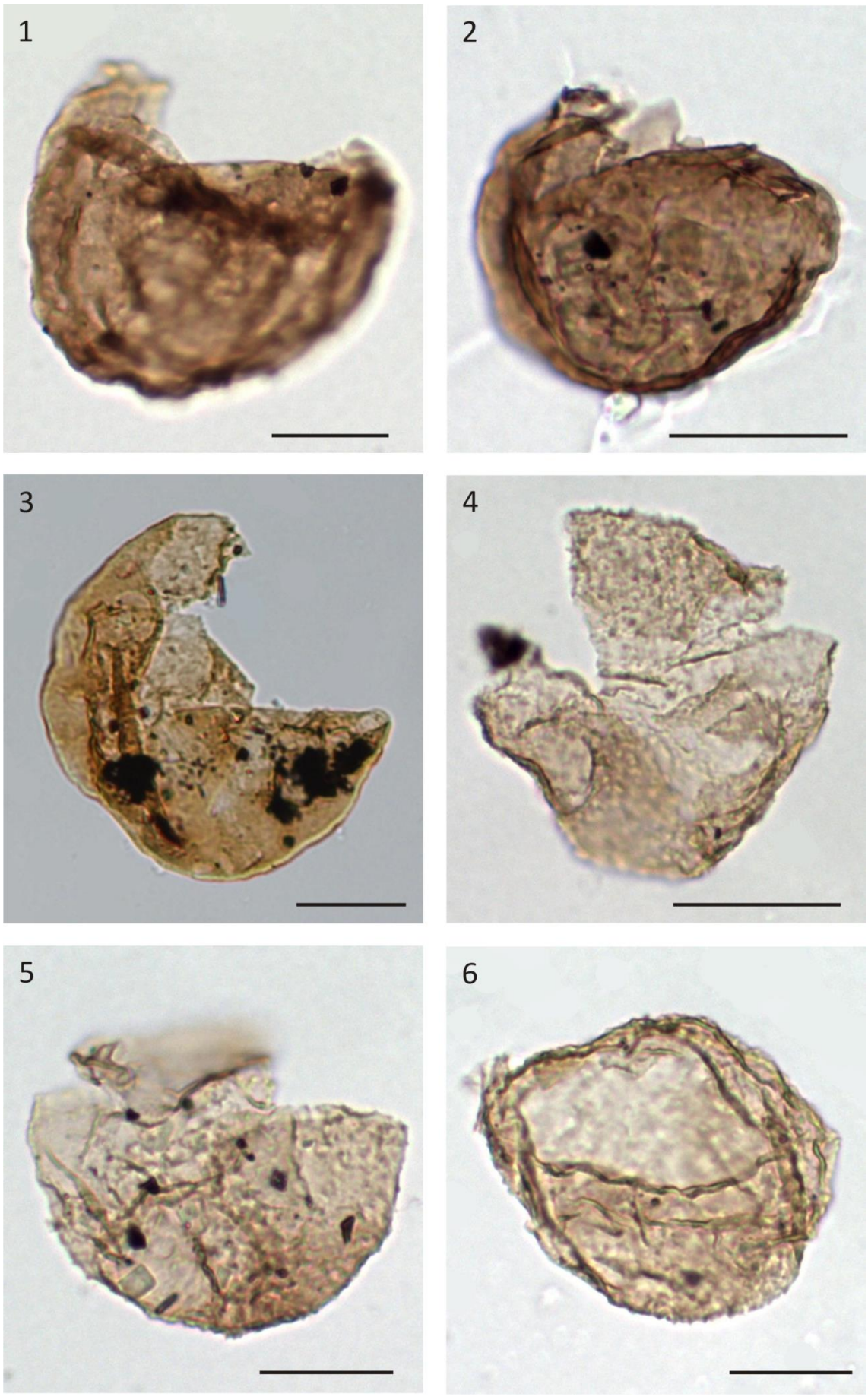
1
2
3
4
5
6

Plate X. *Sentusidinium* spp.

Note the apical archaeopyle and the accessory archaeopyle sutures.

1. *Sentusidinium* sp. cf. *S. explanatum* (Bujak in Bujak et al. 1980) Wood et al. 2016. Cabo Mondego section, lower Bajocian (*Witchellia laeviuscula–Sonninia propinquans* ABs), sample AB108, slide 1, J32. Note the smooth autophragm.
2. *Sentusidinium* sp. 1. Cabo Mondego section, lower Bajocian (*Witchellia laeviuscula–Sonninia propinquans* ABs), sample AB108, slide 1, Q38/3. Note the granulate autophragm.
3. *Sentusidinium* sp. 1. Cabo Mondego section, lower Bajocian (*Witchellia laeviuscula–Sonninia propinquans* ABs), sample AB108, slide 1, X38.
4. *Sentusidinium* sp. 1. Cabo Mondego section, lower Bajocian (*Witchellia laeviuscula–Sonninia propinquans* ABs), sample AB108, slide 1, W55/1.
5. *Sentusidinium* sp. 1. Cabo Mondego section, lower Bajocian (*Witchellia laeviuscula–Sonninia propinquans* ABs) sample AB116, slide 1, W51/2. Note the scabrate to granulate autophragm.
6. *Sentusidinium* sp. 1. Cabo Mondego section, lower Bajocian (*Sonninia propinquans* AB), sample AB178a, slide 1, L38/4. Photomicrograph taken using differential interference contrast.
7. *Sentusidinium* sp. 1. Cabo Mondego section, lower Bajocian (*Sonninia propinquans* AB), sample AB178a, slide 1, J29/2.
8. *Sentusidinium* sp. 1. Cabo Mondego section, lower Bajocian (*Stephanoceras humphriesianum* AB), sample AB192, slide 1, T25.
9. *Sentusidinium* sp. 1. Cabo Mondego section, lower Bathonian (*Zigzagiceras zigzag* AB), sample Bt134, slide 1, W26.
10. *Sentusidinium* sp. 1. Cabo Mondego section, lower Bathonian (*Zigzagiceras zigzag* AB), sample Bt164, slide 1, Z34/2.
11. *Sentusidinium* sp. cf. *S. asymmetrum* (Fenton et al. 1980) Lentin & Williams 1981. Cabo Mondego section, lower Bajocian (*Stephanoceras humphriesianum* AB), sample AB192, slide 1, Q33. Note the antapical granulate ornamentation.
12. *Sentusidinium* sp. 2. Cabo Mondego section, upper Bajocian (*Parkinsonia parkinsoni* AB), sample Bt106, slide 1, W28. Note the scabrate autophragm with dense short spines.

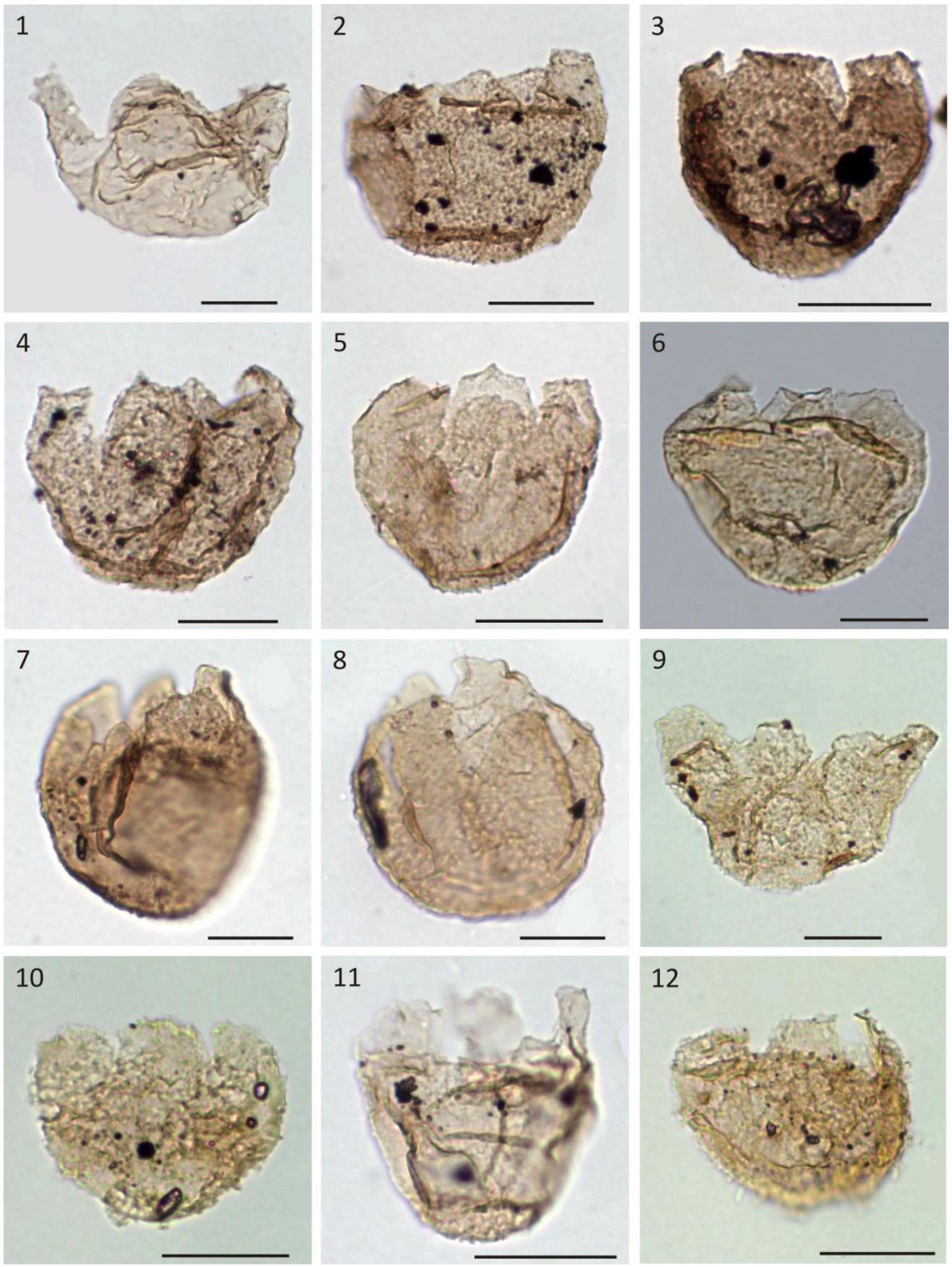
1
2
3
4
5
6
7
8
9
10
11
12

Plate XI. *Meiourogonyaulax* spp.

Note the apical archaeopyle and the cingulum.

1. *Meiourogonyaulax* sp. 1. . Cabo Mondego section, lower Bajocian (*Witchellia laeviuscula–Sonninia propinquans* ABs), sample AB108, slide 1, F59/3.
2. *Meiourogonyaulax* sp. 2. Cabo Mondego section, lower Bajocian (*Sonninia propinquans* AB), sample AB178a, slide 1, R43/4.
3. *Meiourogonyaulax* sp. 2. Cabo Mondego section, lower Bajocian (*Sonninia propinquans* AB), sample AB178a, slide 1, T60/3.
4. *Meiourogonyaulax* sp. 2. Cabo Mondego section, lower Bajocian (*Sonninia propinquans* AB), sample AB178a, slide 2, K48/1.
5. *Meiourogonyaulax* sp. 3. Cabo Mondego section, upper Bajocian (*Parkinsonia parkinsoni* AB), sample Bt106, slide 1, H37/4. Note the cingulum and sulcus.
6. *Meiourogonyaulax* sp. 3. Cabo Mondego section, upper Bajocian (*Parkinsonia parkinsoni* AB), sample Bt110, slide 1, N24/1.

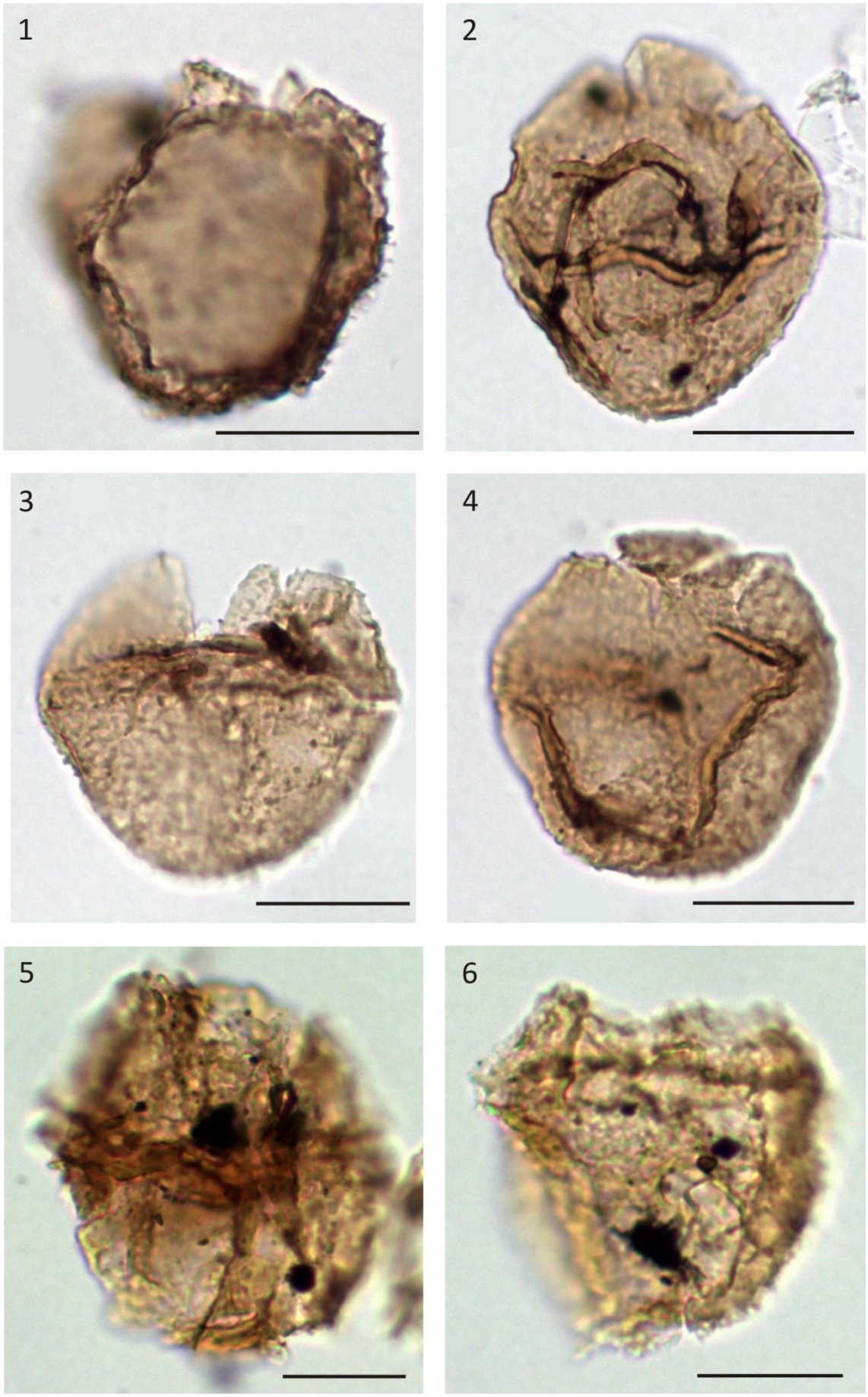
1
2
3
4
5
6

Plate XII. *Ctenidodinium* spp.

Note the epicystal archaeopyle and the sutural spines.

1–4. *Ctenidodinium sellwoodii* (Sarjeant 1975) Stover & Evitt 1978.

1. Cabo Mondego section, lower Bajocian (*Sonninia propinquans* AB), sample AB138, slide 1, P22/2.
2. Cabo Mondego section, upper Bajocian (*Parkinsonia parkinsoni* AB), sample Bt106, slide 1, R25/1. Note the large antapical plate (1"").
3. Cabo Mondego section, lower Bathonian (*Zigzagiceras zigzag* AB), sample Bt126, slide 1, G23/4.
4. Cabo Mondego section, upper Callovian (*Peltoceras athleta* AB), sample CM12, slide 1, J48/4. Hypocyst.
5. *Ctenidodinium* sp. Cabo Mondego section, lower Bathonian (*Zigzagiceras zigzag* AB), sample Bt210, slide 1, T33/1. Note the relatively long antapical spines, compared with *C. sellwoodii*.
6. *Ctenidodinium* sp. Cabo Mondego section, lower Bathonian (*Zigzagiceras zigzag* AB), sample Bt210, slide 1, Q38/1. Note the relatively long antapical spines, compared with *C. sellwoodii*.

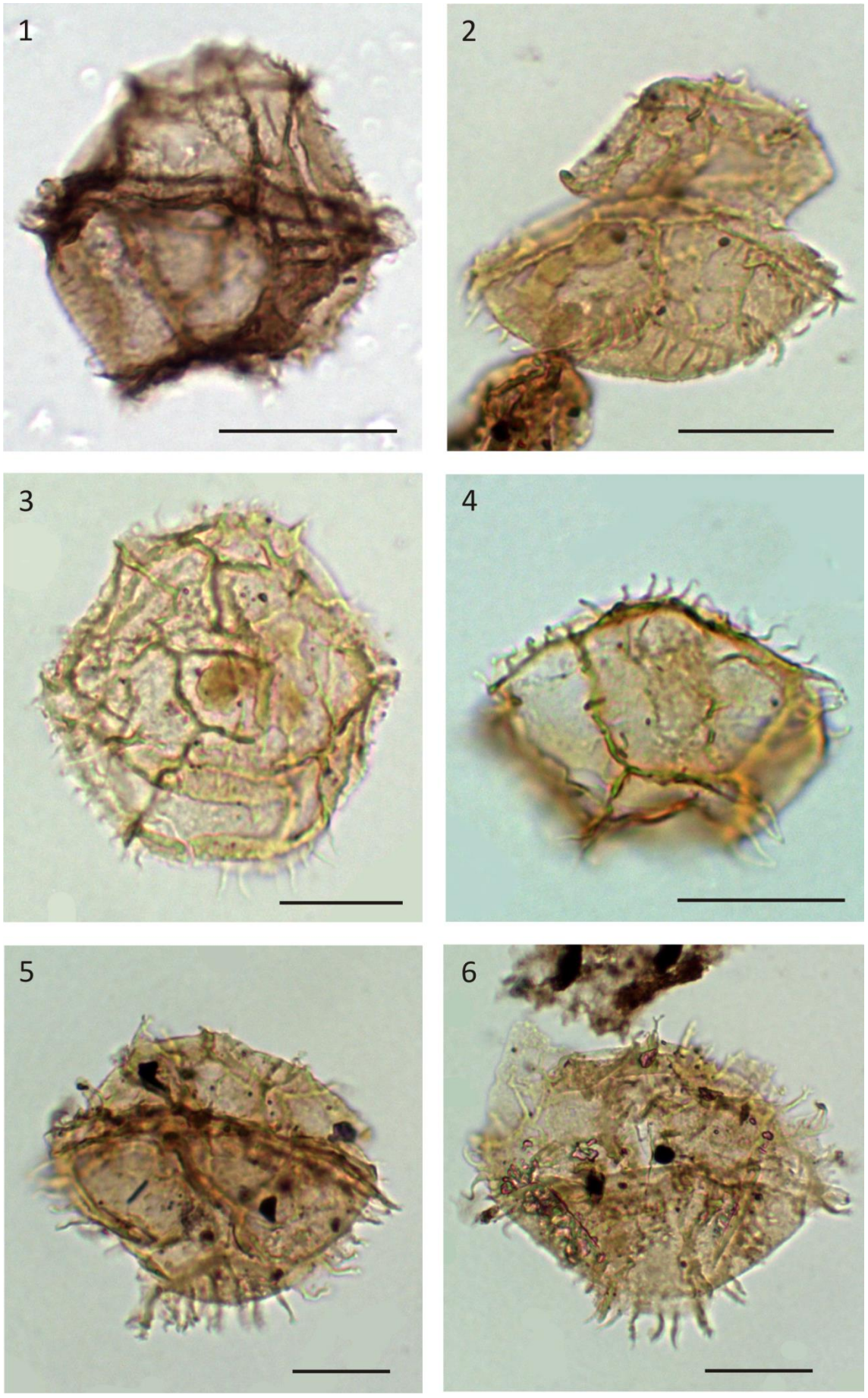
1
2
3
4
5
6

Plate XIII. *Valensiella ovulum* (Deflandre 1947) Eisenack 1963.

Note the apical archaeopyle and the reticulate ornamentation.

1. Cabo Mondego section, lower Bathonian (*Zigzagiceras zigzag* AB), sample Bt134, slide 1, H33.
2. Cabo Mondego section, lower Bathonian (*Zigzagiceras zigzag* AB), sample Bt134, slide 1, C32. Apical view.
3. Cabo Mondego section, lower Bathonian (*Zigzagiceras zigzag* AB), sample Bt164, slide 1, W31.
4. Cabo Mondego section, lower Bathonian (*Zigzagiceras zigzag* AB), sample Bt200, slide 1, S30.
5. Cabo Mondego section, lower Bathonian (*Zigzagiceras zigzag* AB), sample Bt200, slide 1, O42.
6. Cabo Mondego section, lower Bathonian (*Zigzagiceras zigzag* AB), sample Bt200, slide 1, F25/2.

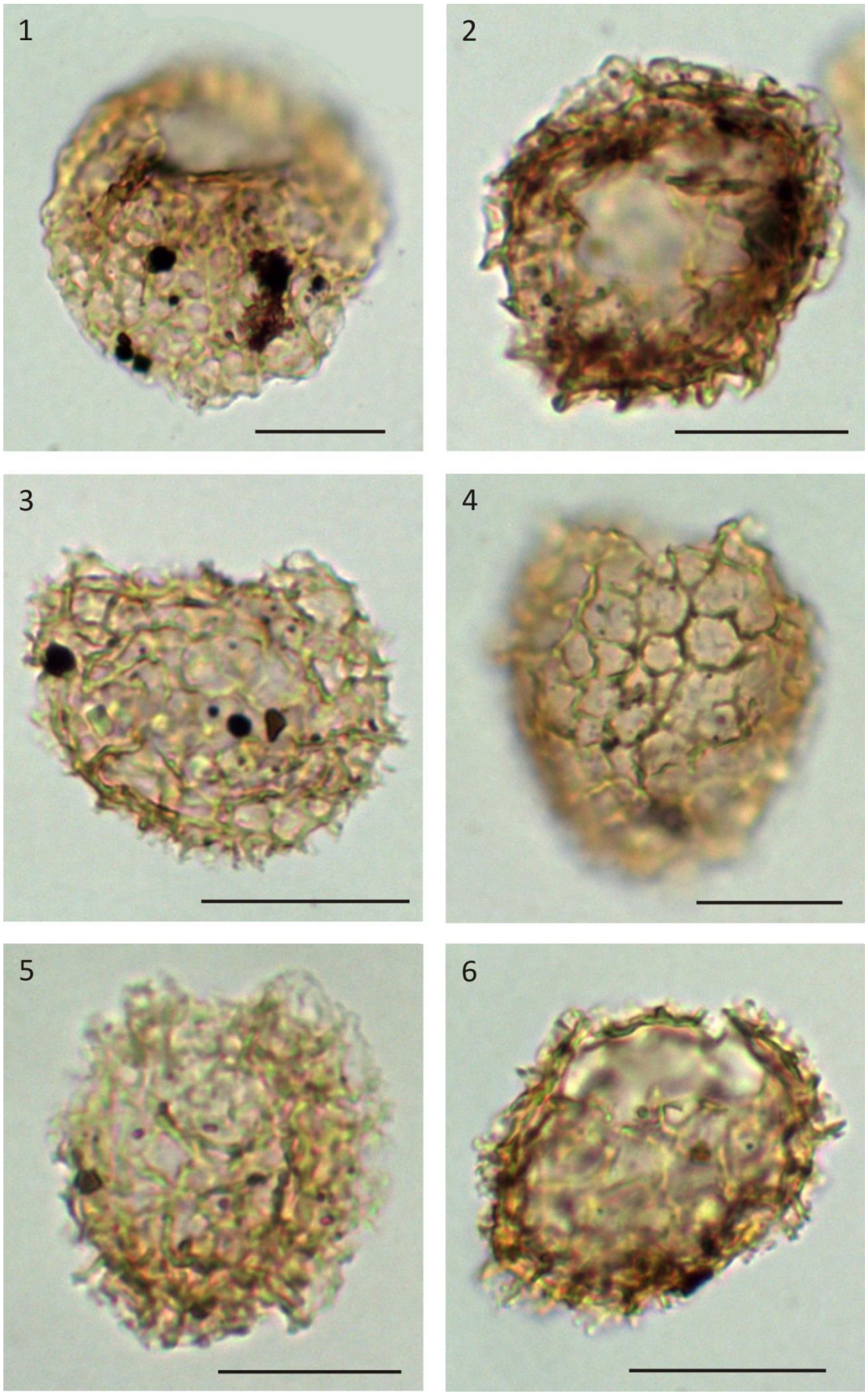
1
2
3
4
5
6

Plate XIV. *Chytroeisphaeridia chytroeides* (Sarjeant 1962) Downie & Sarjeant 1965.

Note the precingular (1P) archaeopyle.

1. Cabo Mondego section, upper Bajocian (*Parkinsonia parkinsoni* AB), sample Bt110, slide 1, T24/4. Left lateral view.
2. Cabo Mondego section, lower Bathonian (*Zigzagiceras zigzag* AB), sample Bt164, slide 1, N35. Oblique dorsal view.
3, 4. Cabo Mondego section, lower Bathonian (*Zigzagiceras zigzag* AB), sample Bt164, slide 1, K35/3. Oblique left lateral view. **3.** - high focus; note the detached operculum (plate 3") inside the body cyst. **4.** - low focus; note the 1P archaeopyle.
5. Cabo Mondego section, lower Bathonian (*Zigzagiceras zigzag* AB), sample Bt164, slide 1, E24. Left lateral view.
6. Cabo Mondego section, lower Bathonian (*Zigzagiceras zigzag* AB), sample Bt200, slide 1, U31. Oblique left lateral view.
7. Cabo Mondego section, upper Bathonian (*Clydoniceras discus* AB) sample CM3, slide 1, V30/1. Oblique dorsal view.
8. Cabo Mondego section, upper Callovian (*Peltoceras athleta* AB), sample CM12, slide 1, E26/2. Oblique dorsal view.

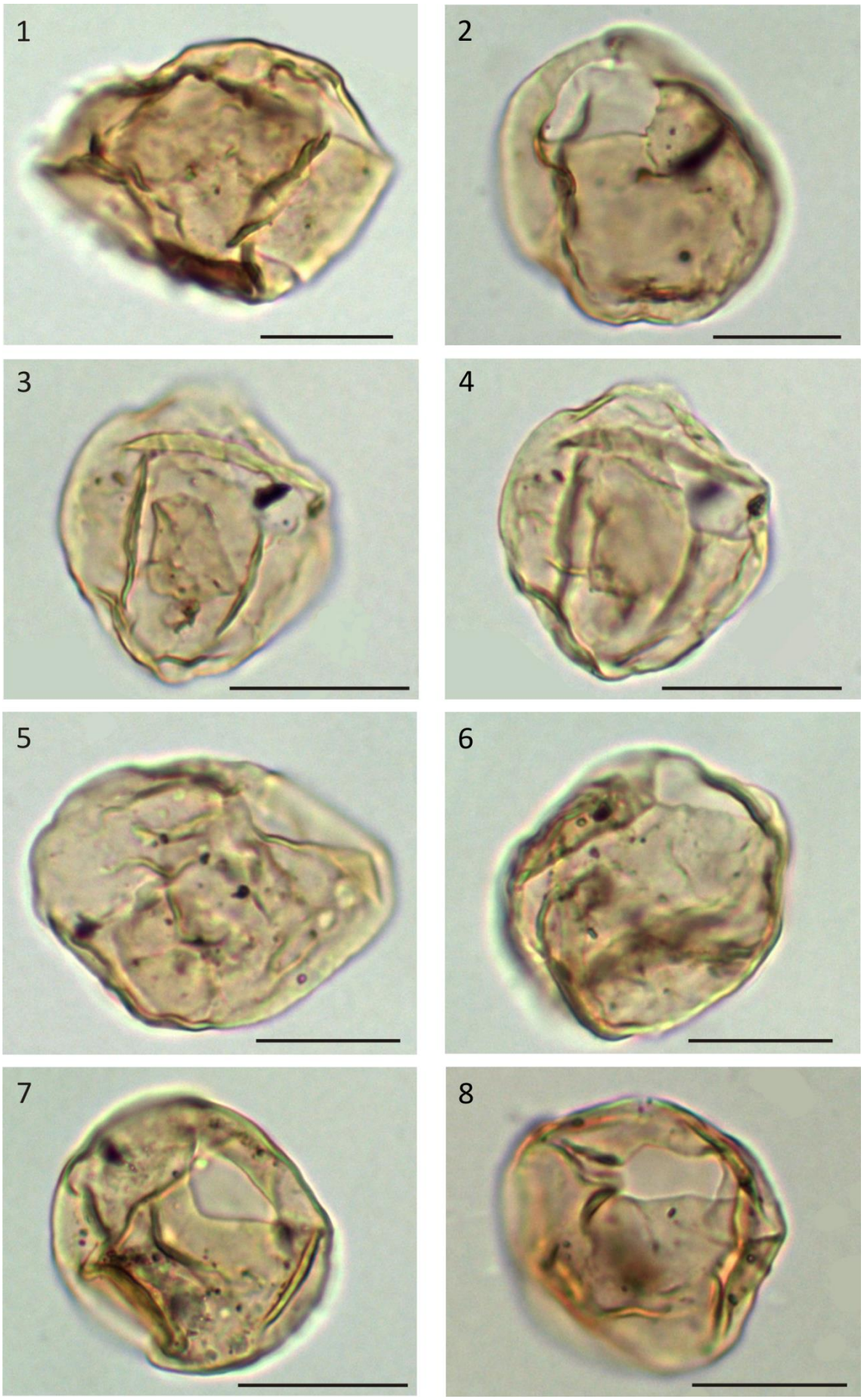
1
2
3
4
5
6
7
8

Plate XV. *Pareodinia* spp.

Note the prominent apical horn and the anterior intercalary archaeopyle.

1. *Pareodinia* sp. Cabo Mondego section, lower Bajocian (*Witchellia laeviuscula–Sonninia propinquans* ABs), sample AB108, slide 1, F22. Note the short apical horn.

2–4. *Pareodinia ceratophora* Deflandre 1947.

2. Cabo Mondego section, upper Bajocian (*Parkinsonia parkinsoni* AB), sample Bt106, slide 1, R31.
3. Cabo Mondego section, lower Bathonian (*Zigzagiceras zigzag* AB), sample Bt126, slide 1, O24.
4. Cabo Mondego section, upper Bathonian (*Clydoniceras discus* AB), sample CM3, slide 1, S54/2.

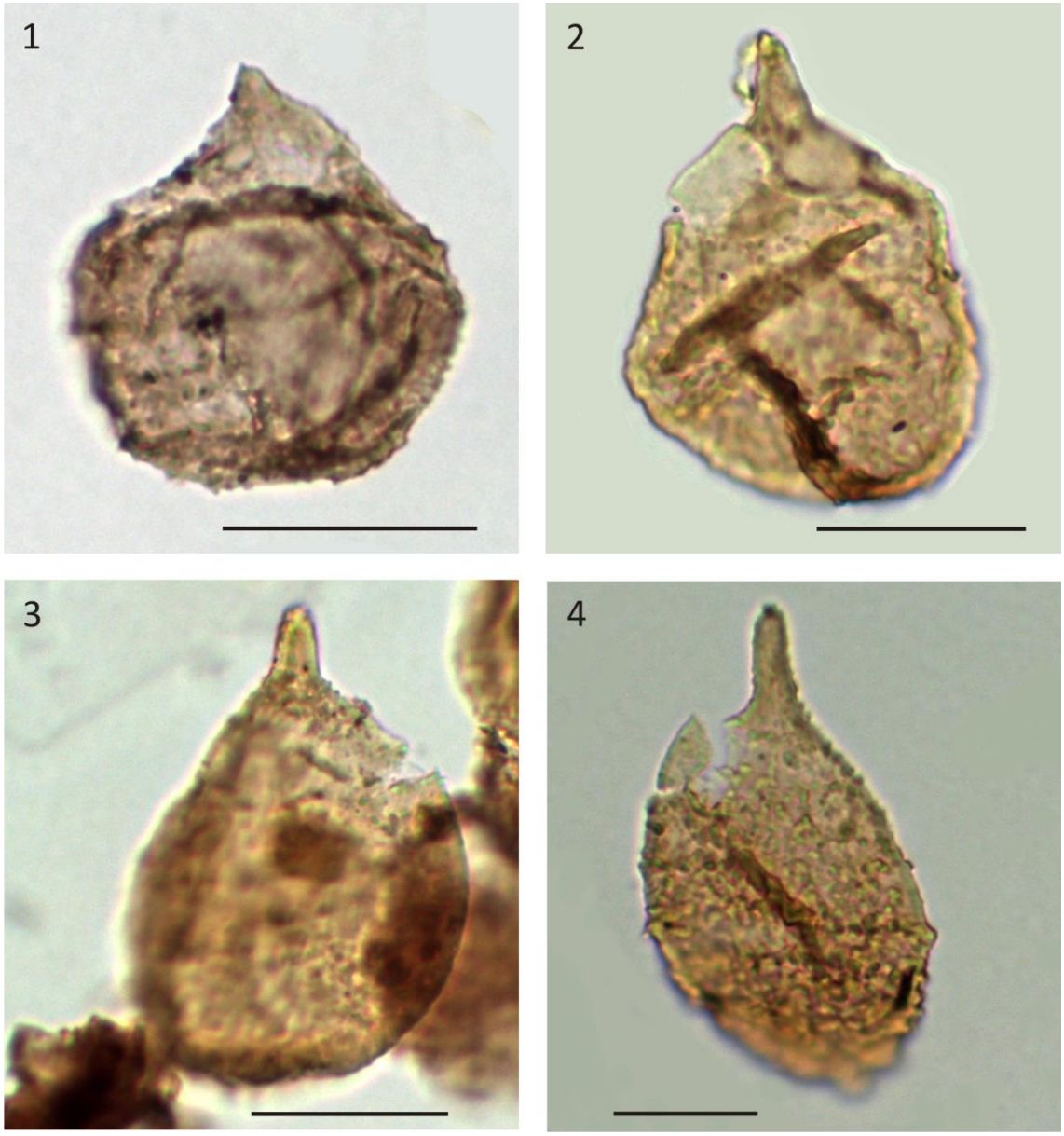
1
2
3
4

Plate XVI. *Gonyaulacysta* spp.

Note the apical horn and the prominent sutural crests with spines.

1–4. *Gonyaulacysta pectinigera* (Gocht 1970) Fensome 1979.

1, 2. Cabo Mondego section, lower Bathonian (*Zigzagiceras zigzag* AB), sample Bt200, slide 1, J25/3. Note the same size of the epicyst and hypocyst. **1**. – dorsal view, high focus; note the 1P archaeopyle and the prominent denticulate sutural crests. **2.** - ventral view, low focus; note the sulcus.

3. Cabo Mondego section, lower Bathonian (*Zigzagiceras zigzag* AB), sample Bt200, slide 1, O28/1. Ventral view.

4. Cabo Mondego section, lower Bathonian (*Zigzagiceras zigzag* AB), sample Bt200, slide 1, T29. Oblique right lateral view; note the 1P archaeopyle.

5, 6. *Gonyaulacysta jurassica* (Deflandre 1938) Norris & Sarjeant 1965 subsp. *adecta* Sarjeant 1982.

5. Cabo Mondego section, upper Bathonian (*Clydoniceras discus* AB) sample CM4, slide 1, N37. Note the sutural crests ornamented with spines. Ventral view, high focus.

6. Cabo Mondego section, upper Callovian (*Peltoceras athleta* AB), sample CM12, slide 1, O29. Note the epicyst longer than the hypocyst and the epicavation. Ventral view, high focus; note the S-type sulcus.

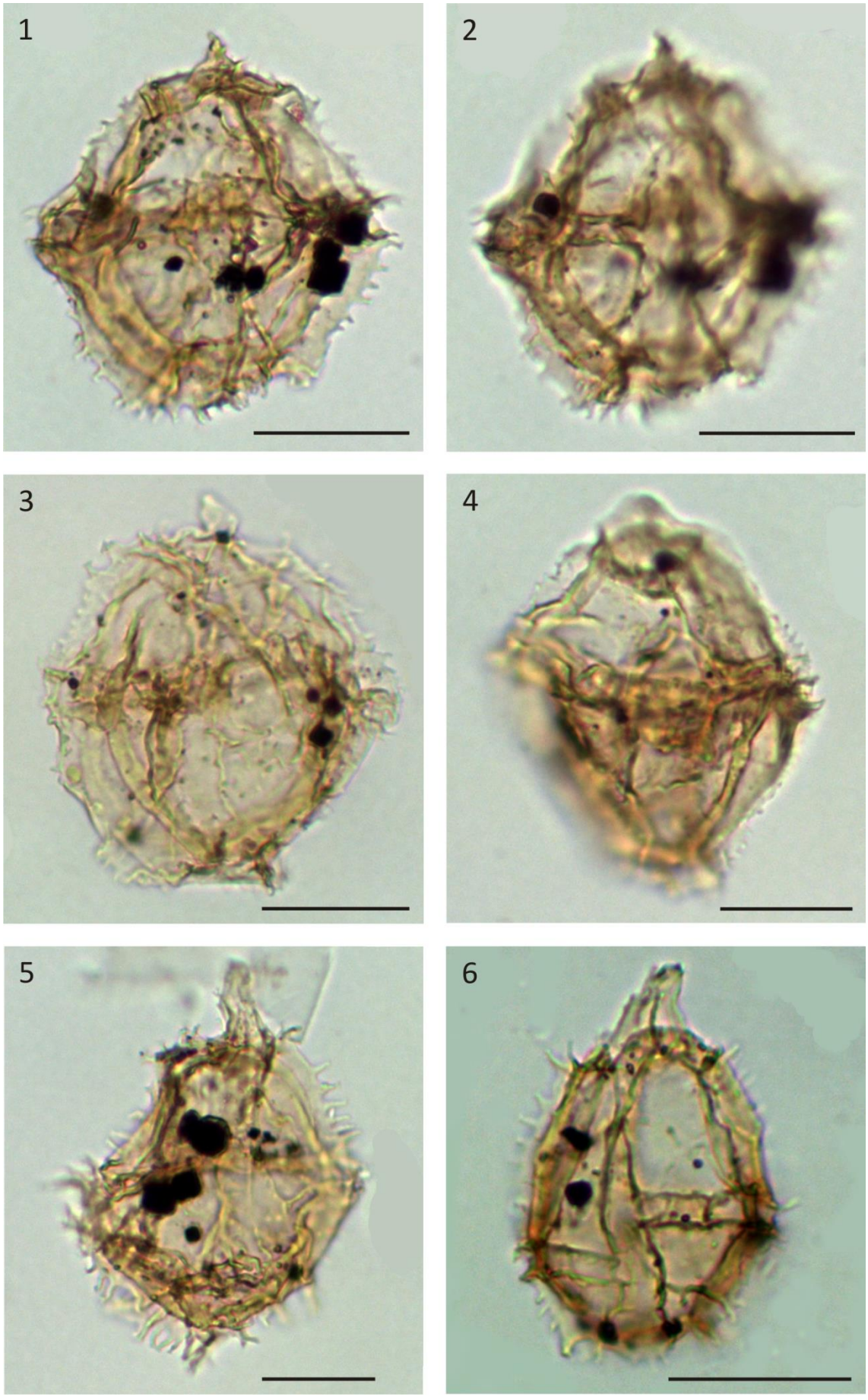
1
2
3
4
5
6

Plate XVII. *Ellipsoidictyum* sp.

Note the apical archaeopyle, the reticulate ornamentation and the cingulum.

1. Cabo Mondego section, lower Bathonian (*Zigzagiceras zigzag* AB), sample Bt126, slide 1, U26/2.
2. Cabo Mondego section, lower Bathonian (*Zigzagiceras zigzag* AB), sample Bt200, slide 1, P44.
3. Cabo Mondego section, lower Bathonian (*Zigzagiceras zigzag* AB), sample Bt200, slide 1, M26/1.
4. Cabo Mondego section, lower Bathonian (*Zigzagiceras zigzag* AB), sample Bt200, slide 1, V25.
5. Cabo Mondego section, lower Bathonian (*Zigzagiceras zigzag* AB), sample Bt200, slide 1, G32/1.
6. Cabo Mondego section, upper Callovian (*Peltoceras athleta* AB), sample CM12, slide 1, S27/1. Note the cingulum and sulcus.

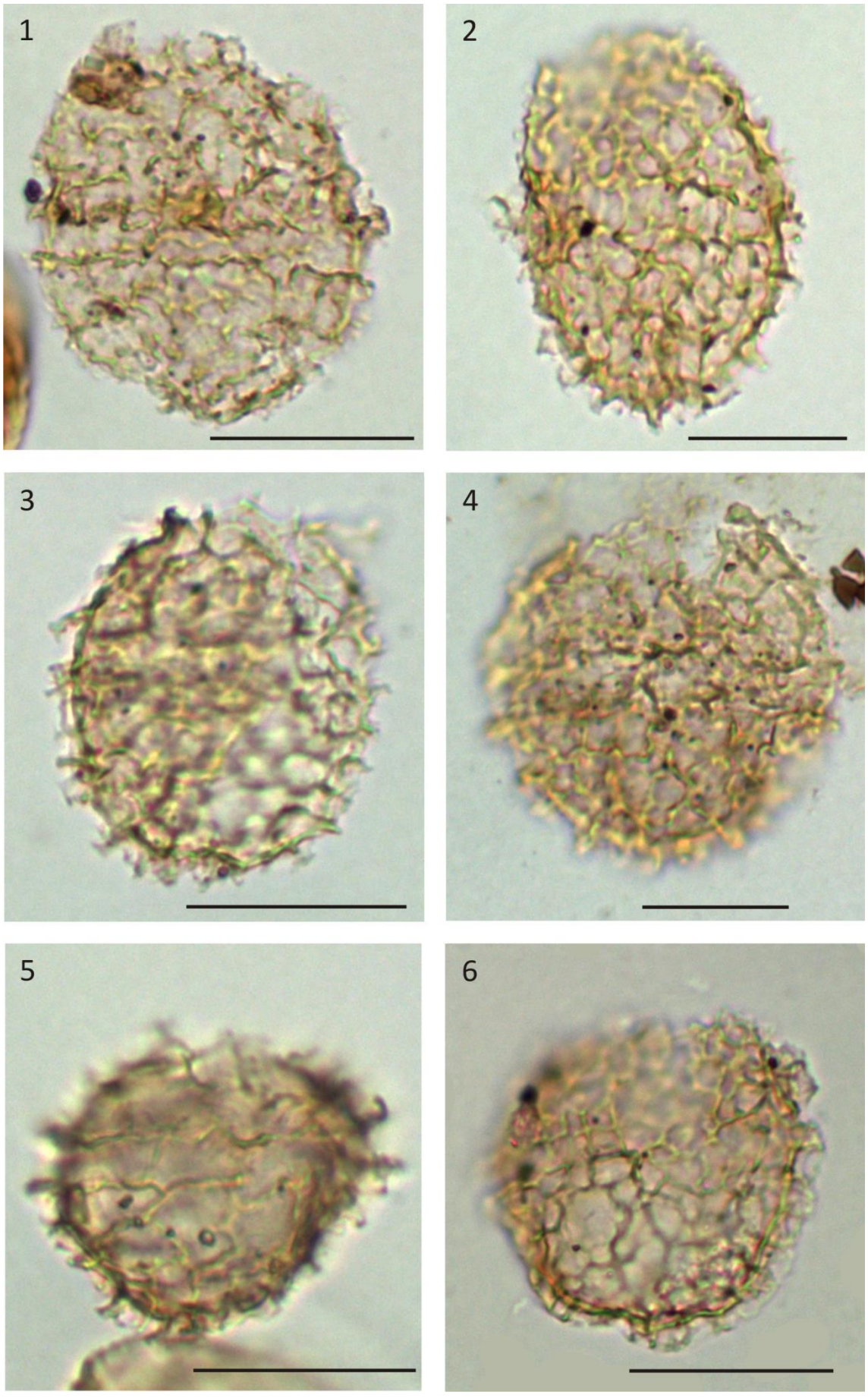
1
2
3
4
5
6

Plate XVIII. *Tubotuberella dangeardii* (Sarjeant 1968) Stover & Evitt 1978.

Note the 1P archaeopyle and the antapical "tube".

1. Cabo Mondego section, lower Bathonian (*Zigzagiceras zigzag* AB), sample Bt126, slide 1, O25/1. Ventral view, high focus.
2. Cabo Mondego section, upper Bathonian (*Clydoniceras discus* AB), sample CM4, slide 1, X35. Oblique ventral view, high focus.

3, 4.Cabo Mondego section, upper Bathonian (*Clydoniceras discus* AB), sample CM3, slide 1, O24. **3**. – dorsal view, high focus; note the 1P archaeopyle. **4.** – ventral view, low focus; note the sulcus and the antapical tube.

5. Cabo Mondego section, lower Callovian (*Bullatimorphites bullatus* AB), sample CM9, slide 1, T30. Oblique dorsal view, low focus.
6. Cabo Mondego section, ?middle Callovian, sample CM 10, slide 1, P22. Ventral view, high focus.

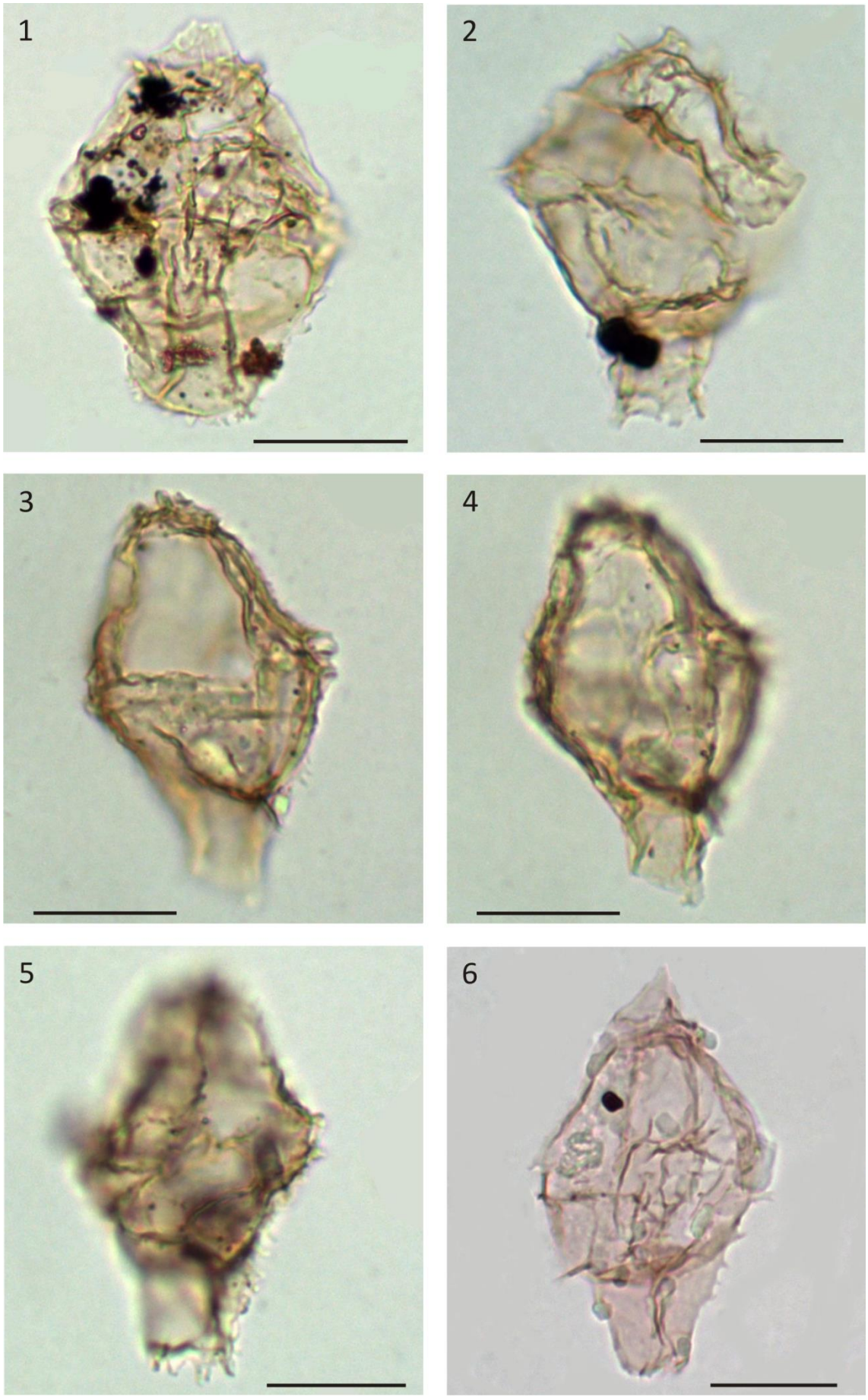
1
2
3
4
5
6

Plate XIX. *Ctenidodinium cornigerum* Valensi 1953.

Note the epicystal archaeopyle and the long sutural spines.

1. Cabo Mondego section, lower Bathonian (*Zigzagiceras zigzag* AB), sample Bt220, slide 1, H24.
2. Cabo Mondego section, ?middle Bathonian, sample CM1, slide 1, Q47/4. Note the sutural crests with simple or bifurcate spines.
3. Cabo Mondego section, ?middle Bathonian sample, CM1, slide 1, G53/1. Note the longer sutural spines (some bifurcate) in the antapical region.
4. Cabo Mondego section, ?middle Bathonian, sample CM1, slide 1, F54/4. Photomicrograph taken using differential interference contrast (40x).
5. Cabo Mondego section, ?middle Bathonian, sample CM1, slide 1, F54/4. Photomicrograph taken using differential interference contrast (20x).
6. Cabo Mondego section, ?middle Bathonian, sample CM1, slide 1, F54/4. General view (10x). Note the high abundance of *C. cornigerum*.

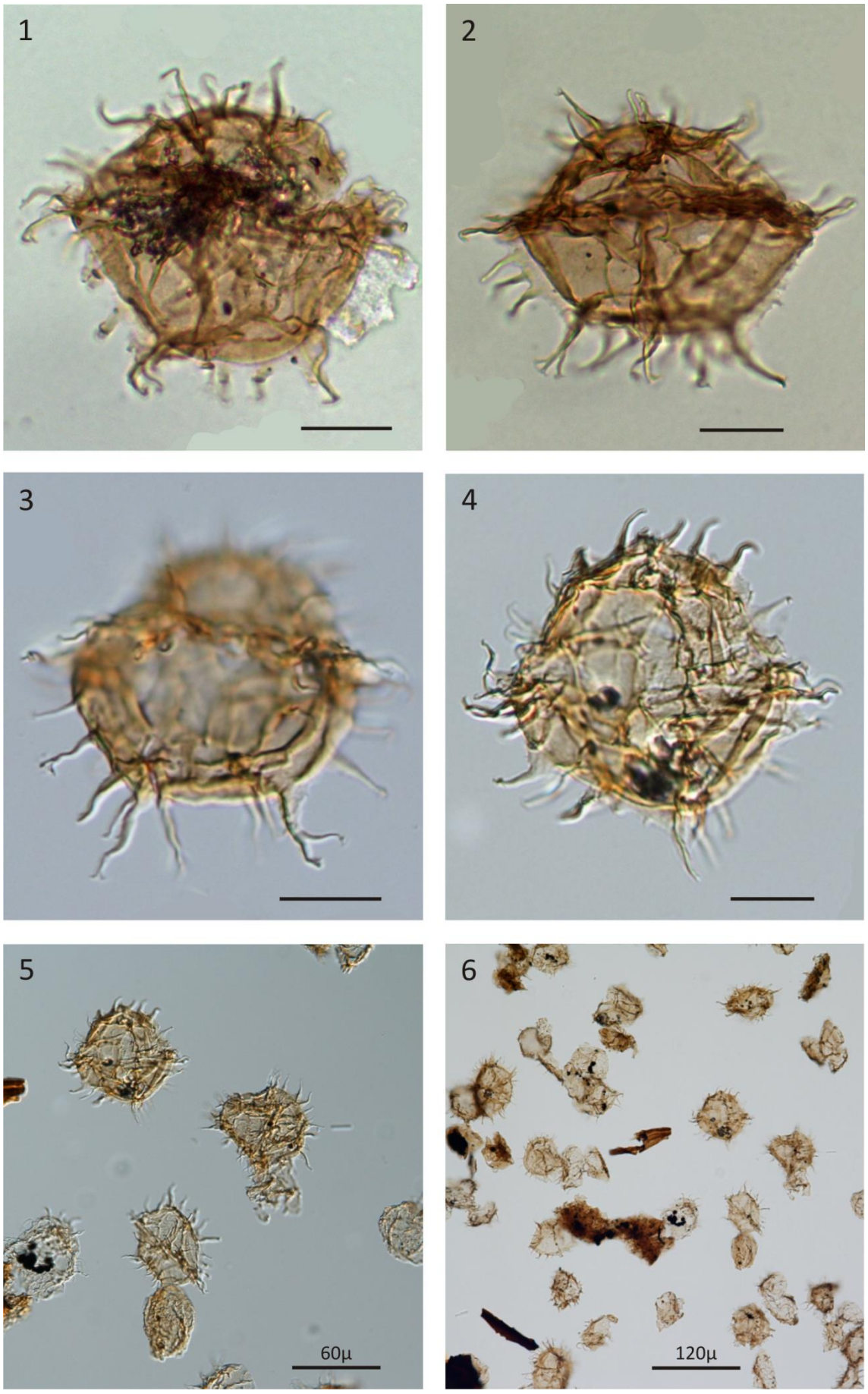
1
2
3
4
5
60µ
6
120µ

Plate XX. Complex chorate dinoflagellate cysts

1. Indeterminate complex chorate dinoflagellate cyst. Cabo Mondego section, lower Bathonian (*Zigzagiceras zigzag* AB), sample Bt210, slide 1, P27.
2. Indeterminate complex chorate dinoflagellate cyst. Cabo Mondego section, Bathonian–Callovian transition, sample CM5, slide 1, S36/3.

3, 4. *Adnatosphaeridium*? *caulleryi* (Deflandre 1939) Williams & Downie1969.

3. Cabo Mondego section, upper Bathonian (*Clydoniceras discus* AB), sample CM4, slide 1, C36.
4. Cabo Mondego section, upper Bathonian (*Clydoniceras discus* AB), sample CM4, slide 1, R39/1.

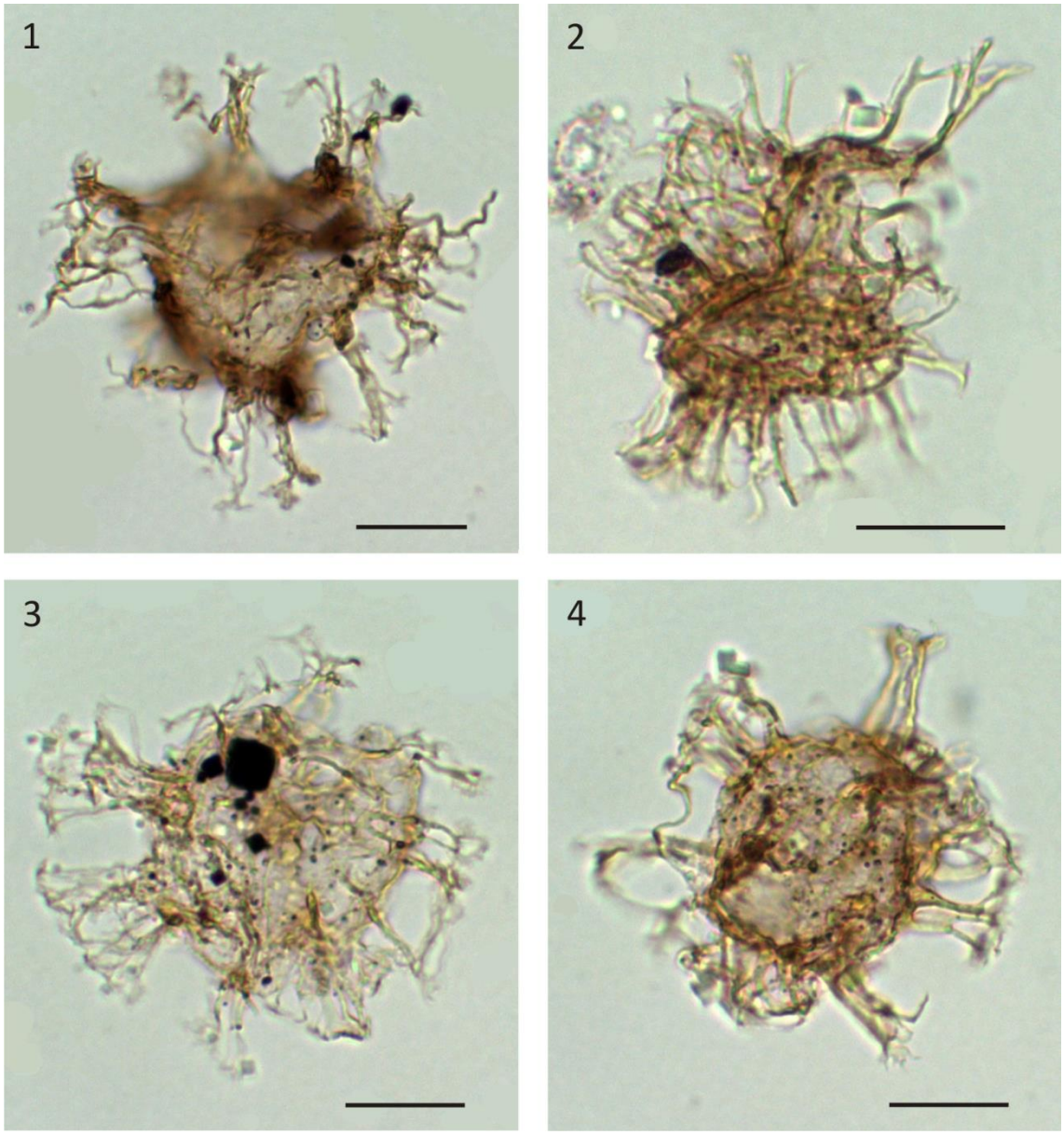
1
2
3
4

Plate XXI. Other Jurassic dinoflagellate cysts

Note these taxa were found in low abundances in the Lusitanian Basin and, some of theme, in poorly preservation.

1. *Valvaeodinium* sp. cf. *V. armatum* Morgenroth 1970. São Gião section, upper Toarcian (*Pleydellia aalensis* AB), sample SG10t, slide 1, O30/2.
2. *Valvaeodinium* sp. Cabo Mondego section, lower Bathonian (*Zigzagiceras zigzag* AB), sample Bt200, slide 1, R24.
3. *Phallocysta elongata* (Beju 1971) Riding 1994. Cabo Mondego section, upper Aalenian (*Graphoceras concavum* AB), sample M319, slide 1, N30/3.
4. *Acanthaulax* sp. cf. *A. crispa* (Wetzel 1967) Woollam & Riding 1983. Cabo Mondego section, lower Bajocian (*Sonninia propinquans* AB), sample AB138, slide 1, M32/3.
5. *Acanthaulax*? sp. Cabo Mondego section, lower Bathonian (*Zigzagiceras zigzag* AB), sample Bt126, slide 1, N26/2.
6. *Wanaea* sp. Cabo Mondego section, lower Bajocian (*Sonninia propinquans* AB), sample AB178a, slide 1, K52. Note the antapical horn.
7. *Bradleyella adela* (Fenton et al. 1980) Woollam 1983. Cabo Mondego section, upper Bajocian (*Parkinsonia parkinsoni* AB), sample Bt94, slide 1, M27/1.

8, 9. *Rhynchodiniopsis*? *regalis* (Gocht 1970) Jan du Chêne 1985.

8. Cabo Mondego section, upper Bajocian (*Parkinsonia parkinsoni* AB), sample Bt94, slide 1, U32/2.
9. Cabo Mondego section, upper Bajocian (*Parkinsonia parkinsoni* AB), sample Bt94, slide 1, Y35/1.

10, 11. *Korystocysta pachyderma* (Deflandre 1938) Woollam 1983.

10. Cabo Mondego section, upper Bajocian (*Parkinsonia parkinsoni* AB), sample Bt106, slide 1, X37/3. Note the intratabular ridges, characteristic of this species.
11. Cabo Mondego, lower Bathonian (*Zigzagiceras zigzag* AB), sample Bt140, slide 1, X45. Note the intratabular ridges.
12. *Korystocysta*? *gochtii* (Sarjeant 1976) Woollam 1983. Cabo Mondego section, lower Bathonian (*Zigzagiceras zigzag* AB), sample Bt200, slide 1, E32/4.

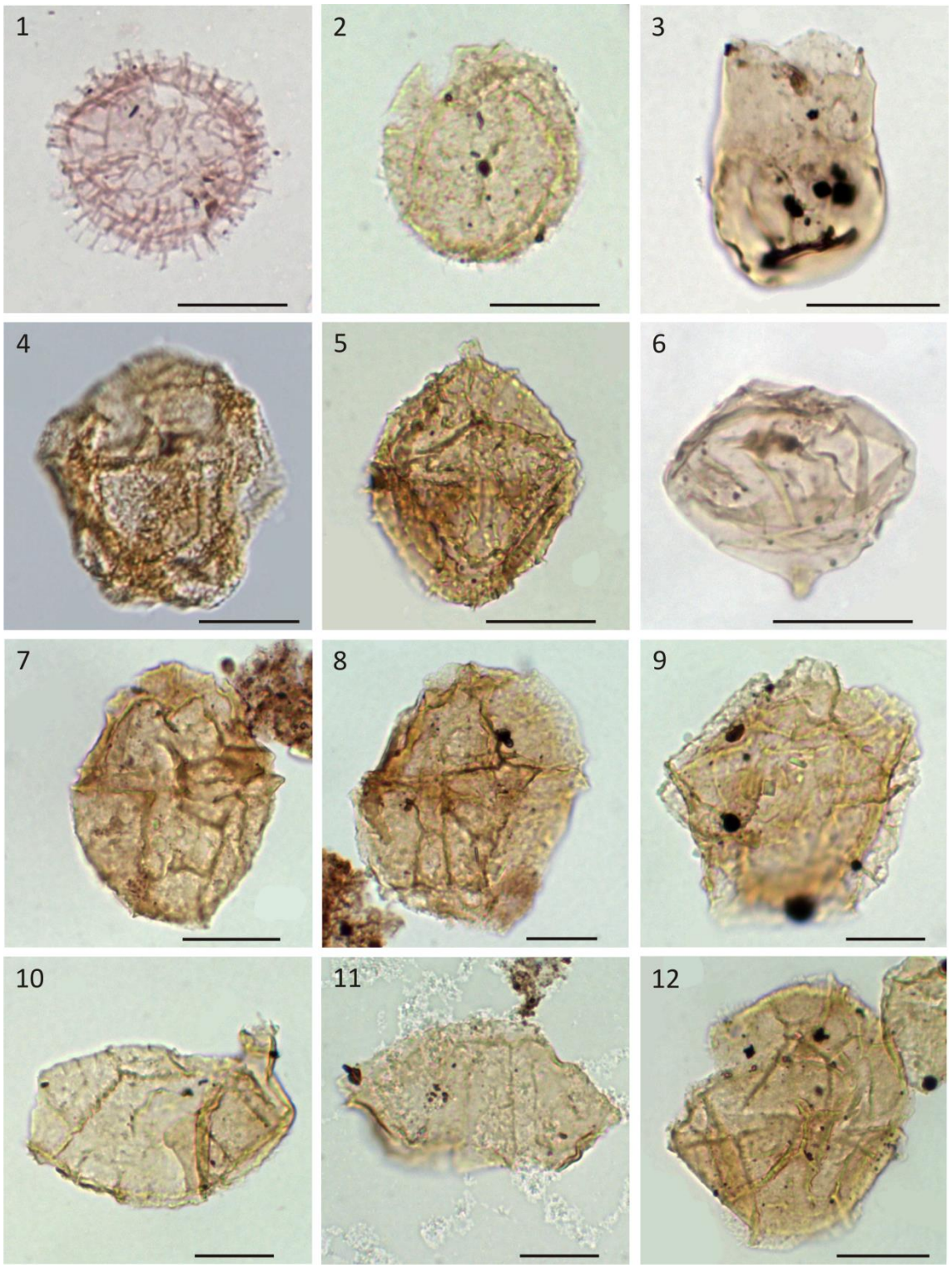
1
2
3
4
5
6
7
8
9
10
11
12

Plate XXII. *Kraeuselisporites reissingeri* (Harris 1957) Morbey 1975.

Note the distinctive apiculate sculpture.

1. São Pedro de Moel section, upper Sinemurian (*Oxynoticeras oxynotum* AB), sample PM3, slide 1, H43.
2. Vale das Fontes section, lower Toarcian (*Dactylioceras polymorphum* AB), sample PVF4, slide 1, R53/3.
3. Vale das Fontes section, lower Toarcian (*Dactylioceras polymorphum* AB), sample PVF5, slide 1, E34/3. Tetrad.
4. Vale das Fontes section, lower Toarcian (*Dactylioceras polymorphum* AB), sample PVF10, slide 1, H26/4.
5. Cabo Mondego section, upper Toarcian (*Pleydellia aalensis* AB), sample M24, slide 1, N60/1.
6. Cabo Mondego section, lower Aalenian (*Leioceras opalinum* AB), sample M43, slide 1, T35/4. Tetrad.

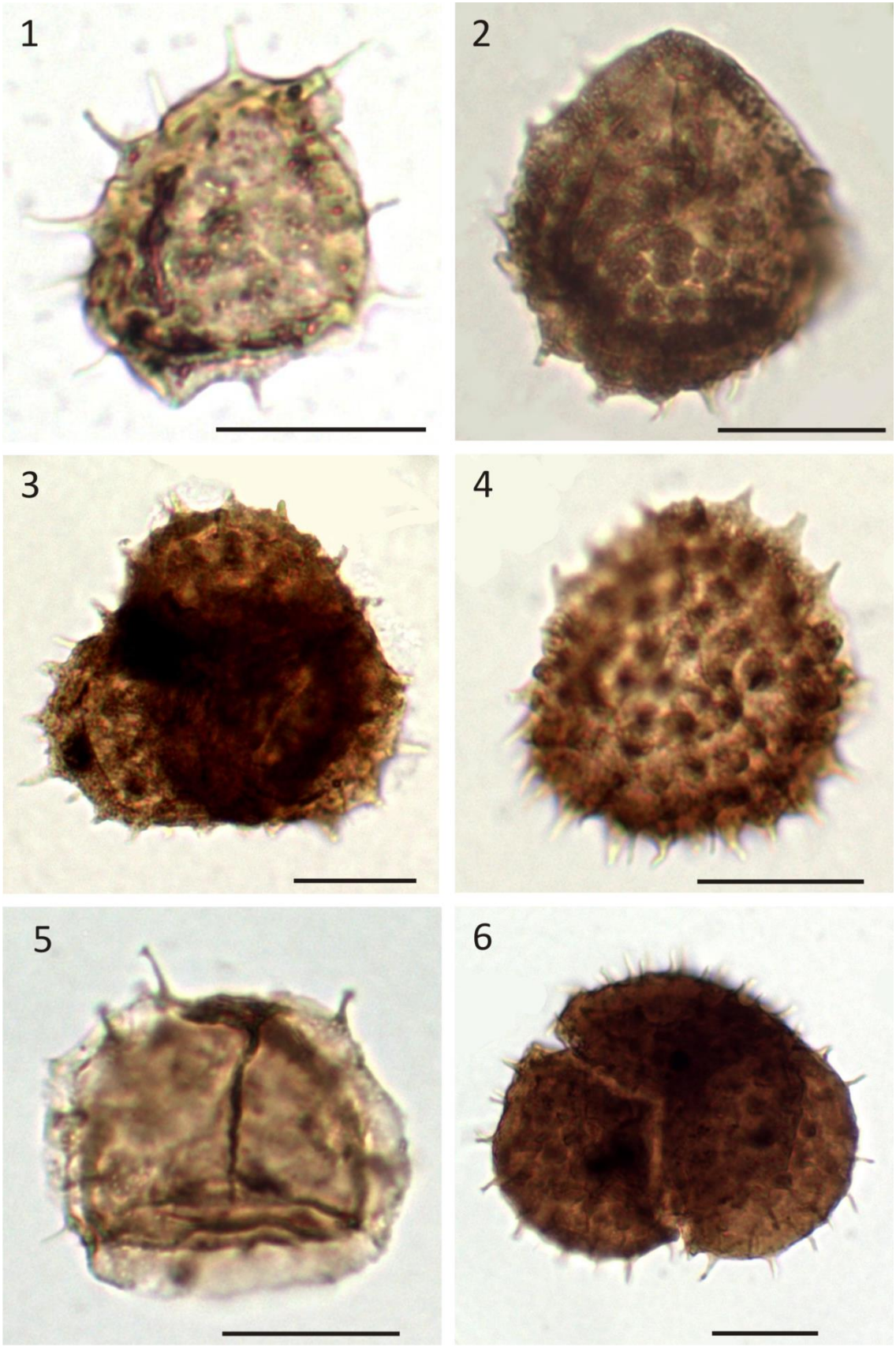
1
2
3
4
5
6

Plate XXIII. *Classopollis* spp.

1–8. *Classopollis classoides* (Pflug 1953) Pocock & Jansonius 1961. Note the subequatorial circumpolar canal and the equatorial striate band.

1. São Pedro de Moel section, upper Sinemurian (*Oxynoticeras oxynotum* AB), sample PM2, slide 1, Q36. Equatorial view.
2. São Pedro de Moel section, upper Sinemurian (*Oxynoticeras oxynotum* AB), sample PM3, slide 1, H50. Tetrad.
3. São Pedro de Moel section, upper Sinemurian (*Oxynoticeras oxynotum* AB), sample PM3, slide 1, W52/4. Polar distal view; note the cryptopore.
4. Peniche section, lower Pliensbachian (*Tragophylloceras ibex* AB), sample P-34, slide 1, Q32/2. Tetrad.
5. Fonte Coberta section, upper Pliensbachian (*Amaltheus margaritatus* AB), sample FC1, slide 1, O35/2. Tetrad.
6. Vale das Fontes section, lower Toarcian (*Dactylioceras polymorphum* AB), sample PVF2, slide 1, H30/2. Polar proximal view; note the trifid tetrad mark.
7. Vale das Fontes section, lower Toarcian (*Dactylioceras polymorphum* AB), sample PVF2, slide 1, K39/3. Tetrad.
8. Vale das Fontes section, lower Toarcian (*Dactylioceras polymorphum* AB), sample PVF10, slide 1, Q33/3. Dyad.
9. *Classopollis* sp. Maria Pares section, middle Toarcian (*Brodieia gradata* AB), sample PZ59, slide 1, Q38/4. Tetrad. Note the high abundance of sculpture elements.

10–12. *Classopollis meyeriana* (Klaus 1960) de Jersey 1973. Note the subequatorial circumpolar canal and the absence of the equatorial striate band.

10. Cabo Mondego section, upper Toarcian (*Pleydellia aalensis* AB), sample M28, slide 1, N41. Tetrad.
11. Cabo Mondego section, lower Aalenian (*Leioceras opalinum* AB), sample M32, slide 1, T44/3. Tetrad.
12. Cabo Mondego section, lower Bajocian (*Sonninia propinquans* AB), sample AB164, slide 1, Q35. Tetrad.

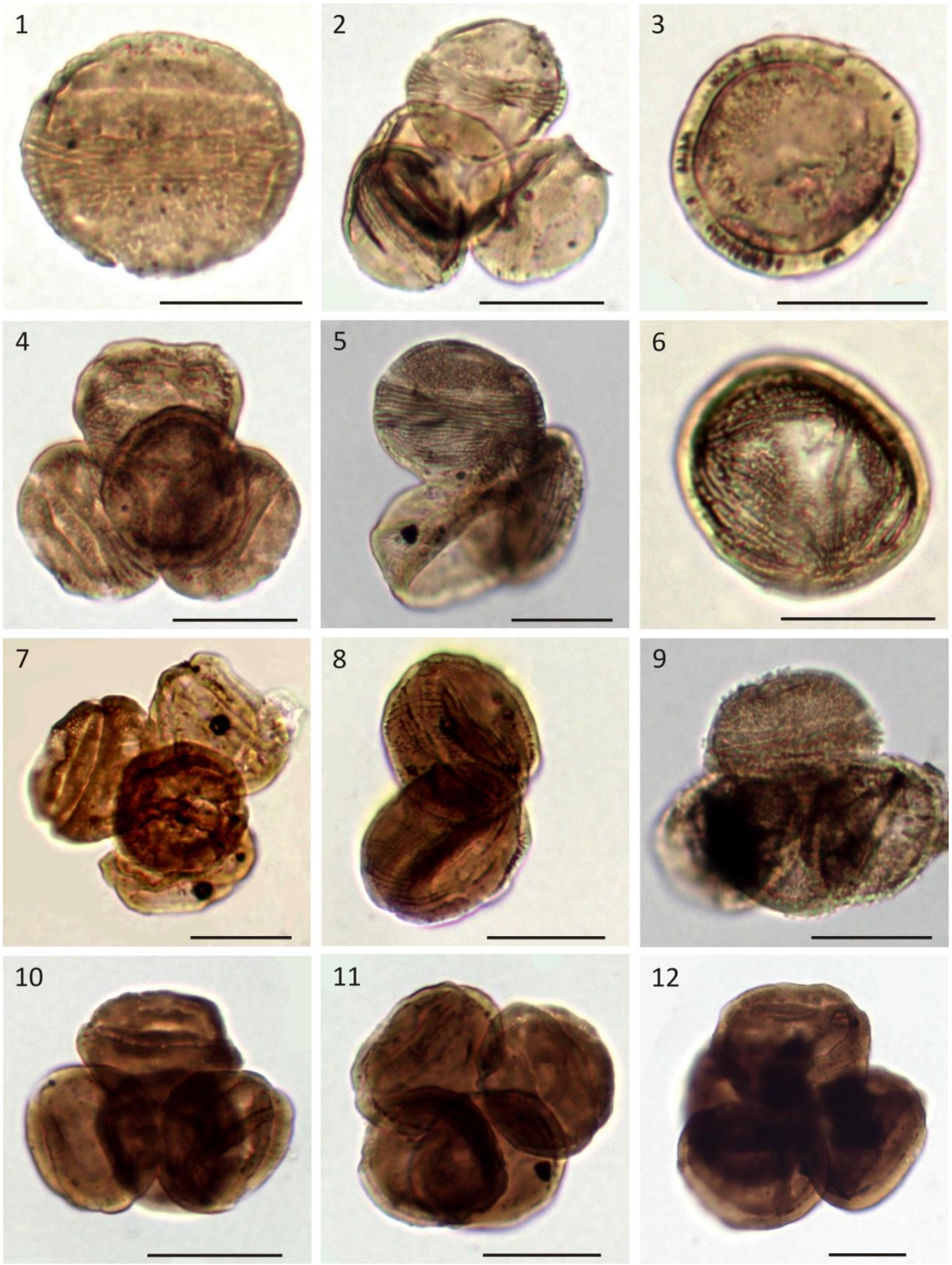
1
2
3
4
5
6
7
8
9
10
11
12

Plate XXIV. *Araucariacites australis* Cookson 1947 ex Couper 1958.

Note the scabrate to granulate exine.

1. Vale das Fontes section, lower Toarcian (*Dactylioceras polymorphum* AB), sample PVF3, slide 1, N30/1.
2. Vale das Fontes section, lower Toarcian (*Dactylioceras polymorphum* AB), sample PVF5, slide 1, O40.
3. Cabo Mondego section, upper Aalenian (*Graphoceras concavum* AB), sample M305, slide 1, K28. Note the strongly granulate sculpture.
4. Cabo Mondego section, lower Bajocian (*Witchellia laeviuscula–Sonninia propinquans* ABs), sample AB108, slide 1, N31/4.
5. Cabo Mondego section, lower Bajocian (*Witchellia laeviuscula–Sonninia propinquans* ABs), sample AB108, slide 1, N49/1.
6. Cabo Mondego section, lower Bajocian (*Sonninia propinquans* AB), sample AB178a, slide 1, Q23/2.
7, 8. Cabo Mondego section, lower Bajocian (*Sonninia propinquans* AB), sample AB178a, slide 2, M59/2. **7.** 40x objective. **8.** 60x objective with oil; note the scabrate sculpture.
9. Cabo Mondego section, lower Bajocian (*Sonninia propinquans* AB), sample AB178a, slide 2, M59. 60x objective with oil; note the scabrate sculpture.
10. Cabo Mondego section, upper Bajocian (*Parkinsonia parkinsoni* AB), sample Bt122, slide 1, B30.
11. Cabo Mondego section, lower Bathonian (*Zigzagiceras zigzag* AB), sample Bt126, slide 1, P28/3.
12. Cabo Mondego section, lower Bathonian (*Zigzagiceras zigzag* AB), sample Bt210, slide 1, D31.

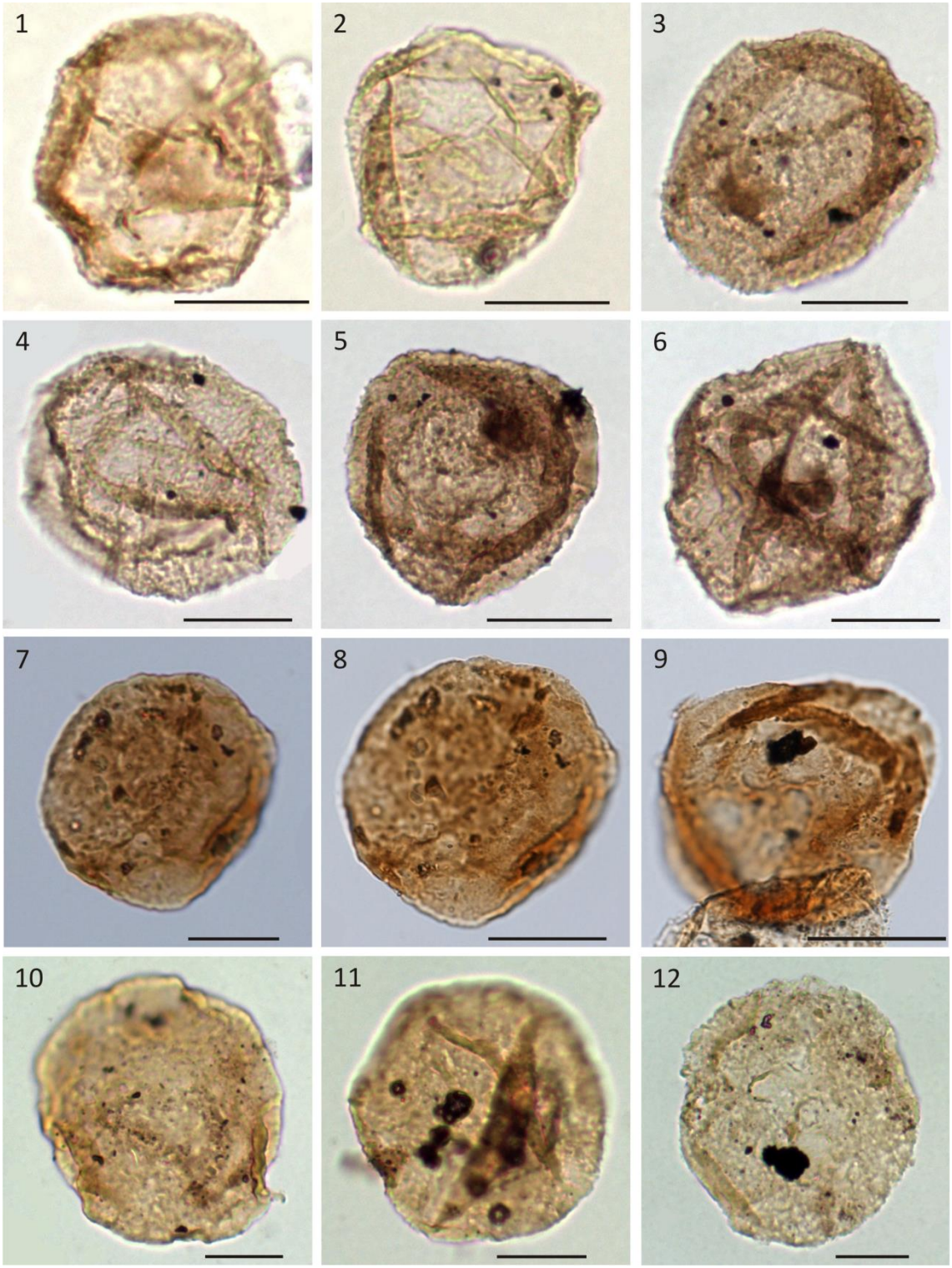
1
2
3
4
5
6
7
8
9
10
11
12

Plate XXV. *Callialasporites* spp.

Note the monosaccate pollen grains.

1–3. *Callialasporites dampieri* (Balme 1957) Dev 1961.

1. Maria Pares section, upper Toarcian (*Hammatoceras speciosum* AB), sample PZ81, slide 3, K29/4.
2. Cabo Mondego, lower Bathonian (*Zigzagiceras zigzag* AB), sample Bt184, slide 1, U55/2.
3. Cabo Mondego section, upper Bathonian (*Clydoniceras discus* AB), sample CM4, slide 1, R38/1.

4–6. *Callialasporites turbatus* (Balme 1957) Schulz 1967.

4. Maria Pares section, upper Toarcian (*Hammatoceras speciosum* AB), sample PZ81, slide 3, N54.
5. Cabo Mondego, lower Bajocian (*Hyperlioceras discites* AB) sample M341, slide 1, N23/2.
6. Cabo Mondego, lower Bathonian (*Zigzagiceras zigzag* AB), sample Bt164, slide 1, E30.

7–9. *Callialasporites segmentatu*s (Balme 1957) Srivastava 1963

7. Cabo Mondego section, upper Aalenian (*Graphoceras concavum* AB), sample M330, slide 2, U31/1.
8. Cabo Mondego section, lower Bajocian (*Witchellia laeviuscula–Sonninia propinquans* ABs) sample AB116, slide 1, J25/2.
9. Cabo Mondego, lower Bathonian (*Zigzagiceras zigzag* AB), sample Bt184, slide 1, H29/2.
10. *Callialasporites minus* (Tralau 1968) Guy 1971. Cabo Mondego, lower Bajocian (*Hyperlioceras discites* AB) sample M341, slide 1, N27.
11. *Callialasporites microvelatus* Schulz 1967. Cabo Mondego, lower Bathonian (*Zigzagiceras zigzag* AB), sample Bt140, slide 1, Z40.
12. *Callialasporites trilobatus* (Balme 1957) Dev 1961. Cabo Mondego section, lower Bajocian (*Sonninia propinquans* AB), sample AB178a, slide 1, Q26/1.

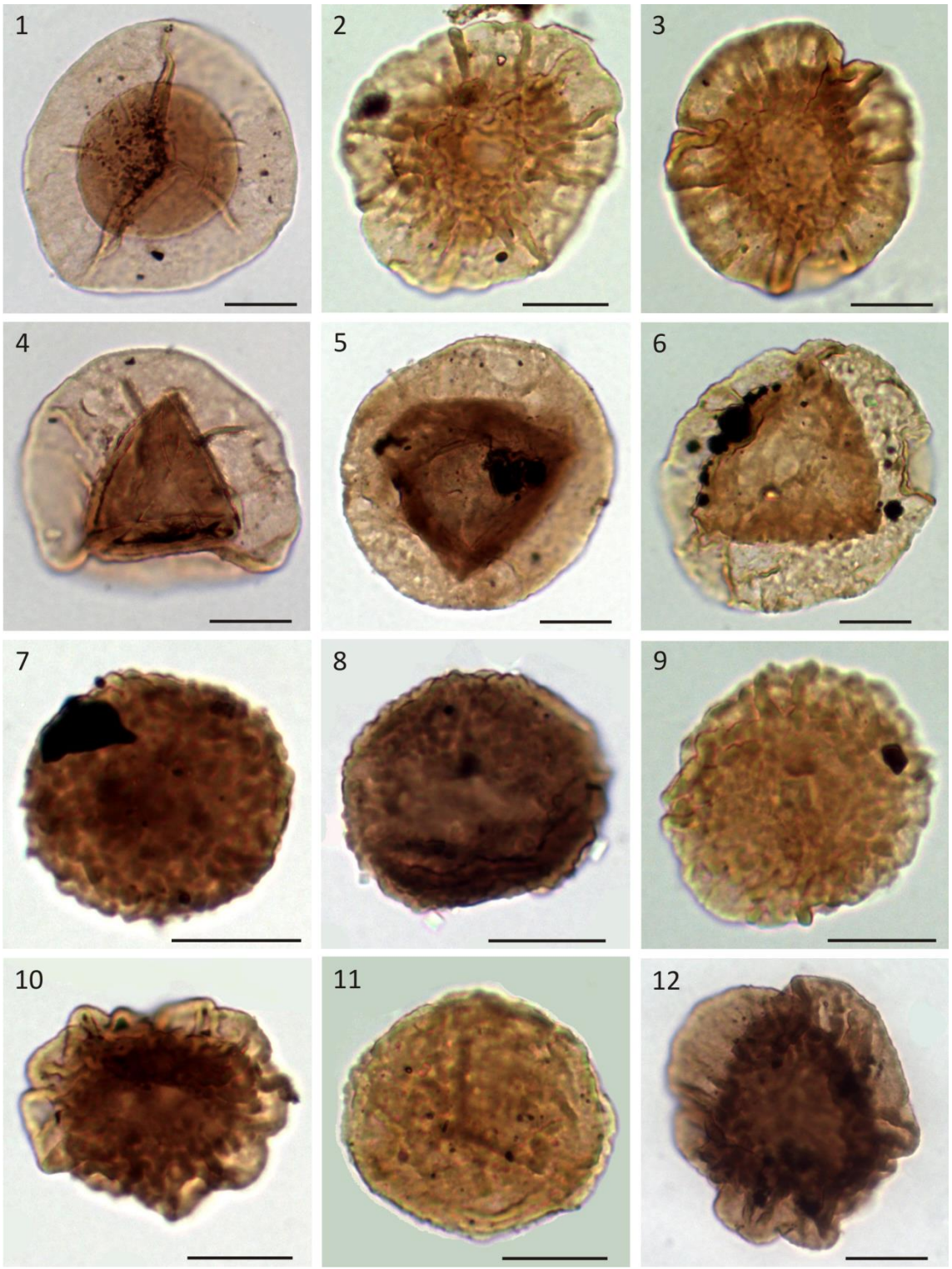
1
2
3
4
5
6
7
8
9
10
11
12